

Physics Department

Centro de Investigación y de Estudios Avanzados del IPN



# Low-energy meson phenomenology with Resonance Chiral Lagrangians

Presented in Partial Fulfilment of the Requirements for the  
Degree of Doctor in Science

by

Adolfo Enrique Guevara Escalante

Thesis advisors:

Dr. Gabriel López Castro and Dr. Pablo Roig Garcés.

*“Life is like a healthy penis,  
it gets hard for no reason.”*

# Table of Contents

<b>Table of Contents</b>	<b>iii</b>
<b>List of Tables</b>	<b>vi</b>
<b>List of Figures</b>	<b>viii</b>
<b>1 Theoretical Framework</b>	<b>7</b>
1.1 Introduction . . . . .	7
1.2 Standard Model . . . . .	7
1.2.1 Introduction . . . . .	7
1.2.2 Electroweak Standard Model . . . . .	8
1.2.3 Strong Interactions and Quantum Chromodynamics . . . . .	16
1.2.4 Standard Model of Particle Physics . . . . .	22
1.2.5 QCD, limitations and Effective Field Theories . . . . .	27
1.2.6 Chiral symmetry of the QCD Lagrangian density . . . . .	29
1.2.7 Inclusion of external currents . . . . .	30
1.3 Chiral Perturbation Theory . . . . .	32
1.3.1 Construction of Chiral Perturbation Theory ( $\chi$ PT) . . . . .	32
1.4 Resonance Chiral Theory ( $R\chi T$ ) . . . . .	35
<b>2 Lepton universality violation and new sources of CP violation</b>	<b>38</b>
2.1 Introduction . . . . .	38
2.2 The $\tau^- \rightarrow \pi^- \nu_\tau \ell^+ \ell^-$ decays as background for BSM interactions . . .	39
2.2.1 Introduction . . . . .	39
2.2.2 Matrix element of the process . . . . .	40
2.2.3 Form Factors . . . . .	42
2.2.4 Short distance constraints . . . . .	45
2.2.5 Branching ratio and invariant mass spectrum . . . . .	47
2.2.6 Conclusions . . . . .	51

2.3	Long-distance contribution to $B^\pm \rightarrow (\pi^\pm, K^\pm)\ell^+\ell^-$ decays. . . . .	52
2.3.1	Introduction . . . . .	52
2.3.2	R $\chi$ T contribution to the Weak Annihilation amplitude . . . .	53
2.3.3	Extending R $\chi$ T for heavy flavor mesons . . . . .	54
2.3.4	The electromagnetic form factor $F_P(q^2)$ . . . . .	58
2.3.5	CP Asymmetry . . . . .	65
2.3.6	Conclusions . . . . .	67
<b>3</b>	<b>New charged current structures</b>	<b>69</b>
3.1	Introduction . . . . .	69
3.2	Matrix Element and Form Factors . . . . .	70
3.3	Meson dominance model prediction . . . . .	72
3.4	Resonance Chiral Theory . . . . .	78
3.4.1	Resonance Lagrangian operators . . . . .	78
3.5	$\tau^- \rightarrow \pi^- \eta^{(\prime)} \gamma \nu_\tau$ as background in the searches for $\tau^- \rightarrow \pi^- \eta^{(\prime)} \nu_\tau$ . . .	94
3.5.1	Meson dominance predictions . . . . .	94
3.5.2	R $\chi$ L predictions . . . . .	98
3.6	Statistical error analysis . . . . .	102
3.7	Conclusions . . . . .	104
<b>4</b>	<b>The <math>VV'P</math> form factors in R<math>\chi</math>T and the <math>\pi - \eta - \eta'</math> light-by-light contribution to the muon <math>g - 2</math></b>	<b>106</b>
4.1	Introduction . . . . .	106
4.2	The anomalous magnetic moment . . . . .	107
4.3	Hadronic contributions . . . . .	111
4.4	Transition Form Factor, TFF . . . . .	113
4.5	$\eta$ - and $\eta'$ - Transition Form Factor . . . . .	116
4.6	Pseudoscalar exchange contribution $a_\mu^{P,HLbL}$ . . . . .	118
4.7	Genuine probe of the $\pi$ TFF . . . . .	121
4.8	Conclusions . . . . .	125

<b>5</b>	<b>Conclusions</b>	<b>127</b>
	<b>Appendices</b>	<b>130</b>

# List of Tables

2.1	The central values of the different contributions to the branching ratio of the $\tau^- \rightarrow \pi^- \nu_\tau \ell^+ \ell^-$ decays ( $\ell = e, \mu$ ) are displayed on the left-hand side of the table. The error bands of these branching fractions are given in the right-hand side of the table. The error bar of the IB contribution stems from the uncertainties on the pion decay constant $F$ and $\tau_\ell$ lepton lifetime [72]. .	48
2.2	LD, SD and their interference contributions to the branching ratio for both channels. . . . .	66
2.3	CP asymmetry computed for different $q^2$ ranges, all values are given as percentages. . . . .	66
3.1	Our fitted values of the coupling parameters. Those involving a photon are given multiplied by the unit of electric charge. . . . .	78
3.2	Branching fractions for different kinematical constraints and parameter space points. . . . .	104
3.3	The main conclusions of our analysis are summarized: Our predicted branching ratios for the $\tau^- \rightarrow \pi^- \eta^{(\prime)} \gamma \nu_\tau$ decays and the corresponding results when the cut $E_\gamma > 100$ MeV is applied. We also compare the latter results to the prediction for the corresponding non-radiative decay (SCC signal) according to ref. [124] and conclude if this cut alone is able to get rid of the corresponding background in SCC searches. .	105
4.1	Different types of contributions to the $a_\mu$ . The hadronic contributions give the main theoretical uncertainty. . . . .	110
4.2	Contributions to $a_\mu$ from diagrams (a), (b) and (c) in fig 4.5 as given in ref. [166]. . . . .	113
4.3	Our result for $a_\mu^{\pi^0, HLbL}$ in eq. (4.22) is compared to other determinations. The method employed in each of them is also given. We specify those works that approximate $a_\mu^{\pi^0, HLbL}$ by the pion pole contribution. It is understood that all others consider the complete pion exchange contribution. . . . .	119

- 4.4 Our result for  $a_\mu^{P,HLbL}$  in eq. (4.26) is compared to other determinations. The method employed in each of them is also given. We specify those works that approximate  $a_\mu^{P,HLbL}$  by the pseudoscalar pole contribution. It is understood that all others consider the complete pseudoscalar exchange contribution. . 120
- 4.5 Our contribution to the  $a_\mu^{HLbL}$  compared to previous computations. . 126

# List of Figures

2.1	Feynman diagrams of the different contributions to the $\tau \rightarrow \pi \ell^+ \ell^- \nu_\tau$ decay. Diagrams (a) to (c) give the model independent contribution, while the structure dependent has been separated into two contributions for convenience . . . . .	40
2.2	Contribution to the vector form factor in eq (2.1), where the circle with cross denotes the weak vertex. . . . .	43
2.3	Contribution to the axial form factor in eq (2.1), where the circle with cross denotes the weak vertex. . . . .	43
2.4	The different contributions to the normalized $e^+e^-$ invariant mass distribution defined in Eq. (2.15) are plotted. A double logarithmic scale was needed. . . . .	49
2.5	The different contributions to the normalized $e^+e^-$ invariant mass distribution defined in Eq. (2.15) are plotted in a magnification for $s_{34} \gtrsim 0.1 \text{ GeV}^2$ intended to better appreciate the $SD$ contributions. A double logarithmic scale was needed. . . . .	50
2.7	All possible contributions to the WA amplitude at leading order in $1/N_C$ . The thick dot denotes interactions between resonances and the fields coupled to the vertex. . . . .	53
2.8	All LD WA Feynman diagrams at leading order in $1/N_C$ . The first row shows the contribution from model independent interactions, while the second and third shows contributions from diagrams with one and two resonances respectively. $V^{(0)}$ stands for light charged (neutral) vector resonances. . . . .	56
2.9	Only non-vanishing structure dependent contribution to the WA LD amplitude. . . . .	58



2.10	BaBar parametrization and our form factor compared with data from BaBar. Here $m_{\parallel} = \sqrt{q^2}$ . Both form factors overlap below 1.4 GeV, which is the dominant region of the form factor in the observables of the studied decays. . . . .	60
2.11	Electromagnetic form factor of the $K$ meson with the BaBar parametrization and our form factor compared with data from BaBar. Here $m_{\parallel} = \sqrt{q^2}$ . . . . .	61
2.12	Real and imaginary parts of $F_K(q^2)$ using $R\chi T$ and GS. . . . .	62
2.13	Real and imaginary parts of $F_{\pi}(q^2)$ using $R\chi T$ and GS. . . . .	63
2.14	The smooth match between LD and QCdf description of $F_K$ at 2 GeV <sup>2</sup> is shown. . . . .	64
2.15	The smooth match between LD and QCdf description of $F_{\pi}$ at 2 GeV <sup>2</sup> is shown. . . . .	65
3.1	Effective hadronic vertex (grey blob) that defines the $V_{\mu\nu}$ and $A_{\mu\nu}$ tensors. 71	
3.2	Photon energy spectra for the leading bremsstrahlung terms in $BR(\tau \rightarrow \pi\eta^{(\prime)}\gamma\nu_{\tau})$ . . . . .	72
3.3	Contributions to the effective weak vertex in the MDM model. The wavy line denotes the photon. . . . .	73
3.4	Contributions from the Wess-Zumino-Witten functional [56] to $\tau^- \rightarrow \pi^- \eta \gamma \nu_{\tau}$ decays. The cross circle indicates the insertion of the charged weak current. . . . .	88
3.5	One-resonance exchange contributions from the $R\chi L$ to the axial-vector form factors of the $\tau^- \rightarrow \pi^- \eta \gamma \nu_{\tau}$ decays. Vertices involving resonances are highlighted with a thick dot. . . . .	89
3.6	Two-resonance exchange contributions from the $R\chi L$ to the axial-vector form factors of the $\tau^- \rightarrow \pi^- \eta \gamma \nu_{\tau}$ decays. Vertices involving resonances are highlighted with a thick dot. . . . .	89

3.7	One-resonance exchange contributions from the $R\chi L$ to the vector form factors of the $\tau^- \rightarrow \pi^- \eta \gamma \nu_\tau$ decays. Vertices involving resonances are highlighted with a thick dot. . . . .	90
3.8	Two-resonance exchange contributions from the $R\chi L$ to the vector form factors of the $\tau^- \rightarrow \pi^- \eta \gamma \nu_\tau$ decays. Vertices involving resonances are highlighted with a thick dot. . . . .	90
3.9	Histogram of $BR(\tau^- \rightarrow \pi^- \eta \gamma \nu_\tau)$ for 100 (left) and 1000 (right) random points in the MDM parameter space are plotted. . . . .	95
3.10	$\tau^- \rightarrow \pi^- \eta \gamma \nu_\tau$ normalized spectra according to MDM in the invariant mass of the $\eta \pi^-$ system (left) and in the photon energy (right) are plotted for some characteristic points in fig. 3.9 . . . . .	96
3.11	Histogram of $BR(\tau^- \rightarrow \pi^- \eta \gamma \nu_\tau)$ where photons with $E_\gamma > 100$ MeV are rejected. . . . .	96
3.12	Histogram of $BR(\tau^- \rightarrow \pi^- \eta' \gamma \nu_\tau)$ for 100 (left) and 1000 (right) random points in the MDM parameter space are plotted. . . . .	97
3.13	$\tau^- \rightarrow \pi^- \eta' \gamma \nu_\tau$ normalized spectra according to MDM in the invariant mass of the $\pi^- \eta'$ system (left) and in the photon energy (right) are plotted for some characteristic points in fig. 3.12 . . . . .	98
3.14	Histogram of $BR(\tau^- \rightarrow \pi^- \eta' \gamma \nu_\tau)$ where photons with $E_\gamma > 100$ MeV are rejected. . . . .	99
3.15	Histogram of $BR(\tau^- \rightarrow \pi^- \eta \gamma \nu_\tau)$ with a sample of 100 $R\chi T$ parameter space points for the complete (left) and neglecting 2R diagrams (right) branching fractions. . . . .	99
3.16	$\tau^- \rightarrow \pi^- \eta \gamma \nu_\tau$ normalized spectra according to $R\chi T$ in the invariant mass of the $\pi^- \eta$ system (left) and in the photon energy (right) are plotted. . . . .	100
3.17	Histogram of $BR(\tau^- \rightarrow \pi^- \eta \gamma \nu_\tau)$ in $R\chi T$ where photons with $E_\gamma > 100$ MeV are rejected. . . . .	101

3.18	Histogram of $BR(\tau^- \rightarrow \pi^- \eta' \gamma \nu_\tau)$ with a sample of 100 $R\chi T$ parameter space points for the complete (left) and neglecting 2R diagrams (right) branching fractions. . . . .	101
3.19	$\tau^- \rightarrow \pi^- \eta' \gamma \nu_\tau$ normalized spectra according to $R\chi T$ in the invariant mass of the $\pi^- \eta'$ system (left) and in the photon energy (right) are plotted. . . . .	102
3.20	Histogram of $BR(\tau \rightarrow \pi \eta' \gamma \nu_\tau)$ in $R\chi T$ where photons with $E_\gamma > 100$ MeV are rejected. . . . .	103
4.1	Next to leading order correction to the anomalous magnetic moment found by Schwinger. . . . .	108
4.2	Feynman diagram of a fermion interaction with a classic electromagnetic field. The blob represents all possible interactions that can happen in between. . . . .	109
4.3	Hadronic Vacuum Polarization contribution to $a_\mu$ , the blob stands for all possible strong interaction processes. . . . .	110
4.4	Light by light scattering insertions for a fermion loop. . . . .	111
4.5	Contributions from Hadronic Light by Light scattering, $a_\mu^{HLbL}$ . . . .	112
4.6	Main contribution to $a_\mu^{HLbL}$ , internal photon lines include the $\rho - \gamma$ mixing . . . . .	113
4.7	Our fit to the BaBar, Belle, CELLO and CLEO data compared to the Brodsky-Lepage behavior. . . . .	115
4.8	Our prediction for the $\eta$ (left) and $\eta'$ (right) TFF cross section (left) using the couplings of eq. 4.27 compared to BaBar [171], CELLO [173] and CLEO [174]. . . . .	118
4.9	The $e^+e^- \rightarrow \mu^+\mu^-\pi^0$ scattering as a probe for $\pi$ TFF with both photons off-shell. . . . .	121
4.10	Our prediction for $\sigma(e^+e^- \rightarrow \mu^+\mu^-\pi^0)$ at different center of mass energies using the couplings in eq. 4.27. . . . .	123

4.11	Our prediction for $\mu^+\mu^-$ distribution at $s = (1.02 \text{ GeV})^2$ using the couplings in eq. 4.27. . . . .	124
4.12	Our prediction for the $\sigma(e^+e^- \rightarrow \mu^+\mu^-\eta)$ cross section (left) and $\mu^+\mu^-$ distribution at $4 \text{ GeV}^2$ (right). . . . .	125

# Agradecimientos

Agradezco de manera muy sincera a mis asesores, Gabriel López Castro y Pablo Roig Garcés, de quienes he obtenido muchísimos conocimientos y que me han ayudado de muchas maneras en mi desarrollo y formación. Gracias a Sally Santiago por ser tan gran soporte para mí en tiempos tan difíciles, en especial el tortuoso lapso de tiempo que pasé sin beca. Agradezco muchísimo a mis sinodales Aurore Courtoy, David Farnández, Iván Heredia, Omar Miranda y Genaro Toledo por su paciencia y ayuda durante mi periodo de formación, en especial en el periodo de revisión de la tesis y el seminario. Agradezco especialmente todas las ayudas recibidas por parte de Eduard de la Cruz. También le doy las gracias al jefe del Departamento, Máximo López (bis) por apoyarme con recursos para que pudiera mostrar mi trabajo en los Rencontres de Moriond.

Debo agradecer también a José Salazar (Chepe), Blanca Cañas (la doctora), Lenin Tostado, Gerardo H. Tomé, Alfonso Jaimes, Jhovanny Mejía, Idalia Sandoval, Bryan Larios y todos los que no logro recordar (y que se quedarán sin ser mencionados por la prisa con la que tuve que escribir esta tesis y no porque no merezcan ser mencionados); es decir, a todos mis amigos... Y Gus (Gustavo Gutiérrez) por tantas discusiones tan fructíferas en el entendimiento del cómo funciona la naturaleza. Especiales agradecimientos a Penguin-San por acompañarnos durante las discusiones de física y otros temas. Gracias, también, a la naturaleza por ser cuántica, debido a que sus fluctuaciones cuánticas a lo largo de la historia del universo me han permitido llegar tan lejos. También, como becario, estoy obligado a dar las gracias a Conacyt por la beca de doctorado, cuyo sistema y personal tienen grandísimas deficiencias que necesitan arreglo urgentemente. Agradezco el apoyo para la obtención de grado por parte del Centro (Cinvestav), así como los apoyos para Curso Especializado con el que asistí a la CERN Latin American School of High Energy Physics y asistencia a Congreso que parcialmente cubrió gastos para asistir a los Rencontres de Moriond.

# Abstract

It is not known how to obtain exactly transition amplitudes in Quantum Field Theory, so that perturbative approximation is the best we can do. Since the fundamental theory of strong interactions (Quantum Chromodynamics) does not admit a perturbative approach for processes with energies near or below the proton mass one needs to see how to overcome this difficulty. What common sense dictates is to construct a theory that admits a perturbative description of phenomena at the energy ranges in which the fundamental theory fails to be perturbative. In this thesis we present the computation of some processes that cannot be obtained through an expansion of the strong coupling intensity, since nothing would guarantee the convergence of such expansion, this is why we use an Effective Field Theory whose main characteristic is chiral invariance.

On the other hand, since the 1970's, the Standard Model of fundamental particles interactions has been so successful that it seems very implausible to see phenomena resulting from interactions beyond this theory (with the exception of everything related to neutrino masses) at leading order in perturbation theory. One then relies on precision tests, for which a very good understanding of the interactions is needed. Since many experiments on the High Intensity Frontier begin to take data in the very near future, in order to improve their power of prediction all possible background in the search for Beyond Standard Model effects must be very well understood.

The observables we have computed are contributions within the Standard Model to processes that either need to have a very well described background or that are not very well understood. Two processes are two different  $\tau$  lepton decays as background for processes with lepton number and lepton flavor violation such as  $\tau^- \rightarrow \pi^+ \ell^- \ell^- \nu_\tau$  and background for second class currents for the decay  $\tau \rightarrow \pi \eta \nu_\tau$ . Another process we computed was the  $B^\pm \rightarrow P^\pm \ell^+ \ell^-$ , where  $P$  is either a pion or a Kaon. This was computed in an effort to try to understand the apparent lepton non-universality mea-

sured at LHCb, where we obtained a rather large CP asymmetry for the  $\pi$  channel. Finally, we computed the pseudoscalar light-by-light contribution to the anomalous magnetic moment of the muon, giving a more robust analysis of the theoretical uncertainties and compatible with previous results.

# Resumen

Actualmente no es posible obtener amplitudes de manera exacta usando Teoría Cuántica de Campos, así que lo mejor que se puede hacer es una aproximación perturbativa. Ya que la teoría fundamental de las interacciones fuertes (la Cromodinámica Cuántica) no admite una descripción perturbativa para procesos a escalas energéticas cerca o por debajo de la masa del protón se vuelve necesario buscar la forma sortear esta dificultad. Lo que marca la intuición es construir una teoría que permita una descripción perturbativa de fenómenos a escalas de energía en que la teoría fundamental no puede dar tal descripción. En este sentido, se presenta el cálculo de varios procesos que no pueden ser obtenidos por medio de algunos procesos que no pueden ser obtenidos por medio de una expansión de la intensidad de interacciones fuertes, ya que no se puede garantizar la convergencia de dicha expansión, por lo que hemos recurrido al uso de una Teoría de Campos Efectiva cuya principal característica es la invarianza quiral.

Por otro lado, desde la década de 1970, el Modelo Estándar de partículas fundamentales ha tenido tanto éxito que parece muy poco probable encontrar algún fenómeno resultante de interacciones más allá de esta teoría (con excepción de todo lo relacionado con las masas de los neutrinos) a primer orden en teoría de perturbaciones. Entonces se vuelve necesario recurrir a pruebas de precisión, para lo cual se necesita un buen entendimiento de las interacciones. Ya que muchos experimentos en la frontera de la alta intensidad empezarán a tomar datos en un futuro muy cercano, para mejorar su poder predictivo es necesario entender muy bien cualquier posible ruido de fondo en la búsqueda de efectos más allá del Modelo Estándar.

Las observables que calculamos son contribuciones del Modelo Estándar a proceso que, ya sea necesitan tener un ruido de fondo muy bien descrito o no están bien entendidos. Dos de los procesos son dos diferentes decaimientos del leptón  $\tau$  como ruido de fondo para procesos con violación de número y sabor leptónico como  $\tau^- \rightarrow$



$\pi^+\ell^-\ell^-\nu_\tau$  y el ruido para el descubrimiento de corrientes de segunda clase en el decaimiento  $\tau \rightarrow \pi\eta\nu_\tau$ . Otro proceso que calculamos fue el decaimiento  $B^\pm \rightarrow P^\pm\ell^+\ell^-$ , donde  $P = \pi, K$ . Esto se calculó como un esfuerzo en tratar de entender la aparente violación de universalidad leptónica medida por LHCb, donde obtuvimos una asimetría de CP grande para el canal del  $\pi$ . Finalmente, calculamos la contribución principal de la dispersión hadrónica luz por luz la momento magnético anómalo del muón, dando un análisis más robusto de la incertidumbre teórica y que es compatible con resultados previos.



# Chapter 1

## Theoretical Framework

### 1.1 Introduction

In this chapter we show the theoretical framework within quantum field theory needed to compute the observables in subsequent chapters. First we give an introduction using a historical approach of the development of the Standard Model of elementary particles. In section 1.3 we develop Chiral Perturbation Theory from the chiral symmetry of the QCD Lagrangian and its Spontaneous Symmetry Breaking into vectorial  $SU(3)$ . In section 1.4 we give the main features of Resonance Chiral Theory, laying the foundations to further enlarge the theory to higher chiral orders.

### 1.2 Standard Model

#### 1.2.1 Introduction

In this section we give a summary of the historical development of the now called Standard Model of elementary particles. In subsection 1.2.2 we follow the development of the electroweak unification starting with the chiral symmetry of neutrinos up to the Glashow-Weinberg-Salam model of electroweak interactions. In subsection 1.2.3 we show the historical development of strong interactions until Ne'eman and Gell-Mann's extension of the isospin model, then introduce the concept of partons and the color charge to conclude with the Lagrangian of strong interactions. In subsection 1.2.4 we briefly summarize  $CP$  violation, the Kobayashi-Maskawa scenario and the dates in which the remaining particles of the Standard Model were discovered. In subsection 1.2.5 we discuss the limitations of QCD and define the concept of Effective Field Theory.

### 1.2.2 Electroweak Standard Model

Since Ernest Rutherford's discovery in 1909 that protons were confined in atomic nuclei positively charged [1], the question of how same charge particles can remain together without repelling each other arose. After James Chadwick's discovery of the neutron in 1932 [2], a *strong* interaction was hypothesized to explain why the nucleus (a bounded state of protons and neutrons, as suggested by Dmitri Ivanenko [3]) remain bounded, where Werner Heisenberg proposed the isospin model [4]. The next year, Enrico Fermi proposed the existence of a new interaction to explain  $\beta$ -decay [5], later known as *weak* interaction, where the interacting term came as products of fermion currents

$$\mathcal{L}_{Fermi} = g \left( \bar{\psi}_p \gamma^\mu \psi_n \right) \left( \bar{\psi}_e \gamma_\mu \psi_\nu \right), \quad (1.1)$$

where the subindex in each fermion operator  $\psi$  denotes the physical field referred to. It also was the first attempt of including the neutrino as a fundamental field. With this and except for gravity, all now known fundamental interactions had been postulated by then at a quantum level.

Fermi's theory of beta decay only included the proton, neutron (both within the isospin model), electron and neutrino fields as fundamental, but could be very easily extended to include muons (earlier called  $\mu$ -mesons), heavier baryons and spin zero fields. Also the particles with strangeness (earlier called  $\eta$ -charge) were able to be allocated in a Fermi-like theory.

Since the Fermi theory was not able to predict some nuclear processes involving  $\Delta J = 0$  between nuclei, a generalization of Fermi's theory was sought by considering all linearly independent combinations of Dirac matrices [6], namely  $\mathbf{1}$ ,  $\gamma_5$ ,  $\gamma_\mu$ ,  $\gamma_\mu \gamma_5$  and  $\sigma_{\mu\nu} = \frac{i}{2}[\gamma_\mu, \gamma_\nu]$ , where the squared brackets denotes the commutator. The Lagrangian reads

$$\mathcal{L} = g_i \left( \bar{\psi}_1 \Gamma_i \psi_2 \right) \left( \bar{\psi}_3 \Gamma_i \psi_4 \right), \quad i = S, P, V, A, T, \quad (1.2)$$

where  $\Gamma_i$  is one of the linearly independent operators and  $S, P, V, A, T$  stands for scalar, pseudoscalar, vector, axial-vector and tensor operators respectively. This implied an effort to experimentally determine the coupling constants  $g_i$ .

The fact that Tsung-Dao Lee and Chen-Ning Yang [7] suggested the non conservation of parity in  $\beta$ -decays (or  $P$  violation, confirmed experimentally some months later in  $\text{Co}^{60}$  decays [8] and in  $\pi^+ \rightarrow \mu^+ + \nu$  and  $\mu \rightarrow e + 2\nu$  decays [9]), lead Abdus Salam to propose what was known as chirality or  $\gamma_5$  invariance [10]. The argument is as follows: since the neutrino is a massless field, no term mixing chiralities exists in its free Lagrangian, this means that under the substitution  $\nu \rightarrow -\gamma_5\nu$  the free Lagrangian remains invariant<sup>1</sup>. Then, it is postulated that no neutrino interaction can generate a self-mass term, *i.e.*, all interactions must respect this non-mixing chirality of neutrino terms. The way of fulfilling this idea is by imposing the  $\gamma_5$  invariance to all the neutrino interaction terms. Therefore, to the lepton<sup>2</sup> current in eq.(1.2) must be added a term violating parity conservation. This is accomplished by taking

$$\mathcal{L} = g_i (\bar{\psi}_1 \Gamma_i \psi_2) [\bar{e} \Gamma_i (1 - \gamma_5) \nu], \quad (1.3)$$

where this added term must have the same coupling constant due to the same  $\gamma_5$  invariance. Since  $\frac{1}{2}(1 - \gamma_5)$  is a projection operator, meaning that it is hermitian and that any power of such operator gives the same operator, it can be noticed that the lepton accompanying the neutrino in the current must have a determined chirality depending on the operator  $\Gamma_i$  in the interaction. In other words, the lepton current can be divided into scalar, pseudoscalar and tensor operators for an electron with opposite chirality than that of the neutrino and into vector and axial for same chiralities.

---

<sup>1</sup>Our convention of  $\gamma_5$  is different from the convention followed in the cited papers, this is

$$\gamma_5^{us} = -i\gamma_5^{\text{Salam}},$$

where  $\gamma_5^{\text{us}}$  is our convention which is used in this thesis and  $\gamma_5^{\text{Salam}}$  is the convention used in the cited papers. However, the expressions in all cited papers will be adjusted to fit our convention.

<sup>2</sup>A lepton is defined as a field which undergoes no strong interactions at tree level.

By making use of a Fierz identity for the muon decay, one is able to detect that two kind of processes may take place. One occurs with the emission of two neutrinos and the other with the emission of a neutrino and an antineutrino

$$\mathcal{L}_A = g_i (\bar{\mu} \Gamma_i e) [\bar{\nu} \Gamma_i (1 - \gamma_5) \nu], \quad i = V, A, \quad (1.4a)$$

$$\mathcal{L}_B = g_i (\bar{\mu} \Gamma_i e^*) [\nu^T \gamma_0 \Gamma_i (1 - \gamma_5) \nu], \quad i = S, P, T. \quad (1.4b)$$

In the previous equations we can see that  $\gamma_5$  invariance would require  $g_V = -g_A$  for vector and pseudo-vector interactions, while it requires  $g_S = g_P$  for scalar and pseudoscalar interactions. These two interaction Lagrangian densities give different values for the Michel parameter<sup>3</sup>  $\rho$ , namely  $\rho_A = \frac{3}{4}$  and  $\rho_B = 0$  for  $\mathcal{L}_A$  and  $\mathcal{L}_B$  respectively. This was the first prediction of the correct  $\rho$  value for the  $\mu$  decay, however the coupling constants in the generalized Fermi theory were not known and there was doubt if all operators would really contribute.

At the moment there was not any certainty in which operators participated in the interactions since some experiments gave inconsistent results among them. However, Richard Feynman [12] showed an inconformity in describing the fundamental fermion field as a four component spinor, arguing that for a spin 0 field (Klein-Gordon) we only need a wave function of one component and therefore the electron field should be described by a two component field. Thus, he showed that the fermion field in the Dirac equation  $(i\partial\!\!\!/ - \mathcal{A})\psi = m\psi$  can be substituted by another fermion field

$$\psi = \frac{1}{m}(i\partial\!\!\!/ - \mathcal{A} + m)\chi, \quad (1.5)$$

---

<sup>3</sup>The Michel parameters [11] in a three body decay give the energy and angular distributions,  $\frac{d^2\Gamma}{x^2 dx d\cos(\theta)}$ , where  $x = E/E_{max}$  is the normalized energy of a final state particle and  $\theta$  is the angle between two final state particle three-momenta, which in the case of muon decay can be given as a function of the angle between the final state charged lepton three-momentum and the spin of the decaying muon.

which, as in the case of the Klein-Gordon field, is described by a second order equation

$$(i\not{\partial} - \not{A})^2\chi = \left[ (i\partial^\mu - A^\mu)(i\partial_\mu - A_\mu) - \frac{1}{2}\sigma^{\mu\nu}F_{\mu\nu} \right] = m^2\chi. \quad (1.6)$$

However,  $\chi$  is still a four component spinor, but since  $\sigma^{\mu\nu}$  commutes with  $\gamma_5$  the  $\chi$  field can be splitted into  $\gamma_5$  eigenvectors of two components, which are  $\gamma_5\chi_- = -\chi_-$  and  $\gamma_5\chi_+ = \chi_+$ . The connection with the original spinor field is given by

$$\chi_{\mp} = \frac{1}{2}(1 \mp \gamma_5)\psi. \quad (1.7)$$

Feynman also states that it is these two-component fields that should be treated as fundamental, and therefore, it is this field which should enter the weak current interaction. Then, connecting with  $\gamma_5$  invariance Feynman postulates that all fermions in the generalized Fermi theory should be inserted with the *left* projection operator. This can only lead to currents of the type  $V - A$ , for the rest must vanish and, therefore, having a universal weak coupling strength. Worth is to mention that also Robert Marshak and George Sudarshan in an independent work [13] showed that a universal Fermi interaction together with  $\gamma_5$  invariance can be achieved only through  $V - A$  currents.

Great success was achieved with this description of weak interactions, however one problem still remained: the Fermi interaction was not renormalizable. A more fundamental approach could be achieved by merging both, weak and electromagnetic interactions in a more general theory. This idea has its origin in some shared characteristics:

- Both forces affect equally all forms of hadrons and charged leptons.
- Both are vector in character.
- Both (individually) possess universal couplings.

Since universality and vector character are features of a gauge theory, these shared

characteristics suggested that weak forces, just as electromagnetic interactions arise from a gauge principle.

In an attempt to give a more fundamental description and a unification of all particle interactions (except for gravity), Julian Schwinger suggested [14] that all intrinsic degrees of freedom are dynamically exhibited by specific interactions, each interaction with its characteristic symmetry properties, and that the final effect of interactions with successively lower symmetry is to produce a spectrum of physically different particles from an initially degenerate state. He also postulated that only unitary groups should be taken into account for internal symmetries, and by assuming a  $SO(6)$  group for describing electromagnetic, weak and strong interactions he made the suggestion that electroweak interactions among leptons could be unified in a *local*  $SO(3)$  subgroup. The fact that the electromagnetic field must be a realization of this symmetry assumed to be a component of a  $SO(3)$  iso-triplet encouraged Schwinger to say that the other two components of the iso-triplet responsible for weak interactions must also be vector particles.

This was the first step towards a consistent perturbative description of electroweak interactions, however there was a problem with Schwinger's theory and all theories that tried to unify electromagnetic and weak interactions as a group  $SU(2)$ . By describing the Maxwell field as the component of such iso-triplet one ends up with an interaction term with charged fermions that *do not* conserve parity, which is undeniably incompatible with electrodynamics. The electromagnetic current found in this way is

$$j_\mu^3 = \bar{\psi} \gamma_\mu O_3 \psi = \bar{\psi} \gamma_\mu \frac{1}{4} [t_3 - \gamma_5(t_3^2 - 2)] \psi, \quad (1.8)$$

where  $t_i$  are generators of the  $SO(3)$  electroweak subgroup.

This was first noticed by Sheldon Glashow [15], who introduced the concept of partial symmetries. This concept states that there might be a symmetry under which



part of the Lagrangian density is invariant; more precisely, it is only the mass terms in the Lagrangian density that break the conservation under a determined symmetry transformation. Then, by proving that an  $SO(3)$  subgroup give the inconsistent results shown in eq (1.8), he arrives to the conclusion that the only way to give a consistent description of a unified theory of electroweak interactions is by adding more vector fields, where the minimal amount of added fields in this case is 1. This field is assumed to be a singlet under the  $SO(3)$  group, meaning that it does not interact with neither the charged weak fields nor with the neutral field. He then introduced the lepton current associated with this boson

$$j_\mu^B = \bar{\psi}\gamma_\mu S\psi = \bar{\psi}\gamma_\mu \frac{3}{4} \left[ t_3 + \gamma_5(t_3^2 - \frac{2}{3}) \right] \psi. \quad (1.9)$$

Thus, it is found that the operator  $S$  satisfies the following relations

$$[\vec{O}, S] = 0, \quad (1.10a)$$

$$O_1^2 + O_2^2 + O_3^2 + S^2 = \mathbf{1}, \quad (1.10b)$$

$$Q := t_3 = O_3 + S \quad (1.10c)$$

Now, eq. (1.10a) means that the field  $B$  associated with the operator  $S$  must be a scalar under  $SO(3)$  transformations, so that  $j_\mu^B$  must remain invariant under such transformations as expected. However, eq. (1.10b) shows that  $S$  is not independent from all the other operators. So, one can find a  $SO(2)$  symmetry to the  $B$  field and the  $W_3$  field associated with the  $O_3$  operator in their own *neutral bosons space*.

$$\begin{pmatrix} A \\ Z \end{pmatrix} = \begin{pmatrix} \cos \theta_W & \sin \theta_W \\ -\sin \theta_W & \cos \theta_W \end{pmatrix} \begin{pmatrix} W_3 \\ B \end{pmatrix}. \quad (1.11)$$

The relation of eq. (1.10c) give a relation resembling the Nakano–Nishijima–Gell-Mann (NNG) relation [16, 17, 18].

This rotation between the neutral fields ends up with one that is associated with a

parity conserving current, and therefore is identified as the Maxwell field. The mixing of these fields was first done to permit an arbitrary choice of strengths of the triplet and singlet interactions, which would explain the difference between the weak and electromagnetic coupling strengths.

Glashow had successfully unified the electromagnetic and weak interactions by relying on a  $SO(3) \otimes U(1)$  symmetry of the interaction Lagrangian density and the kinetic free Lagrangian density, but, as Glashow said, the mass terms do not preserve any weak interaction symmetry. This was a problem, since by adding a mass term to the free Lagrangian density for the intermediate weak bosons one has to add the term  $k^\mu k^\nu / m^2 (k^2 - m^2)$  to the propagator of the gauge bosons.

$$D_W(k) = \frac{-g_{\mu\nu}}{k^2 - m_W^2} \rightarrow -\frac{g_{\mu\nu} + \frac{k_\mu k_\nu}{m_W^2}}{k^2 - m_W^2} \quad (1.12)$$

The problem with this term in the propagator is that it made loop corrections not renormalizable. So, the problem of having a perturbatively consistent theory was not solved yet.

The solution thought was that the masses of the vector bosons should be generated dynamically. It was proven by Abdus Salam and John Clive Ward [19] that a non-zero vacuum expectation value of a scalar field interacting with other fields may give mass to the latter, however with a non-zero vacuum expectation value breaking a global symmetry scalar bosons with zero mass must come about. This was first conjectured [20] and the proven by Jeffrey Goldstone, Abdus Salam and Steven Weinberg [21] by using the Källén-Lehmann spectral representation. Then, François Englert and Robert H. Brout [22] and Peter Higgs [23] showed that one may be able to *exorcise out* the Goldstone bosons by choosing a gauge in which this scalar particles could be transformed into the longitudinal mode of some of the gauge bosons propagators.

Then, Weinberg [24] gave the correct description of the complete unification of

electromagnetic and weak interactions with the correct mechanism that gives mass to all fields in the model (except for neutrinos and the photon fields) by taking the weak interaction symmetry to be  $SU(2)_L \otimes U(1)_Y$  with a spontaneous symmetry breaking (SSB) of the  $SU(2)$  symmetry given by the introduction of a weak doublet of scalar fields  $\phi = \begin{pmatrix} \phi^- \\ \phi^0 \end{pmatrix}$  that interact with the gauge bosons. Weinberg's Lagrangian is given by

$$\begin{aligned} \mathcal{L} = & -\frac{1}{4}W_{\mu\nu}W^{\mu\nu} - \frac{1}{4}B_{\mu\nu}B^{\mu\nu} - \bar{R}\not{D}_R R - \bar{L}\not{D}_L L - \frac{1}{2}|(\partial - D_L)\phi|^2 \\ & - Y(\bar{L}\phi R + \bar{R}\phi^\dagger L) - \mu^2\phi^\dagger\phi + \frac{\lambda}{24}|\phi^\dagger\phi|^2, \quad (1.13) \end{aligned}$$

where  $W_{\mu\nu} = \partial_\mu W_\nu - \partial_\nu W_\mu + g\varepsilon_{abc}W_\mu^a W_\nu^b$ ,  $B_{\mu\nu} = \partial_\mu B_\nu - \partial_\nu B_\mu$ ,  $L = \frac{1}{2}(1 - \gamma_5) \begin{pmatrix} \nu_e \\ e \end{pmatrix}$ ,  $R = \frac{1}{2}(1 + \gamma_5)e$ ,  $D_R = \partial - igB$ ,  $D_L = \partial + ig\vec{t} \cdot \vec{W} - i\frac{1}{2}g'B$  and  $t$  are the generators of the  $W$  fields algebra. As in the case of the  $K$  meson isospin doublet (see subsection 1.2.4 below), both scalar form a charge doublet, so that the  $\bar{\phi}^0$  should be differentiated from the  $\phi^0$ , therefore three of the states are absorbed (two charged and one neutral), the remaining one is called the Brout-Englert-Higgs (BEH) boson.

There are completely analogous terms to those consisting of the electron field and a neutrino with same leptonic charge as the electron field but for muon and the neutrino related to muon production. This neutrino was found to be different to the one produced in beta decay by Leon Lederman, Melvin Schwartz and Jack Steinberger at Brookhaven [25], which was used by Weinberg to construct a  $\mu$   $SU(2)_L$  doublet analogous to the electron one.

Salam also arrived at these expressions from a more general symmetry principle by stating that it should be  $SU(2)_L \otimes U(1)_Y$  the symmetry that unifies electromagnetic and weak gauge bosons[26, 27]. Following Higgs' idea of *gauging out* the Goldstone bosons, Salam showed that with the most general model for a scalar autointeracting

field the symmetry breaking would then absorb three of the scalar fields into the  $SU(2)$  gauge bosons in order to give them mass. The Glashow angle now played the role of choosing the interaction strength  $g \sin \theta_W$  such that one can find the appropriate massless vector boson to identify it as the Maxwell field. He also noticed that since the theory before spontaneous symmetry breaking is renormalizable, it should keep like this after breaking the symmetry, solving thus the problem of finding a perturbative description of a unified theory of electromagnetic and weak interactions later known as the Standard Model of Electroweak interactions. But the problem still remained for particles that undergo strong interactions, which led Glashow to the conclusion that this was just an academic exercise if this model is not general enough so that it also applies for fields that can interact via strong interactions. So, a theory of strong interactions should be developed which was compatible with the electroweak Standard Model.

### 1.2.3 Strong Interactions and Quantum Chromodynamics

The eta-charge, now known as strangeness, in particle physics was conjectured by Toshiyuki Nakano, Kazuhiko Nishijima [16, 17] and Murray Gell-Mann [18] where they proposed the relation known as the Nakano–Nishijima–Gell-Mann (NNG) relation

$$Q = I_3 + \frac{1}{2}(B + S), \quad (1.14)$$

where  $Q$  is the electric charge of the particle,  $I_3$  is the isotopic spin third component,  $B$  is the baryon number and  $S$  is the strangeness (or  $\eta$ -charge) of the particle.

The NNG relation used to identify new baryons had been very successful describing newfound particles, which seemed like there should be a more fundamental principle behind the relation. This was the thought followed by Soichi Sakata [28], making an analogy with the coincidence between the mass number of atomic nuclei and its spin: when the spin is integer the mass number is even, while if the spin is half-integer the mass number should be odd. After Chadwick’s discovery of the neutron, this puzzle

was solved by developing the isotopic spin model. So this even-odd rule for nuclei was explained by means of the sub-atomic particles. Therefore, Sakata showed us that, in analogy with the even-odd rule the NNG relation may be explained if one assumes the existence of new particles from which all newfound hadrons should be made of<sup>4</sup>. He also stresses out the lack of interaction laws between such fundamental particles.

Then, Yuval Ne'eman [29] and Murray Gell-Mann [30] proposed both in 1961 a  $SU(3)$  symmetry between the currents generated with the fundamental Sakata fields (also called sakatons) called the eight-fold way or symmetric Sakata model. This was intended as an extension to  $SU(2)$  isospin to include strangeness. These sakatons were  $p$ ,  $n$  and  $\Lambda$ , with the same quantum numbers as the proton, neutron and  $\Lambda$  baryon. The statement was that sakatons should interact via a massive vector boson, and that these interactions should be invariant under the  $SU(3)$  symmetry. Now, for weak currents of sakatons, one should arrive at the expressions

$$J_\mu = i\bar{p}\gamma_\mu(1 - \gamma_5)n + i\bar{p}\gamma_\mu(1 - \gamma_5)\Lambda, \quad (1.15)$$

which can be achieved by taking the combinations of currents

$$J_\mu = i\bar{b}\gamma_\mu\frac{1}{2}(\lambda_1 + i\lambda_2 + \lambda_4 + i\lambda_5)b, \quad (1.16)$$

where  $b = \begin{pmatrix} p \\ n \\ \Lambda \end{pmatrix}$  is the baryon triplet and  $\lambda_i$  is the  $i$ th Gell-Mann matrix. It should be noticed the lack of  $(\lambda_6 \pm i\lambda_7)$  currents that would couple the  $n$  and  $\Lambda$  fields giving rise Flavor Changing Neutral Current (FCNC) which were not seen by the time this theory was postulated. (The combinations of  $\lambda_3$  and  $\lambda_8$  will give the diagonal charged current.)

---

<sup>4</sup>In his paper, Sakata gives credit for the first composite model to Markov (Rep. Acad. Sci. USSR, 1955), although we were not able to track down such paper.

By making use of the  $V - A$  model of weak interactions [12, 13] and the eight-fold way model, Nicola Cabibbo found in 1963 that weak currents of strongly interacting fields should have some additional symmetry[31]; those belonging to a  $SU(3)$  representation of the symmetric Sakata model with  $\Delta S = 0$ , and  $\Delta Q = 1$ ,  $j_\mu^{(0)}$ , should be related to currents  $j_\mu^{(1)}$  with  $\Delta S = \Delta Q = 1$ , the former with selection rule  $\Delta I = 1$ , the latter with  $\Delta I = \frac{1}{2}$ . In this model, strangeness changing weak current should be blended with  $\Delta S = 0$  currents since a  $SU(3)$  transformation would necessarily mix  $N$  and  $\Lambda$  in the general weak current for sakatons in eq. (1.16). Thus, the total weak current for strongly interacting fields is

$$J_\mu = aj_\mu^{(0)} + bj_\mu^{(1)}, \quad (1.17)$$

where  $a$  and  $b$  should have some universality constraint stemming from the mix between strangeness conserving and changing currents. A naive universality relation would be  $a = b = 1$ ; however this might give rise to uncoupled currents. Therefore, Cabibbo assumes a weaker form of universality, namely that  $J_\mu$  should be of ‘unit-length’, *i.e.*,  $a^2 + b^2 = 1$ . Hence,  $J_\mu$  can be re-expressed as<sup>5</sup>

$$J_\mu = \cos(\theta)j_\mu^{(0)} + \sin(\theta)j_\mu^{(1)}. \quad (1.18)$$

This weaker form of universality solved several experimental discrepancies between different processes that implied the use of weak currents of strongly interacting particles.

The symmetric Sakata model was successful explaining the octuplet allocation of pseudoscalar mesons, however it failed in constructing the nucleons from the sakatons.

---

<sup>5</sup>A similar expression following the same universality statement was obtained first by Gell-Mann and Lèvy[32], but using the relation

$$\bar{p}\gamma_\mu(n + \epsilon\Lambda)(1 + \epsilon^2)^{-\frac{1}{2}}$$

which is a very good approximation to the expression given by Cabibbo when expanded near  $\theta \approx 0$ . Gell-Mann and Lèvy take  $\epsilon^2 \sim 0.06$ , which gives  $\sin \theta \sim \epsilon \approx 0.26$  a very good approximation.

This is why in 1964 George Zweig [33] proposed some fundamental fields called aces instead of sakatons. (Gell-Mann made the same proposition also in 1964, calling the fundamental fields quarks [34].) These fields should have fractional electric charge with spin 1/2 and should form a triplet of the same  $SU(3)$  symmetry

$$q = \begin{pmatrix} u^{\frac{2}{3}} \\ d^{-\frac{1}{3}} \\ s^{-\frac{1}{3}} \end{pmatrix}, \quad (1.19)$$

where the super-index denotes the electric charge of each ace or quark in units of the proton electric charge  $e$ . Since quarks have spin 1/2, baryons should be composed from an odd number of quarks and mesons by an even number of quarks. Then, by taking products of quarks and anti-quarks baryons should be represented as the product of three quark fields since  $(qqq) = \mathbf{1} \oplus \mathbf{8} \oplus \mathbf{8} \oplus \mathbf{10}$ , and mesons as the product of a quark and an anti-quark since  $(q\bar{q}) = \mathbf{1} \oplus \mathbf{8}$ , where  $\mathbf{1}$ ,  $\mathbf{8}$  and  $\mathbf{10}$  are one, eight and ten dimensional representations of  $SU(3)$ . For example, the meson octet would be composed by  $\pi$ ,  $K$  and  $\eta$  mesons. Further more, a 27 dimensional representation that must be considered in the symmetric Sakata model not found experimentally should be absent in the quark model.

Unsatisfied with having a fractional electric charge (in units of the proton charge), Moo-Young Han and Yoichiro Nambu postulated that the fundamental fields should be each one a triplet of an  $SU(3)$  symmetry [35] which was not the one proposed by Ne'eman. These should be (as Schwinger had proposed [14]) a local gauge group, leading to eight neutral vector bosons, named *gluons*, that mediate the strong interactions and does not mix the triplets. Since it was derived as a subgroup of an embedding  $SU(6)$  symmetry, the fundamental triplets should interact through other  $SU(3)$  symmetry which, as the weak interaction does, would blend the three interacting triplets. In this case, similar to the Salam  $SU(6)$  model where the correct symmetry was the subgroup  $SU(2) \otimes U(1)$ , the correct group seemed to be the one with the eight vector bosons which did not mix the triplets of fermions. This necessarily implies a new

charge for these fields. This new charge would explain the fact that the newfound  $\Omega^-$  had  $S = -3$  and  $J = \frac{3}{2}$  [37] and the existence of the  $\Delta^{++}$  baryon with same spin as the  $\Omega^-$  but with isospin  $I = \frac{3}{2}$  found in 1951 [38], since without this extra charge, the Pauli exclusion principle would forbid the existence of these baryons. The fact the  $\Delta^{++}$  and  $\Omega^-$  baryons should be each made of three identical fermions made the fractional charge model of quarks the most viable model discarding the integer charge model since in the Han-Nambu model it is not possible to reproduce the  $\Omega^-$ .

However, quarks were still fundamental fields understood mainly as mathematical objects with no physical evidence of their existence. Then, in 1968 James D. Bjorken studying the inelastic lepton-proton scattering, demonstrated that in the limit of infinite energy transfer the structure functions upon which the cross section depends remain finite [39], furthermore, he showed that these structure functions can be expressed as dependent of the ratio of the virtual photon four-momentum squared  $q^2$  and the initial energy of the proton  $P_0$ , which is taken as constant as one takes the limit  $q_0, P_0 \rightarrow \infty$ . So, the structure functions have no dependence on the scaling of the energy of the process, meaning that no structure can be discerned as the energy of the process is augmented. Since by reducing the de Broglie wavelength one has a higher energy state, by taking a higher center of mass energy one will have a greater resolution scale, probing smaller space regions. Therefore, the electrons scattered must be interacting with free point-like particles inside the proton.

With only three kind of quarks, the theory of weak interactions seemed to have some problems with experimental selection rules of weak processes. By using the Pauli-Villars regularization technique, a cut-off energy remarkably small of  $\Lambda \sim 3$  GeV seemed necessary. Also there should be amplitudes with  $\Delta S = 2$  contributing to  $K$  decays that were not observed since a  $\bar{s}\gamma^\mu d$  hadronic neutral current was not prohibited by the electroweak model with three quarks. In 1970, Sheldon Glashow, Jean (Ιωάννης) Iliopoulos and Luciano Maiani proposed the existence of a new quark [40] in analogy with the electroweak model for four leptons ( $e, \nu_e, \mu$  and  $\nu_\mu$ ) leading



to the hadronic current

$$J_\mu^H = \bar{q} C_H \gamma_\mu (1 - \gamma_5) q, \quad (1.20)$$

where  $q = (c, u, d, s)$ , and in order for  $J_\mu^H$  to be unit charge current,  $C_H$  must have the following form

$$C_H = \begin{pmatrix} \mathbf{0} & U \\ \mathbf{0} & \mathbf{0} \end{pmatrix}, \quad (1.21)$$

where  $\mathbf{0}$  is a  $2 \times 2$  zero matrix and  $U$  is a matrix that must be unitary in analogy with the leptonic weak current. By rephasing the quark fields one gets the most general form

$$U = \begin{pmatrix} -\sin \theta & \cos \theta \\ \cos \theta & \sin \theta \end{pmatrix}. \quad (1.22)$$

This proposed quark should have  $Q = \frac{2}{3}$ ,  $Y = -\frac{2}{3}$  and, since it must be an isospin singlet, a new quantum number called *charm*<sup>6</sup>. In this model, the weak symmetry group for quarks  $SU(2) \otimes U(1)$  is a partial symmetry (in the sense of Glashow's paper [15]) of the gluonic  $SU(3)$  symmetry of strong interactions. With this, Glashow, Iliopoulos and Maiani gave the term complementary to the Glashow-Salam-Weinberg theory of leptonic weak interactions, completing the theory of weak interactions. On the other hand, the 3 GeV cut needed without the charm quark can be qualitatively explained with the model including the charm quark since  $\Lambda \sim m_c$ , where  $m_c$  is the charm quark mass, this is, the charm quark becomes an active degree of freedom of the theory only above these energies.

In 1972, William Bardeen, Harald Fritzsch and Murray Gell-Mann proposed that the quarks should have the extra charge mentioned above and coined the term *color* for this new quantum number. Each quark should exist with one of three possible color values, 'say red, white and blue' [42]. Also, all physical states and all observable quantities must be color  $SU(3)$  singlets. This theory solved immediately the tension

---

<sup>6</sup> Although Glashow had already proposed a charm number to describe a different quantum number, Iliopoulos affirmed that the name *charm* used to baptize the new quark was thought of as a good-luck charm for them so that it would exist and be detected soon [41].

between the quark model predicted  $BR(\pi^0 \rightarrow \gamma\gamma)$  and the experimental result that gave a factor 9 greater. Eventually, this became the standard theory for strong interactions that has been used since then to describe all strong interactions.

### 1.2.4 Standard Model of Particle Physics

There was still one problem with the Lagrangian of elementary particles. As Nakano and Nishijima showed, the  $K^0$  must be different from  $\bar{K}^0$ , then, they must belong to two different isospin doublets and have different strangeness. These states can be expressed as a linear combination of  $CP$  symmetry eigenstates,  $K_1$  and  $K_2$  which makes them identifiable by their decay products into pions. Since the  $\pi$  has intrinsic parity  $P = -1$  and  $C = 1$ , the  $K_1$  being  $CP$  even should decay into two pions and the  $K_2$  into three, so each state would have definite mass and lifetime. Since one has a longer lifetime, they were called  $K$  short ( $K_S = K_1$ ) and  $K$  long ( $K_L = K_2$ ). However, as it was shown by James Christenson, James Cronin, Val Logsdon Fitch and René Turlay<sup>7</sup> at the Alternating Gradient Synchrotron at Brookhaven [43], there were a small probability that  $K_L$  would decay in the channel that  $K_S$  does, giving a clear indication of  $CP$  symmetry violation.

Within the models of electroweak and strong interactions there is no  $CP$  violation, meaning that something should be still missing. In 1972, Makoto Kobayashi and Toshihide Maskawa suggested four possible scenarios within the electroweak model to include  $CP$  violation [44]. One of them was the scenario where two more quarks should be included in a left  $SU(2)_L$  doublet and two right handed singlets, so that including these extra quarks the matrix in eq. (1.21) must now have a non-factorisable phase responsible for  $CP$  violation.

Then, in 1977 the E288 experimental team lead by Leon Lederman at Fermilab discovered a meson resonance which should have a different content of quarks [45].

---

<sup>7</sup>Only Cronin and Fitch were awarded with the Physics Nobel Prize despite the four of them contributed to the same work.

This new quark was named *bottom* and should be part of a new  $SU(2)_L$  doublet. two years earlier, Martin Lewis Perl discovered the tau lepton with the SLAC-LBL group [47]. The top quark, which was the left weak doublet partner of the bottom was discovered in 1995 in the CDF and DØ experiments at Fermilab [46]. The tau neutrino was discovered in the year 2000 by the DONUT collaboration [48] completing the Kobayashi-Maskawa frame (also generalized to leptons).

Thus, the Standard Model (SM) is the theory that describes the interactions between charged leptons, neutrinos, quarks and gauge bosons, which are the mediators of the electromagnetic, weak and strong interactions. The internal symmetry that generates these gauge bosons is thus  $SU(3)_C \otimes SU(2)_L \otimes U(1)_Y$ , with a weak gauge spontaneous symmetry breaking field experimentally discovered in 2012 at the Large Hadron Collider experiments [49]. The electroweak Standard Model (EWSM) Lagrangian is thus expressed as the sum of four terms,

$$\mathcal{L}_{EWSM} = \mathcal{L}_{fermion} + \mathcal{L}_{gauge} + \mathcal{L}_\phi + \mathcal{L}_{Yukawa}, \quad (1.23)$$

the kinetic term of the fermions and their interaction with the gauge bosons ( $\mathcal{L}_{fermion}$ ), the pure gauge bosons contributions (kinetic and interactions) ( $\mathcal{L}_{gauge}$ ), the BEH field and interaction with gauge bosons ( $\mathcal{L}_\phi$ ) and the Yukawa interaction between the BEH field and the SM fermions ( $\mathcal{L}_{Yukawa}$ ). Each term is invariant under the  $SU(2)_L \otimes U(1)_Y$  symmetry group. Since the electroweak symmetry is non abelian, there will be an interaction term among gauge bosons that is included in

$$\mathcal{L}_{gauge} = W_{\mu\nu}^a W_a^{\mu\nu} + B_{\mu\nu} B^{\mu\nu}, \quad (1.24)$$

where  $W_a^{\mu\nu} = (\partial^\mu W_a^\nu - \partial^\nu W_a^\mu - gf_{abc}W_b^\mu W_c^\nu)$ ,  $f$  is the structure constant of the group and  $B_{\mu\nu} = \partial_\mu B_\nu - \partial_\nu B_\mu$ . The correct interaction term of the gauge bosons with the fermions is obtained by the standard method of making an arbitrary local gauge

transformation, obtaining thus

$$\mathcal{L}_{fermion} = \sum_i \bar{\chi}_L^i (i\not{\partial} - g\tau_a W_a - g' \not{B}) \chi_L^i, \quad (1.25)$$

where  $i$  runs through all the lepton flavors  $l$  and quark doublets  $q$ ,  $\tau_a$  are the  $2 \times 2$  Pauli matrices and  $g$  and  $g'$  are the  $SU(2)_L$  and  $U(1)_Y$  coupling constants respectively. As Weinberg showed us [24], the correct representation of the SM fermions is through doublets defined as

$$\chi_L^l = \begin{pmatrix} \psi_\ell \\ \nu_\ell \end{pmatrix}_L \quad \text{and} \quad \chi_L^q = \begin{pmatrix} \psi_u \\ \psi_d \end{pmatrix}_L, \quad (1.26)$$

where  $\psi_u$  is an up-type quark and  $\psi_d$  its corresponding down-type quark ( $u \leftrightarrow d, c \leftrightarrow s, t \leftrightarrow b$ ). The subindex  $L$  denotes the left projection of the fermion field, *i.e.*,  $\psi_L = \frac{1}{2}(1 - \gamma_5)\psi$ .

The scalar fields term in the Lagrangian is obtained in an analogous way to the fermion case, and reads

$$\mathcal{L}_\phi = (D^\mu \phi)^\dagger D_\mu \phi - V(\phi) \quad (1.27)$$

The field  $\phi$  is realized as a  $SU(2)_L$  doublet  $\phi = \begin{pmatrix} \phi^+ \\ \phi^0 \end{pmatrix} = \frac{1}{\sqrt{2}} \begin{pmatrix} \phi_1 - i\phi_2 \\ \phi_3 - i\phi_4 \end{pmatrix}$ , where the  $\phi_i$  are all real fields. The covariant derivative is  $D^\mu = \partial^\mu + ig\frac{\tau_a}{2}W_a^\mu - ig'\frac{B^\mu}{2}$ . The  $V(\phi)$  term is made of the self-interacting terms of the introduced scalar fields

$$V(\phi) = \mu^2 |\phi|^2 + \frac{\lambda}{4!} |\phi|^4, \quad (1.28)$$

where by taking  $\mu^2 < 0$  one obtains a non-zero vacuum expectation value  $vev$ , which gives the SSB of the electroweak symmetry into the electromagnetic symmetry  $SU(2)_L \otimes U(1)_Y \rightarrow U(1)_{EM}$ . As was said above, three of the scalar fields are absorbed by the weak bosons as longitudinal component of these fields leaving only one physical scalar field, the BEH field. Since the remaining scalar has non-zero  $vev$ , we

can take the covariant derivative term acting on the  $vev$  of the BEH field to get

$$\begin{aligned}
\left| \left( ig \frac{\tau_a}{2} W_a^\mu + i \frac{g}{2} B^\mu \right) \begin{pmatrix} 0 \\ v \end{pmatrix} \right|^2 &= \frac{1}{8} v^2 g^2 (W_1^\mu W_{1\mu} + W_2^\mu W_{2\mu}) \\
&\quad + \frac{1}{8} v^2 (g' B_\mu - g W_{3\mu})(g' B^\mu - g W_3^\mu) \\
&= \left( \frac{1}{2} v g \right)^2 W^+_\mu W^{-\mu} + \frac{1}{8} v^2 (W_\mu^3, B_\mu) \begin{pmatrix} g^2 & -gg' \\ -gg' & g'^2 \end{pmatrix} \begin{pmatrix} W^{3\mu} \\ B^\mu \end{pmatrix},
\end{aligned} \tag{1.29}$$

where  $W^\pm = \frac{1}{\sqrt{2}} (W^1 \mp iW^2)$ . All terms in the previous expression are mass terms since they are quadratic forms of the fields, to see this we need to express  $W^3$  and  $B$  in a base which has no terms of the kind  $W^3 \cdot B$ , this is, no gauge boson mix terms. In order to obtain these mass eigenstates a rotation of the neutral current bosons  $W^3$  and  $B$  is done

$$\begin{pmatrix} A_\mu \\ Z_\mu \end{pmatrix} = \begin{pmatrix} \cos \theta_W & \sin \theta_W \\ -\sin \theta_W & \cos \theta_W \end{pmatrix} \begin{pmatrix} B_\mu \\ W_\mu^3 \end{pmatrix}. \tag{1.30}$$

To obtain such states one finds that the relation  $\tan \theta_W = g/g'$  must be fulfilled so that one of the states remains massless. This field is identified, as Glashow, Weinberg and Salam did, as the Maxwell (electromagnetic) field. Therefore, the mass of the other fields are  $m_W = vg/2$  and  $m_Z = \frac{1}{2}\sqrt{g^2 + g'^2}$ . With this, the interaction of the fermions with the electroweak gauge bosons can be written as follows

$$\mathcal{L}_{CC} = \frac{g}{2\sqrt{2}} W_\mu^- \left\{ \sum_\ell \bar{\psi}_\ell \gamma^\mu (1 - \gamma_5) \psi_{\nu_\ell} + \sum_i \bar{\psi}_{di} \gamma^\mu (1 - \gamma_5) \psi_{ui} \right\} + \text{h.c.}, \tag{1.31}$$

where  $\ell$  runs on the lepton number,  $i$  on the quark family and h.c. is the hermitian conjugate of the previous terms. For the weak neutral one has

$$\begin{aligned}
\mathcal{L}_{NC} = \frac{g}{2 \cos \theta_W} Z_\mu \sum_{i,\ell} \left[ \bar{\psi}_{u_{iL}} \gamma^\mu \psi_{u_{iL}} - \bar{\psi}_{d_{iL}} \gamma^\mu \psi_{d_{iL}} + \bar{\psi}_{\nu_{\ell L}} \gamma^\mu \psi_{\nu_{\ell L}} - \bar{\psi}_{\ell L} \gamma^\mu \psi_{\ell L} \right. \\
\left. - 2 \sin^2 \theta_W \left( \frac{2}{3} \bar{\psi}_{u_i} \gamma^\mu \psi_{u_i} - \frac{1}{3} \bar{\psi}_{d_i} \gamma^\mu \psi_{d_i} - \bar{\psi}_\ell \gamma^\mu \psi_\ell \right) \right]. \tag{1.32}
\end{aligned}$$

The remaining piece of the Lagrangian is the interactions of the fermions with the scalar doublet introduced to induce the SSB of the EW gauge. This is given by

$$\mathcal{L}_{Yukawa} = - \sum_{j,k} \left[ \Gamma_{jk}^u \bar{\chi}_L^{qj} \tilde{\phi} (\psi_{u_k})_R + \Gamma_{jk}^d \bar{\chi}_L^{qj} \phi (\psi_{d_k})_R + \Gamma_{jk}^l \bar{\chi}_L^{lj} \phi (\psi_{l_k})_R + \text{h.c.} \right], \quad (1.33)$$

where a different convention to that of Weinberg has been used for the terms with right-handed up-type quarks, here  $\tilde{\phi} = i\tau_2 \phi^\dagger$ . Since in the broken EW gauge the scalar doublet field is just  $\phi = \begin{pmatrix} 0 \\ v + H \end{pmatrix}$ , one finds for the  $u$  type quarks (for the down-type quarks and the leptons a completely analogous procedure follows) the Lagrangian density

$$\mathcal{L}_{Yuk} = \sum_{jk} \left( \bar{\psi}_{u_j} \right)_L Y_{jk}^u (\psi_{u_k})_R + \text{h.c.}, \quad (1.34)$$

where the matrix  $Y$  is in general neither hermitian, nor diagonal. Since the physical states are the mass eigenstates we need to express the previous equation in terms of mass eigenstates. Since any matrix can be diagonalized by multiplying it by the left and by the right with the adequate unitary matrices, the left and right fermion fields are transformed with unitary matrices mixing all the  $u$  type quarks. Therefore, by making  $\psi_{uL} \rightarrow A_L^u \psi_{uL}$  and  $\psi_{uR} \rightarrow A_R^u \psi_{uR}$  one finds

$$A_L^{u\dagger} M^u A_R^u = \begin{pmatrix} m_u & 0 & 0 \\ 0 & m_c & 0 \\ 0 & 0 & m_t \end{pmatrix}. \quad (1.35)$$

There are analogous terms for the down-type quarks and for the charged leptons. Notice that since in the SM neutrinos are assumed massless, there is no such term for these fields. If one forbids the right-handed projection of the neutrino field, no mass term can be generated in eq. (1.33).

It is trivially verified that this unitary transformation does not affect the neutral

currents of the standard model, since they include a  $\bar{\psi}_X$  and a  $\psi_X$  factor and all SM operators are diagonal in flavor space<sup>8</sup>. However, charged currents are modified by these rotations since they involve fields of two different kinds (e.g.  $\bar{\psi}_e$  and  $\psi_{\nu_e}$ ). These matrices will give one unitary matrix in the interaction Lagrangian since the product of two unitary matrices is a unitary matrix. The parameters of this unitary matrix can be diminished by rephasing the fermion fields. So, for the hadronic charged currents one has

$$\mathcal{L}_{cc}^q = \frac{g}{2\sqrt{2}} W_\mu^+ \left\{ (\bar{d}, \bar{s}, \bar{b}) V_{CKM}^\dagger \gamma^\mu (1 - \gamma_5) \begin{pmatrix} u \\ c \\ t \end{pmatrix} \right\} + \text{h.c.} , \quad (1.36)$$

where  $V_{CKM}$  is the unitary matrix generated by the transformation done to obtain the mass eigenstates of the quarks, which after rephasing the quark fields has three real parameters and one phase. This phase is the responsible for  $CP$  violation which was detected in  $K^0$  and  $\bar{K}^0$  decays. Notice that since no right-handed projection of the neutrino field exist in the SM, no Yukawa term can be generated for these fields, so that there is no special unitary transformation in the flavor space of the neutrinos to diagonalize a  $Y$  matrix as in eq. (1.34). Therefore, when one transforms the charged lepton fields, the same unitary transformation can be applied to the neutrino field so that the resulting matrix is the identity. Thus, no mixing matrix is obtained for leptons as it is for quarks.

### 1.2.5 QCD, limitations and Effective Field Theories

Quantum Chromodynamics (QCD), as was previously stated, is described by a local  $SU(3)$  symmetry, with a Lagrangian density

$$\mathcal{L}_{QCD} = \mathcal{L}_{quark} + \mathcal{L}_{gluon}, \quad (1.37)$$

---

<sup>8</sup>Flavor is defined as the attributes that distinguish quarks and charged leptons, namely the  $u$ ,  $d$ ,  $s$ ,  $c$ ,  $b$ ,  $t$  for quarks and the  $e$ ,  $\mu$  and  $\tau$  for leptons.

where  $\mathcal{L}_{gluon}$  is analogous to  $\mathcal{L}_{gauge}$  in eq. (1.23). It can be obtained by taking the first term in eq. (1.24) and changing the weak ( $W$ ) for the gluon ( $G$ ) fields and by taking  $f$  as the structure constant of  $SU(3)$ . The quark term is

$$\mathcal{L}_{quark} = \sum_r \bar{q}_{r\alpha} i \not{D}_\beta^\alpha q_r^\beta, \quad (1.38)$$

where  $r$  runs over all flavors and  $\alpha$  and  $\beta$  are color indices. The covariant derivative is found in an analogous way to the EW case, and reads

$$D_{\alpha\beta}^\mu = \delta_{\alpha\beta} \partial^\mu + i \frac{g_s}{2} G_i^\mu \lambda_{\alpha\beta}^i, \quad (1.39)$$

where  $g_s$  is the strong interaction constant,  $\delta$  is the Kronecker  $\delta$  and  $\lambda$  are the generators of the  $su(3)$  algebra. With these all the terms of the SM have been described.

As has been said, all the processes computed within the SM give outstandingly precise predictions of a very vast amount of processes. This relies on the renormalizability of the whole model, as a result the coupling constant varies with the energy of the studied process. Nevertheless, when QCD is renormalized it is found that the coupling constant diverges as one approaches the 1 GeV energy region (where the energy at which it diverges is called the Landau pole) and the theory, despite being correct becomes not perturbative. Since there is no way known of computing exactly amplitudes in Quantum Field Theory, QCD is of no use without a perturbative description of phenomena. A way to overcome this problem is using an Effective Field Theory (EFT) which relies on some symmetries of the original QCD Lagrangian.

There are two kinds of EFTs [50], namely

- Decoupling EFTs: These are characterized by an energy scale  $\Lambda$  below which only light degrees of freedom are left and the heavy ones are frozen and so can



be *integrated out*. Such theories are described by Lagrangians such as

$$\mathcal{L}_{eff} = \mathcal{L}_{d \leq 4} + \sum_{d > 4} \frac{1}{\Lambda^{d-4}} \sum_{i_d} g_{i_d} \mathcal{O}_{i_d}, \quad (1.40)$$

where  $d$  is the dimension of the operator  $\mathcal{O}$  in natural units.

- Non-decoupling EFTs: The transition from fundamental to effective theory is made through a phase transition via a SSB generating Goldstone bosons. Processes with different number of Goldstone bosons relate  $d \leq 4$  with  $d > 4$  terms, so that one cannot distinguish between these terms.

### 1.2.6 Chiral symmetry of the QCD Lagrangian density

One needs to rely on EFTs to compute processes involving strong interaction at energies near or below the Landau pole, so the question of how to construct such EFT comes about. First of all, as previously stated a symmetry of the underlying theory is needed to develop the EFT. By reviewing the historical development of the theories of strong interactions in the previous section it becomes appealing to rely on some kind of flavor symmetry due to its great success in the Symmetric Sakata model and the quark model in describing phenomena below the lepton-nucleon inelastic scattering,  $\sim 1$  GeV, where the structure of the nucleons becomes apparent. Since we are interested in regions around and below the Landau pole, the QCD Lagrangian density (1.37) can be split into light and heavy degrees of freedom,

$$\mathcal{L}_{quark} = \sum_{q=u,d,s} \bar{q} i \not{D} q + \mathcal{L}_{heavy \text{ quarks}} = \sum_{q=u,d,s} (\bar{q}_L i \not{D} q_L + \bar{q}_R i \not{D} q_R) + \mathcal{L}_{heavy \text{ quarks}}. \quad (1.41)$$

By separating the light quarks in their right and left chiral parts it becomes apparent a  $SU(3)_L \otimes SU(3)_R \otimes U(1)_V \otimes U(1)_A$  symmetry. The  $U(1)_V$  is just the baryon number conservation and the  $U(1)_A$  is not conserved at the quantum level. The remaining  $G = SU(3)_L \otimes SU(3)_R$  is called the chiral group. Notice that only the weak symmetry  $SU(2)_L$  is explicitly broken by including a mass term for the quarks, meaning that

QCD does not forbid a mass term for the quarks. This mass term breaks explicitly the chiral group symmetry. However one can exclude the quark masses and include them later in a consistent way.

The Noether currents of the chiral symmetry  $G$  are  $\bar{q}\gamma^\mu\frac{1}{2}(1\pm\gamma_5)\frac{\lambda^a}{2}q$  for right and left quark currents, with which one can construct the vector and axial quark currents

$$V^{\mu,\alpha} = R^{\mu,\alpha} + L^{\mu,\alpha} = \bar{q}\gamma^\mu\frac{\lambda^a}{2}q, \quad (1.42a)$$

$$A^{\mu,\alpha} = R^{\mu,\alpha} - L^{\mu,\alpha} = \bar{q}\gamma^\mu\gamma_5\frac{\lambda^a}{2}q. \quad (1.42b)$$

In this way one arrives to a  $SU(3)_V \otimes SU(3)_A$  symmetry. This basis is chosen since theoretically and experimentally there is evidence that the chiral group must be spontaneously broken to  $SU(3)_V$  [50, 51]. A way to see this is with a similar argument to that used by Scherer [52]: If  $SU(3)_V \otimes SU(3)_A$  was the symmetry of the meson spectrum, to the lowest lying octet of vector mesons would correspond an octet of opposite parity and with same spin and mass, *i.e.*, the lowest lying axial-vector mesons. The fact that empirically both octets have significantly different masses (eg.  $m_{a_1} \approx 2m_\rho$ ) means that  $SU(3)_A$  must be broken. Since the Lagrangian density is invariant under the complete chiral group, this means that  $SU(3)_A$  must be spontaneously broken, generating eight Goldstone bosons. Since the Goldstone bosons inherit the properties of the generators of the broken symmetry, they must be pseudoscalar, with zero baryon number.

### 1.2.7 Inclusion of external currents

Aiming to construct a theory which can be obtained through a generating functional, external currents are introduced in order to generate Green functions of quark currents. These external fields do not propagate and can be introduced by extending the

Lagrangian density adding quark currents coupled to some external hermitian fields

$$\mathcal{L} = \mathcal{L}_{quarks} + \bar{q}\gamma^\mu(v_\mu + a_\mu\gamma_5)q - \bar{q}(s - ip\gamma_5)q. \quad (1.43)$$

The major advantages of this method is that one can include the electroweak gauge boson interactions by making

$$r_\mu = v_\mu + a_\mu = -eQA_\mu^{ext} \quad (1.44a)$$

$$\ell_\mu = v_\mu - a_\mu = -eQA_\mu^{ext} - \frac{e}{\sqrt{2}\sin\theta_W}(W_\mu^{ext,+}T_+) \quad (1.44b)$$

Where  $Q = \frac{1}{3}\text{diag}(2, -1, -1)$ ,  $(T_+)_{ij} = \delta_{i1}(\delta_{j2}V_{ud} + \delta_{j3}V_{us})$  and  $V_{ij}$  are the Cabibbo-Kobayashi-Maskawa mixing matrix. Also, one can include (as previously said) the quark masses by means of the scalar external current, this is, symmetry breaking terms can be introduced by means of the external fields. If one takes  $v = a = p = 0$  and

$$s = \begin{pmatrix} m_u & 0 & 0 \\ 0 & m_d & 0 \\ 0 & 0 & m_s \end{pmatrix}, \quad (1.45)$$

one can include symmetry breaking terms in a manifestly chiral invariant way. The inclusion of external fields promotes chiral symmetry to a local one. The transformation rules of the external fields are

$$r^\mu \rightarrow g_R r^\mu g_R^\dagger + ig_R \partial^\mu g_R^\dagger, \quad (1.46a)$$

$$\ell^\mu \rightarrow g_L \ell^\mu g_L^\dagger + ig_L \partial^\mu g_L^\dagger, \quad (1.46b)$$

$$s + ip \rightarrow g_R(s + ip)g_L^\dagger \quad (1.46c)$$

$$s - ip \rightarrow g_L(s - ip)g_R^\dagger. \quad (1.46d)$$

Since now chiral symmetry has been promoted to a local one the derivative of the quark fields must be modified in order to keep the chiral invariance also, by introducing a field strength tensor that transforms like  $F_x^{\mu\nu} \rightarrow g_x F_x^{\mu\nu} g_x^\dagger$  for  $x = r, \ell$ . Thus,

one has

$$F_R^{\mu\nu} = \partial^\mu r^\nu - \partial^\nu r^\mu - i[r^\mu, r^\nu], \quad (1.47a)$$

$$F_L^{\mu\nu} = \partial^\mu \ell^\nu - \partial^\nu \ell^\mu - i[\ell^\mu, \ell^\nu]. \quad (1.47b)$$

We have now all the elements needed to construct the EFT. The covariant derivative will be defined in the next section once the symmetry has been realized.

## 1.3 Chiral Perturbation Theory

### 1.3.1 Construction of Chiral Perturbation Theory ( $\chi$ PT)

Weinberg showed that in order to get consistent results, one must use a non-linear realization of the chiral symmetry, so that soft pions cannot be emitted from virtual particles in hard scattering processes [53]. A year later, Callan, Coleman, Wess and Zumino developed a generalized way to construct non-linear realizations of arbitrary symmetry groups [54]. For the chiral symmetry  $G$ , SSB generates eight pseudoscalar bosons which are identified with the lightest octet of pseudoscalar mesons. So, these are the fundamental fields upon which the theory is constructed. These meson fields are collected in a unitary matrix using the Gell-Mann matrices

$$U(\varphi) = \exp(i\sqrt{2}\lambda_a\varphi^a/F), \quad \lambda_a\varphi^a = \begin{pmatrix} \frac{\pi^0}{\sqrt{2}} + \frac{\eta_8}{\sqrt{6}} & \pi^+ & K^+ \\ \pi^- & -\frac{\pi^0}{\sqrt{2}} + \frac{\eta_8}{\sqrt{6}} & K^0 \\ K^- & \bar{K}^0 & -2\frac{\eta_8}{\sqrt{6}} \end{pmatrix}, \quad (1.48)$$

where  $\lambda_a$  are the eight Gell-Mann matrices and  $F_\pi = F[1 + \mathcal{O}(m_q)] \sim 92.4$  MeV is the pion decay constant. As stated at the end of the previous subsection, the promotion of  $G$  to a local symmetry lead us to define a covariant derivative, given by

$$D_\mu U = \partial_\mu U - ir_\mu U + iU\ell_\mu, \quad (1.49)$$

and which transforms as  $D_\mu U \xrightarrow{G} g_R D_\mu U g_L^{-1}$ .

Since one is able to construct a mass term for quarks stemming from the interaction with a constant external scalar current, a mass term of the mesons might arise by making them interact with an external scalar current  $\chi = 2B(s + ip)$ , the constant  $B$  is related to the quark condensate  $\langle 0 | \bar{q}q | 0 \rangle = -F^2 B [1 + \mathcal{O}(m_q)]$ . The lowest dimension operator which is also chiral invariant that can be constructed is

$$\mathcal{L}_{mass} = \frac{F^2}{4} \langle \chi U^\dagger + \chi^\dagger U \rangle, \quad (1.50)$$

where  $\langle A \rangle = \text{Tr}(A)$ . One can obtain, by expanding the  $U$  fields to  $\mathcal{O}(\varphi^2)$  the relations

$$M_{\pi^+}^2 = 2mB \quad (1.51a)$$

$$M_{\pi^0}^2 = 2mB + \mathcal{O} \left[ \frac{(m_u - m_d)^2}{m_s - m} \right] \quad (1.51b)$$

$$M_{K^+}^2 = (m_u + m_s)B \quad (1.51c)$$

$$M_{K^0}^2 = (m_d + m_s)B \quad (1.51d)$$

$$M_{\eta_8}^2 = \frac{2}{3}(m + 2m_s)B + \mathcal{O} \left[ \frac{(m_u - m_d)^2}{m_s - m} \right], \quad (1.51e)$$

where  $m = \frac{1}{2}(m_u + m_d)$ . A relation between quark and pseudoscalar meson masses has been now constructed.

Given the realization of the chiral symmetry through the matrix  $U(\varphi)$ , the general Lagrangian density can be constructed by means of this matrix and the external fields. However, the question of how to do this in a systematic way including only the relevant terms comes naturally. An answer to this question is given by Weinberg [55], where he conjectures that, since Quantum Field Theory by itself has no content beyond analyticity, unitarity, cluster decomposition<sup>9</sup> and symmetry, by giving all the

---

<sup>9</sup>In a QFT having the property of Cluster decomposition means that the vacuum-to-vacuum expectation value of a product of many operators defined in two disjoint small space-time regions  $A$

terms consistent with the assumed symmetry principles one gets the most general Lagrangian density, and calculating the matrix elements with this Lagrangian density to any given order in perturbation theory the result is the most general possible S-matrix consistent with analyticity, perturbative unitarity, cluster decomposition and the assumed symmetry principles. This, however, is of no use by itself since an infinite number of terms should be considered in the Lagrangian to give the most general S-matrix.

Nevertheless, one can rescale the moments and the meson masses, taking  $p \rightarrow tp$  and  $m_P \rightarrow tm_P$ . Then, the chiral dimension is defined as

$$\mathcal{M}(tp_i, tm_P) = t^D \mathcal{M}(p_i, m_P) \quad (1.52)$$

with

$$D = 2 + \sum_{n=1}^{\infty} (d-2)N_d + 2N_L, \quad (1.53)$$

where  $N_L$  is the number of loops,  $N_d$  is the number of vertices formed from interactions with  $d$  derivatives. Thus, by stating that amplitudes with the lowest chiral counting  $D$  will give a dominant contribution and with aid of Weinberg's conjecture one is able to construct, order by order in chiral expansion the most general Lagrangian consistent with all features of QFT and chiral symmetry.

The elements to construct Chiral Perturbation Theory are shown with their chiral order

$$U = \mathcal{O}(p^0), \quad D_\mu U = \mathcal{O}(p), \quad r_\mu, l_\mu = \mathcal{O}(p), \quad F_{\mu\nu}^{L/R} = \mathcal{O}(p^2), \quad \chi = \mathcal{O}(p^2). \quad (1.54)$$

Now, the most general chiral invariant Lagrangian density that can be constructed

---

and  $B$  with very large separation equals the vacuum-to vacuum expectation value of the products of operators in region  $A$  times the vacuum-to-vacuum expectation value of the product of operators in region  $B$ , meaning that the effects of operators in  $A$  cannot affect what happens in  $B$  and vice-versa.

at lowest chiral order  $D = 2$  is

$$\boxed{\mathcal{L}_2 = \frac{F^2}{4} \text{Tr}[D_\mu U (D^\mu U)^\dagger] + \frac{F^2}{4} \text{Tr}(\chi U^\dagger + U \chi^\dagger)}. \quad (1.55)$$

In the same way as it was done for  $\mathcal{L}_2$ , the chiral Lagrangian of order  $D = 4$  can be constructed using the operators which give the most general lagrangian at this order invariant under  $G$ . However, its associated functional will only give Green functions with even powers of Goldstone bosons (even intrinsic parity sector). From the  $U(1)_A$  anomaly one can construct the most general Lagrangian with chiral dimension  $D = 4$  that will give Green functions that involve only odd numbers of Goldstone bosons (odd intrinsic parity sector), this is the Wess-Zumino-Witten Lagrangian  $\mathcal{L}_{WZW}$  [56]. The corresponding functional is given by

$$Z[U, l, r] = -\frac{iN_C}{240\pi^2} \int_{M^5} d^5x \varepsilon^{ijklm} \langle \Sigma_i^L \Sigma_j^L \Sigma_k^L \Sigma_l^L \Sigma_m^L \rangle \\ - \frac{iN_C}{48\pi^2} \int d^4x \varepsilon_{\mu\nu\rho\sigma} (W(U, l, r)^{\mu\nu\rho\sigma} - W(\mathbf{1}, l, r)^{\mu\nu\rho\sigma}) \quad (1.56)$$

where  $\langle A \rangle = \text{Tr}(A)$ ,

$$W(U, l, r)_{\mu\nu\rho\sigma} = \langle U \ell_\mu \ell_\nu \ell_\rho U^\dagger r_\sigma + \frac{1}{4} U \ell_\mu U^\dagger r_\nu U \ell_\rho U^\dagger r_\sigma + i U \partial_\mu \ell_\nu \ell_\rho U^\dagger r_\sigma \\ + i \partial_\mu r_\nu U \ell_\rho U^\dagger r_\sigma - i \Sigma_\mu^L \ell_\nu U^\dagger r_\rho U \ell_\sigma + \Sigma_\mu^L U^\dagger \partial_\nu r_\rho U \ell_\sigma \\ - \Sigma_\mu^L \Sigma_\nu^L U^\dagger r_\rho U \ell_\sigma + \Sigma_\mu^L \ell_\nu \partial_\rho \ell_\sigma + \Sigma_\mu^L \partial_\nu \ell_\rho \ell_\sigma - i \Sigma_\mu^L \ell_\nu \ell_\rho \ell_\sigma \\ + \frac{1}{2} \Sigma_\mu^L \ell_\nu \Sigma_\rho^L \ell_\sigma - i \Sigma_\mu^L \Sigma_\nu^L \Sigma_\rho^L \ell_\sigma - (L \leftrightarrow R) \rangle, \quad (1.57)$$

and  $\Sigma_\mu^L = U^\dagger \partial_\mu U$ ,  $\Sigma_\mu^R = U \partial_\mu U^\dagger$ .

## 1.4 Resonance Chiral Theory ( $\text{R}\chi\text{T}$ )

Chiral Perturbation Theory [55, 57, 58, 59, 60] has been very successful, however it has some serious limitations. Chiral Perturbation Theory is only reliable at energies

below  $\sim 500$  MeV. Above this energy, other meson resonances become active degrees of freedom. So, to push Chiral Perturbation Theory to higher energies one needs to include resonances as active degrees of freedom. The way to do this is relying not only in chiral symmetry, but in  $1/N_C$  expansion [61] from which Chiral Perturbation Theory can be obtained with the restoration of the  $U(1)_A$  anomaly [62]. Therefore,  $1/N_C$  is completely compatible with chiral symmetry. It has been shown that at low energies ( $< 500$  MeV)  $\mathcal{L}_4$  is completely described by the lowest-lying resonance exchange [63], so that the most general Lagrangian will be given by  $\mathcal{L}_2 + \mathcal{L}_{WZW}$  and all possible contributions from resonance exchange. For the sake of simplicity, a different representation is used for the realization of the Goldstone bosons, namely the matrix  $u$  defined by the relation  $U = u^2$ , and which transforms under  $G$  as

$$u(\varphi) \xrightarrow{G} g_R u(\varphi) h(\varphi)^\dagger = h(\varphi) u(\varphi) g_L^\dagger, \quad (1.58)$$

where  $h \in SU(3)_V$ . Also, the fields  $\chi_\pm$  and  $f_\pm^{\mu\nu}$  are used instead of  $\chi$  and  $F_{R/L}^{\mu\nu}$ , which are defined as

$$f_\pm^{\mu\nu} = u F_L^{\mu\nu} u^\dagger \pm u^\dagger F_R^{\mu\nu} u, \quad (1.59a)$$

$$\chi_\pm = u^\dagger \chi u^\dagger \pm u \chi^\dagger u \quad (1.59b)$$

Depending on the nature of the resonance field one can write down a chiral invariant interaction term to couple the resonance field with the chiral objects in eq. (1.54) [63, 64]. The realization of  $G$  on resonance fields in the antisymmetric tensor formalism is given by

$$R_{\mu\nu} \xrightarrow{G} h(\varphi) R_{\mu\nu} h(\varphi)^\dagger, \quad (1.60)$$

with covariant derivative

$$\nabla_\mu R = \partial_\mu R + [\Gamma_\mu, R], \quad (1.61)$$

$$\Gamma_\mu = \frac{1}{2} [u^\dagger (\partial_\mu - i r_\mu) u + u (\partial_\mu - i \ell_\mu) u^\dagger]. \quad (1.62)$$



By using the covariant derivative, the kinetic Lagrangian density can now be written down

$$\mathcal{L}_{kin}(R_{\mu\nu}) = -\frac{1}{2}\langle\nabla^\lambda R_{\lambda\mu}\nabla_\nu R^{\nu\mu} - \frac{1}{2}M_R^2 R_{\mu\nu}R^{\mu\nu}\rangle. \quad (1.63)$$

Similarly, one can write the interaction terms at the leading  $1/N_C$  order in the following way

$$\mathcal{L}_2(V) = \frac{F_V}{2\sqrt{2}}\langle V_{\mu\nu}f_+^{\mu\nu}\rangle + \frac{iG_V}{\sqrt{2}}\langle V_{\mu\nu}u^\mu u^\nu\rangle, \quad (1.64a)$$

$$\mathcal{L}_2(A) = \frac{F_A}{2\sqrt{2}}\langle A_{\mu\nu}f_-^{\mu\nu}\rangle, \quad (1.64b)$$

$$\mathcal{L}_2(S) = c_d\langle Su_\mu u^\mu\rangle + c_m\langle S\chi_+\rangle, \quad (1.64c)$$

$$\mathcal{L}_2(P) = id_m\langle P\chi_-\rangle. \quad (1.64d)$$

In this antisymmetric tensor formalism, the propagator of the meson resonance is given by the following relation [63]

$$\begin{aligned} \langle 0|T\{R_{\mu\nu}R_{\rho\sigma}\}|0\rangle = i\frac{1}{M_R^2}\int\frac{d^4ke^{-ik(x-y)}}{(2\pi)^4(M_R^2-k^2-i\epsilon)}\Big[ & M^2g_{\mu\rho}g_{\nu\sigma} + g_{\mu\rho}k_\nu k_\sigma \\ & - g_{\mu\sigma}k_\nu k_\rho - k^2g_{\mu\rho}g_{\nu\sigma} - (\mu\leftrightarrow\nu)\Big], \end{aligned} \quad (1.65)$$

corresponding to the normalization

$$\langle 0|R_{\mu\nu}|R,p\rangle = i\frac{1}{M_R}[p_\mu\epsilon_\nu(p) - p_\nu\epsilon_\mu(p)]. \quad (1.66)$$

The final ingredient of this theory is a match between QCD and this EFT. The way to do this is by taking the Green function due to some process and then take the high energy limit, by comparing this result with the exact QCD prediction one is able to find constrictions in some of the coupling constants. This reduces significantly the number of free parameters in the theory.

## Chapter 2

# Lepton universality violation and new sources of CP violation

### 2.1 Introduction

In the Standard Model (SM) all lepton currents couple with the same strength to the weak gauge bosons. This is an interesting property of the SM, since any deviation from this prediction would be a clear signal of Beyond SM (BSM) interactions, therefore all processes in which a false signal of lepton universality might come about due to kinematical or dynamical effects stemming from processes unrelated to real lepton universality. Since High Intensity Frontier experiments such as Belle-II will be able to look up for processes with lepton universality violation it becomes mandatory to know well all the processes that may be an important background for the observation of BSM effects in these decays.

In order to get reliable predictions one needs to have under control all the hadronic effects in the processes studied. Therefore, predictions of background in the search for BSM effects have to be taken into account so that this background can improve the predictions of the experiments. Some experimental results show effects that cannot be explained by means of the SM (although, not so far from the SM  $\lesssim 4\sigma$ ). Therefore, the hadronic effects on such processes need to be under very good control.

Since CP asymmetries have been measured recently in  $B$  meson decays, the hadronic effects in these decays need to be very well studied to increase the precision in the search for BSM phenomena and determine whether these measurements agree with the Standard Model or needs an explanation from effects beyond it. Therefore, the hadronic parts in potential background in the search for BSM phenomena

needs to be very well known and under control.

## 2.2 The $\tau^- \rightarrow \pi^- \nu_\tau \ell^+ \ell^-$ decays as background for BSM interactions

### 2.2.1 Introduction

Being the heaviest of the leptons, the  $\tau$  offers an opportunity that neither of its lighter copies can provide, namely the chance to study in a clean way the production of hadrons. This unique characteristic makes it appealing for the analysis of all kind of processes involving leptons and hadrons. One such effect is Lepton Flavor Violation (LFV) and Lepton Number Violation (LNV), as well as lepton universality violation in semileptonic  $\tau$  decays [65]. Lepton universality violation has been suggested in heavy meson decays including  $\tau$ 's in the final state, therefore to ensure that no spurious violation of this universality is been measured due to  $\tau$  decays one has to compute the possible configurations in which such effect could be induced. The hadronic effects in the studies of LFV in  $\tau$  decays has to be very well understood, since otherwise this effects can give different orders of magnitude[66, 67, 68, 69]

In this section we study the  $\tau^- \rightarrow \pi^- \nu_\tau \ell^+ \ell^-$  decays, where the effective vertex  $W\gamma^*\pi$  comes about. The presence of this effective vertex makes the processes appealing for one more reason, which is the fixing of parameters for the pion transition form factor by means of a weak isospin rotation (and its correction factor) where both gauge bosons are off-shell and also with high virtualities. In subsection 2.2.2 we show the different contributions to the total amplitude and their complete expressions. In subsection 2.2.3 the expressions of the form factors are given, as well as the Feynman diagrams needed for computing them. In subsection 2.2.4 we show the form in which the couplings in the form factors are constrained through the short distance behavior of QCD. In subsection 2.2.5 we show our results for the total branching fraction and the different contributions for the process, also, the invariant mass spectra for both

decay channels are shown.

### 2.2.2 Matrix element of the process

The study of the  $\tau^-(p_\tau) \rightarrow \pi^-(p)\nu_\tau(q)\ell^+(p_+)\ell^-(p_-)$  decays is a generalization of the computation in ref [70], where the photon is real. The opportunity of studying this process for virtual photon turns out to be interesting since by a weak isospin rotation one can determine the principal contribution to the Hadronic Light by Light scattering to the anomalous magnetic moment of the muon  $a_\mu$ . So, if this process could be measured one could in principle constraint the relevant parameters for the relevant contribution in the  $a_\mu$ . It also opens the possibility of studying lepton universality violation by comparing the  $\gamma^* \rightarrow e^+e^-$  and  $\gamma^* \rightarrow \mu^+\mu^-$  processes. Also, a Majorana neutrino exchange could give place to LNV for which this process might become a very important background [71].

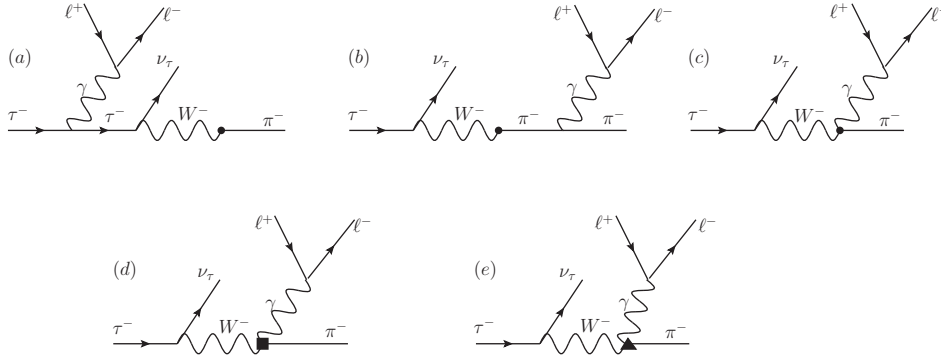


Figure 2.1: Feynman diagrams of the different contributions to the  $\tau \rightarrow \pi\ell^+\ell^-\nu_\tau$  decay. Diagrams (a) to (c) give the model independent contribution, while the structure dependent has been separated into two contributions for convenience

To describe this process we need to compute the relevant amplitude, which is given by one model independent and two structure dependent contributions. The model independent contribution has the bremsstrahlung off the  $\tau$  (a), off the  $\pi$  (b) and the diagram with the local vertex  $W\gamma^*\pi$  (c) shown in figure 2.1 which are given by pure

QED assuming a point-like pion. The contributions to the amplitude are thus

$$\begin{aligned}
\mathcal{M}_{IB} &= -iG_F V_{ud} \frac{e^2}{k^2} F M_\tau \bar{u}(p_-) \gamma_\mu v(p_+) \bar{u}(q) (1 + \gamma_5) \left[ \frac{2p^\mu}{2p \cdot k + k^2} + \frac{2p_\tau^\mu - \not{k} \gamma^\mu}{-2p_\tau \cdot k + k^2} \right] u(p_\tau), \\
\mathcal{M}_V &= -G_F V_{ud} \frac{e^2}{k^2} \bar{u}(p_-) \gamma^\nu v(p_+) F_V(p \cdot k, k^2) \epsilon_{\mu\nu\rho\sigma} k^\rho p^\sigma \bar{u}(q) \gamma^\mu (1 - \gamma_5) u(p_\tau), \\
\mathcal{M}_A &= iG_F V_{ud} \frac{2e^2}{k^2} \bar{u}(p_-) \gamma_\nu v(p_+) \left\{ F_A(p \cdot k, k^2) [(k^2 + p \cdot k) g^{\mu\nu} - k^\mu p^\nu] - \frac{1}{2} A_2(k^2) k^2 g^{\mu\nu} \right. \\
&\quad \left. + \frac{1}{2} A_4(k^2) k^2 (p + k)^\mu p^\nu \right\} \bar{u}(q) \gamma_\mu (1 - \gamma_5) u(p_\tau).
\end{aligned} \tag{2.1}$$

Here  $G_F$  is the Fermi constant,  $V_{ud}$  is the first entry of the CKM matrix,  $k = p_+ + p_-$  is the virtual photon four-momentum and all the values for the SM parameters were taken from the Particle Data Group Review on Particle Physics [72].  $\mathcal{M}_{IB}$  is the total model independent contribution and  $\mathcal{M}_V$  and  $\mathcal{M}_A$  are the vector and axial-vector structure dependent contributions, respectively.

By inspection of the previous expressions it can be seen that the decay amplitudes for the real photon are obtained by making  $\frac{e}{k^2} \bar{u}(p_-) \gamma_\mu v(p_+) \rightarrow \epsilon(k)_\mu^*$ , for  $\epsilon_\mu^*(k)$  the polarization of the real photon, then setting  $k^2 \rightarrow 0$ . Our computation of the form factors  $F_A$  and  $F_V$  agrees in the  $k^2 \rightarrow 0$  limit with the expressions from ref [70]. In addition, we provide for the first time their dependence on the photon virtuality. The additional axial form factors  $A_2(k^2)$  and  $A_4(k^2)$  can be seen in ref [73]. These can be expressed in terms of one form factor at the order we are interested in computing the process (further details can be seen on ref [74]). By defining  $B(k^2) := -\frac{1}{2} A_2(k^2)$  one gets  $\frac{1}{2} A_4(k^2) = -B(k^2)/(k^2 + 2p \cdot k)$ , so that the amplitude simplifies to

$$\begin{aligned}
\mathcal{M}_A &= iG_F V_{ud} \frac{2e^2}{k^2} \bar{u}(p_-) \gamma_\nu v(p_+) \left\{ F_A(p \cdot k, k^2) [(k^2 + p \cdot k) g^{\mu\nu} - k^\mu p^\nu] \right. \\
&\quad \left. + B(k^2) k^2 \left[ g^{\mu\nu} - \frac{(p + k)^\mu p^\nu}{k^2 + 2p \cdot k} \right] \right\} \bar{u}(q) \gamma_\mu (1 - \gamma_5) u(p_\tau).
\end{aligned} \tag{2.2}$$

The  $k$  dependence of the amplitudes gives us an idea of what to expect. All the amplitudes have a factor  $1/k^2$ , nevertheless the structure independent amplitude

will give the dominant contribution when  $k$  is small since it has extra  $1/k$  factors compared to the structure dependent part, which has an  $\mathcal{O}(k)$  dependence. Instead, for  $k^0 \sim m_\tau - m_\pi$  the structure dependent terms will give the main contribution to the process. Since the mass of the electron is 200 times smaller than that of the muon one would expect to see this decay channel dominated by the pure QED contribution. Being the muon nearly as heavy as the pion, one would expect that hadronic effects would be more important since the structure dependent amplitude  $\sim \mathcal{O}(k)$ .

It should be noticed that ref [72] neglects the  $A_4(k^2)$  in the  $\pi \rightarrow \mu\nu_\mu e^+ e^-$  for kinematic reasons, however, given the different phase space of our process we will keep this form factor.

The decay rate will be conveniently separated in six terms which will be given by the squared moduli of the three amplitudes and three interference terms.

$$\Gamma_{total} = \Gamma_{IB} + \Gamma_{VV} + \Gamma_{AA} + \Gamma_{IVB} + \Gamma_{IVA} + \Gamma_{VA} \quad (2.3)$$

where the integrals for  $d\Gamma(\tau^- \rightarrow \pi^- \ell^+ \ell^- \nu_\tau)$  were obtained using the phase space configuration of reference [75]. All the squared amplitudes sum over final and averaged over initial polarizations are shown in appendix 5.

### 2.2.3 Form Factors

The expressions for the form factors are obtained by computing the Feynman diagrams in figure 2.2 for the vector and in figure 2.3 for axial form factors. These contributions are computed by means of R $\chi$ T since at the energies probed in the  $\tau$  decay, the resonances region is available. However, near the mass of the  $\tau$  the process is kinematically suppressed, therefore contributions of higher multiplets of resonances can be safely neglected.

Since both gauge bosons in the  $W\gamma\pi$  vertex are off-shell, the effective vertex will depend upon two Lorentz invariants, which we choose as  $t := (p + k)^2$  and  $k^2$ . In ref [70] the same diagrams were obtained, however the one with the contribution to the



Figure 2.2: Contribution to the vector form factor in eq (2.1), where the circle with cross denotes the weak vertex.



Figure 2.3: Contribution to the axial form factor in eq (2.1), where the circle with cross denotes the weak vertex.

electromagnetic form factor (the second in fig 2.3), is zero for on-shell photon, so the extra form factor is expected to be proportional to the electromagnetic form factor of the pion for  $\rho - \gamma$  mixing.

Therefore, the expression of the vector form factor is expressed in the following way

$$\begin{aligned}
 F_V(t, k^2) = & -\frac{N_C}{24\pi^2 F} + \frac{2\sqrt{2}F_V}{3FM_V} \left[ (c_2 - c_1 - c_5)t + (c_5 - c_1 - c_2 - 8c_3)m_\pi^2 + 2(c_6 - c_5)k^2 \right] \times \\
 & \left[ \frac{\cos^2\theta}{M_\phi^2 - k^2 - iM_\phi\Gamma_\phi} \left( 1 - \sqrt{2}\text{tg}\theta \right) + \frac{\sin^2\theta}{M_\omega^2 - k^2 - iM_\omega\Gamma_\omega} \left( 1 + \sqrt{2}\text{cotg}\theta \right) \right] \\
 & + \frac{2\sqrt{2}F_V}{3FM_V} D_\rho(t) \left[ (c_1 - c_2 - c_5 + 2c_6)t + (c_5 - c_1 - c_2 - 8c_3)m_\pi^2 + (c_2 - c_1 - c_5)k^2 \right] \\
 & + \frac{4F_V^2}{3F} D_\rho(t) \left[ d_3(t + 4k^2) + (d_1 + 8d_2 - d_3)m_\pi^2 \right] \times \\
 & \left[ \frac{\cos^2\theta}{M_\phi^2 - k^2 - iM_\phi\Gamma_\phi} \left( 1 - \sqrt{2}\text{tg}\theta \right) + \frac{\sin^2\theta}{M_\omega^2 - k^2 - iM_\omega\Gamma_\omega} \left( 1 + \sqrt{2}\text{cotg}\theta \right) \right], \quad (2.4)
 \end{aligned}$$

where  $\theta$  is the mixing of  $\omega - \phi$  vector mesons and

$$D_R(t) = \frac{1}{M_R^2 - t - iM_R\Gamma_R(t)}, \quad (2.5)$$

and  $\Gamma_R(t)$  is the off-shell width of the resonance meson. The  $c_i$  and  $d_k$  are couplings of the VJP and VVP operators respectively, given in section 3.4. The off-shell width can be read from appendix 5 [76]. If the ideal mixing of vector mesons  $\omega - \phi$  is

considered,

$$\begin{pmatrix} \omega_1 \\ \omega_8 \end{pmatrix} = \begin{pmatrix} \sqrt{\frac{2}{3}} & -\frac{1}{\sqrt{3}} \\ \frac{1}{\sqrt{3}} & \sqrt{\frac{2}{3}} \end{pmatrix} \begin{pmatrix} \omega \\ \phi \end{pmatrix}, \quad (2.6)$$

the contribution from the  $\phi$  meson vanishes. Since these are rather narrow resonances, their energy dependent widths will be taken constant and equal to their total widths.

In the case of the axial form factors one finds

$$F_A(t, k^2) = \frac{F_V^2}{F} \left(1 - \frac{2G_V}{F_V}\right) D_\rho(k^2) - \frac{F_A^2}{F} D_{a_1}(t) + \frac{F_A F_V}{\sqrt{2}F} D_\rho(k^2) D_{a_1}(t) \left(-\lambda'' t + \lambda_0 m_\pi^2\right), \quad (2.7)$$

where we have used the notation

$$\begin{aligned} \sqrt{2}\lambda_0 &= -4\lambda_1 - \lambda_2 - \frac{\lambda_4}{2} - \lambda_5, \\ \sqrt{2}\lambda'' &= \lambda_2 - \frac{\lambda_4}{2} - \lambda_5, \end{aligned} \quad (2.8)$$

for the relevant combinations of couplings of the VAP operators shown in section 3.4. Again, the off-shell width of the  $a_1$  meson is shown in appendix 5.

What one gets for the  $B(k^2)$  form factor is, as previously mentioned, completely related to the electromagnetic form factor of the pion for  $\rho - \gamma$  mixing.

$$B(k^2) = F \left[ \frac{F_V^{\pi^+\pi^-}|_\rho(k^2) - 1}{k^2} \right], \quad (2.9)$$

The form factor  $F_V^{\pi^+\pi^-}|_\rho(k^2)$  has been obtained by means of dispersion relations in ref. [77, 78, 79, 80], although, we follow the approach in ref. [81] and use a dispersive representation of the form factor at low energies matched to a phenomenological description at intermediate energies, including the excited resonance contribution. So, the form factor is obtained through a three times subtracted dispersion relation



$$F_V^\pi(s) = \exp \left[ \alpha_1 s + \frac{\alpha_2}{2} s^2 + \frac{s^3}{\pi} \int_{s_{\text{thr}}}^\infty ds' \frac{\delta_1^1(s')}{(s')^3 (s' - s - i\epsilon)} \right], \quad (2.10)$$

where [82]

$$\tan \delta_1^1(s) = \frac{\Im m F_V^{\pi(0)}(s)}{\Re e F_V^{\pi(0)}(s)}, \quad (2.11)$$

with

$$\begin{aligned} F_V^{\pi(0)}(s) &= \frac{M_\rho^2}{M_\rho^2 \left[ 1 + \frac{s}{96\pi^2 F^2} (A_\pi(s) + \frac{1}{2} A_K(s)) \right] - s} \\ &= \frac{M_\rho^2}{M_\rho^2 \left[ 1 + \frac{s}{96\pi^2 F^2} \Re e (A_\pi(s) + \frac{1}{2} A_K(s)) \right] - s - i M_\rho \Gamma_\rho(s)}. \end{aligned} \quad (2.12)$$

The loop function is ( $\mu$  can be taken as  $M_\rho$ )

$$A_P(k^2) = \ln \left( \frac{m_P^2}{\mu^2} \right) + 8 \frac{m_P^2}{k^2} - \frac{5}{3} + \sigma_P^3(k^2) \ln \left( \frac{\sigma_P(k^2) + 1}{\sigma_P(k^2) - 1} \right), \quad (2.13)$$

and the phase-space factor  $\sigma_P(k^2)$  is defined after the  $\rho$  width in appendix 5.

The parameters  $\alpha_1$ ,  $\alpha_2$  and the  $\rho(770)$  resonance parameters entering  $B(k^2)$  will be extracted [81] from fits to BaBar  $\sigma(e^+e^- \rightarrow \pi^+\pi^-)$  data [83] excluding the  $\omega(782)$  contribution. We have used the fitted values with corresponding errors, as discussed in ref [80]  $\alpha_1 = 1.87$ ,  $\alpha_2 = 4.26$ .

## 2.2.4 Short distance constraints

One of the main advantages of R $\chi$ T is the fact that the couplings from operators in the theory can be constrained by means of the QCD behavior at infinite energies, specifically the Green functions behavior. The Large  $N_C$  description of QCD gives us a way to relate the quark Green functions to those generated by means of meson exchange, therefore, by matching consistently the leading order Operator Product Expansion result to a given order in the  $1/N_C$  expansion Green functions in both descriptions, the relations among them will constrain the couplings of the effective

theory. When the energy in the quark current in the Green function is very large ( $E \rightarrow \infty$ , this is, when the distance between the points of the Green function  $\rightarrow 0$ ) the quarks Green function must be equal to the meson exchange Green function, this is called quark-hadron duality. Assuming quark-hadron duality, the study of two point spin-one Green functions in pQCD shows that the imaginary part of the quark loop must be constant at infinite momentum transfer [84] and can be understood as a sum of infinitely many positive contributions from intermediate hadron states. Since all these infinite positive contributions must add up to a constant value at high energies, each of these contributions must vanish in this limit.

In principle all resonance excitations must enter the short distance relations, however most experimental processes can be very well described by considering the lowest-lying (vector and axial) resonances approximation [85]. The effect of the excited resonances usually give very small corrections to the short distance relations (see some examples in [86, 87, 74]). Therefore, by assuming this lowest-lying resonances dominance and the sum rules given by Weinberg [88] we get the results

$$\begin{aligned}
c_1 - c_2 + c_5 &= 0, \\
2(c_6 - c_5) &= \frac{-N_C M_V}{64\pi^2 F}, \\
c_1 - c_2 - 8c_3 + c_5 &= 0, \\
d_1 + 8d_2 - d_3 &= \frac{1}{16}, \\
d_3 &= \frac{-N_C M_V^2}{128\pi^2 F^2} + \frac{1}{16}, \\
G_V &= \frac{F}{\sqrt{2}}, \\
F_V &= \sqrt{2}F, \\
F_A &= F, \\
\lambda' &= \frac{1}{2}, \\
\lambda'' &= 0, \\
\lambda_0 &= \frac{1}{8}.
\end{aligned} \tag{2.14}$$

Given the corrected short distance relations of reference [89] a reanalysis of the process should be done, however this effect would give a small correction (even for the  $\ell = \mu$  channel), so that the conclusion in this thesis and in ref. [74] stands. For the branching fraction of the process we will take  $M_V = 775$  MeV.

### 2.2.5 Branching ratio and invariant mass spectrum

The form factors given in eqs. (2.4), (2.7) and (2.9) parametrize the structure dependent contribution. With the information on the couplings of the form factors, we are now ready to compute all the contributions to the branching fraction and the invariant mass spectrum. The branching fractions are, therefore, predicted with the values [74] of table 2.1, where we let a variation of a 20% around the short distance prediction of couplings is allowed in order to estimate a theoretical uncertainty. These are the errors of the structure dependent contributions in table 2.1, the errors in the completely structure independent contribution comes from the numerical integration

of this contribution. The error ranges are basically given by the uncertainties in  $F_V, G_V, F_A, d_3$  and  $c_5 - c_6$ .

	$\ell = e$	$\ell = \mu$	$\ell = e$	$\ell = \mu$
IB	$1.461 \cdot 10^{-5}$	$1.600 \cdot 10^{-7}$	$\pm 0.006 \cdot 10^{-5}$	$\pm 0.007 \cdot 10^{-7}$
IB-V	$-2 \cdot 10^{-8}$	$1.4 \cdot 10^{-8}$	$[-1 \cdot 10^{-7}, 1 \cdot 10^{-7}]$	$[-4 \cdot 10^{-9}, 4 \cdot 10^{-8}]$
IB-A	$-9 \cdot 10^{-7}$	$1.01 \cdot 10^{-7}$	$[-3 \cdot 10^{-6}, 2 \cdot 10^{-6}]$	$[-2 \cdot 10^{-7}, 6 \cdot 10^{-7}]$
VV	$1.16 \cdot 10^{-6}$	$6.30 \cdot 10^{-7}$	$[4 \cdot 10^{-7}, 4 \cdot 10^{-6}]$	$[1 \cdot 10^{-7}, 3 \cdot 10^{-6}]$
AA	$2.20 \cdot 10^{-6}$	$1.033 \cdot 10^{-6}$	$[1 \cdot 10^{-6}, 9 \cdot 10^{-6}]$	$[2 \cdot 10^{-7}, 6 \cdot 10^{-6}]$
V-A	$2 \cdot 10^{-10}$	$-5 \cdot 10^{-11}$	$\sim 10^{-10}$	$\sim 10^{-10}$
TOTAL	$1.710 \cdot 10^{-5}$	$1.938 \cdot 10^{-6}$	$(1.7^{+1.1}_{-0.3}) \cdot 10^{-5}$	$[3 \cdot 10^{-7}, 1 \cdot 10^{-5}]$

Table 2.1: The central values of the different contributions to the branching ratio of the  $\tau^- \rightarrow \pi^- \nu_\tau \ell^+ \ell^-$  decays ( $\ell = e, \mu$ ) are displayed on the left-hand side of the table. The error bands of these branching fractions are given in the right-hand side of the table. The error bar of the IB contribution stems from the uncertainties on the pion decay constant  $F$  and  $\tau_\ell$  lepton lifetime [72].

We computed also the invariant (di-lepton) mass spectrum normalized to the  $\tau$  total width for both channels

$$\frac{1}{\Gamma_\tau} \cdot \frac{d\Gamma(\tau^- \rightarrow \pi^- \nu_\tau \ell^+ \ell^-)}{dk^2}. \quad (2.15)$$

As it was noticed in subsection 2.2.2, since the electron can reach very low invariant mass values, the decay width for this channel is mainly given by the model independent part of the amplitude and the structure dependent part gives a negligible contribution. This behavior of the invariant mass spectrum is shown in figure 2.4, where  $s_{34} = k^2$  is the invariant mass of the di-lepton [74].

Thus, we can see that for the muon channel the the opposite of the electron case happens. Since the mass of the muon is nearly that of the pion, the energy region probed in this decay has a great contribution from the hadronic processes (structure dependent).

In Figs. 2.4-2.6 vertical fluctuations can be appreciated in certain energy regions of the normalized invariant-mass distributions. In order to compute these distributions

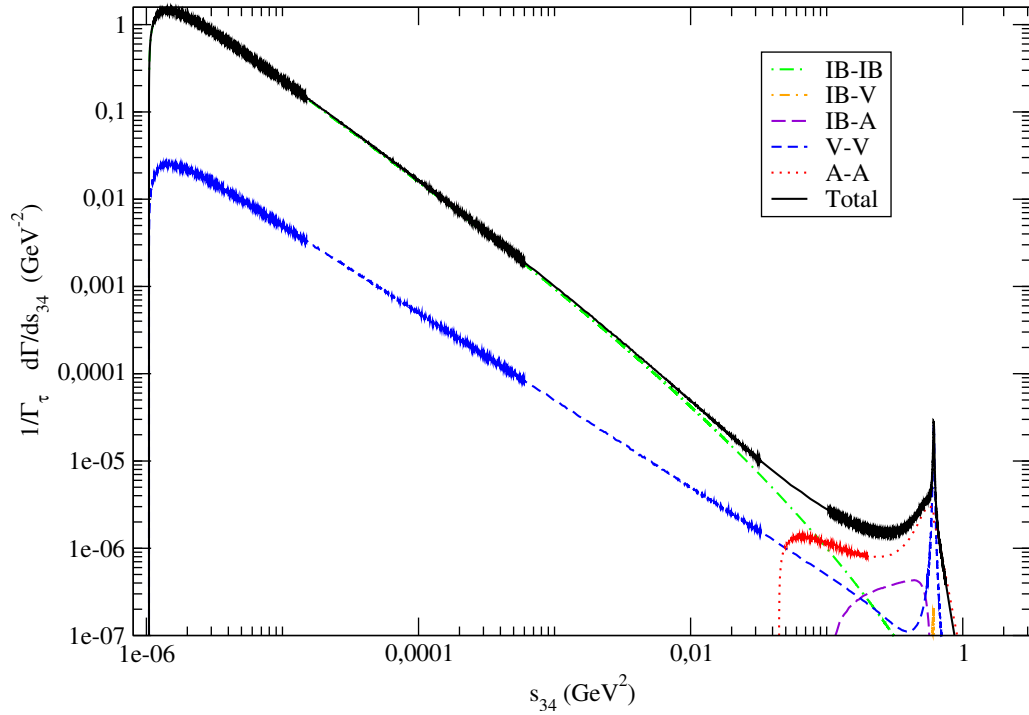


Figure 2.4: The different contributions to the normalized  $e^+e^-$  invariant mass distribution defined in Eq. (2.15) are plotted. A double logarithmic scale was needed.

in the  $s_{34}$  variable, we have integrated numerically the decay probability over the remaining four independent kinematical variables. The observed fluctuations arise from the Monte Carlo evaluation over the four-body phase space integration. The branching fractions shown in Table 2.1 were obtained by integrating numerically these invariant-mass distributions and checked from a direct integration over the five independent kinematical variables.

The fact that, in both decays, the contribution to the decay width of the  $s_{34} > 1$   $\text{GeV}^2$  region is negligible justifies our assumption of including only the lightest multiplet of vector and axial-vector resonances. This result is not trivial in the axial-vector case and in the vector case it is not modified even if the  $\rho(1450)$  exchange is included phenomenologically [90].

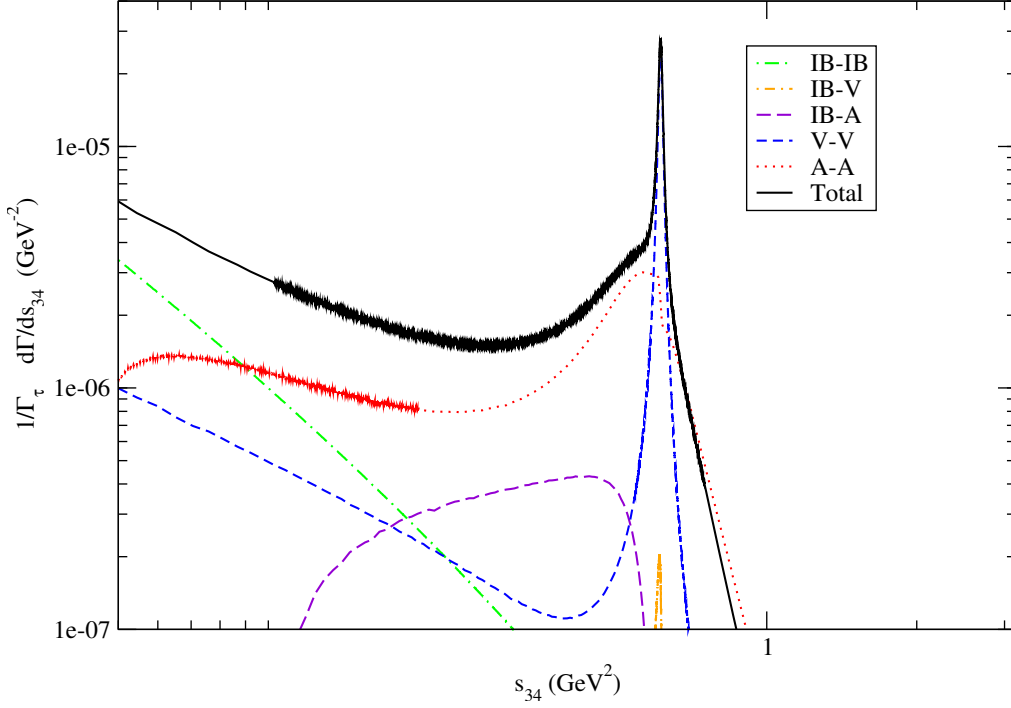


Figure 2.5: The different contributions to the normalized  $e^+e^-$  invariant mass distribution defined in Eq. (2.15) are plotted in a magnification for  $s_{34} \gtrsim 0.1 \text{ GeV}^2$  intended to better appreciate the  $SD$  contributions. A double logarithmic scale was needed.

We can see the effect of including the  $B(k^2)$  form factor into the axial amplitude by neglecting its contribution and then comparing it to the full axial contribution (squared  $A$  modulus plus the interference with  $IB$ ). The effect in both of the parts are 33 and 25% respectively of the values in table 2.1. It becomes essential to include this contribution since the muon channel is dominated by the axial amplitude. Thus, it drops a 44% of the value in table 2.1 when one neglects this contribution. This explains the peak in the axial amplitude around the rho mass, since  $B(k^2)$  is proportional to the electromagnetic form factor of the pion with only  $\rho - \gamma$  mixing.

It is worth to notice the difference between the total branching fractions for the electron and (for its central value) the muon channels. If this effect is not taken into account in the search for lepton universality violation might lead to spurious signal of beyond Standard Model effects.

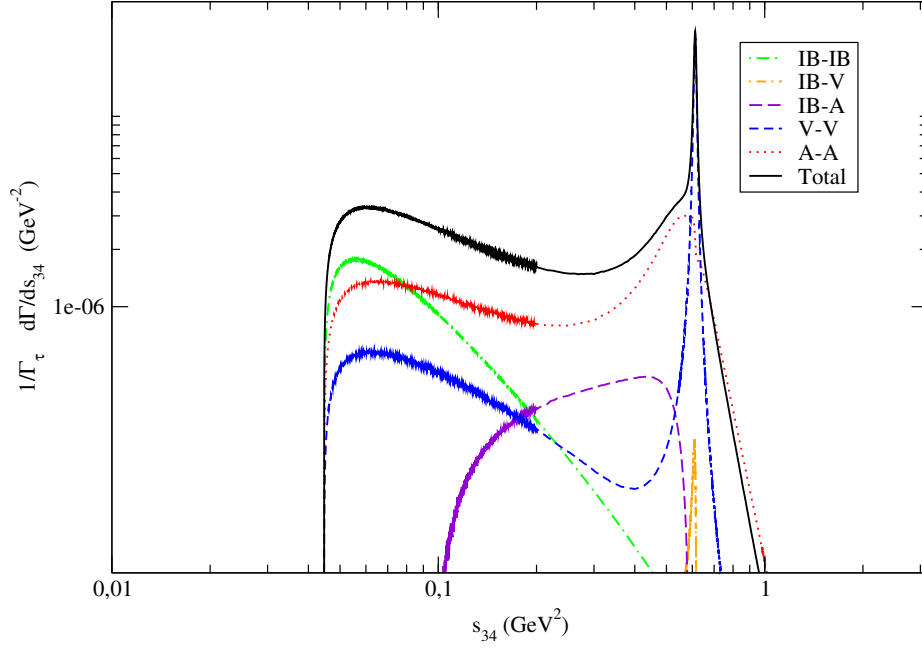


Figure 2.6: The different contributions to the normalized  $\mu^+\mu^-$  invariant mass distribution are plotted. A double logarithmic scale allows to display the different contributions more clearly.

### 2.2.6 Conclusions

We have studied for the first time the branching ratio of the  $\tau \rightarrow \pi \ell^+ \ell^- \nu_\tau$  decays as well as the normalized invariant di-lepton mass spectrum. The analysis of this decays lead to a lepton universality violation induced by dynamic and kinematical effects. If this effect is not taken into account, the study of lepton flavor violation in heavy hadrons involving  $\tau$  leptons in the final state might lead to a non-universality induced effect which might be confused with a genuine BSM effect.

As previously mentioned, the observables in this process are needed in order to give a good estimate of the background for the search of lepton flavor violation processes as  $\tau \rightarrow \ell' \ell^+ \ell^-$  or lepton number violation as in the process  $\tau^- \rightarrow \pi^+ \ell^- \ell^- \nu_\tau$  [71]. This form factors were coded in the R $\chi$ T based version of TAUOLA, which is the standard Monte Carlo generator for  $\tau$  decays [91, 92].

## 2.3 Long-distance contribution to $B^\pm \rightarrow (\pi^\pm, K^\pm)\ell^+\ell^-$ decays.

### 2.3.1 Introduction

Being the lightest element of the third generation quark doublet, all  $b$ -flavored hadrons occur through generation changing processes. This means that all amplitudes will be  $\mathcal{O}(\lambda)$  suppressed, within the Wolfenstein parameterization [93] of the CKM matrix. Thus, several processes involving  $b$ -flavored mesons will be highly suppressed in the Standard Model yielding an excellent ground to search for Beyond Standard Model Physics.

In 2014 several interesting precision tests of the Standard Model were made at the LHCb experiment, in particular a test of lepton universality in  $B^\pm \rightarrow K^\pm\ell^+\ell^-$  decays,

$$R_K := BR(B \rightarrow K\mu^+\mu^-)/BR(B \rightarrow Ke^+e^-) = 0.745_{-0.074}^{+0.090} \pm 0.036 \quad (2.16)$$

within the squared invariant mass of the lepton pair in the range  $[1, 6] \text{ GeV}^2$  [94], where the errors shown are the first statistic and the second systematic. This very interesting result contrasts with current SM prediction, which is  $R_K^{SM} = 1 + (3.0_{-0.7}^{+1.0}) \cdot 10^{-4}$  [95]. We saw previously (in  $\tau \rightarrow \pi^-\ell^+\ell^-\nu_\tau$  decays) [96] that the weak radiative pion vertex gives different values by taking either  $\ell = \mu$  or  $\ell = e$  for the model dependent terms, especially close to 1 GeV, where they became relevant. This analysis hinted the possibility that such violation of lepton universality might be due to hadronic effects at the GeV scale.

In this chapter we compute a Long-Distance (LD) term of the Weak Annihilation contribution of  $B^\pm \rightarrow P^\pm\ell^+\ell^-$  decays which, by extending  $R_{\chi T}$  to include  $b$ -flavored mesons and after computing all possible diagrams, we find that the only non-negligible



contribution comes from the  $P$  meson electromagnetic form factor for  $P = \pi, K$ . Also, to have reference point, we used the Gounaris-Sakurai (GS) parametrization used by the BaBar collaboration in the fit of their data to the mentioned form factors [97]. The observables are computed for invariant dilepton mass below the charmonium threshold  $q^2 \leq 8 \text{ GeV}^2$ , overlapping the experimental  $q^2$  range in the measurement of

$$R_P := BR(B^\pm \rightarrow P^\pm \mu^+ \mu^-) / BR(B^\pm \rightarrow P^\pm e^+ e^-), \quad (2.17)$$

where  $P$  is either  $\pi$  or  $K$ . Our short distance (SD) analysis of the amplitude was based in the results given in ref [95].

### 2.3.2 $R_{\chi T}$ contribution to the Weak Annihilation amplitude

The QCD factorization (QCdf) [98, 99] contribution to the  $B^\pm \rightarrow (\pi^\pm, K^\pm) \ell^+ \ell^-$  decays [95, 96, 100] is taken at next to leading order, where a comparable uncertainty to that obtained using  $R_{\chi T}$  with only the leading terms is expected. In this approximation the small contribution of the Weak Annihilation (WA) of the valence quarks in the  $B$  meson becomes relevant. At this order in  $1/N_C$ , the quark currents of both mesons can be *naively factorized*, since a gluon exchange would mean a higher order term in  $1/N_C$ ; this means that the hadronic current can be written as products of decay constants and/or form factors [99] which is described by the diagrams in Figure 2.7.



Figure 2.7: All possible contributions to the WA amplitude at leading order in  $1/N_C$ . The thick dot denotes interactions between resonances and the fields coupled to the vertex.

Now, at leading order in QED the leptonic current can be factorized from the

hadronic current since no photon exchange exists except for the one connecting the lepton current with the hadronic one. Thus, the LD WA amplitude can be written as the coupling of the leptonic current and an effective hadronic electromagnetic current ( $\mathcal{M}_\mu^{WA}$ )

$$\mathcal{M}_{LD}^{WA} = \frac{e^2}{q^2} \bar{\ell} \gamma^\mu \ell \mathcal{M}_\mu^{WA}, \quad (2.18)$$

where  $q^2$  is the dilepton invariant mass squared and, by conservation of the electromagnetic current, the effective hadronic electromagnetic current takes the form

$$\mathcal{M}_\mu^{WA} = \left[ (p_B + p_P)_\mu - \frac{m_B^2 - m_P^2}{q^2} q_\mu \right] F(q^2), \quad (2.19)$$

where  $m_{B/P}$  is the  $B$  meson (pseudo-Goldstone boson) mass and  $p_{B/P}$  is the  $B$  meson (pseudo-Goldstone boson) four-momentum. All strong, weak and electromagnetic interactions happening within the  $B \rightarrow P\gamma^*$  transition are embedded in the form factor  $F(q^2)$ . Since  $q_\mu \bar{\ell} \gamma^\mu \ell = 0$ , only the first term in the previous equation contributes where, by the same argument  $p_B + p_P$  can be replaced by  $2p_B$ . The next section shows the framework to compute the form factor of the  $B^\pm \rightarrow \gamma^* W^{*\pm}$  effective vertex.

### 2.3.3 Extending $R_\chi T$ for heavy flavor mesons

To obtain the form factor of the interactions of the effective vertex shown in Figure 2.7, we proceed in analogy with the extension of Resonance Chiral Theory to include  $c$ -flavored quarks,  $c$ -flavored resonances and the interactions between them, the Goldstone bosons and the light resonances [101]. This model *does not* rely on the heaviness of the charm quark and therefore cannot ensure a better description depending on the mass of the heavy quark in the meson, nevertheless it can be extended in a straightforward way to  $b$ -flavored mesons.

The  $b$ -flavored mesons are included by constructing a flavor triplet in a convenient realization and demanding it to transform linearly under the chiral group  $G$ ,

$$B := \begin{pmatrix} B^- \\ B_d^0 \\ B_s^0 \end{pmatrix}, \quad B \xrightarrow{G} h(\varphi)B, \quad (2.20)$$

where  $h(\varphi) \in SU(3)_V$ . In other words,  $B$  mesons are taken to be the components of a  $SU(3)_V$  triplet which is a linear realization of  $SU(3)_V$ . The same procedure is followed for  $b$ -flavored resonances where, as SSB of the chiral group dictates,  $B^V$  and  $B^A$  will have different masses.

Analogously to the chiral theory for light mesons, the electroweak interactions are introduced as non-propagating external fields where they have to be extended to  $SU(4)$  hermitian fields coupling to the two quark doublets of weak  $SU(2)_L$  via

$$\mathcal{L} = \mathcal{L}_{QCD}^0 - m_b \bar{b}b + \bar{q}\gamma^\mu \left[ \frac{1}{2}(1 - \gamma_5)\tilde{\ell}_\mu + \frac{1}{2}(1 + \gamma_5)\tilde{r}_\mu \right] q - i\bar{q}(\tilde{s} - i\gamma_5\tilde{p})q. \quad (2.21)$$

Even when all external fields vanish, the mass term for the  $b$  quark still remains. Since the fields have to be extended, at the meson level a new realization is needed in order to couple the pseudoscalar mesons to the external currents. This means extending the  $U$  matrix in the chiral group to a  $4 \times 4$  operator  $\tilde{U}$ . The way to realize this is by constructing a matrix  $4 \times 4$  including the  $B$  triplet

$$\tilde{U} = \tilde{u}_R^\dagger \tilde{u}_L, \quad (2.22)$$

where

$$\tilde{u}_R^\dagger = \begin{pmatrix} u(\varphi) & \frac{i}{\sqrt{2}f_B}u(\varphi)B \\ \frac{i}{\sqrt{2}f_B}B^\dagger & f_B/F \end{pmatrix}, \quad \tilde{u}_L = \begin{pmatrix} u(\varphi) & \frac{i}{\sqrt{2}f_B}B \\ \frac{i}{\sqrt{2}f_B}u(\varphi)B^\dagger & f_B/F \end{pmatrix}, \quad (2.23)$$

with  $f_X$  the decay constant of meson  $X$ . In a similar way, the resonance fields can be extended to  $SU(4)$

$$\tilde{R} = \begin{pmatrix} R & B^R \\ B^{R\dagger} & 0 \end{pmatrix}. \quad (2.24)$$

The important thing to notice here is that in this model, the Goldstone bosons and the light resonances enter as non-linear realizations and  $b$ -flavored mesons as linear realizations. That is to say, the  $SU(4)$  realization is only introduced to see how the external currents have to be implemented, meaning that this is *not* an implementation of a chiral realization with four flavors whatsoever.

The coupling to weak interactions through external currents comes from the definition

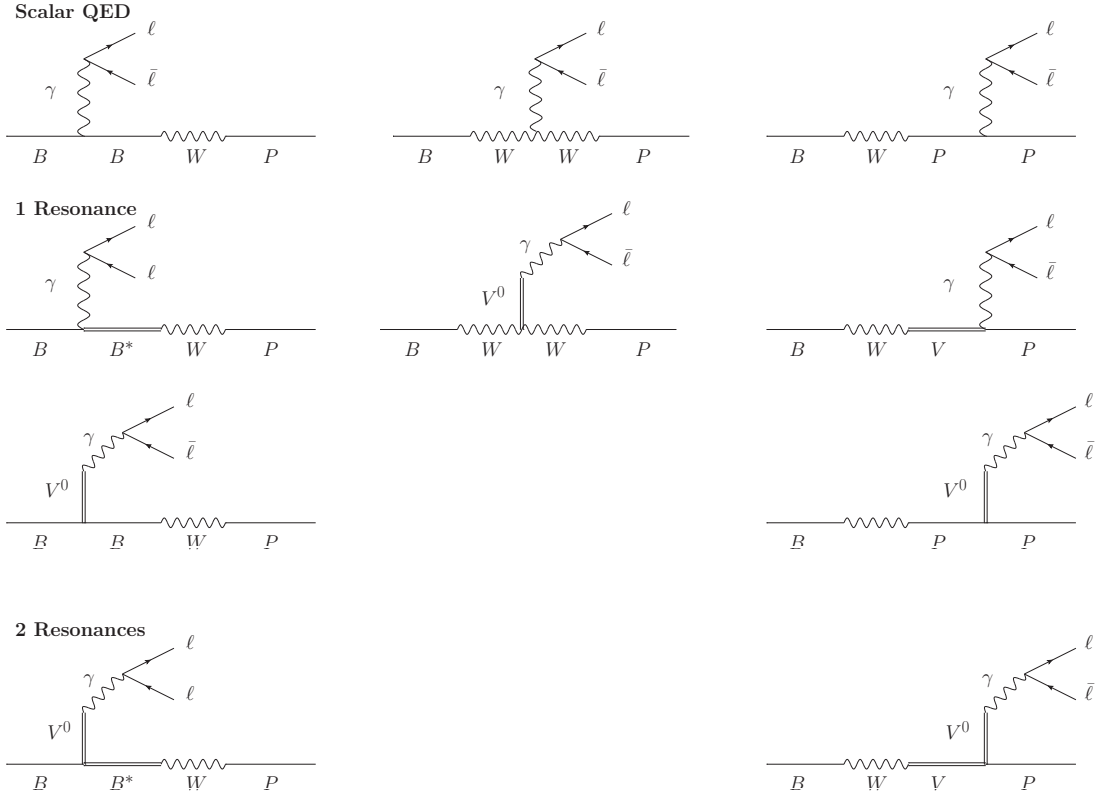


Figure 2.8: All LD WA Feynman diagrams at leading order in  $1/N_C$ . The first row shows the contribution from model independent interactions, while the second and third shows contributions from diagrams with one and two resonances respectively.  $V^{(0)}$  stands for light charged (neutral) vector resonances.

of the covariant derivatives on the relevant objects

$$D_\mu \tilde{U} = \partial_\mu \tilde{U} - i\tilde{r}\tilde{U} + i\tilde{U}\tilde{\ell}, \quad (2.25a)$$

$$\nabla_\mu \tilde{R} = \partial_\mu \tilde{R} + [\tilde{\Gamma}_\mu, \tilde{R}], \quad (2.25b)$$

where

$$\tilde{\Gamma}_\mu = \frac{1}{2} \left\{ \tilde{u}_R [\partial_\mu - i\tilde{r}] \tilde{u}_R^\dagger + \tilde{u}_L [\partial_\mu - i\tilde{\ell}] \tilde{u}_L^\dagger \right\}. \quad (2.26)$$

The extended right ( $\tilde{r}$ ) and left ( $\tilde{\ell}$ ) external fields are

$$\tilde{r}_\mu = \begin{pmatrix} r_\mu & 0 \\ 0 & \gamma_\mu \end{pmatrix} \quad \tilde{\ell}_\mu = \begin{pmatrix} l_\mu & \omega_\mu \\ \omega_\mu^\dagger & \delta_\mu \end{pmatrix} \quad (2.27)$$

where

$$\gamma_\mu = -\frac{1}{3}e [A_\mu - \tan \theta_W Z_\mu], \quad (2.28a)$$

$$\delta_\mu = -\frac{1}{3}e A_\mu + e \left[ -\frac{1}{\sin 2\theta_W} + \frac{1}{3} \tan \theta_W \right] Z_\mu, \quad (2.28b)$$

$$\omega_\mu = 2m_W \sqrt{\frac{G_F}{\sqrt{2}}} \begin{pmatrix} V_{ub} \\ 0 \\ 0 \end{pmatrix} W_\mu. \quad (2.28c)$$

Now, the covariant derivative acting on the  $B$  resonances is defined in the following way

$$\nabla_\mu B^{(R)} = \left[ \partial_\mu + \Gamma_\mu + \frac{i}{2}(\gamma_\mu + \delta_\mu) \right] B^{(R)}. \quad (2.29)$$

At the lowest chiral order, the whole set of operators that can be constructed regarding the relevant objects defined previously can be obtained from ref [101] by making the substitutions  $B \rightarrow C$  and  $F_C \rightarrow f_B$  and using the definitions given above for all the operators.

Once all operators have been constructed, the Feynman diagrams that need to be computed are those shown in Figure 2.8. All  $b$ -flavored resonances in the Feynman diagrams will have a propagator  $D_{B^*}$  (left-hand side diagrams of Figure 2.8) with invariant mass  $k^2 = m_P^2$  equals to the pseudo-Goldstone mass, such contributions are

not taken into account due to the suppression of the heavy resonance,

$$D_{B^*}(m_P^2) = \frac{1}{m_{B^*}^2 - m_P^2}. \quad (2.30)$$

By electromagnetic gauge invariance, the structure independent terms computed with scalar QED, are found to vanish. The diagram in the middle of the first line in Figure 2.8 is obtained by computing the bremsstrahlung off the  $B$  and the corresponding diagram for  $P$  and then applying the Ward-Takahashi identity, which by gauge invariance gives a relation between the sum of the bremsstrahlung diagrams and the remaining one. Also, after computing the remaining diagrams it is found that several vanish too. The only non-vanishing diagrams are those described only by the electromagnetic form factor of the mesons, namely those of Figure 2.9.

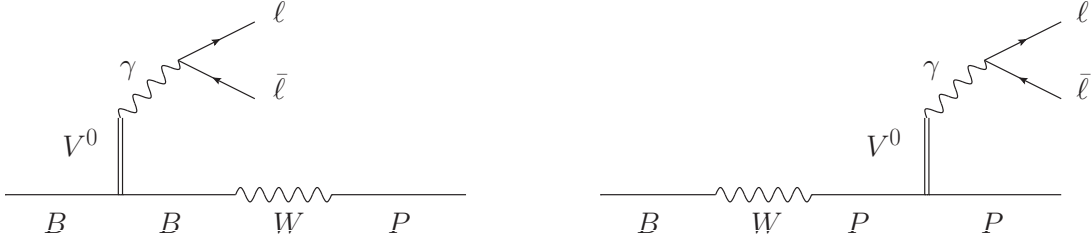


Figure 2.9: Only non-vanishing structure dependent contribution to the WA LD amplitude.

### 2.3.4 The electromagnetic form factor $F_P(q^2)$

Therefore, the amplitude of eq. (2.19) will be fully described by the electromagnetic form factors of the pseudo-Goldstone and the  $B$  meson. Thus, this amplitude can be written in the following way

$$\mathcal{M}_{LD}^{WA} = \frac{\sqrt{2}G_F(4\pi\alpha)V_{ub}V_{ud}^*f_Bf_P}{q^2(m_B^2 - m_P^2)} [m_B^2 (F_P(q^2) - 1) - m_P^2 (F_B(q^2) - 1)] p_{B\mu} \bar{\ell} \gamma^\mu \ell. \quad (2.31)$$

Since the second term is smaller by a factor  $m_P^2/m_B^2$ , it can be neglected once it can be claimed that  $F_B(q^2)$  is not too large compared to  $F_P(q^2)$ . By using the formalism developed in the previous section, the electromagnetic form factor of the

$B$  meson is found to be

$$F_B(q^2) = 1 + \frac{3}{2}q^2 \left( \frac{1}{M_\rho^2 - q^2 - iM_\rho\Gamma_\rho(q^2)} - \frac{1}{3[M_\omega^2 - q^2 - iM_\omega\Gamma_\omega(q^2)]} \right), \quad (2.32)$$

where  $\Gamma_X(s)$  is the off-shell width of the  $X$  meson resonance [76] with invariant mass  $\sqrt{s}$ . So that it becomes apparent that  $F_B(q^2)$  will not surpass the suppression factor  $m_P^2/m_B^2$  so that it can be neglected, only considering the electromagnetic form factor of the light pseudoscalar.

On the other hand, QCDf gives the following amplitude [95, 100, 96]

$$\mathcal{M}_{QCDf} = \frac{G_F\alpha}{\sqrt{2}\pi} V_{tb}V_{tD}^* \xi_P(q^2) p_B^\mu [F_V(q^2) \bar{\ell}\gamma_\mu \ell + F_A(q^2) \bar{\ell}\gamma_\mu \gamma_5 \ell], \quad (2.33)$$

where  $V_{tx}$  is the CKM mixing term between the top quark and the down-type quark  $x$ ,  $\xi$  is a long-distance form factor obtained through Light Cone Sum Rules (LCSM) [102] and  $F_V$  and  $F_A$  are functions of the Wilson Coefficients of the Operator Product Expansion. (All the details about the computation of the QCDf amplitude can be seen in Sergio Lennin Tostado Robledo's Ph. D. thesis.) By comparing this expression with eq. (2.31) it can be seen that the LD WA amplitude<sup>1</sup> can be absorbed in the vector form factor of the QCDf amplitude by doing the replacement

$$\xi_P(q^2)F_V \rightarrow \xi_P(q^2)F_V + \kappa_P m_B^2 \left[ \frac{F_P(q^2) - 1}{q^2} \right], \quad (2.34)$$

where

$$\kappa_P = -8\pi^2 \frac{V_{ub}V_{uD}^*}{V_{tb}V_{tD}^*} \frac{f_B f_P}{m_B^2 - m_P^2} \quad (2.35)$$

is a dimensionless constant  $\sim \mathcal{O}(10^{-2}) \times \frac{V_{ub}V_{uD}^*}{V_{tb}V_{tD}^*}$ . This means that for  $P = K$  (*i.e.*  $D = s$ ) there will be an extra suppression  $\sim \mathcal{O}(\lambda^2)$  compared to the case when  $P = \pi$  (*i.e.*  $D = d$ ), where the CKM factors are  $\mathcal{O}(\lambda^0)$ . Resonance Chiral Theory with only the lightest vector multiplet gives the functional form of the light pseudoscalar form

---

<sup>1</sup>Although the  $B$  meson form factor is neglected, in the rest of the chapter, it was included in the numerical results. No difference is noticed in the observables computed by including it.

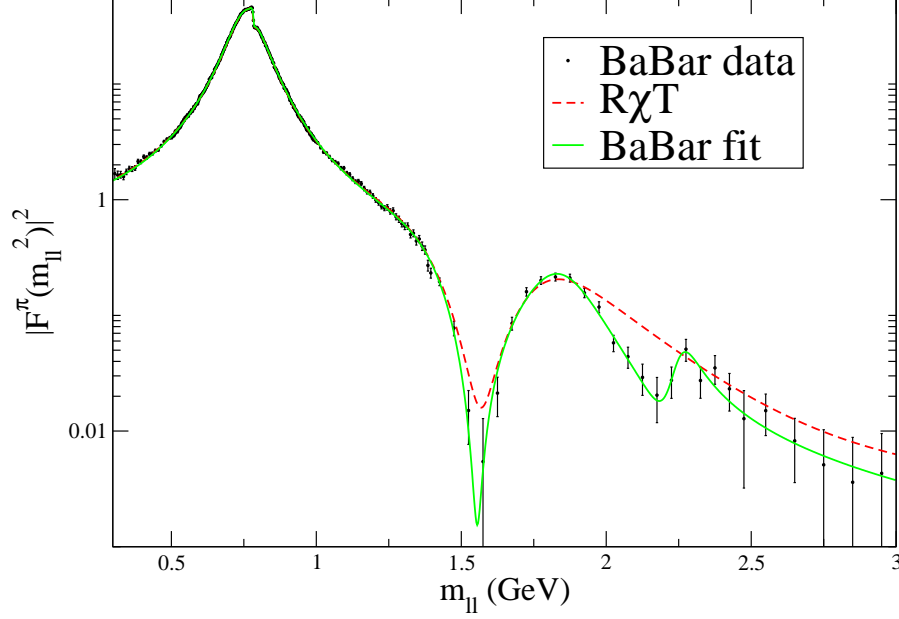


Figure 2.10: BaBar parametrization and our form factor compared with data from BaBar. Here  $m_{||} = \sqrt{q^2}$ . Both form factors overlap below 1.4 GeV, which is the dominant region of the form factor in the observables of the studied decays.

factor

$$F_P(q^2) = 1 + \frac{F_V G_V}{F^2} \frac{q^2}{M_V^2 - q^2}. \quad (2.36)$$

In the previous expression, by demanding a Brodsky Lepage behavior [103] of the form factor one gets the relation  $F_V G_V = F^2$  (also at LO in  $1/N_C$ ). This expression for the form factor must be improved to obtain a more precise determination of the amplitude through the off-shell width of the resonances, (in the  $P = \pi$  case) heavier vector multiplets and the dominant isospin breaking effect in the  $\rho - \omega$  mixing giving the factor [104]

$$1 - \theta_{\rho\omega} \frac{q^2}{3m_\rho^2} \frac{1}{m_\omega^2 - q^2 - im_\omega \Gamma_\omega}, \quad (2.37)$$

where  $\theta_{\rho\omega} = (-3.3 \pm 0.5) \cdot 10^{-3} \text{ GeV}^2$  [105]. For the  $F_\pi(q^2)$  we used the parametrization given in ref [106] including three vector resonances with same quantum numbers ( $\rho(770)$ ,  $\rho(1450)$  and  $\rho(1700)$ ) and a resummation of final state interactions encoded



through chiral loop functions.

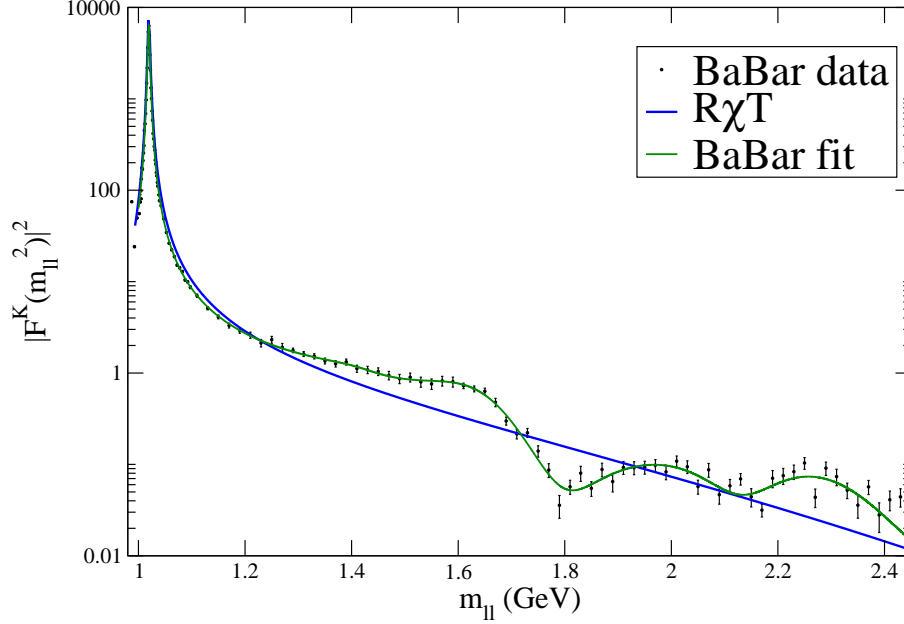


Figure 2.11: Electromagnetic form factor of the  $K$  meson with the BaBar parametrization and our form factor compared with data from BaBar. Here  $m_{||} = \sqrt{q^2}$ .

The comparison between our form factors and those used by BaBar for fitting their data [107] are shown in Figures 2.10 for  $P = \pi$  with energy region  $2m_\pi \leq \sqrt{q^2} \leq 3\text{GeV}$ , where the GS parametrization includes an extra iso-vector resonance. In these plots it is made evident the lack of the latter resonance ( $\rho(2250)$ ), also small differences can be seen in the region where the  $\rho(1450)$  interferes with the  $\rho(1700)$ . All these differences are taken into account to obtain the uncertainty induced by  $F_\pi(q^2)$ .

For the  $P = K$  case, we also made use of the BaBar parametrization of the form factor [108] to compare it with our form factor as can be seen in Figure 2.11. In this case, the  $\phi(1020)$  resonance peak is so large that no other multiplet of resonances need to be considered to improve the precision of the LD WA amplitude for  $P = K$ , since there is a very good match between the data and our form factor around the peak of this resonance and, in addition, the squared modulus of the form factor drops 4 orders

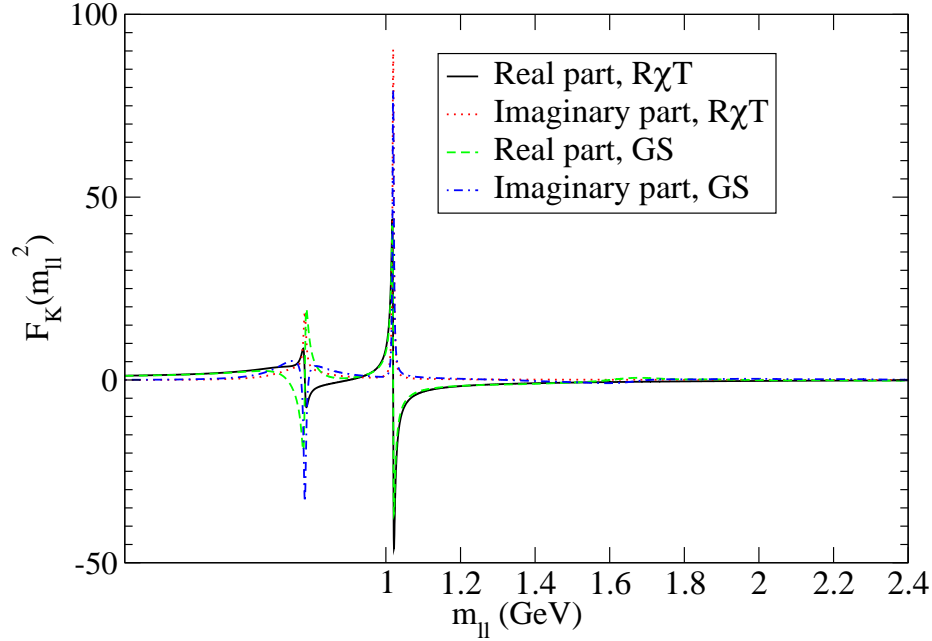


Figure 2.12: Real and imaginary parts of  $F_K(q^2)$  using  $R\chi T$  and GS.

of magnitude just outside the peak of the resonance. That is to say,  $R\chi T$  gives a very good description from threshold to around 1.3 GeV and deviations at higher energies will have a negligible effect on the integrated observables. The remaining structure shown in the BaBar fit (above 1.3 GeV) is due to heavier vector resonances (two  $\phi$ , three  $\rho$  and three  $\omega$ ), which also includes the lightest iso-vector multiplet included in the  $R\chi T$  description.

As previously mentioned, the WA is also considered in the QCDf amplitude, thus, at some point this would mean making a double counting of the same process. Therefore, a check on whether this is happening is needed. To do so, it must be remarked that QCDf is expected to give a more precise description of phenomena for high  $q^2$  region of energy. Also, since  $R\chi T$  is expected to give adequate description of phenomena at small  $q^2$ , we assume there is an intermediate energy scale where both models describe adequately this process. This match must be done at the form factor level,

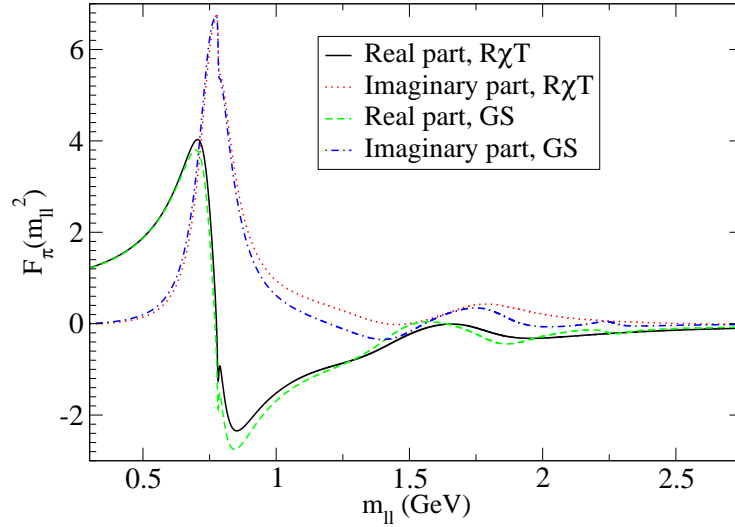


Figure 2.13: Real and imaginary parts of  $F_\pi(q^2)$  using  $R\chi T$  and GS.

meaning that the real (imaginary) part of one model must match the real (imaginary) part of the other model if our assumption is correct. So, a comparison between our model and the fit done by the BaBar collaboration has to be made before trying to match the QCdf and the chiral Lagrangian descriptions. This is shown in Figure 2.13, where we can see that both parametrizations give a similar description of the form factor for  $q^2 \geq 1$  GeV, *i.e.*, in the  $q^2$  region of the  $R_P$  observable. The fact that both parametrizations are significantly different at low  $q^2$  (specifically around the  $\rho(770)$  resonance) for  $P = K$  is expected, since chiral Lagrangians are more precise the lower the energy of the process is.

At the precision order of the QCdf amplitude  $F_V(q^2) = C_9^{\text{eff}}$  is found to make a very smooth match with the chiral Lagrangians description at around 2 GeV<sup>2</sup>. This match is shown in Figure 2.14 and Figure 2.15. This shows that it is meaningless to compute the observables as we proposed, where the chiral Lagrangian amplitude must be taken (for  $q^2 < 1$  GeV<sup>2</sup>, otherwise GS also gives a good parameterization) up to 2 GeV<sup>2</sup> and the QCdf amplitude from  $q^2 = 2$  GeV<sup>2</sup> up to the  $c\bar{c}$  threshold. Our branching ratio for the  $P = \pi$  case can be compared with that of ref [109], however

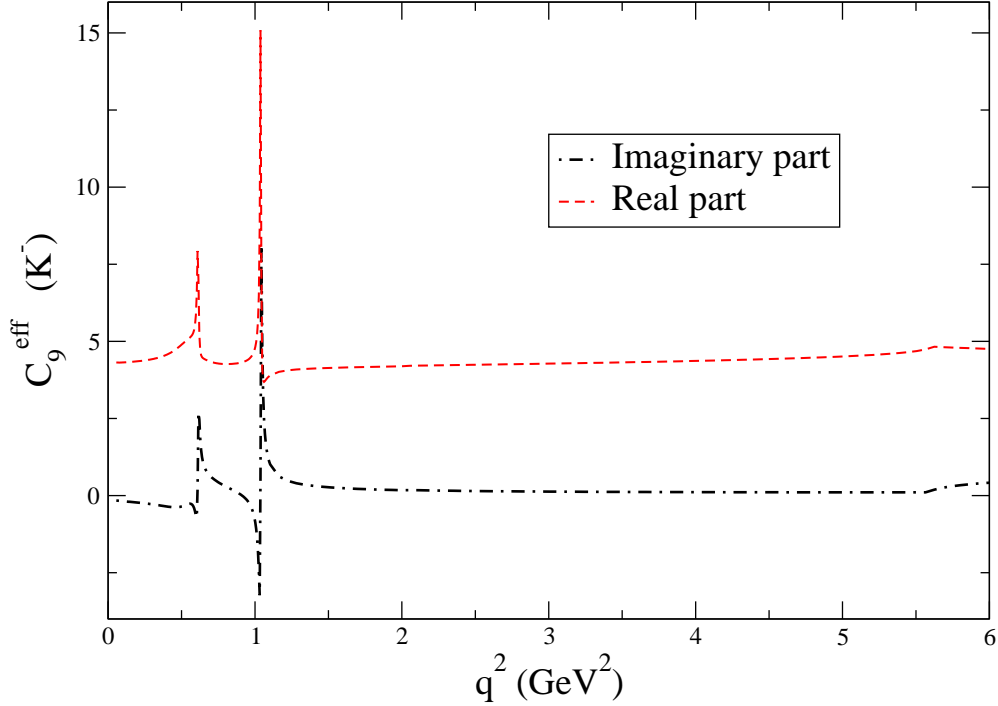


Figure 2.14: The smooth match between LD and QCDf description of  $F_K$  at  $2 \text{ GeV}^2$  is shown.

in their analysis of QCDf parameters, these were fitted to reproduce  $B^+ \rightarrow \pi^0 \ell^+ \nu_\ell$  data. The branching fractions obtained are shown in table 2.2, and since no dedicated study of the errors stemming from the QCDf contribution was made, the errors shown were obtained by rescaling the errors in ref [109] for  $P = \pi$  and in [95] for  $P = K$  according to the different central values obtained by them and us. Also, by using different quark mixing values ([110] and [111]) the branching ratio is  $\sim 5\%$  larger when the parameters from the CKM fitter group is used compared to the result using the PDG values. And thus, the  $R_P$  ratios are  $R_K = 1.0003(1)$  in the  $(1,6) \text{ GeV}^2$  range and  $R_\pi = 1.0006(1)$  in the  $(1,8) \text{ GeV}^2$  range. Finally, to compare our result with that of reference [109] we computed the branching ratio in the whole kinematical domain, which gives  $BR(B^- \rightarrow \pi^- \ell^+ \ell^-) = (2.6_{-0.3}^{+0.4}) \cdot 10^{-8}$ . For the  $K$  channel we find  $BR(B^- \rightarrow K^- \ell^+ \ell^-) = (1.92_{-0.41}^{+0.69}) \cdot 10^{-8}$  for  $q^2 \in [1, 6] \text{ GeV}^2$ . Comparing our

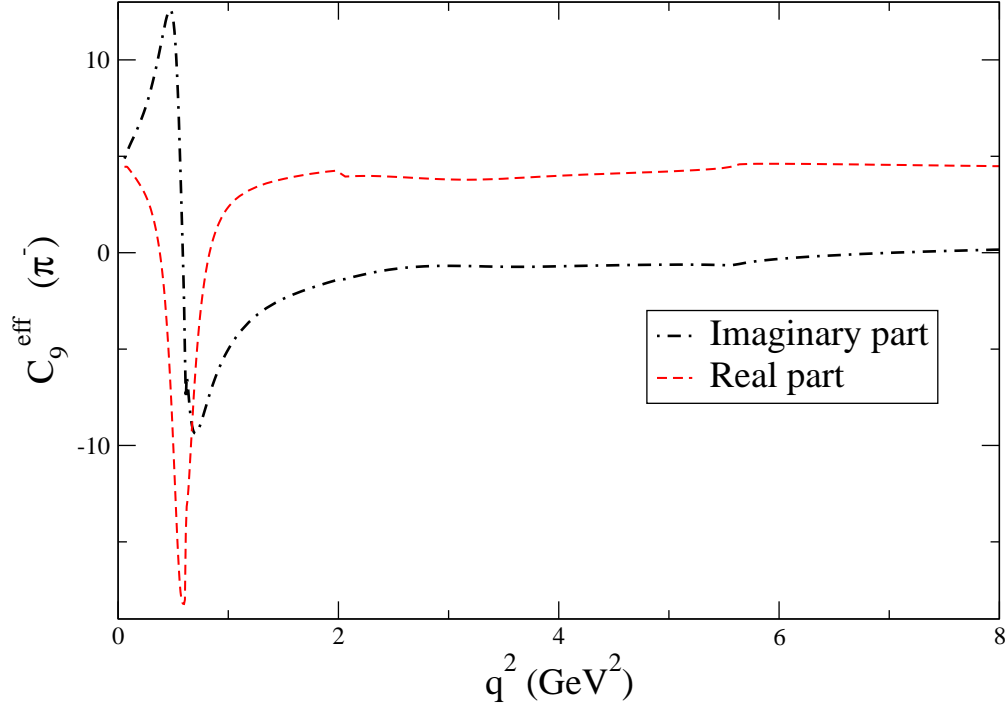


Figure 2.15: The smooth match between LD and QCDf description of  $F_\pi$  at  $2 \text{ GeV}^2$  is shown.

results with the measurements done at BaBar [94, 112]

$$BR(B^- \rightarrow \pi^- \mu^+ \mu^-) = (2.3 \pm 0.6 \pm 0.1) \cdot 10^{-8}, \quad (2.38a)$$

$$BR(B^- \rightarrow K^- e^+ e^-) = (1.56^{+0.20}_{-0.16}) \cdot 10^{-7}, \quad \text{for } 1 < q^2 < 6 \text{ GeV}^2, \quad (2.38b)$$

we see there is a very good agreement within errors.

### 2.3.5 CP Asymmetry

We can analyze further the decays proposed by computing the CP asymmetry in the dilepton invariant mass region where our description works. The interest in this observable stems from the proposal made in ref [113] (within QCDf) that, in these

	$P = \pi$	$P = \pi$	$P = K$
	$0.05 \leq q^2 \leq 8 \text{ GeV}^2$	$1 \leq q^2 \leq 8 \text{ GeV}^2$	$1 \leq q^2 \leq 6 \text{ GeV}^2$
$LD$	$(9.16 \pm 0.15) \cdot 10^{-9}$	$(5.47 \pm 0.05) \cdot 10^{-10}$	$(1.70 \pm 0.21) \cdot 10^{-9}$
Interf	$(-2.62 \pm 0.13) \cdot 10^{-9}$	$(-2_{-1}^{+2}) \cdot 10^{-10}$	$(-6 \pm 2) \cdot 10^{-11}$
$SD$	$(9.83_{-1.04}^{+1.49}) \cdot 10^{-9}$	$(8.71_{-0.90}^{+1.35}) \cdot 10^{-9}$	$(1.90_{-0.41}^{+0.69}) \cdot 10^{-7}$

Table 2.2: LD, SD and their interference contributions to the branching ratio for both channels.

decays a large CP asymmetry might come about. By inspecting the behavior of the form factor in Figure 2.15 a measurable CP asymmetry seems possible, due to the large values of the real and imaginary parts of  $P_\pi(q^2)$ . Since the off-shell width of the vector resonances describes the imaginary part of the electromagnetic form factor of the pseudo-Goldstone bosons, it will be responsible for the strong phase required to generate the CP asymmetry. The CP asymmetry is defined as follows,

$$A_{CP}(P) = \frac{\Gamma(B^+ \rightarrow P^+ \ell^+ \ell^-) - \Gamma(B^- \rightarrow P^- \ell^+ \ell^-)}{\Gamma(B^+ \rightarrow P^+ \ell^+ \ell^-) + \Gamma(B^- \rightarrow P^- \ell^+ \ell^-)}. \quad (2.39)$$

As just mentioned above, the CP asymmetry will be mainly consequence of the off-shell width of vector resonances, but for  $q^2 \geq 2 \text{ GeV}^2$  it must be verified that QCDf also gives a measurable asymmetry. There are, in fact two sources of such asymmetry. The first stems from on-shell radiating light quarks, since heavy quarks bremsstrahlung is suppressed by a factor  $m_q/m_b$ , where  $m_{q(b)}$  is the mass of the light ( $b$ ) quark. The second source arises from light  $q\bar{q}$  loops ref [113]. The CP asymmetry taking into account all the previously mentioned effects for different  $q^2$  ranges is shown in Table 2.3.

$(q_{\min}^2, q_{\max}^2)$	Ref [113]	$P = \pi$	$P = K$
$(1, 8) \text{ GeV}^2$	$13 \pm 2$	$7.8 \pm 2.9$	—
$(1, 6) \text{ GeV}^2$	$16 \pm 2$	$9.2 \pm 1.7$	$-1.0 \pm 0.3$
$(2, 6) \text{ GeV}^2$	$13_{-3}^{+2}$	$7.7 \pm 0.5$	—
$(0.05, 8) \text{ GeV}^2$	—	$16.1 \pm 1.9$	—

Table 2.3: CP asymmetry computed for different  $q^2$  ranges, all values are given as percentages.

For  $P = \pi$ , in the  $(0.05, 8) \text{ GeV}^2$  range, 83% of the  $A_{CP}$  has a LD WA origin,

while in the  $(1,8)$   $\text{GeV}^2$  this contribution is reduced to a 31%. For  $P = K$ , 70% of the asymmetry is due to LD WA. As seen in Table 2.3, in ref [113] the  $A_{CP}(\pi)$  was predicted to be larger than ours, while in ref [114] reports a result that lies between both predictions (for  $(1,6)$   $\text{GeV}^2$  they predict  $A_{CP}(\pi) = (14.3^{+2.9}_{-3.5})\%$ ).

A remark regarding the  $F_B(q^2)$  needs to be done. By computing the CP asymmetry from muon threshold we obtained a contribution to this observable that is completely negligible, since its contribution is smaller than the uncertainty, namely  $\mathcal{O}(10^{-4})$ . Also note that the asymmetry becomes significantly larger as  $q^2$  becomes smaller. That is to say, the CP asymmetry becomes larger as  $q_{min}^2$  moves towards the region where the predictions based on QCDf are not reliable.

Currently, experimental data gives  $A_{CP}$  values consistent with zero ( $A_{CP}(K) = 0.011 \pm 0.017$  [110] and  $A_{CP}(\pi) = -0.11 \pm 0.12$ ), but within errors are also compatible with the different theoretical predictions.

Despite the fact that one-photon exchange diagrams at leading order give a small contribution to the decay rates, within the Standard Model they can generate a non-negligible CP asymmetry. This CP asymmetry together with measurements of the decay rates can be used as test in the decays studied in this chapter. This makes us emphasize the need of a dedicated measurement of these observables at LHCb in the next run and in the forthcoming Belle-II experiment.

### 2.3.6 Conclusions

We computed the  $\mathcal{M}(B \rightarrow P\ell^+\ell^-)$  amplitude for  $P = \pi, K$  obtaining a contribution that had not been considered before in the analysis of this process. Our contribution for the  $K$  channel is a correction  $\sim 1\%$ , which we believe cannot be measured in the forthcoming experiments.

However, for  $P = \pi$  the contribution becomes very significant when  $q_{min}^2$  is lowered near the threshold. This suggests that the  $[1, 8]$   $\text{GeV}^2$  range is free from hadronic

pollution (within current experimental errors). On the other hand, more refined measurements of the fully integrated branching fraction for this decay could be sensitive to our contribution once the error is reduced below half of the current uncertainty.

Interestingly, the different weak and strong phases of the QCDf and LD WA one photon exchange contributions are capable to generate a CP asymmetry. Again, this CP asymmetry is large in the case of a pion in the initial state for  $q$  taken from threshold, but also sizable and worth to measure in the experimental range for the leptons squared invariant mass. For the  $K$ , the range  $1 \leq q^2 \leq 6 \text{ GeV}^2$  is optimal for such search. Our CP asymmetry result and the magnitudes of the decay rates at LHCb and future Belle II can provide another non-trivial test of the SM.



# Chapter 3

## New charged current structures

### 3.1 Introduction

The question of whether weak charged currents are different to those coupled with the  $W$  boson has a great relevance in nowadays High Intensity Frontier experiments, as it offers an excellent place for the search of Beyond Standard Model (BSM) effects. Several extensions to the SM predict new charged currents whose origins might stem, for example, on quark-lepton symmetries (leptoquarks) or additional copies of the BEH scalar doublet (charged Higgs), which would induce a scalar charged current instead of the  $V - A$  weak current described in chapter 1.

In semileptonic processes, these currents can be classified by means of  $G$ -parity into first and Second Class Currents (SCC). This parity taken as an extension of the charge conjugation  $C$  is defined by  $G := Ce^{i\pi I_2}$ , where  $I_2$  is the generator of isospin rotations [115]. If  $G$ -parity was an exact symmetry, there would only be first class currents in the SM, however, it is not since isospin violating processes will induce SCC. Although SCC are present within the SM, they are highly suppressed with respect to the first class ones, which keeps the feature of a good test of the SM.

In this chapter we compute the  $\tau \rightarrow \pi\eta^{(\prime)}\gamma\nu_\tau$  decay as a background for the search of SCC. We compare our results with the  $\tau \rightarrow \pi\eta^{(\prime)}\nu_\tau$  decay, which is the cleanest channel of those proposed for the search of these currents [116] with predicted  $BR \lesssim 10^{-5}$  [119]. The latter can be induced by  $G$ -parity breaking, while the former will receive contributions from first class currents and a very suppressed contribution from second class ones. Experimental limits on these processes are near the theoretical estimates based on isospin breaking [120, 121, 122]. Since Belle-II increase considerably the luminosity compared to previous B-factories, these isospin breaking

decays are likely to be measured. We, therefore, look for a sufficiently low cut in the photon energy such that the radiative process (above such cut) can be neglected as background in the search for BSM SCC.

In section 3.2 we show the relevant

### 3.2 Matrix Element and Form Factors

The  $\tau \rightarrow \pi\eta^{(\prime)}\gamma\nu_\tau$  process does not present  $G$ -parity suppression, since the photon is not an isospin eigenstate. It also will have, as stated before, bremsstrahlung contributions stemming from the  $G$  suppressed process which will be further suppressed by a factor  $\alpha$ . Contributions from the effective vertex  $W\pi\eta\gamma$ , which does not present the  $G$  suppression, is expected to give an effect comparable to the non radiative process.

To check this assertion we compute the amplitude with the convention  $\tau^-(P) \rightarrow \pi^-(p)\eta^{(\prime)}(p_0)\nu(p')\gamma(k, \epsilon)$ , given by

$$\mathcal{M} = \frac{eG_F V_{ud}^*}{\sqrt{2}} \epsilon^{*\mu} \{ (V_{\mu\nu} - A_{\mu\nu}) \bar{u}(p') \gamma^\nu (1 - \gamma_5) u(P) \} . \quad (3.1)$$

where the bremsstrahlung contribution has been neglected, *i. e.*, eq. (3.1) gives the leading contribution to our process which originates from the  $W\pi\eta\gamma$  effective vertex. Here, the hadronic tensors  $V_{\mu\nu}$  and  $A_{\mu\nu}$  are directly related to the vector and axial-vector contributions to the effective vertex in fig. 3.1 and are parametrized as follows [117, 118]

$$\begin{aligned} V_{\mu\nu} &= v_1(p.k g_{\mu\nu} - p_\mu k_\nu) + v_2(g_{\mu\nu} p_0.k - p_{0\mu} k_\nu) \\ &\quad + v_3(p_\mu p_0.k - p_{0\mu} p.k) p_\nu + v_4(p_\mu p_0.k - p_{0\mu} p.k) p_{0\nu} \\ A_{\mu\nu} &= i\varepsilon_{\mu\nu\rho\sigma} (a_1 p_0^\rho k^\sigma + a_2 k^\rho W^\sigma) + i\varepsilon_{\mu\rho\sigma\tau} k^\rho p^\sigma p_0^\tau (a_3 W_\nu + a_4 (p_0 + k)_\nu) , \end{aligned} \quad (3.2)$$

where  $W = P - p' = p + p_0 + k$ . These tensors depend on four vector ( $v_i$ ) and four axial ( $a_i$ ) form factors, respectively, depending on three Lorentz scalars.

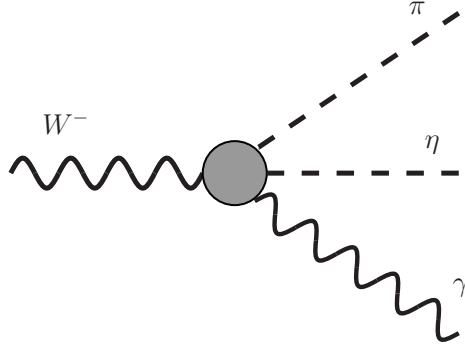


Figure 3.1: Effective hadronic vertex (grey blob) that defines the  $V_{\mu\nu}$  and  $A_{\mu\nu}$  tensors.

We have argued that bremsstrahlung amplitudes will give a negligible contribution to the process, however we can go further and try to give an estimate of whether this is true for a reasonable experimental cut in the energy of the photon. The way to do this is by using Low's theorem [123], which tells that an amplitude with a real photon will have the dependence

$$\mathcal{M}_\gamma = \frac{A}{k} + B + \mathcal{O}(k), \quad (3.3)$$

where  $A$  and  $B$  are given in terms of the non radiative amplitude  $\mathcal{M}_0$ . Since the four momentum is taken to be very small, one can expand the radiative amplitude as

$$\mathcal{M}_\gamma = -e\mathcal{M}_0 \left( \frac{P \cdot \epsilon}{P \cdot k} - \frac{p \cdot \epsilon}{p \cdot k} \right) + \dots, \quad (3.4)$$

and the amplitude  $\mathcal{M}_0$  can be taken to be independent of  $k$ . Then, the  $\mathcal{M}_0$  amplitude can be calculated with the expressions of ref. [124]. The infrared divergence might surpass the suppression and give a comparable contribution, therefore one needs to establish a minimum energy in order to determine the kinematical region of the phase space to be probed. By choosing this threshold as 10 MeV, photons with smaller energies will not be included. Thus, we obtain the bremsstrahlung contribution to the branching fractions  $BR(\tau \rightarrow \pi\eta\gamma\nu_\tau) \sim 2.5 \times 10^{-8}$  and for  $BR(\tau \rightarrow \pi\eta'\gamma\nu_\tau) \sim 4.6 \times$

$10^{-12}$  for an energy cut  $E_\gamma > 10$  MeV, and the corresponding photon energy spectra is shown in fig. 3.2. Now we can safely neglect the bremsstrahlung contribution to our process.

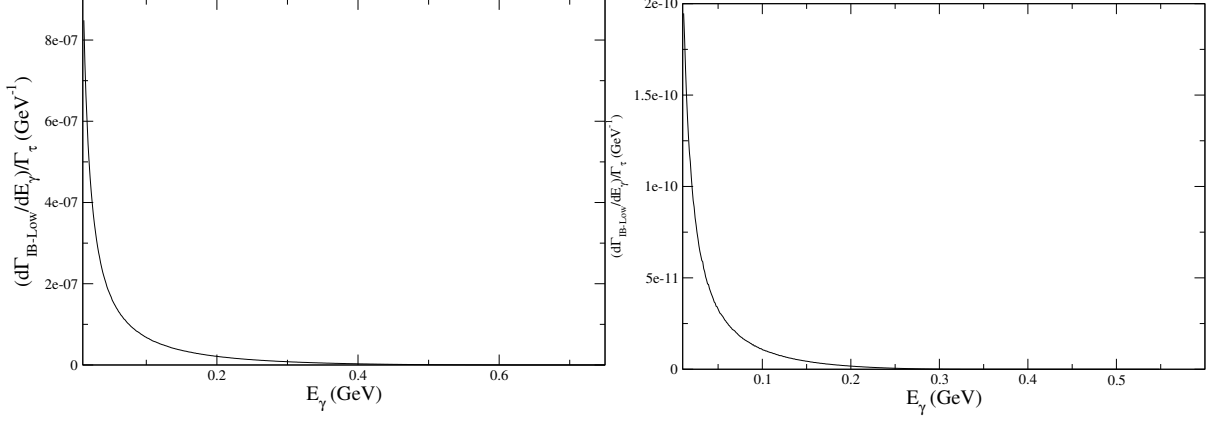


Figure 3.2: Photon energy spectra for the leading bremsstrahlung terms in  $BR(\tau \rightarrow \pi\eta^{(\prime)}\gamma\nu_\tau)$

### 3.3 Meson dominance model prediction

Before trying to give the very complex description of the problem within R $\chi$ T, we will estimate the form factors of the process in the Meson Dominance Model (MDM) [75], which are given by a considerably smaller amount of diagrams. In this model weak and electromagnetic couplings are dominated by the exchange of a few light mesons and their excitations. The determination of the relevant couplings is done phenomenologically and by symmetry relations of the theory.

Therefore one needs to compute all the processes in fig. 3.3 to obtain the MDM contribution to the form factors, where the diagram with the  $b_1(1235)$  exchange can be neglected given  $BR(b_1 \rightarrow \pi\gamma) = (1.6 \pm 0.4)10^{-3}$  and  $BR(b_1 \rightarrow \rho\eta) < 10\%$ . Also, the contribution from the pion pole in the last diagram in figure 3.3 will be suppressed since the pion will be far off its mass-shell.

The Feynman rules for the different vertices in the diagrams are

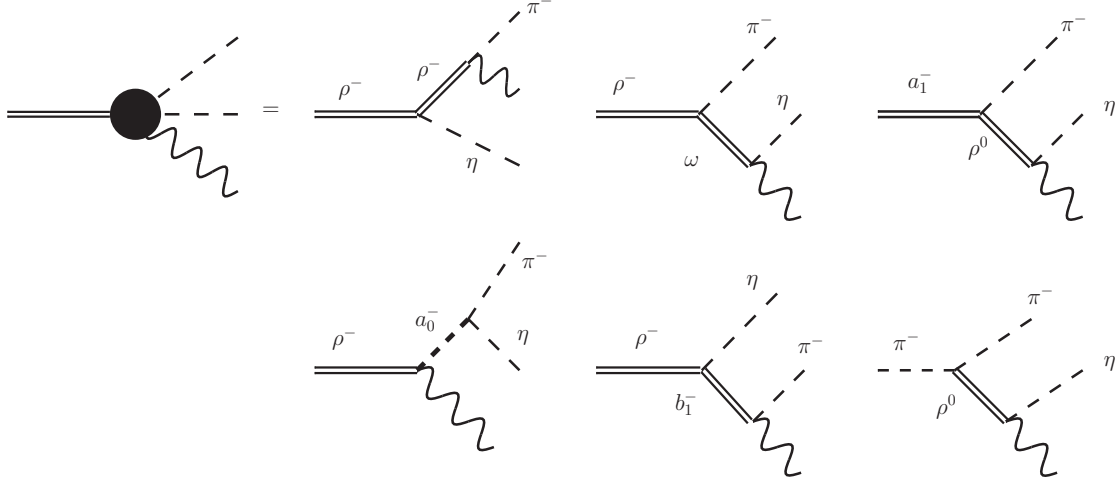


Figure 3.3: Contributions to the effective weak vertex in the MDM model. The wavy line denotes the photon.

$$V'^{\mu}(r) \rightarrow V^{\alpha}(s)P(t) : ig_{V'VP}\epsilon^{\mu\alpha\rho\sigma}s_{\rho}t_{\sigma}, \quad (3.5)$$

$$V^{\mu}(r) \rightarrow \gamma^{\alpha}(s)P(t) : ig_{VP\gamma}\epsilon^{\mu\alpha\rho\sigma}s_{\rho}t_{\sigma}, \quad (3.6)$$

$$A^{\mu}(r) \rightarrow V^{\alpha}(s)P(t) : ig_{VAP}(r \cdot sg_{\mu\alpha} - r_{\alpha}s_{\mu}), \quad (3.7)$$

$$V^{\mu}(r) \rightarrow \gamma^{\alpha}(s)S(t) : ig_{VS\gamma}(r \cdot sg_{\mu\alpha} - r_{\alpha}s_{\mu}), \quad (3.8)$$

$$S(r) \rightarrow P(s)P'(t) : ig_{SPP'}. \quad (3.9)$$

The following contributions to the effective weak vertex are found (the superscripts denote the ordering of diagrams in the right-hand side of figure 3.3), from left to right and from top to bottom; we have used the following definition  $\mathcal{H}_{\nu} = (V_{\mu\nu}^{SD} - A_{\mu\nu})\epsilon^{*\mu}$ :

$$\mathcal{H}_\nu^a = \frac{i\sqrt{2}m_\rho^2}{g_\rho} g_{\rho^-\rho^-\eta} g_{\rho^-\pi^-\gamma} \frac{1}{D_\rho(W^2)} \frac{1}{D_\rho((p+k)^2)} \times \varepsilon_{\nu\alpha\rho\sigma} (p+k)^\rho p_0^\sigma \varepsilon^{\alpha\mu\gamma\delta} k_\gamma p_{0\delta} \epsilon_\mu^*, \quad (3.10)$$

$$\mathcal{H}_\nu^b = \frac{i\sqrt{2}m_\rho^2}{g_\rho} g_{\rho^-\omega\pi^-} g_{\omega\eta\gamma} \frac{1}{D_\rho(W^2)} \frac{1}{D_\omega((p_0+k)^2)} \times \varepsilon_{\nu\alpha\rho\sigma} (p_0+k)^\rho p^\sigma \varepsilon^{\alpha\mu\gamma\delta} k_\gamma p_{0\delta} \epsilon_\mu^*, \quad (3.11)$$

$$\mathcal{H}_\nu^c = \frac{i\sqrt{2}m_{a_1}^2}{g_{a_1}} g_{\rho^0 a_1^- \pi^-} g_{\rho^0 \eta \gamma} ((p_0+k) \cdot W g_{\nu\alpha} - W_\alpha (p_0+k)_\nu) \times \frac{1}{D_{a_1}(W^2) D_\rho((p_0+k)^2)} \varepsilon^{\alpha\mu\gamma\delta} k_\gamma p_{0\delta} \epsilon_\mu^*, \quad (3.12)$$

$$\mathcal{H}_\nu^d = \frac{i\sqrt{2}m_\rho^2}{g_\rho} g_{\rho^-\alpha_0^- \gamma} g_{\alpha_0^- \pi^-\eta} (W \cdot k g_{\mu\nu} - k_\nu W_\mu) \epsilon^{*\mu} \frac{1}{D_\rho(W^2) D_{a_0}((p+p_0)^2)}. \quad (3.13)$$

In the above expressions, we have defined  $D_X(Q^2)$  as the denominator of the meson propagator, which may (or not) have an energy-dependent width;  $g_X$  represents the weak couplings of spin-one mesons, defined here as  $\langle X | J_\mu | 0 \rangle = i\sqrt{2}m_X^2/g_X \eta_\mu$  ( $\eta_\mu$  is the polarization four-vector of meson  $X$ ) and  $g_{XYZ}$  denotes the trilinear coupling among mesons  $XYZ$ . The effects of the  $\rho$  meson excitations can be taken into account through the following replacement

$$\frac{\sqrt{2}m_\rho^2}{g_\rho} \frac{1}{D_\rho(W^2)} \rightarrow \frac{\sqrt{2}}{g_{\rho\pi\pi}} \frac{1}{1+\beta_\rho} [BW_\rho(W^2) + \beta_\rho BW_{\rho'}(W^2)], \quad (3.14)$$

where

$$BW_\rho(W^2) = \frac{m_\rho^2}{m_\rho^2 - W^2 - im_\rho \Gamma_\rho(W^2)}, \quad (3.15)$$

with  $BW_\rho(0) = 1$  and  $\beta_\rho$  encodes the strength of the  $\rho' = \rho(1450)$  meson contribution. The  $\rho \rightarrow \pi\pi$  coupling is denoted  $g_{\rho\pi\pi}$  and  $BW_{a_0}(X^2)$ ,  $BW_{a_1}(X^2)$  and  $BW_\omega(X^2)$  are defined in analogy to  $BW_\rho(W^2)$ .

Note that all the amplitudes in eqs. (3.10) to (3.13) are of  $\mathcal{O}(k)$  in agreement with Low's theorem. All of them correspond to contributions to the vector current, except eq. (3.12), which is due to the axial-vector current.

The MDM leads to the following form factors:

$$v_1^{MDM} = iC_\rho(W^2) \left[ -\frac{g_{\rho^- \rho^- \eta} g_{\rho^- \pi^- \gamma}}{D_\rho[(p+k)^2]} p \cdot p_0 + \frac{g_{\rho^- \omega \pi^-} g_{\omega \eta \gamma}}{D_\omega[(p_0+k)^2]} p_0 \cdot (p_0 + k) + \frac{g_{\rho^- a_0^- \gamma} g_{a_0^- \pi^- \eta}}{D_{a_0}[(p+p_0)^2]} \right], \quad (3.16)$$

$$v_2^{MDM} = iC_\rho(W^2) \left[ \frac{g_{\rho^- \rho^- \eta} g_{\rho^- \pi^- \gamma}}{D_\rho[(p+k)^2]} p \cdot (p+k) - \frac{g_{\rho^- \omega \pi^-} g_{\omega \eta \gamma}}{D_\omega[(p_0+k)^2]} p \cdot p_0 + \frac{g_{\rho^- a_0^- \gamma} g_{a_0^- \pi^- \eta}}{D_{a_0}[(p+p_0)^2]} \right], \quad (3.17)$$

$$v_3^{MDM} = iC_\rho(W^2) \left[ -\frac{g_{\rho^- \rho^- \eta} g_{\rho^- \pi^- \gamma}}{D_\rho[(p+k)^2]} \right], \quad (3.18)$$

$$v_4^{MDM} = iC_\rho(W^2) \left[ \frac{g_{\rho^- \omega \pi^-} g_{\omega \eta \gamma}}{D_\omega[(p_0+k)^2]} \right], \quad (3.19)$$

$$a_1^{MDM} = C_A(W^2) \left[ \frac{g_{\rho^0 a_1^- \pi^-} g_{\rho^0 \eta \gamma}}{D_\rho[(p_0+k)^2]} \right] (p_0 + k) \cdot W, \quad (3.20)$$

$$a_2^{MDM} = 0, \quad (3.21)$$

$$a_3^{MDM} = 0, \quad (3.22)$$

$$a_4^{MDM} = -\frac{a_1^{MDM}}{(p_0 + k) \cdot W}. \quad (3.23)$$

In the above equations the shorthand notation  $C_X(W^2) = \sqrt{2}m_X^2/[g_X D_X(W^2)]$  has been used.

The coupling constants required in MDM are defined in equations (3.5)-(3.9). Comparisons of the calculated and measured rates allows to determine the relevant coupling constants assuming they are real and positive as indicated in the following.

- We can use the  $\tau^- \rightarrow (\rho, a_1)^- \nu_\tau$  decays to extract the (axial-)vector weak coupling constants defined as indicated before. We use the decay width for  $\tau^- \rightarrow X^- \nu_\tau$

$$\Gamma(\tau^- \rightarrow \nu_\tau X^-) = \frac{G_F^2 |V_{ud}|^2}{8\pi M_\tau^3} \frac{M_X^2}{g_X^2} (M_\tau^2 - M_X^2)^2 (M_\tau^2 + 2M_X^2). \quad (3.24)$$

For the  $a_1(1260)$  we assume  $BR(\tau^- \rightarrow a_1^- \nu_\tau) = 0.1861 \pm 0.0013$  [72]. Similarly, we can extract  $g_\rho$  from  $\tau^- \rightarrow \rho^- \nu_\tau$  decays; instead, we compare the measured value of the  $\rho^0 \rightarrow \ell^+ \ell^-$  decay width with

$$\Gamma(\rho^0 \rightarrow \ell^+ \ell^-) = \frac{4\pi}{3} \left( \frac{\alpha}{g_\rho} \right)^2 \left( 1 + \frac{2m_\ell^2}{M_V^2} \right) \sqrt{M_V^2 - 4m_\ell^2}. \quad (3.25)$$

- We extract the coupling constants  $g_{VP\gamma}$  from the  $V^\mu \rightarrow \gamma^\alpha(s)P(t)$  decays, using the decay width

$$\Gamma(V \rightarrow P\gamma) = \frac{|g_{VP\gamma}|^2}{96\pi M_V^3} (M_V^2 - M_P^2)^3. \quad (3.26)$$

This expression, together with  $\Gamma(\rho/\omega \rightarrow \pi/\eta \gamma)$  [72] allows to determine four of the required coupling constants.

- In order to fix the  $\rho a_1 \pi$  coupling we consider the decay amplitude  $\mathcal{M} = ig_{\rho a_1 \pi}(r \cdot sg_{\mu\alpha} - r_\alpha s_\mu) \eta_{a_1}^\mu \eta_\rho^{*\alpha}$ , for  $a_1^\mu(r, \eta_{a_1}) \rightarrow \rho^\alpha(s, \eta_\rho) \pi(t)$  decays. This gives the decay rate ( $\lambda(a, b, c)$  is the ordinary Kälén function)

$$\Gamma(a_1 \rightarrow \rho\pi) = \frac{|g_{\rho a_1 \pi}|^2}{96\pi M_{a_1}^3} [\lambda(M_{a_1}^2, M_\rho^2, m_\pi^2) + 6M_\rho^2 M_{a_1}^2] \lambda^{1/2}(M_{a_1}^2, M_\rho^2, m_\pi^2). \quad (3.27)$$

According to the PDG16 [72]  $a_1 \rightarrow \rho\pi$  decays make up 61.5% [125] of the total decay width of  $a_1(1260)$ , which we take as  $\Gamma_{a_1} = (475 \pm 175)$  MeV [72]. Using isospin symmetry to relate the two decay modes of charged  $a_1$  mesons lead us to the result in Table 3.1.

- The following partial widths of  $a_0(980)$  meson

$$\Gamma(a_0 \rightarrow \gamma\gamma) = \frac{|g_{a_0\gamma\gamma}|^2}{32\pi} M_{a_0}^3, \quad (3.28)$$

$$\Gamma(a_0 \rightarrow \pi\eta) = \frac{|g_{a_0\pi\eta}|^2}{16\pi M_{a_0}^3} \lambda^{1/2}(M_{a_0}^2, m_\eta^2, m_\pi^2), \quad (3.29)$$

can be used to extract the required coupling constants involving the  $a_0$  meson. Neither of these individual  $a_0$  decay rates have been measured separately. Instead, measurements of their product have been reported by several groups with



good agreement among them. The average value reported in PDG16 [72] is

$$\Gamma(a_0 \rightarrow \gamma\gamma) \times \frac{\Gamma(a_0 \rightarrow \pi\eta)}{\Gamma_{a_0}} = (0.21_{-0.04}^{+0.08}) \text{ keV}. \quad (3.30)$$

We can extract the product of coupling constants of the  $a_0$  by comparing the previous equations and using  $\Gamma_{a_0} = (75.6 \pm 1.6_{-10.0}^{+17.4}) \text{ MeV}$  [126] for the total decay width.

- The coupling  $g_{\rho\omega\pi}$  was fixed using the relation

$$g_{\rho\omega\pi} = \frac{G^8}{\sqrt{3}} \left[ \sin\theta_V + \sqrt{2}r\cos\theta_V \right], \quad (3.31)$$

where  $G^8$  ( $G^0$ ) is the  $SU(3)$  invariant coupling of one pseudoscalar meson with two octets (one octet and one singlet) of vector mesons, and  $r \equiv G^0/G^8$ . Using the rates of  $V \rightarrow P\gamma$  decays and assuming ideal  $\omega - \phi$  mixing,  $\theta_V = \tan^{-1} \left( \frac{1}{\sqrt{2}} \right)$ , one gets  $G^8 = (1.052 \pm 0.032) \cdot 10^{-2} \text{ MeV}^{-1}$  and  $r = 1.088 \pm 0.018$  [75].

- The following MDM relations between strong and electromagnetic couplings

$$g_{\rho\rho\eta} = \frac{g_\rho}{e} g_{\rho\eta\gamma}, \quad g_{a_0\rho\gamma} = \frac{g_\rho}{e} g_{a_0\gamma\gamma}. \quad (3.32)$$

can be used to extract other relevant coupling constants.

- Finally for the decays involving the  $\eta'$  meson, the couplings  $g_{a_0\pi\eta'}$ ,  $g_{\rho\rho\eta'}$ ,  $g_{\omega\eta'\gamma}$  and  $g_{\rho\eta'\gamma}$  need to be determined. Employing the above formulas it is straightforward to obtain the last two from the measured  $\Gamma(\eta' \rightarrow \omega\gamma)$  and  $\Gamma(\eta' \rightarrow \rho\gamma)$  decays [72].  $g_{\rho\rho\eta'}$  is fixed in terms of  $g_{\rho\eta'\gamma}$  in analogy to eq. (3.32). It is not possible to determine  $g_{a_0\pi\eta'}$  easily, because the involved masses forbid all possible one-to-two body decays. However, according to [127],  $g_{a_0\pi\eta'} \ll g_{a_0\pi\eta}$ . We will take  $g_{a_0\pi\eta'}/g_{a_0\pi\eta} \leq 0.1$  as a conservative estimate.

In table 3.1 we show the values of the coupling constants obtained using the above procedure. The errors are propagated from the experimental ones adding

Coupling constant	Fitted value
$g_\rho$	$5.0 \pm 0.1$
$g_{a_1}$	$7.43 \pm 0.03$
$eg_{\rho\eta\gamma}$	$(4.80 \pm 0.16) \times 10^{-1} \text{ GeV}^{-1}$
$g_{\rho\rho\eta}$	$(7.9 \pm 0.3) \text{ GeV}^{-1}$
$eg_{\omega\eta\gamma}$	$(1.36 \pm 0.06) \times 10^{-1} \text{ GeV}^{-1}$
$eg_{\rho\pi\gamma}$	$(2.19 \pm 0.12) \times 10^{-1} \text{ GeV}^{-1}$
$g_{\rho\omega\pi}$	$(11.1 \pm 0.5) \text{ GeV}^{-1}$
$g_{a_1\rho\pi}$	$(3.9 \pm 1.0) \text{ GeV}^{-1}$
$eg_{\rho a_0\gamma}$	$(9.2 \pm 1.6) \times 10^{-2} \text{ GeV}^{-1}$
$g_{a_0\pi\eta}$	$(2.2 \pm 0.9) \text{ GeV}$
$eg_{\rho\eta'\gamma}$	$(4.01 \pm 0.13) \times 10^{-1} \text{ GeV}^{-1}$
$eg_{\omega\eta'\gamma}$	$(1.30 \pm 0.08) \times 10^{-1} \text{ GeV}^{-1}$
$g_{\rho\rho\eta'}$	$(6.6 \pm 0.2) \text{ GeV}^{-1}$
$g_{a_0\pi\eta'}/g_{a_0\pi\eta}$	$\leq 0.1$

Table 3.1: Our fitted values of the coupling parameters. Those involving a photon are given multiplied by the unit of electric charge.

them in quadrature. In section 3.5.1 we will present the MDM predictions for the  $\tau^- \rightarrow \pi^- \eta^{(\prime)} \gamma \nu_\tau$  decays using these inputs.

## 3.4 Resonance Chiral Theory

### 3.4.1 Resonance Lagrangian operators

The interaction terms linear in resonance fields which -upon their integration out- contribute to the low-energy constants of the  $\chi PT$  Lagrangian at  $\mathcal{O}(p^4)$  were also derived in refs. [63, 64, 128]. These are

$$\begin{aligned}
\mathcal{L}^R = & c_d \langle S u^\mu u_\mu \rangle + c_m \langle S \chi_+ \rangle + i d_m \langle P \chi_- \rangle + i \frac{d_{m0}}{N_F} \langle P \rangle \langle \chi_- \rangle \\
& + \frac{F_V}{2\sqrt{2}} \langle V_{\mu\nu} f_+^{\mu\nu} \rangle + i \frac{G_V}{\sqrt{2}} \langle V_{\mu\nu} u^\mu u^\nu \rangle + \frac{F_A}{2\sqrt{2}} \langle A_{\mu\nu} f_-^{\mu\nu} \rangle .
\end{aligned} \tag{3.33}$$

The last two operators on the first line involving pseudoscalar resonances do not play any role in our study <sup>1</sup> because they couple the pseudoscalar resonances to spin-zero sources instead of to the weak  $V - A$  current.

Resonant operators contributing at  $\mathcal{O}(p^6)$  in the chiral expansion (in the low-energy limit) were studied systematically in refs. [130] and [129] for the even- and odd-intrinsic parity sectors, respectively. We will be discussing those entering our study of  $\tau^- \rightarrow \pi^- \eta^{(\prime)} \gamma \nu_\tau$  decays in the following.

We will consider first the even-intrinsic parity sector and start with the operators containing one resonance field. There, only one of the operators involving a scalar resonance matters to our analysis:  $\mathcal{O}_{15}^S = \langle S f_+^{\mu\nu} f_{+\mu\nu} \rangle$  [130], while again no operators including pseudoscalar resonances contribute (in either intrinsic parity sector).

The corresponding Lagrangian with one vector resonance field was derived in ref. [130]:

$$\mathcal{L}_{(4)}^V = \sum_{i=1}^{22} \lambda_i^V \mathcal{O}_i^V, \quad (3.34)$$

---

<sup>1</sup>Although it may seem that the operator with coefficient  $d_{m0}$  is suppressed with respect to the others in eq. (3.33) because of its additional trace, this is not the case since it is enhanced due to  $\eta'$  exchange [129].

with the operators

$$\begin{aligned}
\mathcal{O}_1^V &= i \langle V_{\mu\nu} u^\mu u_\alpha u^\alpha u^\nu \rangle \quad , \quad \mathcal{O}_2^V = i \langle V_{\mu\nu} u^\alpha u^\mu u^\nu u_\alpha \rangle , \\
\mathcal{O}_3^V &= i \langle V_{\mu\nu} \{ u^\alpha, u^\mu u_\alpha u^\nu \} \rangle \quad , \quad \mathcal{O}_4^V = i \langle V_{\mu\nu} \{ u^\mu u^\nu, u^\alpha u_\alpha \} \rangle , \\
\mathcal{O}_5^V &= i \langle V_{\mu\nu} f_-^{\mu\alpha} f_-^{\nu\beta} \rangle g_{\alpha\beta} \quad , \quad \mathcal{O}_6^V = \langle V_{\mu\nu} \{ f_+^{\mu\nu}, \chi_+ \} \rangle , \\
\mathcal{O}_7^V &= i \langle V_{\mu\nu} f_+^{\mu\alpha} f_+^{\nu\beta} \rangle g_{\alpha\beta} \quad , \quad \mathcal{O}_8^V = i \langle V_{\mu\nu} \{ \chi_+, u^\mu u^\nu \} \rangle , \\
\mathcal{O}_9^V &= i \langle V_{\mu\nu} u^\mu \chi_+ u^\nu \rangle \quad , \quad \mathcal{O}_{10}^V = \langle V_{\mu\nu} [ u^\mu, \nabla^\nu \chi_- ] \rangle , \\
\mathcal{O}_{11}^V &= \langle V_{\mu\nu} \{ f_+^{\mu\nu}, u^\alpha u_\alpha \} \rangle \quad , \quad \mathcal{O}_{12}^V = \langle V_{\mu\nu} u_\alpha f_+^{\mu\nu} u^\alpha \rangle , \\
\mathcal{O}_{13}^V &= \langle V_{\mu\nu} ( u^\mu f_+^{\nu\alpha} u_\alpha + u_\alpha f_+^{\nu\alpha} u^\mu ) \rangle \quad , \quad \mathcal{O}_{14}^V = \langle V_{\mu\nu} ( u^\mu u_\alpha f_+^{\alpha\nu} + f_+^{\alpha\nu} u_\alpha u^\mu ) \rangle , \\
\mathcal{O}_{15}^V &= \langle V_{\mu\nu} ( u_\alpha u^\mu f_+^{\alpha\nu} + f_+^{\alpha\nu} u^\mu u_\alpha ) \rangle \quad , \quad \mathcal{O}_{16}^V = i \langle V_{\mu\nu} [ \nabla^\mu f_-^{\nu\alpha}, u_\alpha ] \rangle , \\
\mathcal{O}_{17}^V &= i \langle V_{\mu\nu} [ \nabla_\alpha f_-^{\mu\nu}, u^\alpha ] \rangle \quad , \quad \mathcal{O}_{18}^V = i \langle V_{\mu\nu} [ \nabla_\alpha f_-^{\alpha\mu}, u^\nu ] \rangle , \\
\mathcal{O}_{19}^V &= i \langle V_{\mu\nu} [ f_-^{\mu\alpha}, h_\alpha^\nu ] \rangle \quad , \quad \mathcal{O}_{20}^V = \langle V_{\mu\nu} [ f_-^{\mu\nu}, \chi_- ] \rangle , \\
\mathcal{O}_{21}^V &= i \langle V_{\mu\nu} \nabla_\alpha \nabla^\alpha ( u^\mu u^\nu ) \rangle \quad , \quad \mathcal{O}_{22}^V = \langle V_{\mu\nu} \nabla_\alpha \nabla^\alpha f_+^{\mu\nu} \rangle .
\end{aligned} \tag{3.35}$$

Two-resonance operators which conserve intrinsic parity are discussed in the following. We begin with the basis of operators for vertices with one  $V$  and one  $A$  resonances and a pseudoscalar meson [131] (here denoted  $P$  in the operators indices, like in the quoted reference) in the normal parity sector. This is

$$\mathcal{L}^{VAP} = \sum_{i=1}^5 \lambda^i \mathcal{O}_{VAP}^i, \tag{3.36}$$

where the operators are

$$\begin{aligned}
\mathcal{O}_{VAP}^1 &= \langle [V^{\mu\nu}, A_{\mu\nu}] \chi_- \rangle , \\
\mathcal{O}_{VAP}^2 &= i \langle [V^{\mu\nu}, A_{\nu\alpha}] h_\mu^\alpha \rangle , \\
\mathcal{O}_{VAP}^3 &= i \langle [\nabla^\mu V_{\mu\nu}, A^{\nu\alpha}] u_\alpha \rangle , \\
\mathcal{O}_{VAP}^4 &= i \langle [\nabla^\alpha V_{\mu\nu}, A_\alpha^\nu] u^\mu \rangle , \\
\mathcal{O}_{VAP}^5 &= i \langle [\nabla^\alpha V_{\mu\nu}, A^{\mu\nu}] u_\alpha \rangle .
\end{aligned} \tag{3.37}$$

There is only one relevant operator with both a  $V$  and a  $S$  field,  $O_3^{SV} = \langle \{ S, V_{\mu\nu} \} f_+^{\mu\nu} \rangle$ , with coupling  $\lambda_3^{SV}$  [130].

Finally, we include the relevant operators with two  $V$  resonances in this even-intrinsic parity sector [130]

$$\mathcal{L}^{VV} = \sum_{i=1}^{18} \lambda_i^{VV} \mathcal{O}_i^{VV}, \quad (3.38)$$

where

$$\begin{aligned} \mathcal{O}_1^{VV} &= \langle V_{\mu\nu} V^{\mu\nu} u^\alpha u_\alpha \rangle, \\ \mathcal{O}_2^{VV} &= \langle V_{\mu\nu} u^\alpha V^{\mu\nu} u_\alpha \rangle, \\ \mathcal{O}_3^{VV} &= \langle V_{\mu\alpha} V^{\nu\alpha} u^\mu u_\nu \rangle, \\ \mathcal{O}_4^{VV} &= \langle V_{\mu\alpha} V^{\nu\alpha} u_\nu u^\mu \rangle, \\ \mathcal{O}_5^{VV} &= \langle V_{\mu\alpha} (u^\alpha V^{\mu\beta} u_\beta + u_\beta V^{\mu\beta} u^\alpha) \rangle, \\ \mathcal{O}_6^{VV} &= \langle V_{\mu\nu} V^{\mu\nu} \chi_+ \rangle, \\ \mathcal{O}_7^{VV} &= i \langle V_{\mu\alpha} V^{\alpha\nu} f_{+\beta\nu} \rangle g^{\beta\mu}. \end{aligned} \quad (3.39)$$

Next we turn to the odd-intrinsic parity sector, where the two terms involving a scalar and an axial-vector resonance [129] are

$$O_1^{SA} = i \epsilon_{\mu\nu\alpha\beta} \langle [A^{\mu\nu}, S] f_+^{\alpha\beta} \rangle, \quad O_2^{SA} = \epsilon_{\mu\nu\alpha\beta} \langle A^{\mu\nu} [S, u^\alpha u^\beta] \rangle. \quad (3.40)$$

In this intrinsic parity sector, operators with only vector resonances and sources and at most one pseudoscalar (again denoted  $P$  in the naming of the operators) were derived in reference [132]

$$\mathcal{L}^{V,odd} = \sum_{a=1}^7 \frac{c_a}{M_V} \mathcal{O}_{VJP}^a + \sum_{a=1}^4 d_a \mathcal{O}_{VVP}^a, \quad (3.41)$$

where the operators are

$$\begin{aligned}
\mathcal{O}_{VJP}^1 &= \varepsilon_{\mu\nu\rho\sigma} \langle \{V^{\mu\nu}, f_+^{\rho\alpha}\} \nabla_\alpha u^\sigma \rangle, \\
\mathcal{O}_{VJP}^2 &= \varepsilon_{\mu\nu\rho\sigma} \langle \{V^{\mu\alpha}, f_+^{\rho\sigma}\} \nabla_\alpha u^\nu \rangle, \\
\mathcal{O}_{VJP}^3 &= i\varepsilon_{\mu\nu\rho\sigma} \langle \{V^{\mu\nu}, f_+^{\rho\sigma}\} \chi_- \rangle, \\
\mathcal{O}_{VJP}^4 &= i\varepsilon_{\mu\nu\rho\sigma} \langle V^{\mu\nu} [f_-^{\rho\sigma}, \chi_+] \rangle, \\
\mathcal{O}_{VJP}^5 &= \varepsilon_{\mu\nu\rho\sigma} \langle \{\nabla_\alpha V^{\mu\nu}, f_+^{\rho\alpha}\} u^\sigma \rangle, \\
\mathcal{O}_{VJP}^6 &= \varepsilon_{\mu\nu\rho\sigma} \langle \{\nabla_\alpha V^{\mu\alpha}, f_+^{\rho\sigma}\} u^\nu \rangle, \\
\mathcal{O}_{VJP}^7 &= \varepsilon_{\mu\nu\rho\sigma} \langle \{\nabla^\sigma V^{\mu\nu}, f_+^{\rho\alpha}\} u_\alpha \rangle; \tag{3.42}
\end{aligned}$$

$$\begin{aligned}
\mathcal{O}_{VVP}^1 &= \varepsilon_{\mu\nu\rho\sigma} \langle \{V^{\mu\nu}, V^{\rho\alpha}\} \nabla_\alpha u^\sigma \rangle, \\
\mathcal{O}_{VVP}^2 &= i\varepsilon_{\mu\nu\rho\sigma} \langle \{V^{\mu\nu}, V^{\rho\sigma}\} \chi_- \rangle, \\
\mathcal{O}_{VVP}^3 &= \varepsilon_{\mu\nu\rho\sigma} \langle \{\nabla_\alpha V^{\mu\nu}, V^{\rho\alpha}\} u^\sigma \rangle, \\
\mathcal{O}_{VVP}^4 &= \varepsilon_{\mu\nu\rho\sigma} \langle \{\nabla^\sigma V^{\mu\nu}, V^{\rho\alpha}\} u_\alpha \rangle. \tag{3.43}
\end{aligned}$$

In our case, however, we will not only need odd-intrinsic parity couplings of a  $V$  resonance, a  $J$  source and a pseudoGoldstone; but also such vertices with two pseudoscalars<sup>2</sup>. In this case, as warned in ref. [132], the set  $\{\mathcal{O}_{VJP}^a\}_{a=1}^7$  is no longer a basis<sup>3</sup> and one needs to use the operator basis with a  $V$  resonance derived in ref. [129]; i. e.

$$\widetilde{\mathcal{L}^{V,odd}} = \varepsilon^{\mu\nu\alpha\beta} \sum_i \kappa_i^V \mathcal{O}_{\mu\nu\alpha\beta}^V, \tag{3.44}$$

---

<sup>2</sup>Obviously, in this case  $J$  has opposite parity than in the case with one pseudoGoldstone since both vertices are of odd-intrinsic parity.

<sup>3</sup>Analogous comment applies to eq. (3.36), as pointed out in ref [131].

with the operators

$$\begin{aligned}
(\mathcal{O}_1^V)^{\mu\nu\alpha\beta} &= i\langle V^{\mu\nu}(h^{\alpha\sigma}u_\sigma u^\beta - u^\beta u_\sigma h^{\alpha\sigma}) \rangle, \\
(\mathcal{O}_2^V)^{\mu\nu\alpha\beta} &= i\langle V^{\mu\nu}(u_\sigma h^{\alpha\sigma} u^\beta - u^\beta h^{\alpha\sigma} u_\sigma) \rangle, \\
(\mathcal{O}_3^V)^{\mu\nu\alpha\beta} &= i\langle V^{\mu\nu}(u_\sigma u^\beta h^{\alpha\sigma} - h^{\alpha\sigma} u^\beta u_\sigma) \rangle, \\
(\mathcal{O}_4^V)^{\mu\nu\alpha\beta} &= i\langle [V^{\mu\nu}, \nabla^\alpha \chi_+] u^\beta \rangle, \\
(\mathcal{O}_5^V)^{\mu\nu\alpha\beta} &= i\langle V^{\mu\nu}[f_-^{\alpha\beta}, u_\sigma u^\sigma] \rangle, \\
(\mathcal{O}_6^V)^{\mu\nu\alpha\beta} &= i\langle V^{\mu\nu}(f_-^{\alpha\sigma} u^\beta u_\sigma - u_\sigma u^\beta f_-^{\alpha\sigma}) \rangle, \\
(\mathcal{O}_7^V)^{\mu\nu\alpha\beta} &= i\langle V^{\mu\nu}(u_\sigma f_-^{\alpha\sigma} u^\beta - u^\beta f_-^{\alpha\sigma} u_\sigma) \rangle, \\
(\mathcal{O}_8^V)^{\mu\nu\alpha\beta} &= i\langle V^{\mu\nu}(f_-^{\alpha\sigma} u_\sigma u^\beta - u^\beta u_\sigma f_-^{\alpha\sigma}) \rangle, \\
(\mathcal{O}_9^V)^{\mu\nu\alpha\beta} &= \langle V^{\mu\nu}\{\chi_-, u^\alpha u^\beta\} \rangle, \\
(\mathcal{O}_{10}^V)^{\mu\nu\alpha\beta} &= \langle V^{\mu\nu} u^\alpha \chi_- u^\beta \rangle, \\
(\mathcal{O}_{11}^V)^{\mu\nu\alpha\beta} &= \langle V^{\mu\nu}\{f_+^{\alpha\rho}, f_-^{\beta\sigma}\} g_{\rho\sigma} \rangle, \\
(\mathcal{O}_{12}^V)^{\mu\nu\alpha\beta} &= \langle V^{\mu\nu}\{f_+^{\alpha\rho}, h^{\beta\sigma}\} g_{\rho\sigma} \rangle, \\
(\mathcal{O}_{13}^V)^{\mu\nu\alpha\beta} &= i\langle V^{\mu\nu} f_+^{\alpha\beta} \rangle \langle \chi_- \rangle, \\
(\mathcal{O}_{14}^V)^{\mu\nu\alpha\beta} &= i\langle V^{\mu\nu}\{f_+^{\alpha\beta}, \chi_- \} \rangle, \\
(\mathcal{O}_{15}^V)^{\mu\nu\alpha\beta} &= i\langle V^{\mu\nu}[f_-^{\alpha\beta}, \chi_+] \rangle, \\
(\mathcal{O}_{16}^V)^{\mu\nu\alpha\beta} &= \langle V^{\mu\nu}\{\nabla^\alpha f_+^{\beta\sigma}, u_\sigma\} \rangle, \\
(\mathcal{O}_{17}^V)^{\mu\nu\alpha\beta} &= \langle V^{\mu\nu}\{\nabla_\sigma f_+^{\alpha\sigma}, u^\beta\} \rangle, \\
(\mathcal{O}_{18}^V)^{\mu\nu\alpha\beta} &= \langle V^{\mu\nu} u^\alpha u^\beta \rangle \langle \chi_- \rangle.
\end{aligned} \tag{3.45}$$

The operators in eq. (3.42) can be written in terms of those in eq. (3.45). This yields the following identities among the corresponding couplings [89]

$$\begin{aligned}
\kappa_1^{VV} &= \frac{-d_1}{8n_f} \\
\kappa_2^{VV} &= \frac{d_1}{8} + d_2, \\
\kappa_3^{VV} &= d_3, \\
\kappa_4^{VV} &= d_4, \\
-2M_V\kappa_5^V &= M_V\kappa_6^V = M_V\kappa_7^V = \frac{c_6}{2}, \\
M_V\kappa_{11}^V &= \frac{c_1 - c_2 - c_5 + c_6 + c_7}{2}, \\
M_V\kappa_{12}^V &= \frac{c_1 - c_2 - c_5 + c_6 - c_7}{2}, \\
n_f M_V\kappa_{13}^V &= \frac{-c_2 + c_6}{4}, \\
M_V\kappa_{14}^V &= \frac{c_2 + 4c_3 - c_6}{4}, \\
M_V\kappa_{15}^V &= c_4, \\
M_V\kappa_{16}^V &= c_6 + c_7, \\
M_V\kappa_{17}^V &= -c_5 + c_6.
\end{aligned} \tag{3.46}$$

$$\tag{3.47}$$

The analogous Lagrangian to eq. (3.44) involving an  $A$  resonance [129] is the last missing piece needed for our computations. This is

$$\mathcal{L}^{A,odd} = \varepsilon^{\mu\nu\alpha\beta} \sum_i \kappa_i^A \mathcal{O}_{i\ \mu\nu\alpha\beta}^A, \tag{3.48}$$



with the operators

$$\begin{aligned}
(\mathcal{O}_1^A)^{\mu\nu\alpha\beta} &= \langle A^{\mu\nu}[u^\alpha u^\beta, u_\sigma u^\sigma] \rangle, \\
(\mathcal{O}_2^A)^{\mu\nu\alpha\beta} &= \langle A^{\mu\nu}[u^\alpha u^\sigma u^\beta, u_\sigma] \rangle, \\
(\mathcal{O}_3^A)^{\mu\nu\alpha\beta} &= \langle A^{\mu\nu}\{\nabla^\alpha h^{\beta\sigma}, u_\sigma\} \rangle, \\
(\mathcal{O}_4^A)^{\mu\nu\alpha\beta} &= i\langle A^{\mu\nu}[f_+^{\alpha\beta}, u^\sigma u_\sigma] \rangle, \\
(\mathcal{O}_5^A)^{\mu\nu\alpha\beta} &= i\langle A^{\mu\nu}(f_+^{\alpha\sigma} u_\sigma u^\beta - u^\beta u_\sigma f_+^{\alpha\sigma}) \rangle, \\
(\mathcal{O}_6^A)^{\mu\nu\alpha\beta} &= i\langle A^{\mu\nu}(f_+^{\alpha\sigma} u^\beta u_\sigma - u_\sigma u^\beta f_+^{\alpha\sigma}) \rangle, \\
(\mathcal{O}_7^A)^{\mu\nu\alpha\beta} &= i\langle A^{\mu\nu}(u_\sigma f_+^{\alpha\sigma} u^\beta - u^\beta f_+^{\alpha\sigma} u_\sigma) \rangle, \\
(\mathcal{O}_8^A)^{\mu\nu\alpha\beta} &= \langle A^{\mu\nu}\{f_-^{\alpha\sigma}, h_\sigma^\beta\} \rangle, \\
(\mathcal{O}_9^A)^{\mu\nu\alpha\beta} &= i\langle A^{\mu\nu} f_-^{\alpha\beta} \rangle \langle \chi_- \rangle, \\
(\mathcal{O}_{10}^A)^{\mu\nu\alpha\beta} &= i\langle A^{\mu\nu} u^\alpha \rangle \langle \nabla^\beta \chi_- \rangle, \\
(\mathcal{O}_{11}^A)^{\mu\nu\alpha\beta} &= i\langle A^{\mu\nu}\{f_-^{\alpha\beta}, \chi_- \} \rangle, \\
(\mathcal{O}_{12}^A)^{\mu\nu\alpha\beta} &= i\langle A^{\mu\nu}\{\nabla^\alpha \chi_-, u^\beta\} \rangle, \\
(\mathcal{O}_{13}^A)^{\mu\nu\alpha\beta} &= \langle A^{\mu\nu}[\chi_+, u^\alpha u^\beta] \rangle, \\
(\mathcal{O}_{14}^A)^{\mu\nu\alpha\beta} &= i\langle A^{\mu\nu}\{f_+^{\alpha\beta}, \chi_+ \} \rangle, \\
(\mathcal{O}_{15}^A)^{\mu\nu\alpha\beta} &= \langle A^{\mu\nu}\{\nabla^\alpha f_-^{\beta\sigma}, u_\sigma\} \rangle, \\
(\mathcal{O}_{16}^A)^{\mu\nu\alpha\beta} &= \langle A^{\mu\nu}\{\nabla_\sigma f_-^{\alpha\sigma}, u^\beta\} \rangle.
\end{aligned} \tag{3.49}$$

We recall that the basis for odd-intrinsic parity operators with two vector resonances and a pseudoscalar meson was given in eq. (3.41).

### Short-distance QCD constraints on the $R\chi L$ couplings

We have discussed in the previous section how symmetry determines the structure of the operators in the  $R\chi L$  though it leaves, however, the corresponding couplings undetermined (as in  $\chi PT$  or any other effective field theory with a corresponding fundamental theory in the strongly coupled regime). It was soon observed [88, 63, 64]

that demanding that the Green functions (and related form factors) computed in the meson theory to match their known asymptotic behavior according to the operator product expansion [133] of QCD relates some of the  $R\chi L$  couplings and thus increases the predictive power of the theory. We will quote in the following the results of this programme interesting to our study.

In the odd-intrinsic parity sector, the analysis of three-point  $VVP$  Green function and associated form factors yields [132, 129, 89]

$$\begin{aligned}
M_V(2\kappa_{12}^V + 4\kappa_{14}^V + \kappa_{16}^V - \kappa_{17}^V) &= 4c_3 + c_1 = 0, \\
M_V(2\kappa_{12}^V + \kappa_{16}^V - 2\kappa_{17}^V) &= c_1 - c_2 + c_5 = 0, \\
-M_V\kappa_{17}^V &= c_5 - c_6 = \frac{N_C M_V}{64\sqrt{2}\pi^2 F_V}, \\
8\kappa_2^{VV} &= d_1 + 8d_2 = \frac{F^2}{8F_V^2} - \frac{N_C M_V^2}{64\pi^2 F_V^2}, \\
\kappa_3^{VV} &= d_3 = -\frac{N_C M_V^2}{64\pi^2 F_V^2}, \\
1 + \frac{32\sqrt{2}F_V d_m \kappa_3^{PV}}{F^2} &= 0, \\
F_V^2 &= 3F^2. \tag{3.50}
\end{aligned}$$

It is remarkable that the last of eqs. (3.50) involves couplings belonging to the even-intrinsic parity  $R\chi L$ , despite it was obtained demanding consistency to the high-energy constraints derived in the odd-intrinsic parity sector [132, 129, 89, 134, 135, 70, 74]. Let us also mention that the short-distance QCD constraint  $\kappa_2^S = 0$  [129] forbids a diagram similar to the third one in fig. 3.7 where this time the coupling to the current would conserve intrinsic parity (it would be thus a contribution to the axial-vector form factors, since  $a_0^- \rightarrow \pi^- \eta$  belongs to the unnatural intrinsic parity sector)<sup>4</sup>. Another relevant short-distance constraint in the odd-intrinsic parity sector

---

<sup>4</sup>For completeness we quote the corresponding operator,  $O_2^S = \epsilon_{\mu\nu\alpha\beta} \langle iS [f_+^{\mu\nu}, f_-^{\alpha\beta}] \rangle$ .

which is derived from the study of the  $VAS$  Green function [129] is  $\kappa_A^{14} = 0$ . Interestingly, this same analysis also yields the relation  $\kappa_4^V = 2\kappa_{15}^V$ , where  $\kappa_4^V$  does not enter the relations (3.46). Other high-energy constraints derived in the quoted study are not relevant to our computation.

In the even-intrinsic parity sector, the study of  $VAP$  and  $SPP$  Green functions<sup>5</sup> and their form factors allowed to derive the following restrictions [138, 136, 130]

$$\begin{aligned}\lambda' &\equiv \frac{1}{\sqrt{2}} \left( \lambda_2 - \lambda_3 + \frac{\lambda_4}{2} + \lambda_5 \right) = \frac{F^2}{2\sqrt{2}F_A G_V}, \\ \lambda'' &\equiv \frac{1}{\sqrt{2}} \left( \lambda_2 - \frac{\lambda_4}{2} - \lambda_5 \right) = \frac{2G_V - F_V}{2\sqrt{2}F_A}, \\ \lambda_0 &\equiv -\frac{1}{\sqrt{2}} \left( 4\lambda_1 + \lambda_2 + \frac{\lambda_4}{2} + \lambda_5 \right) = \frac{\lambda' + \lambda''}{4}, \\ \kappa_1^{SA} &\equiv \frac{F^2}{32\sqrt{2}c_m F_A},\end{aligned}\tag{3.51}$$

supplemented by  $F_V G_V = F^2$ ,  $F_A = \sqrt{2}F$  and  $F_V = \sqrt{3}F$  (this one in accord with the result found in the odd-intrinsic parity sector) [88, 63, 85]. Since  $\lambda_{21}^V = 0 = \lambda_{22}^V$  [130], we will not consider the contribution of the corresponding operators. The well-known relation  $c_d c_m = F^2/4$  [139] arising in the study of strangeness-changing scalar form factors will also be employed.

Although not all the operators appearing in section 3.4.1 do actually contribute to the considered decays, the number of asymptotic relations looks too small compared to the number of free couplings to allow a meaningful general phenomenological study of the  $\tau^- \rightarrow \pi^- \eta^{(\prime)} \gamma \nu_\tau$  decays within  $R_\chi L$ . Also there is not enough phenomenological information on the couplings of eqs. (3.45) and (3.49), for instance. Due to that we will first consider only the diagrams with at most one resonance and then comment on the possible extension to include two-resonance diagrams in section 3.5.2.

---

<sup>5</sup>Four-point functions have been studied in ref. [137].

### Form factors according to Resonance Chiral Lagrangians

The relevant Feynman diagrams are shown in figures 3.4 to 3.6 <sup>6</sup>. Fig. 3.4 corresponds to the model-independent contribution given by the chiral  $U(1)$  anomaly, fixed by QCD <sup>7</sup>. The left-hand side diagram is the purely local contribution while, in the one on the right, the Wess-Zumino-Witten functional provides the  $\pi\pi\eta\gamma$  vertex (and all hadronic information corresponding to the coupling of the pion to the axial-vector current is encoded in the pion decay constant). The anomalous vertices violate intrinsic parity, as these two diagrams do. Figs. 3.5 to 3.8 are, on the contrary, model-dependent. Figs. 3.5 and 3.6 (3.7 and 3.8) correspond to the one- and two-resonance mediated contributions to the axial-vector (vector) form factors in eqs. (3.1) to (3.2), respectively.

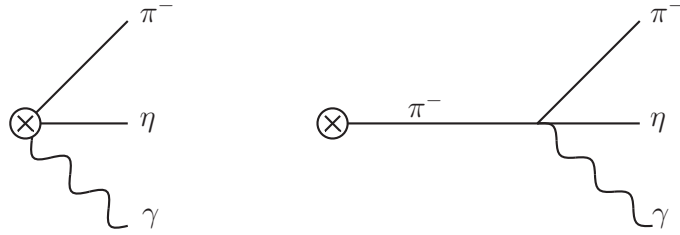


Figure 3.4: Contributions from the Wess-Zumino-Witten functional [56] to  $\tau^- \rightarrow \pi^- \eta \gamma \nu_\tau$  decays. The cross circle indicates the insertion of the charged weak current.

As a general fact, the axial-vector form factors in radiative tau decays to two pseudoscalars violate intrinsic parity as it can be checked for all contributing diagrams in figs. 3.5 and 3.6. The last vertex in all diagrams in the first line of fig. 3.5 is of odd-intrinsic parity (as well as it happens with the second diagram in the second line of this figure). In the first and third diagrams of the second line of fig. 3.5 intrinsic parity is violated in the coupling to the weak (thus axial-vector) current. The odd-intrinsic parity violating vertices appearing in the diagrams in fig. 3.6 are  $\rho^0 \rightarrow \eta\gamma$ ,

<sup>6</sup>We remind that only diagrams which do not violate G-parity are considered.

<sup>7</sup>We note that this contribution is absent in the MDM approach.

$a^{-\mu} \rightarrow a_1^- \eta$  ( $a^\mu$  stands for the axial-vector current),  $a_1^- \rightarrow \pi^- \eta$  and  $a_1^- \rightarrow a_0^- \gamma$ .

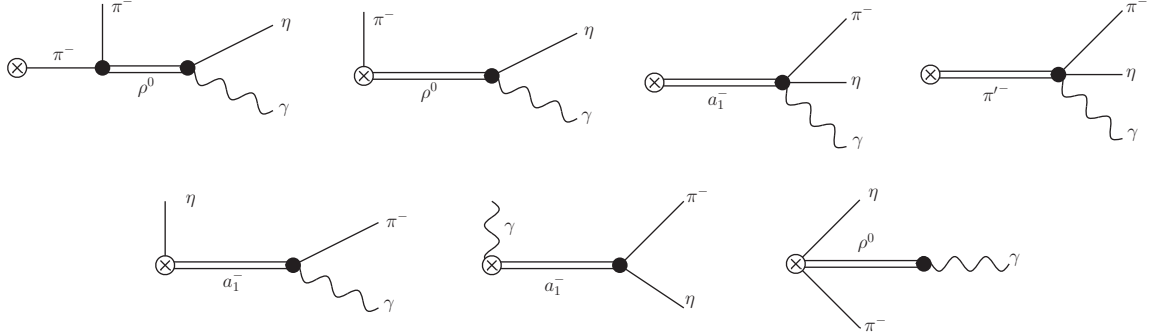


Figure 3.5: One-resonance exchange contributions from the  $R_\chi L$  to the axial-vector form factors of the  $\tau^- \rightarrow \pi^- \eta \gamma \nu_\tau$  decays. Vertices involving resonances are highlighted with a thick dot.

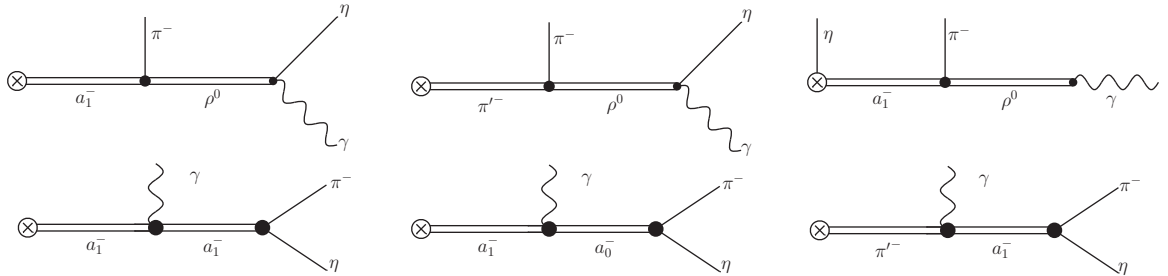


Figure 3.6: Two-resonance exchange contributions from the  $R_\chi L$  to the axial-vector form factors of the  $\tau^- \rightarrow \pi^- \eta \gamma \nu_\tau$  decays. Vertices involving resonances are highlighted with a thick dot.

We note that the first two diagrams of figs. 3.7 contain only odd-intrinsic parity violating vertices while the last three diagrams in this figure contain only even-intrinsic parity vertices in such a way that intrinsic-parity is not violated in neither of them (as it corresponds to the vector form factors). Similarly, in fig. 3.8, the first, second and fourth diagram contain two intrinsic parity violating vertices and the third and fifth diagram contain only even-intrinsic parity vertices. Thus, again intrinsic parity

is conserved in these diagrams as well.

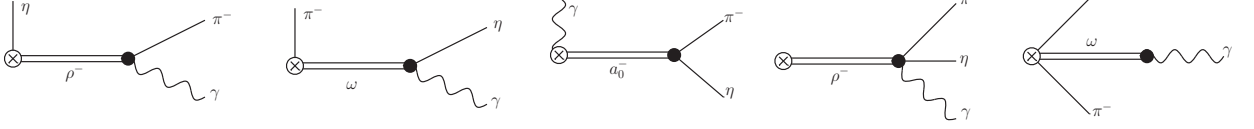


Figure 3.7: One-resonance exchange contributions from the  $R\chi L$  to the vector form factors of the  $\tau^- \rightarrow \pi^- \eta \gamma \nu_\tau$  decays. Vertices involving resonances are highlighted with a thick dot.

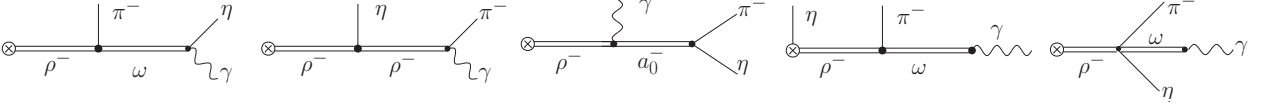


Figure 3.8: Two-resonance exchange contributions from the  $R\chi L$  to the vector form factors of the  $\tau^- \rightarrow \pi^- \eta \gamma \nu_\tau$  decays. Vertices involving resonances are highlighted with a thick dot.

Using the  $R\chi L$  introduced in section 3.4.1, it is straightforward to verify that all three diagrams involving the  $\pi'$  resonance vanish (in figs. 3.5 and 3.6). Also the last diagram of fig. 3.7 is null but all other diagrams in figures 3.4 to 3.8 contribute non trivially to the considered  $\tau^- \rightarrow \pi^- \eta^{(\prime)} \gamma \nu_\tau$  decays. Since the left-handed weak current has both vector and axial-vector components, one could expect to have two different contributions per given topology, with intrinsic parity conserving and violating coupling to the weak charged current, respectively. However, we point out that using the Lagrangian introduced in section 3.4.1 this only happens for the last diagrams in figs. 3.5 and 3.7. In our computation we have neglected subleading contributions in the chiral counting, namely the coupling to the weak current in the second diagram of fig. 3.5 receives contributions from the piece of the Lagrangian in eq. (3.33). Correspondingly, we are not considering the contributions given by the Lagrangian

in eq. (3.34), which are suppressed by one chiral order.

Comparing the  $R\chi L$  diagrams in figs. 3.4 to 3.8 with the MDM diagrams in fig. 3.1, we see first that the model-independent contribution of both diagrams in fig. 3.4 (axial-form factors at lowest order in the chiral expansion) is not included in the MDM approach. Among the 13 contributions in figs. 3.5 and 3.6 (which are subleading in the chiral regime) only one is considered in MDM<sup>8</sup> (the first diagram in figure 3.6). Finally, 10 diagrams appear in figs. 3.7 and 3.8 but only three of them (those including the vertices  $\rho - \omega - \pi$ ,  $\rho - a_0 - \gamma$  and  $\rho - \rho - \eta$ ) enter the MDM description.

We would like to make a final comment regarding gauge invariance before quoting our form factor results using  $R\chi L$ . It can be checked that the contribution of  $\mathcal{O}_{10}^A$  to the third diagram in fig. 3.5 is not gauge invariant by itself. However, for this particular operator, the cancellation of gauge-dependent pieces involves the diagrams with radiation off the  $a_1$  and off the weak vertex in figs. 3.5 and 3.6. As a result of this mechanism, we note the presence of  $D_{a_1}(W^2)$  and  $D_{a_1}[(p+k)^2]$  factors and the absence of  $D_{a_1}[(p+p_0)^2]$  terms in the corresponding contributions to the axial-vector form factors<sup>9</sup>.

For convenience, we will quote the individual contributions to each form factor figure by figure (following the order of the diagrams in a given figure). We will start with the axial-vector form factors. The diagrams in fig. 3.4 give

$$a_1^{\chi PT} = \frac{N_C C_q}{6\sqrt{2}\pi^2 F^2}, \quad a_3^{\chi PT} = \frac{a_1^{\chi PT}}{D_\pi[W^2]}, \quad (3.52)$$

which is a model-independent result coming from the QCD anomaly.

---

<sup>8</sup>The diagram with the pion pole also appears in fig. 3.3, but it is neglected.

<sup>9</sup>We note that, among the  $\mathcal{O}_i^A$  operators, only  $\mathcal{O}_{10}^A$  couples to  $\pi^- \eta^{(\prime)}$ . This vertex does not contribute to the corresponding non-radiative decays because at least an additional independent momentum is needed for a non-vanishing contraction with the Levi-Civita symbol.

The contribution of the remaining diagrams (figures 3.5 and 3.6 for the axial-vector form factors and 3.7 and 3.8 for the vector form factors) is collected in appendix A. The corresponding off-shell width of meson resonances used in our numerical analysis can be found in appendix B. We will discuss in the next section if further insight can be gained on the  $R\chi L$  couplings values restoring to phenomenology and using the expected scaling of the low-energy constants of the  $\chi PT$  Lagrangian.

### Phenomenological estimation of $R\chi L$ couplings

Although the relations in section 3.4.1 only reduce the number of unknowns in eqs. (3.52) and (5.46) to (5.64), some of the remaining free couplings can still be estimated phenomenologically. The high-energy constraint  $c_d c_m = F^2/4$  leaves either  $c_d$  or  $c_m$  as independent. We will use  $c_d = (19.8^{+2.0}_{-5.2})$  MeV [127]. In this way all relevant couplings in eq.(3.33) have been determined.

$\lambda_{15}^S$  is the only leading operator contributing to  $a_0 \rightarrow \gamma\gamma$ . From  $\Gamma(a_0 \rightarrow \gamma\gamma) = (0.30 \pm 0.10)$  keV =  $\frac{64\pi\alpha^2}{9} M_{a_0}^3 |\lambda_{15}^S|^2$  we can estimate  $|\lambda_{15}^S| = (1.6 \pm 0.3) \cdot 10^{-2}$  GeV<sup>-1</sup>. We note that the coupling relevant for the  $a_1 - a_0 - \gamma$  vertex,  $\kappa_1^{SA}$  is fixed by a short-distance constraint in eqs. (3.51).

We turn now to the  $\lambda_i$  couplings in eq. (3.36). Short-distance constraints leave two such couplings undetermined. The three combinations of them that are predicted by high-energy conditions have the following numerical values:

$$\lambda' \sim 0.4, \quad \lambda'' \sim 0.04, \quad \lambda_0 \sim 0.12. \quad (3.53)$$

The same linear combination of  $\lambda_4$  and  $\lambda_5$  enters all couplings in eq. (3.53). Therefore we can take one them as independent ( $\lambda_4$  for us). We will choose as the other independent coupling  $\lambda_2$ , which enters all couplings in eq. (3.53). A conservative estimate would be  $|\lambda_2| \sim |\lambda_4| \leq 0.4$ , to which we will stick in our numerical analysis.



According to ref. [130] the  $\lambda_i^V$  couplings can be estimated from the expected scaling of the NNLO low-energy constants of the  $\chi PT$  Lagrangian (we also employ short-distance QCD constraints on the  $R\chi L$  couplings to write the following expression conveniently) as

$$\lambda_i^V \sim 3C_i^R \frac{M_V^2}{F} \sim 0.05 \text{ GeV}^{-1}, \quad (3.54)$$

that can be considered an upper bound on  $|\lambda_i^V|$  because the employed relation  $C_i^R \sim \frac{1}{F^2(4\pi)^4}$  is linked to  $L_i^R \sim \frac{1}{(4\pi)^2} \sim 5 \cdot 10^{-3}$ , which is basically the size of  $L_9^R$  and  $|L_{10}^R|$  but clearly larger than the remaining eight  $L_i^R$  [63, 140]. There is not that much information on the values of the  $C_i^R$  (see, however ref. [141]). We will take  $|\lambda_i^V| \leq 0.04 \text{ GeV}^{-1}$  for the variation of these couplings ( $i = 6, 11, 12, 13, 14, 15$  are relevant to our analysis), although it may be expected that only one or two of them (if any) are close to that (upper) limit. Proceeding similarly we can estimate  $\lambda_i^{VV} \sim \frac{M_V^4}{2F^2} C_i^R$  and  $\lambda_i^{SV} \sim \sqrt{2} \frac{M_S^2 M_V^2}{c_m F} C_i^R$ . This sets a reasonable upper bound  $|\lambda_i^{SV}| \sim |\lambda_i^{VV}| \lesssim 0.1$  that we will assume in the numerics.

We discuss next the values of the  $c_i$  ( $\kappa_i^V$ ) couplings in eqs. (3.41) and (3.44). Eqs. (3.50) predict the vanishing of two linear combinations of  $c_i$ 's. The numerical value for the predicted  $c_6 - c_5$  is  $-0.017$ . There are some determinations of  $c_3$ . It was estimated (although with a sign ambiguity) studying  $\tau^- \rightarrow \eta \pi^- \pi^0 \nu_\tau$  decays [142]. Taking into account the determinations by Y. H. Chen *et al.* [143, 144, 145] as well, we will use  $c_3 = 0.007_{-0.012}^{+0.020}$ .  $c_4$  was first determined studying  $\sigma(e^+e^- \rightarrow KK\pi)$  in ref. [90], although with a value yielding inconsistent results in  $\tau^- \rightarrow K^- \gamma \nu_\tau$  [70]. We will take the determination  $c_4 = -0.0024 \pm 0.0006$  [144] as the most reliable one. Two other independent  $c_i$  combinations appear in our form factors. We will take them as  $c_5$  and  $c_7$  whose modulus we will vary in the range  $[0, 0.03]$ . Using eqs. (3.46) to relate the  $c_i$  and  $\kappa_i^V$  couplings we can find reasonable guesses on the latter from  $|c_i| \lesssim 0.03$ . Thus, we will take  $|\kappa_i^V| \leq 0.04 \text{ GeV}^{-1}$  for their variation.

There is very little information on the  $\kappa_i^A$  couplings. As a reasonable estimate we

will make them vary in the same interval as the  $\lambda_i^V$  and  $\kappa_i^V$  couplings.

The numerical values of the two  $d_i$  couplings (VVP operators) which were determined in eq. (3.50) are  $d_1 + 8d_2 \sim 0.15$  and  $d_3 \sim -0.11$ .  $d_2$  has been determined jointly with  $c_3$  (discussed above). According to the quoted references we will employ  $d_2 = 0.08 \pm 0.08$ . Then only  $d_4$  would remain free. Given the previous values for the other  $d_i$ 's we will assume  $|d_4| < 0.15$ .

We will discuss in the next section the phenomenology of  $\tau^- \rightarrow \pi^- \eta^{(\prime)} \gamma \nu_\tau$  decays, focusing on the background they constitute to the searches of SCC in their corresponding non-radiative decays. We will start discussing the simplified case of *MDM*, according to eqs.(3.16), to turn next to the *R $\chi$ L* prediction corresponding to eqs. (3.52) and (5.46) to (5.64).

### 3.5 $\tau^- \rightarrow \pi^- \eta^{(\prime)} \gamma \nu_\tau$ as background in the searches for

$$\tau^- \rightarrow \pi^- \eta^{(\prime)} \nu_\tau$$

#### 3.5.1 Meson dominance predictions

The SM values for the non radiative process  $\tau^- \rightarrow \eta^{(\prime)} \pi^- \nu_\tau$  mark the threshold below which no SCC stemming from BSM interactions will be detected in these decays, therefore, one needs to provide a clean scenario for the experimental study of this process. Since the radiative decay can be a considerable background in measuring the non radiative one, the former must be determined in such a way that its effect can be discerned from the latter. The way to do this is by imposing an energy cut on the photon above which we discard all the contributions to the observables.

One has to choose the cut in order to fairly reduce the background, but leaving a photon energy range that can be explored in the experiment. As explained in ref.

[146], 50 MeV can be a too stringent cut for the process and, therefore, we take 100 MeV as the upper limit on photon energy. Notice that since no bremsstrahlung of on-shell particles will enter the structure dependent description (see section 3.2), our computation of the relevant observables is free of infrared divergences, however to be consistent with the disregarding of the bremsstrahlung contribution a lower energy bound should be taken experimentally. This gives us the photon energy range  $10 \text{ MeV} \leq E_\gamma \leq 100 \text{ MeV}$ . To verify this assertion we must analyze the photon energy spectrum. The statistical uncertainties in both models are given assuming a Gaussian distribution of the parameters and letting them to randomly vary within such distribution.

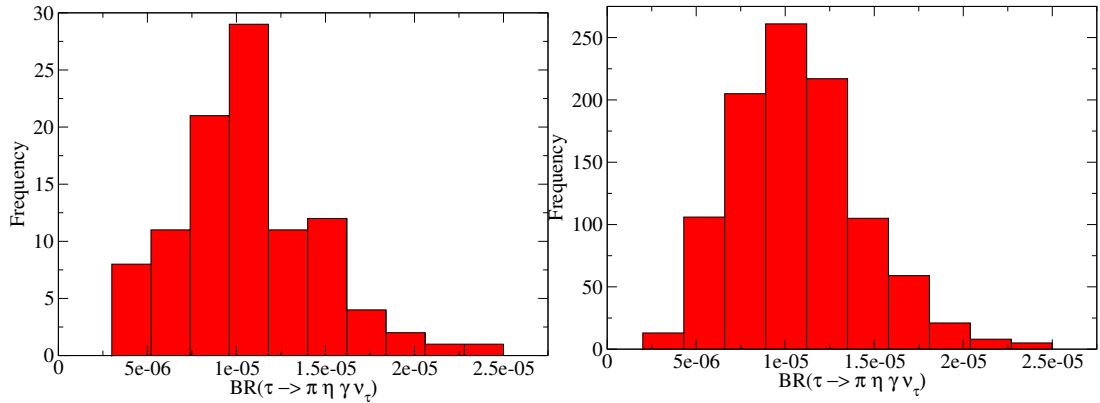


Figure 3.9: Histogram of  $BR(\tau^- \rightarrow \pi^- \eta \gamma \nu_\tau)$  for 100 (left) and 1000 (right) random points in the MDM parameter space are plotted.

The purpose of computing the observables in the MDM is to have an estimation of the magnitude of the process and to compare it with the  $R_\chi T$ , therefore no errors are including due to model uncertainties. We use the values of the couplings in table 3.1, where the error in the prediction of MDM will come by their variation, as told in the previous paragraph. We will first plot the predicted branching ratios when sampling these 10 parameters within one-sigma uncertainties (using normal distributions). This information is collected in figures 3.9, where the branching ratio for the variation of these 10 parameters is shown using 100 points (left) and 1000 (right) in the parameter space scan.

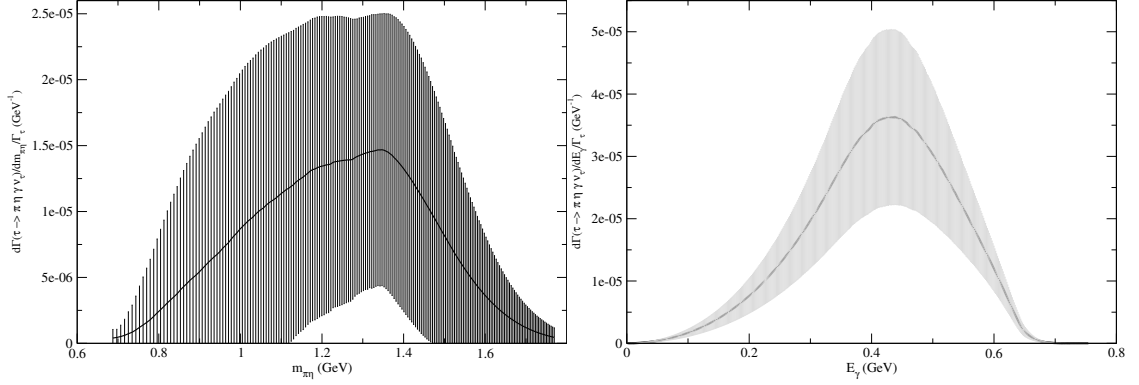


Figure 3.10:  $\tau^- \rightarrow \pi^- \eta \gamma \nu_\tau$  normalized spectra according to MDM in the invariant mass of the  $\eta\pi^-$  system (left) and in the photon energy (right) are plotted for some characteristic points in fig. 3.9

We find the Branching ratios  $BR_{100} = (1 \pm 1) \times 10^{-5}$  for a hundred points and  $BR_{1000} = (1.1 \pm 0.3) \times 10^{-5}$  using a thousand points. Then, by using the same phase space integrals given in ref [75] and taking 100 random sets of points in parameter space we computed the  $\pi\eta$  invariant mass  $m_{\pi\eta}$  spectrum dividing the domain length in 200 steps (left) and the photon energy dividing its domain length into 500 steps  $E_\gamma$  spectrum (right), both spectra normalized to the  $\tau$  lepton lifetime are shown in figure 3.10.

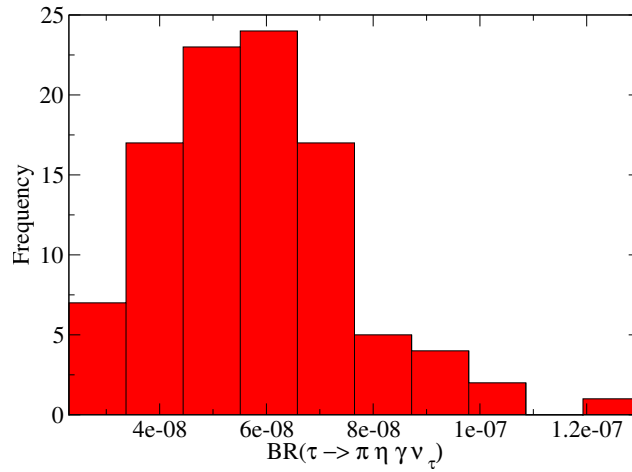


Figure 3.11: Histogram of  $BR(\tau \rightarrow \pi \eta \gamma \nu_\tau)$  where photons with  $E_\gamma > 100$  MeV are rejected.

It can be noticed the peak in the  $1.15 \text{ GeV} \leq m_{\pi\eta} \leq 1.35 \text{ GeV}$  region for the  $m_{\pi\eta}$  spectrum, however there is not any marked dynamics responsible for this effect. As was discussed previously, the effect of bremsstrahlung will become greater at lower energies, while by Low's theorem [123] the structure dependent amplitude will give greater contributions at large photon energies stemming from its dependence on  $k$  ( $\sim \mathcal{O}(k)$ ). Thus, the photon energy spectrum gives the possibility to analyze the effect of the lowest upper bound imposed for the energy of the photon. Since, as already discussed (ref [146]), a 50 MeV cut is too restrictive we will take the 100 MeV cut. Using this cut, we reevaluated the branching fraction with 100 parameter space points obtaining the plot in fig. 3.11. Thus, the upper bound obtained for the branching ratio with a larger simulation sample (not shown in ) is  $BR \leq 0.6 \times 10^{-7}$ , two orders of magnitude smaller than the non radiative decay [124].

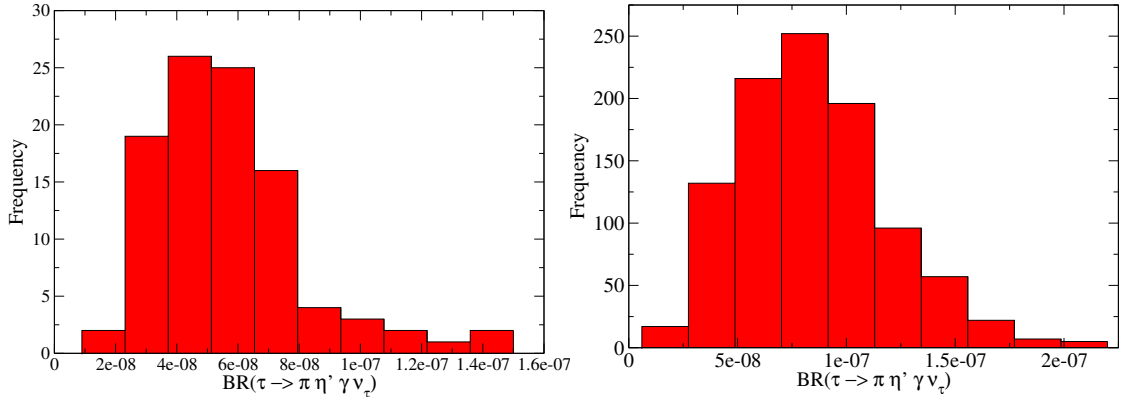


Figure 3.12: Histogram of  $BR(\tau^- \rightarrow \pi^- \eta' \gamma \nu_\tau)$  for 100 (left) and 1000 (right) random points in the MDM parameter space are plotted.

For the  $\eta'$  channel the procedure is completely analogous. We first plot the branching ratio for 100 (1000) normally sampled points in the parameter space in fig 3.12, where the corresponding branching fractions are  $BR_{100} \sim 6 \times 10^{-8}$  and  $BR_{1000} = (0.8 \pm 0.8) \times 10^{-8}$ . Just as in the case of the  $\eta$ , we obtained the  $m_{\pi\eta'}$  spectrum shown in figure 3.13 dividing the domain length in 200 steps (left) and the photon energy dividing its domain length into 500 steps  $E_\gamma$  spectrum (right) both for a 100 random points in parameter space. Since the limited phase space does not

allow an on-shell  $a_0$  meson exchange, no possible related substructure arises.

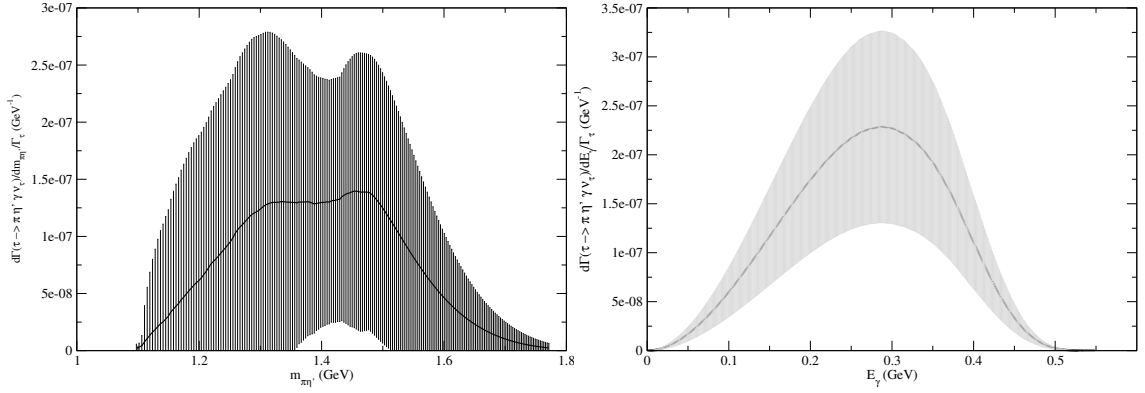


Figure 3.13:  $\tau^- \rightarrow \pi^- \eta' \gamma \nu_\tau$  normalized spectra according to MDM in the invariant mass of the  $\pi^- \eta'$  system (left) and in the photon energy (right) are plotted for some characteristic points in fig. 3.12

Completely analogous to the  $\eta$  decay, the branching fraction is reanalyzed imposing the cut in photon energy of 100 MeV and shown in fig 3.14 using 100 points of parameter space. The branching fraction obtained thus is  $\leq 0.2 \times 10^{-8}$ , which was obtained by using a thousand parameter space points. This is suppressed by a factor of 50 with respect to the non radiative decay. It must be noticed that the MDM contribution to this process is mainly given by the last diagram in figure 3.1, when all the other contributions are neglected we find that  $\sim 80\%$  of the process is given by this contribution in the  $\eta$  channel, while for the  $\eta'$  it is essentially saturated by it [146]. All the results will be compared to  $R\chi T$  predictions in the next section.

### 3.5.2 $R\chi L$ predictions

Contrary to the MDM case which has only contributions from diagrams involving two resonances, in  $R\chi T$  we have point interaction and one Goldstone exchange contributions arising from the WZW functional along with diagrams including one and two resonances. All the observables obtained with MDM are computed using  $R\chi T$  and then compared using all contributions to those without the two resonances exchange diagrams.

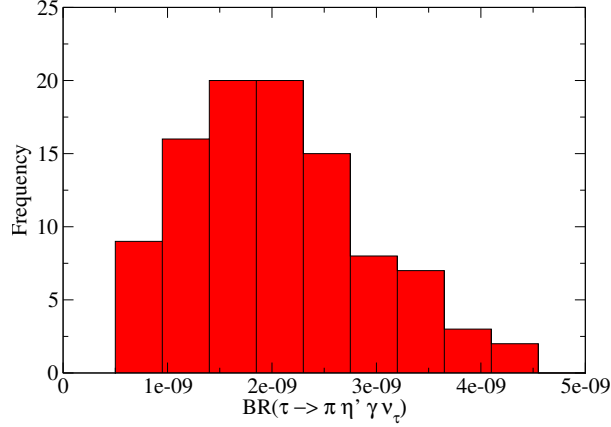


Figure 3.14: Histogram of  $BR(\tau \rightarrow \pi \eta' \gamma \nu_\tau)$  where photons with  $E_\gamma > 100$  MeV are rejected.

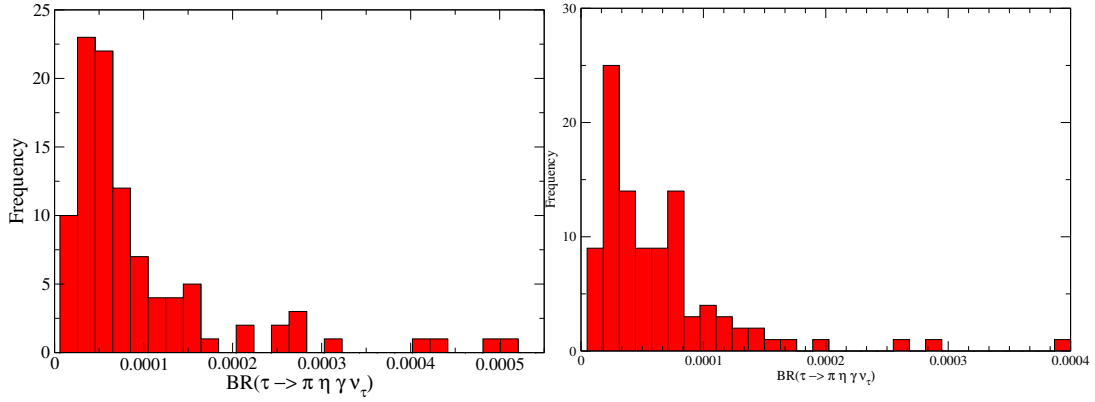


Figure 3.15: Histogram of  $BR(\tau^- \rightarrow \pi^- \eta \gamma \nu_\tau)$  with a sample of 100 R $\chi$ T parameter space points for the complete (left) and neglecting 2R diagrams (right) branching fractions.

As was stated above in subsection 3.5.1, a Gaussian distribution of the parameters is assumed. With this, a sample of 100 points in parameter space is studied, which throws a result of  $BR_{100} = (1.0 \pm 0.2) \times 10^{-4}$ , where the error is statistical. This error can be largely reduced by sampling a larger region of the parameter space, however the error will now be saturated by systematic theoretical error. Thus we find a  $BR_{1000} = (0.98 \pm 0.15) \times 10^{-4}$ , where the error is statistical. To give a more reliable result one has to consider theoretical uncertainties from the model, where one can estimate the error by assigning a  $1/N_C$  uncertainty to the amplitude (which is leading order in  $1/N_C$ ), which gives a  $1/N_C^2$  error that becomes comparable to the statistical error. A conservative estimation of the theoretical un-

certainty, which accounts an uncertainty twice larger, in this branching fraction is  $\sim 0.22 \times 10^{-4}$ . So, by adding in quadratures the statistical and systematic errors we find  $BR(\tau \rightarrow \pi\eta\gamma\nu_\tau) = (0.98 \pm 0.27) \times 10^{-4}$  including all contributions. One should be careful when comparing the results from MDM and  $R\chi T$ , since they are different by an order of magnitude. This will be contrasted to the result using a less general statistical error analysis, discussed in section 3.6, where the results agree with the VMD ones. The result for 1000 points is plotted in fig 3.15 (left), along with the contribution neglecting two resonance (2R) diagrams (right). These last one gives a reduced branching ratio  $BR(1R) = (0.65 \pm 0.17) \times 10^{-4}$ .

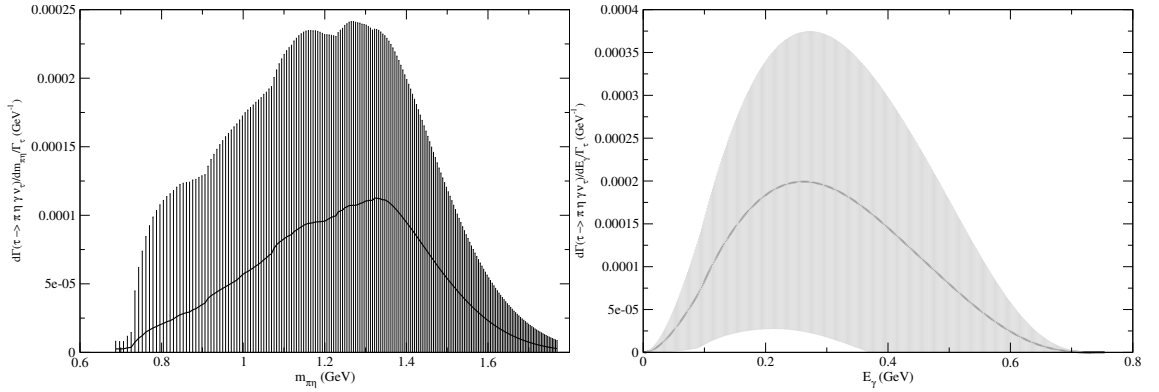


Figure 3.16:  $\tau^- \rightarrow \pi^- \eta \gamma \nu_\tau$  normalized spectra according to  $R\chi T$  in the invariant mass of the  $\pi^- \eta$  system (left) and in the photon energy (right) are plotted.

In fig 3.16 we plot the normalized spectra in  $m_{\pi\eta}$  with 200 steps and  $E_\gamma$  with 500 steps. Further analysis of the spectra dependence on the statistics will be given in section 3.6. Despite the dependence of the total decay width with respect to the statistics of the error, an agreement is found with MDM respecting the (1.15,1.35) GeV  $m_{\pi\eta}$  region, this is, the enhancement in this region is also reproduced. Also, it seems that the  $R\chi T$  for the  $E_\gamma$  spectrum confirms our guess that a cut  $\sim 100$  MeV will give a strong enough suppression. These features do not seem to affect the analysis neglecting 2R diagrams. Further agreement with MDM is seen in the missing of any  $a_0$  meson sign in the  $m_{\pi\eta}$  spectrum.



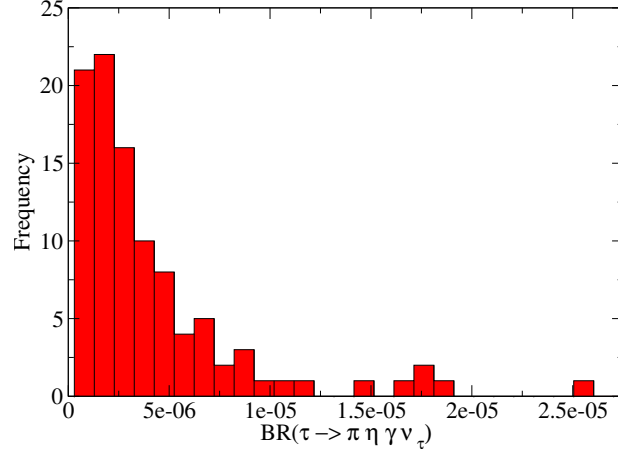


Figure 3.17: Histogram of  $BR(\tau \rightarrow \pi \eta \gamma \nu_\tau)$  in  $R\chi T$  where photons with  $E_\gamma > 100$  MeV are rejected.

In fig. 3.17 we present the branching fraction for a cut in the photon energy of 100 MeV using 100 parameter space points. This yields a branching ratio  $(0.44 \pm 0.06) \times 10^{-6}$ . By neglecting photons with energies above 100 MeV the ratio of background events to non radiative decay event should be reduced to 1/4. By neglecting 2R contributions the branching ratio changes to  $(0.30 \pm 0.04) \times 10^{-6}$ , which lead us to the same conclusion.

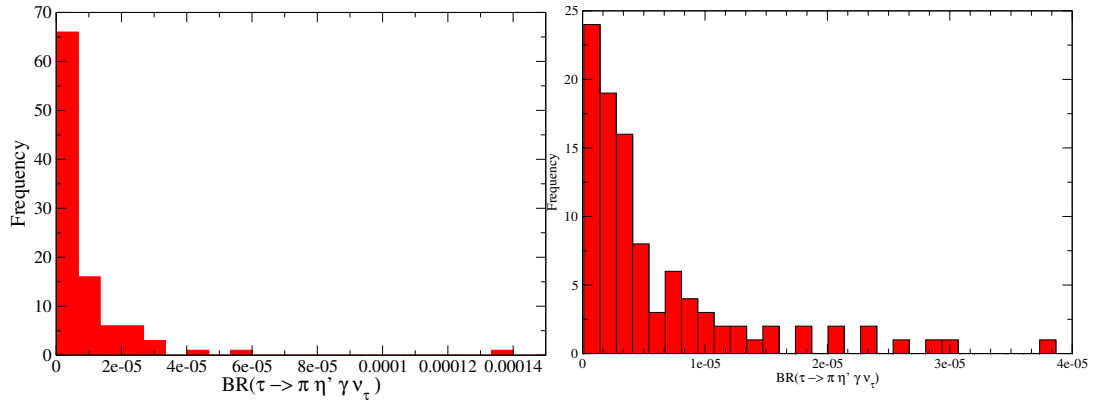


Figure 3.18: Histogram of  $BR(\tau^- \rightarrow \pi^- \eta' \gamma \nu_\tau)$  with a sample of 100  $R\chi T$  parameter space points for the complete (left) and neglecting 2R diagrams (right) branching fractions.

Figure 3.18 gives analogous plots to those in fig 3.15 for the  $\eta'$  mode, this is, whole contribution (left) and neglecting the 2R contributions (right). For 100 parameter

space points the branching ratio we get is  $BR_{100} = (0.9 \pm 0.4) \times 10^{-5}$ , which is still larger than the non radiative process. As in the case for the  $\eta$ , as one takes an increasingly larger region of the parameter space, the systematic theoretical error becomes the dominant uncertainty. Then, by taking the corresponding theoretical uncertainty we get  $BR_{1000} = (0.84 \pm 0.06) \times 10^{-5}$  including all contributions, while neglecting 2R contributions we get  $BR_{1000} = (0.65 \pm 0.05) \times 10^{-6}$ . Again, the dependence on the statistics for the error is analyzed in section 3.6.

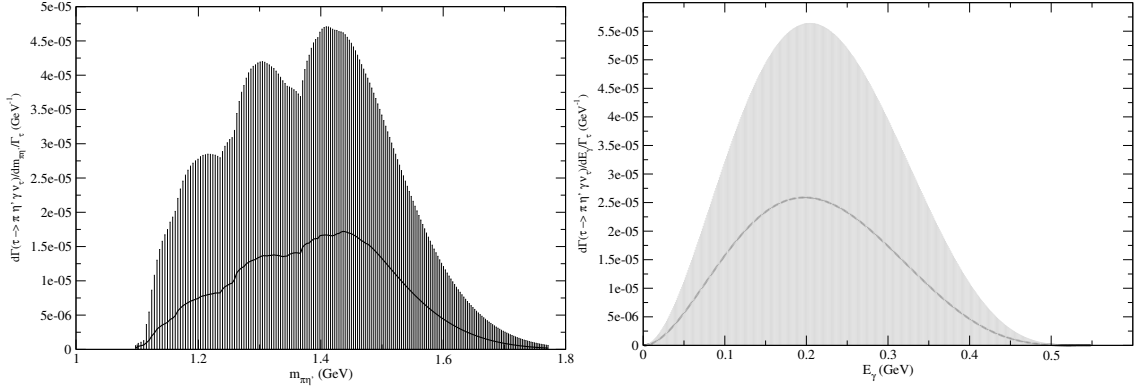


Figure 3.19:  $\tau^- \rightarrow \pi^- \eta' \gamma \nu_\tau$  normalized spectra according to  $R\chi T$  in the invariant mass of the  $\pi^- \eta'$  system (left) and in the photon energy (right) are plotted.

In fig. 3.19 the normalized spectra in  $m_{\pi\eta'}$  with 200 steps (left) and  $E_\gamma$  with 500 steps (right) is shown. For the  $m_{\pi\eta'}$  spectrum, a maximum is expected around the  $[1.30, 1.45]$  GeV region. Also, the photon energy spectrum suggest a  $\sim 100$  MeV cut on the photon energy. The spectra barely changes when neglecting the 2R contributions.

By applying the cut on the photon energy a  $BR = (0.9 \pm 0.2) \times 10^{-6}$ , this result is shown in fig 3.20. By neglecting 2R contributions one gets  $BR = (0.7 \pm 0.2) \times 10^{-6}$ .

### 3.6 Statistical error analysis

A different assignment of distribution for the parameters of both theories were done in the computation of these decays. In the case of MDM, the first consists in taking only the mean value for the couplings and letting them vary randomly within 1 sigma independently. For  $R\chi T$  the same procedure is followed, but some of the couplings have rather large uncertainties due to the fact that those parameters cannot be fixed

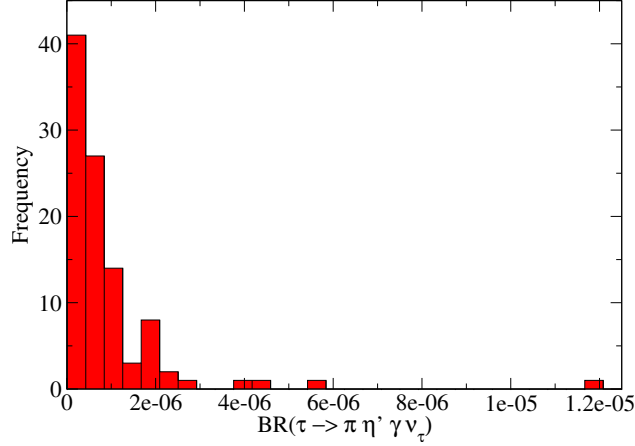


Figure 3.20: Histogram of  $BR(\tau \rightarrow \pi \eta' \gamma \nu_\tau)$  in  $R\chi T$  where photons with  $E_\gamma > 100$  MeV are rejected.

by nowadays experimental data and we still do not know how to constrain them from short distance QCD. From here on, this will be called the 1 sigma approach.

In the previous sections, the coupling parameters were assigned as a Gaussian distribution around the mean value of the fit in the case of MDM. Since almost all coupling parameters within this theory must be fitted phenomenologically from independent physical processes, the Gaussian behavior of the coupling constant gives a very good description of such parameters.

What happens when we try to use the same Gaussian description for the  $R\chi T$  is rather startling at first, since the mean value of the branching ratios seem to augment considerably (an order of magnitude in both channels). The problem here seems to rely on the fact that some of the couplings take values mainly outside the 68% around the mean value, leading to an artificial enhancement of the branching fractions. However, this error analysis has a serious bias stemming from the fact that several of the known and unknown couplings must be related through short distance constraints and should not be varied independently. The correct way to vary the parameters should be by means of constructing a parameter vector and then assign a covariant matrix that would then correct correlation among the different parameters.

The determination of the covariant matrix would be such a formidable task that is far beyond the scope of this work. Therefore, for R $\chi$ T the most reliable description of the decays under study will be the 1 sigma approach. The corresponding values of the branching ratios are given in table 3.2.

	complete $\tau \rightarrow \pi\eta\gamma\nu_\tau$	without 2R $\tau \rightarrow \pi\eta\gamma\nu_\tau$	complete $\tau \rightarrow \pi\eta'\gamma\nu_\tau$	without 2R $\tau \rightarrow \pi\eta'\gamma\nu_\tau$
100 points	$(2.3 \pm 0.9) \cdot 10^{-5}$	—	$(2.3 \pm 3.5) \cdot 10^{-6}$	$(2.1 \pm 1.8) \cdot 10^{-6}$
1000 points	$(3.0 \pm 0.6) \cdot 10^{-5}$	$(2.3 \pm 0.5) \cdot 10^{-5}$	$(2.2 \pm 0.4) \cdot 10^{-6}$	$(2.0 \pm 0.4) \cdot 10^{-6}$
$E_\gamma < 100$ MeV	$(1.0 \pm 0.3) \cdot 10^{-6}$	$(1.2 \pm 0.6) \cdot 10^{-6}$	$(2 \pm 1) \cdot 10^{-7}$	$(2 \pm 1) \cdot 10^{-7}$

Table 3.2: Branching fractions for different kinematical constraints and parameter space points.

### 3.7 Conclusions

The near start of Belle-II data taking brings us an excellent opportunity to search for second class currents, since the current limit on these ( $BR(\tau \rightarrow \pi\eta\gamma\nu_\tau) \lesssim 9 \times 10^{-5}$  and  $BR(\tau \rightarrow \pi\eta'\gamma\nu_\tau) \lesssim 7 \times 10^{-6}$ ) are very near to the expected predictions based on isospin breaking. Belle-II has become a very promising experiment to look for SCC in  $\tau$  decays due to its promised high precision.

We have seen that a less restrictive error estimation might lead to an artificial enhancement of the observables computed within R $\chi$ T due to the dependence amidst known and/or unknown couplings. So, an appropriate description of the errors of the parameters must be done, restricting them to lie within a certain error margin that can ensure the proper variation of parameters without introducing bias due to this dependence.

Using the appropriate error description for R $\chi$ T we found the results given in table 3.3, where we can guarantee background rejection for  $\tau \rightarrow \pi\eta\gamma\nu_\tau$ , but not for the  $\eta'$  channel.

SCC bkg	BR (no cuts)	BR ( $E_\gamma^{\text{cut}} = 100 \text{ MeV}$ )	BR SCC signal	Bkg rejection
$\tau^- \rightarrow \pi^- \eta \gamma \nu_\tau$	$(3.0 \pm 0.6) \cdot 10^{-5}$	$(1.2 \pm 0.6) \cdot 10^{-6}$	$\sim 1.7 \cdot 10^{-5}$	Yes
$\tau^- \rightarrow \pi^- \eta' \gamma \nu_\tau$	$(2.2 \pm 0.4) \cdot 10^{-6}$	$(2 \pm 1) \cdot 10^{-7}$	$[10^{-7}, 10^{-6}]$	No

Table 3.3: The main conclusions of our analysis are summarized: Our predicted branching ratios for the  $\tau^- \rightarrow \pi^- \eta^{(\prime)} \gamma \nu_\tau$  decays and the corresponding results when the cut  $E_\gamma > 100 \text{ MeV}$  is applied. We also compare the latter results to the prediction for the corresponding non-radiative decay (SCC signal) according to ref. [124] and conclude if this cut alone is able to get rid of the corresponding background in SCC searches.

It is also interesting to note our finding that, within the  $R\chi L$  frame, a simplified description of these decays neglecting the two-resonance mediated contributions is a good approximation for branching ratios and decay spectra, which will ease the coding of the corresponding form factors in the Monte Carlo generators.

We have pointed out for the first time the importance of the process studied as an important background on the search for SCC. We also found that  $G$ -parity violation gives a suppression comparable to the  $\alpha$ , and thus neglect the bremsstrahlung contribution to the radiative process by making a reasonable lower cut. Also, that by cutting photons with energies above 100 MeV will give the necessary suppression to neglect the contribution from this process to the background in the search for SCC. (The cut is done leaving only small regions for the detection of  $\pi^0$  and  $\eta^{(\prime)}$  through their decay into photons.)

## Chapter 4

# The $VV'P$ form factors in $R_\chi T$ and the $\pi - \eta - \eta'$ light-by-light contribution to the muon $g - 2$

### 4.1 Introduction

The anomalous magnetic moment has been of such importance to physics that it led the way in constructing the quantum theory of the non-relativistic interactions of particles. Furthermore, once quantum field theory was constructed the anomalous magnetic moment of the electron played a fundamental role in the understanding of renormalization and the perturbativity of QED. This observable continues to be a very interesting one since currently there is a discrepancy of  $\sim 3.5\sigma$  between the latest measurement of the anomalous magnetic moment of the muon and the prediction within the Standard Model. It has become more interesting since, recently it has been announced that in the very near future the experimental accuracy will be improved by a factor of 4. This makes mandatory for theoreticians to reduce the uncertainty in the predictions for this observable if one wants to explore the plausibility of higher energy Beyond Standard Model effects that can be studied in this process.

In section 4.2 we introduce the anomalous magnetic moment along with some historical development and the contributions to it. In section 4.3 we introduce the hadronic contributions to the anomalous magnetic moment of the muon and show the main contribution to the Hadronic Light by Light scattering. In section 4.4 we show our result for the pion transition form factor and how the couplings of the theory are obtained. In section 4.5 we show the way to relate the pion transition form factor with the  $\eta$  and  $\eta'$  ones and give our prediction for them. In section 4.6 we give the

contribution of the Goldstone exchange diagram. In section 4.7 we propose a new form of measuring the transition form factor when both photons are off-shell.

## 4.2 The anomalous magnetic moment

There is a fundamental property of particles that played a key role in the construction and understanding of Quantum Mechanics: the spin. The spin is one of the two Casimir invariants of the Poincaré group (the other being the mass) upon which all particles in a theory invariant under Minkowski space-time isometries are classified. The quantum nature of spin as an intrinsic angular momentum of fundamental particles was first discovered by Otto Stern and Walther Gerlach in 1922 by constructing a collimated beam of silver atoms passing through an inhomogeneous magnetic field [147]. What they measured was a magnetic dipole moment quantization due to a single electron in the outermost occupied shell, this is, the electron could have only two possible magnetic moment values with the same magnitude. At the classical level, the magnetic moment is defined through the relation

$$\boldsymbol{\mu} = \frac{q}{2m} \mathbf{L}, \quad (4.1)$$

where  $q$  is the charge,  $m$  the mass and  $L$  the angular momentum. At the quantum level, a massive particle with non-zero intrinsic angular momentum  $\mathbf{s}$  must have a magnetic moment

$$\boldsymbol{\mu} = g \frac{q}{2m} \frac{\mathbf{s}}{2}, \quad (4.2)$$

where  $\mathbf{s}$  is the spin operator, and  $g$  is defined as the adimensional gyromagnetic factor.

In Quantum Electrodynamics (QED), the way to obtain the magnetic moment of a fundamental particle is by making it interact with an electromagnetic field. At leading order in QED one gets the Dirac result  $g = 2$ . However, in 1947 Isidor Isaac Rabi and his team measured a deviation from Dirac's prediction in hyperfine splitting

of the ground state of hydrogen and deuterium [148], which was

$$a_e := \delta\mu/\mu = \frac{g_e - 2}{2} = 0.00126 \pm 0.00019, \quad (4.3)$$

where  $a_\ell$  is defined as the anomalous magnetic moment of lepton  $\ell$ , and could be successfully explained by Julian Schwinger by computing a next order term as a correction to the vertex [149] as shown in figure 4.1, where the correction is  $\delta\mu/\mu = \alpha/2\pi = 0.00116\dots$  in perfect agreement with the experimental value. Ever since, more and more precise predictions and measurements of  $a$  have been done. This is why it has become a suitable observable for BSM phenomena.



Figure 4.1: Next to leading order correction to the anomalous magnetic moment found by Schwinger.

In their review of the anomalous magnetic moment of the muon  $a_\mu$ , Fred Jegerlehner and Andreas Nyffeler state that by the Appelquist-Carrazzone theorem a heavier particle will have an enhanced sensibility to high energy scale phenomena [150], since it would decouple from a lighter field. The dependence on the mass of the particle and the scale of new phenomena is given by [150]

$$\delta a_\ell \propto \frac{m_\ell^2}{\Lambda^2} \quad \text{for} \quad M \gg m_\ell \quad (4.4)$$

This leads naturally to search deviations from the Standard Model in the anomalous magnetic moment of heavier particles. Since the anomalous magnetic moment of the electron  $a_e$  is very well known, the best option is the muon, which has a mass nearly 200 times greater than the electron. This makes it more reliable to find effects that cannot be explained within the SM.



Being nearly 17 times heavier than the muon, the  $a_\tau$  should be the observable where to look for deviations from the SM. Nevertheless, the muon is preferred instead of the  $\tau$  since its lifetime is so short ( $\tau_\tau/\tau_\mu \sim 10^{-7}$ ) that makes it really difficult to measure its magnetic moment using spin precession techniques. Nowadays the experimental determination of the tau lepton anomalous magnetic moment  $a_\tau$  is compatible with zero [151].

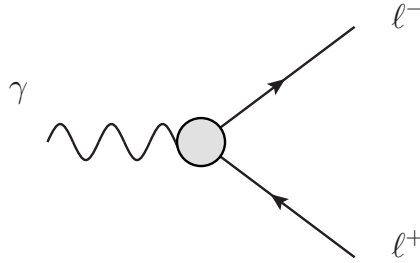


Figure 4.2: Feynman diagram of a fermion interaction with a classic electromagnetic field. The blob represents all possible interactions that can happen in between.

Now, the most general vertex for magnetic moment is represented by the diagram in figure 4.2 where all possible interactions are hidden in the blob (QED, EW and strong interactions)

$$a_\ell = a_\ell^{QED} + a_\ell^{EW} + a_\ell^{Had}. \quad (4.5)$$

One can parametrize all the possible interactions in the blob into two form factors by making use of the Gordon identity and separating the fermion current into a vector ( $\gamma_\mu$ ) and a tensor interaction ( $\sigma_{\mu\nu}$ ) current. The tensor interaction will then have attached the Pauli (or magnetic) form factor  $F_M(q^2)$ , which at  $q^2 = 0$  gives the anomalous magnetic moment.

The hadronic part has two contributions stemming from Hadronic Vacuum Polarization (HVP) diagrams (fig. 4.3) and Hadronic Light by Light (HLbL) (figs. 4.4 and 4.5). The former can be fully obtained by experimental data, while in the latter one has to rely on a model to predict its contribution. All the contributions to the

Type of contribution	Contribution to $a_\mu \times 10^{11}$	Error $\times 10^{11}$
QED	116'584,718.95	0.08
EW	153.6	1.0
Had	6930	$(42)_{HVP}(26)_{HLbL}$
Total	116'591,803	$(1)(42)(26)$
Exp	116'592,091	$(54)(33)$

Table 4.1: Different types of contributions to the  $a_\mu$ . The hadronic contributions give the main theoretical uncertainty.

$a_\mu$  are given in table 4.1, where it can be seen that HVP gives a main source of error followed by HLbL. Nevertheless, the HVP error can be reduced by using a better set of experimental data, while the HLbL error is given by the uncertainty from the theory and the fitting of the parameters used to compute it.

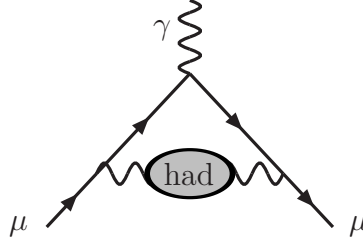


Figure 4.3: Hadronic Vacuum Polarization contribution to  $a_\mu$ , the blob stands for all possible strong interaction processes.

Here we discuss the contributions and errors from table 4.1: As can be seen in the Particle Data Group Review of Particle Physics [72], the anomalous magnetic moment of the muon is almost fully determined by pure QED interaction, with an uncertainty  $80 \times 10^{-14}$  [152]; the contribution arising from weak boson exchange is very little, but non-negligible  $(153.6 \pm 1.0) \times 10^{-11}$  and the contributions stemming from strong interactions give the dominant uncertainty to the anomalous magnetic moment of the muon  $\sim 53 \times 10^{-11}$ , which is comparable with the experimental error  $\sim 63 \times 10^{-11}$  [72]. The Fermilab [153] and J-Parc [154] are planning to reduce the present experimental error in a factor of 4, leading to an error  $\sim 16 \times 10^{-11}$ . This is what makes mandatory from the theoretical point to reduce the uncertainty in the prediction of the  $a_\mu^{HLbL}$ , since the error from  $a_\mu^{HVP}$  can be reduced with further

experimental data.

### 4.3 Hadronic contributions

There is a contribution arising at order  $\alpha^2$  where in the Schwinger correction the virtual photon polarizes the vacuum leading to a loop correction in the propagator of the photon. The QED contribution when the fermions in the loop are leptons has been computed exactly and is included in the QED correction [155]. One of the hadronic contributions to the  $a_\mu$ , the Hadronic Vacuum Polarization (HPV), is obtained by changing the leptons in the loop by quarks, where the strong interactions will come about since the energy scale in the loop covers the region where quarks are confined in hadrons. The hadronic contribution is obtained by means of a dispersion relation which can be connected by the optical theorem with the cross section  $\sigma(e^+e^- \rightarrow \text{hadrons})$

$$a_\mu^{HVP} = \left(\frac{\alpha m_\mu}{3\pi}\right)^2 \int ds \frac{R(s)K(s)}{s^2} + \mathcal{O}(\alpha^3), \quad (4.6)$$

where  $R = \sigma(e^+e^- \rightarrow \text{hadrons})$  and the functional for of  $K(s)$  can be found in ref [150], thus obtained by fitting data up to the charmonium region (5.2 GeV) and the bottomonium region ([9.46,13] GeV), the rest is obtained using pQCD. The greatest error in  $a_\mu$  comes from this contribution  $\sim 42 \times 10^{-11}$ , but this can be reduced by augmenting the quality and quantity of experimental data. In the expression for the  $a_\mu^{HLbL}$  eq. (4.6) it can be seen the dominance of low-energy contributions.

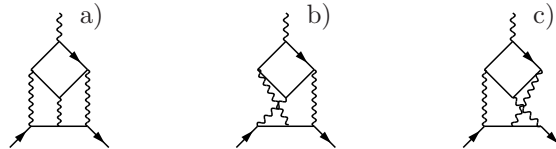


Figure 4.4: Light by light scattering insertions for a fermion loop.

One can see that at the  $\alpha^3$  order in the QED expansion a new kind of phenomena shows up, namely the *light by light* scattering (LbL) insertions. Some typical

diagrams for these contributions are shown in fig 4.4. This effect cannot be present in  $\alpha^2$  contributions ( $\gamma\gamma \rightarrow \gamma$ ), since a closed fermion loop coupled to three photons would vanish due to Furry's theorem. These contributions can be separated into three categories, one that gives a universal contribution to the  $g - 2$  where the particle in the loop is the same as the one under study to determine its magnetic moment. One contribution comes from particles lighter than the one under study and the other from particles heavier than it. The latter ones are suppressed by ratios of squared masses, the former are enhanced by logarithms of the mass ratio [156]. As in the HVP case, if we replace the leptons in the loop by quarks we get the corresponding hadronic contribution, namely the Hadronic Light by Light scattering (HLbL), which cannot be obtained from data and has to be theoretically predicted. Despite the fact that the Appelquist-Carrazone theorem cannot be applied to hadronic couplings, it can give us a lead on which hadrons will contribute the most in the HLbL.

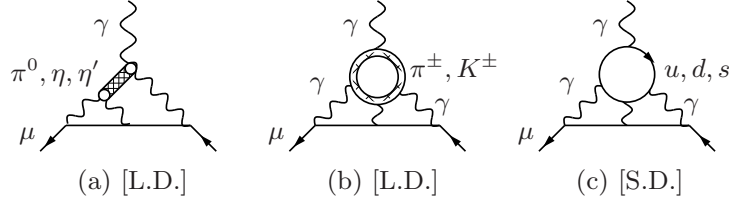


Figure 4.5: Contributions from Hadronic Light by Light scattering,  $a_\mu^{HLbL}$

Since HLbL cannot be fully obtained experimentally (See however recent progress in this direction in Refs. [157, 159, 158, 160, 161, 162, 163]), we will focus on this contribution to the  $a_\mu$  trying to reduce the theoretical uncertainty. There has been also a great advance in Lattice computations [164, 165]. In R $\chi$ T, the contribution comes from diagrams as those shown in fig. 4.5, where to the Goldstone bosons exchange shown in the diagram one has to add resonances exchange. However by the argument of the previous paragraph one would expect these contributions suppressed with respect to that of the Goldstone exchange. A previous computation of the resonances contribution showed that they are, in fact suppressed with respect to the Goldstone ones [166]. The diagrams (b) and (c) of fig. 4.5 give a total contribution suppressed

with respect to the pseudoscalar exchange, therefore we will only focus in the main contribution to the  $a_\mu^{HLbL}$  [166] as shown in table 4.2. It was at first assumed that the main contribution to HLbL would come from energy regions around the muon mass, but it was noticed that some important contributions also come from the  $[0.5, 1]$  GeV region [167, 167], so that one has to extend  $\chi$ PT to include resonances in order to include that energy region.

$a_\mu^{(a)}$	$a_\mu^{(b)}$	$a_\mu^{(c)}$
$(6.5 \pm 0.6) \times 10^{-10}$	$(-5.1 \pm 0.4) \times 10^{-10}$	$(6.0 \pm 0.4) 10^{-10}$

Table 4.2: Contributions to  $a_\mu$  from diagrams (a), (b) and (c) in fig 4.5 as given in ref. [166].

## 4.4 Transition Form Factor, TFF

All the relevant diagrams to the pseudoscalar exchange are shown in figure 4.6. Therefore, all we need to know to completely characterize the Goldstone exchange contribution is the form factor of the effective vertex  $\pi^* \gamma^* \gamma^*$ . Since the external photon must be taken with  $q = 0$  and the form factor depends only on the squared of the momenta of the virtual photons, one finds that only three of the integrals in the loop are non-trivial [169]. The total pion exchange integrals to compute the contribution  $a_\mu^{\pi^0, LbL}$  are given by the expressions in appendix 5.

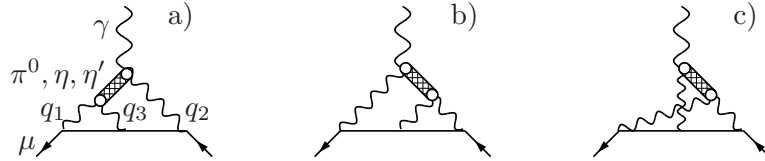


Figure 4.6: Main contribution to  $a_\mu^{HLbL}$ , internal photon lines include the  $\rho - \gamma$  mixing

Previous computations of the  $\pi$  Transition Form Factor ( $\pi$ TFF) were made using the naive simplification of taking the pion on-shell, which might be seen as taking

only the  $\mu$  mass region ( $m_\mu \approx m_\pi$ ) as told in the previous section. This was shown to be an over-simplification of the problem [167, 168]. The following expression gives the general  $\pi$ TFF when all particles are off-shell [129, 170]

$$\begin{aligned} \mathcal{F}_{\pi^0\gamma^*\gamma^*}(p^2, q^2, r^2) = & \frac{2r^2}{3F} \left[ -\frac{N_C}{8\pi^2 r^2} + 4F_V^2 \frac{d_3(p^2 + q^2)}{(M_V^2 - p^2)(M_V^2 - q^2)r^2} \right. \\ & + \frac{4F_V^2 d_{123}}{(M_V^2 - p^2)(M_V^2 - q^2)} + \frac{16F_V^2 P_3}{(M_V^2 - p^2)(M_V^2 - q^2)(M_P^2 - r^2)} \\ & \left. - \frac{2\sqrt{2}}{M_V^2 - p^2} \left( \frac{F_V}{M_V} \frac{r^2 c_{1235} - p^2 c_{1256} + q^2 c_{125}}{r^2} + \frac{8P_2 F_V}{(M_P^2 - r^2)} \right) + (q^2 \leftrightarrow p^2) \right], \quad (4.7) \end{aligned}$$

where  $p$ ,  $q$  and  $r$  are the photons and pion four-momenta, respectively. In the case where the pion is taken to be on-shell one gets

$$\begin{aligned} \mathcal{F}_{\pi^0\gamma^*\gamma^*}(p^2, q^2, r^2 = 0) = & \frac{2}{3F} \left[ -\frac{N_C}{8\pi^2} + \frac{4F_V^2 d_3(p^2 + q^2)}{(M_V^2 - p^2)(M_V^2 - q^2)} + 2\sqrt{2} \frac{F_V}{M_V} \frac{p^2 c_{1256} - q^2 c_{125}}{M_V^2 - p^2} \right. \\ & \left. + 2\sqrt{2} \frac{F_V}{M_V} \frac{q^2 c_{1256} - p^2 c_{125}}{M_V^2 - q^2} \right]. \quad (4.8) \end{aligned}$$

One finds that the couplings in this form factor are all fixed from short distance constraints[89]. These couplings are given in the following expression

$$\begin{aligned} F_V = \sqrt{3}F, \quad c_{125} = 0, \quad c_{1256} = -\frac{N_C M_V}{32\sqrt{2}\pi^2 F_V} \sim -3.26 \cdot 10^{-2}, \\ c_{1235} = 0, d_{123} = \frac{F^2}{8F_V^2} = \frac{1}{24}, \quad d_3 = -\frac{N_C M_V^2}{64\pi^2 F_V^2} \sim -0.112 \end{aligned} \quad (4.9)$$

where the condition we find for the coupling constant  $d_3$  can be expressed in a different manner for convenience,

$$d_3 = -\frac{N_C}{64\pi^2} \frac{M_V^2}{F_V^2} + \frac{F^2}{8F_V^2} + \frac{4\sqrt{2}P_2}{F_V}, \quad (4.10)$$

provided the pseudoscalar resonance coupling  $P_2 \equiv d_m \kappa_3^{PV}$ , where  $\kappa_3^{PV}$  is the pseu-

doscalar vector coupling of  $\mathcal{O}_3^{PV}$  of ref [129] fulfills the relation

$$P_2 = -\frac{F^2}{32\sqrt{2}F_V} = -\frac{F}{32\sqrt{6}}, \quad (4.11)$$

which belongs to the consistent set of short distance constraints [89].

Contrary to ref. [129], we take the asymptotic value given by the short distance constraints of  $F_V = \sqrt{3}F$  and estimate the error varying it around a 10% from the SD prediction. We rely on this estimation since a fit done to BaBar data [91] gives a variation around the 5% of the asymptotic value. With this, we find the behavior given in figure 4.7. The  $P_3$  coupling is fixed phenomenologically from the combined analyses of the  $\pi(1300) \rightarrow \gamma\gamma$  and  $\pi(1300) \rightarrow \rho\gamma$  [129], giving

$$P_3 = -(1.2 \pm 0.3) \cdot 10^{-2} \text{ GeV}^2. \quad (4.12)$$

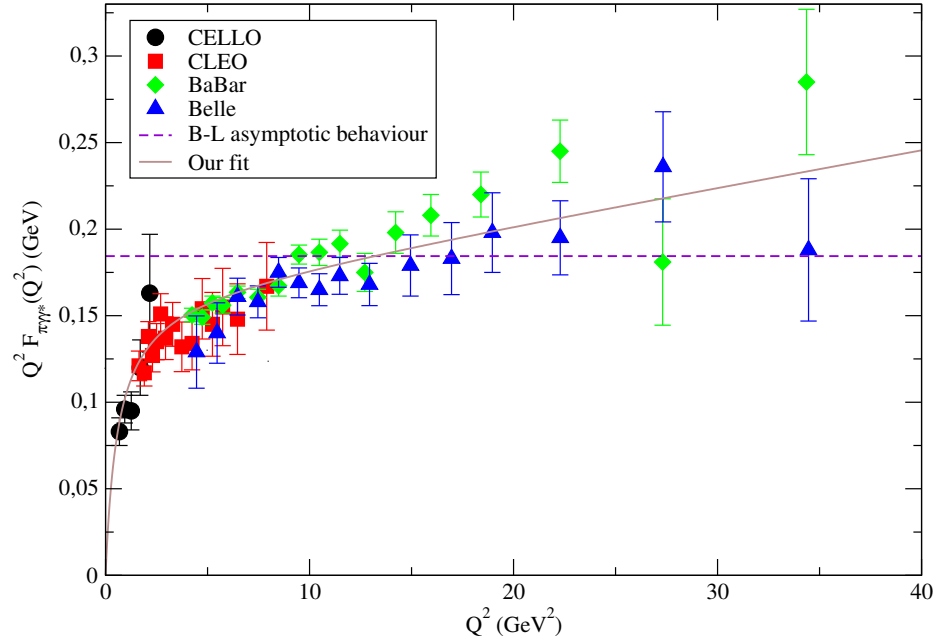


Figure 4.7: Our fit to the BaBar, Belle, CELLO and CLEO data compared to the Brodsky-Lepage behavior.

Relying on the Brodsky-Lepage [103] behavior, which predicts the following limit

of the form factor at high  $q^2$  for one on-shell photon

$$\lim_{q^2 \rightarrow \infty} \mathcal{F}_{\pi\gamma\gamma^*}(0, q^2, m_\pi^2) \sim \frac{2F}{q^2}, \quad (4.13)$$

one finds a deviation from BaBar data [171]. Since the high energy description of the form factor is given mainly by the  $P_2$  coupling we fix all the other couplings from equations (4.9) and fit  $P_2$  to BaBar [171], Belle [172], CELLO [173] and CLEO [174] data of the TFF. We, thus, find that the best fit is given by

$$P_2 = -(1.13 \pm 0.12) \times 10^{-3} \text{ GeV}, \quad (4.14)$$

with the statistic test  $\chi^2/\text{degrees of freedom} = 1.01$ . With this, we find that the best fit for BaBar data is  $\sim 4\%$  away from the Brodsky-Lepage constraint. However, more accurate measurements of the  $\pi$ TFF at large  $q^2$  and  $p^2$  are needed to elucidate whether the Brodsky-Lepage-like asymptotic behavior (approached by Belle) or its violation (hinted by BaBar) describe the high-energy data. Since a best fit of the form factor would be with the two photons being off-shell we propose a new observable from which to fit the TFF (see section 4.7).

## 4.5 $\eta$ - and $\eta'$ - Transition Form Factor

In this section we evaluate the contributions of the next lightest pseudoscalar mesons ( $\eta$  and  $\eta'$ ) to  $a_\mu^{HLbL}$ . In order to do that we take advantage of the relation of the respective TFF with the  $\pi$ TFF. We will treat the  $\eta$ - $\eta'$  mixing in the two-angle mixing scheme (consistent with the large- $N_C$  limit of QCD [175]) and work in the quark flavor basis [176] where

$$\text{diag}(u) = \left( \frac{\pi^0 + C_q\eta + C_{q'}\eta'}{\sqrt{2}}, \frac{-\pi^0 + C_q\eta + C_{q'}\eta'}{\sqrt{2}}, -C_s\eta + C_{s'}\eta' \right), \quad (4.15)$$



in which

$$\begin{aligned}
C_q &\equiv \frac{F}{\sqrt{3}\cos(\theta_8 - \theta_0)} \left( \frac{\cos\theta_0}{f_8} - \frac{\sqrt{2}\sin\theta_8}{f_0} \right), \\
C_{q'} &\equiv \frac{F}{\sqrt{3}\cos(\theta_8 - \theta_0)} \left( \frac{\sqrt{2}\cos\theta_8}{f_0} + \frac{\sin\theta_0}{f_8} \right), \\
C_s &\equiv \frac{F}{\sqrt{3}\cos(\theta_8 - \theta_0)} \left( \frac{\sqrt{2}\cos\theta_0}{f_8} + \frac{\sin\theta_8}{f_0} \right), \\
C_{s'} &\equiv \frac{F}{\sqrt{3}\cos(\theta_8 - \theta_0)} \left( \frac{\cos\theta_8}{f_0} - \frac{\sqrt{2}\sin\theta_0}{f_8} \right).
\end{aligned} \tag{4.16}$$

The values of the pairs of decay constants and mixing angles are [176]

$$\theta_8 = (-21.2 \pm 1.6)^\circ, \quad \theta_0 = (-9.2 \pm 1.7)^\circ, \tag{4.17a}$$

$$f_8 = (1.26 \pm 0.04) F, \quad f_0 = (1.17 \pm 0.03) F. \tag{4.17b}$$

We will consider these errors as independent in the following.

Within this mixing scheme, the  $\eta$  and  $\eta'$  TFF can be easily related to the  $\pi$ TFF

$$\begin{aligned}
\mathcal{F}_{\eta\gamma\gamma}(p^2, q^2, r^2) &= \left( \frac{5}{3}C_q - \frac{\sqrt{2}}{3}C_s \right) \mathcal{F}_{\pi\gamma\gamma}(p^2, q^2, r^2), \\
\mathcal{F}_{\eta'\gamma\gamma}(p^2, q^2, r^2) &= \left( \frac{5}{3}C_{q'} + \frac{\sqrt{2}}{3}C_{s'} \right) \mathcal{F}_{\pi\gamma\gamma}(p^2, q^2, r^2).
\end{aligned} \tag{4.18}$$

We have therefore predicted the  $\eta$  and  $\eta'$  TFF using our results for the  $\pi$ TFF. The corresponding error is completely dominated by the  $\eta$ - $\eta'$  mixing. In fig. 4.8 we confront them to BaBar [171], CELLO [173] and CLEO [174] data. In the case of the  $\eta$ TFF good agreement can be seen, although BaBar data tend to lie in the border of our predicted lower limit. Even though data from different experiments on the  $\eta'$ TFF show slight tension, the overall agreement of our prediction with them is quite good. We observe that our  $\pi$ TFF-based prediction tends to show a tiny larger slope than the  $\eta$  and  $\eta'$  TFF data. This feature may be caused by BaBar data on the  $\pi$ TFF. It

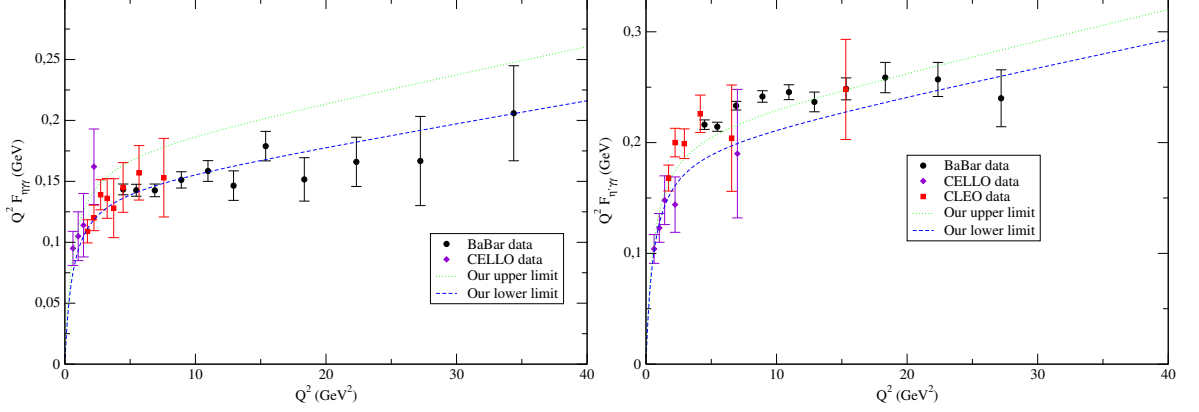


Figure 4.8: Our prediction for the  $\eta$  (left) and  $\eta'$  (right) TFF cross section (left) using the couplings of eq. 4.27 compared to BaBar [171], CELLO [173] and CLEO [174].

remains to be seen if new, more accurate, measurements of these TFF confirm this tendency or not.

## 4.6 Pseudoscalar exchange contribution $a_\mu^{P,HLbL}$

Using all the information in the previous sections and the integrals of appendix 5 we can now compute the total pseudoscalar exchange contribution to the  $a_\mu$ . However, before computing it, further analysis of the error in the  $\pi$ TFF can be done to the classic WZW result in the chiral limit at very-low energy [150]. A small contribution to such value of the  $\pi$ TFF is included [177, 178] by considering the correction at these limits stemming from the short distance constraints on  $c_{1235}$  and  $d_{123}$  and the non-zero mass of the pion. The correction enters as follows,

$$\mathcal{F}_{\pi\gamma\gamma}(0) = -\frac{N_C}{4\pi^2 F}(1 - \Delta), \quad (4.19)$$

where the correction is

$$\Delta = \frac{4\pi^2}{3} \frac{F^2}{M_V^2} \frac{m_\pi^2}{M_V^2} \sim 5.9 \times 10^{-3}. \quad (4.20)$$

Further corrections to the previous expression should be suppressed by further powers of  $m_\pi^2/M_V^2$  and can be safely neglected.

$a_\mu^{\pi^0, HLbL} \cdot 10^{10}$	Method and reference
$5.58 \pm 0.05$	Extended NJL Model [179] (Bijnens, Pallante and Prades [168])
$5.56 \pm 0.01$	Naive VMD Model (Hayakawa, Kinoshita [and Sanda] [167][180])
$5.8 \pm 1.0$	Large- $N_C$ with two vector multiplets, $\pi$ -pole contribution [169]
$7.7 \pm 1.0$	Large- $N_C$ with two vector multiplets, $\pi$ -pole contribution [181]
$7.2 \pm 1.2$	$\pi$ -exchange contribution corresponding to [169] evaluated in [150]
6.9	Holographic models of QCD [182]
$6.54 \pm 0.25$	Holographic models of QCD [183]
$6.58 \pm 0.12$	Lightest Pseudoscalar and Vector Resonance saturation [129]
$6.49 \pm 0.56$	Rational Approximants [184]
$5.0 \pm 0.4$	Non-local chiral quark model [185]
$6.66 \pm 0.21$	This work, short-distance constraints of [129] revisited and data set updated

Table 4.3: Our result for  $a_\mu^{\pi^0, HLbL}$  in eq. (4.22) is compared to other determinations. The method employed in each of them is also given. We specify those works that approximate  $a_\mu^{\pi^0, HLbL}$  by the pion pole contribution. It is understood that all others consider the complete pion exchange contribution.

Although the uncertainty stemming from this correction is negligible to the observables computed with the TFF (including those of section 4.7), it is not so for the  $a_\mu^{P, HLbL}$ , since the uncertainty in this contribution is essentially given by the low-energy correction. Including this correction we find

$$a_\mu^{\pi^0, HLbL} = (5.75 \pm 0.06) \times 10^{-10} \quad (4.21)$$

for the pion-pole simplification, *i. e.*, for on-shell pion and

$$a_\mu^{\pi^{0*}, HLbL} = (6.66 \pm 0.21) \times 10^{-11}. \quad (4.22)$$

We can see, as said above, that the pion-pole simplification underestimates the  $a_\mu^{\pi^0, HLbL}$  by a 14% and the error by a factor 4. The off-shell result is shown in table 4.3, where other results are quoted for comparison. For the  $\eta$  and  $\eta'$  we made the same comparison between the pole estimation and the complete TFF, where we found

$$a_\mu^{\eta,HLbL} = (1.44 \pm 0.26) \cdot 10^{-10}, \quad a_\mu^{\eta',HLbL} = (1.08 \pm 0.09) \cdot 10^{-10} \quad (4.23)$$

for the pole contribution and

$$a_\mu^{\eta,HLbL} = (2.04 \pm 0.44) \cdot 10^{-10}, \quad a_\mu^{\eta',HLbL} = (1.77 \pm 0.23) \cdot 10^{-10} \quad (4.24)$$

for the whole exchange contribution.

$a_\mu^{P,HLbL} \cdot 10^{10}$	Method and reference
$8.5 \pm 1.3$	Extended NJL Model [179] (Bijnens, Pallante and Prades [168])
$8.27 \pm 0.64$	Naive VMD Model (Hayakawa, Kinoshita [and Sanda] [167][180])
$8.3 \pm 1.2$	Large- $N_C$ with two vector multiplets, $P$ -pole contribution [169]
$11.4 \pm 1.0$	Large- $N_C$ with two vector multiplets, $P$ -pole contribution [181]
$9.9 \pm 1.6$	$\pi$ -exchange contribution corresponding to [169] evaluated in [150]
10.7	Holographic models of QCD [182]
$9.0 \pm 0.7$	Rational Approximants [187] using half-width rule [188], $P$ -pole contribution
$5.85 \pm 0.87$	Non-local chiral quark model [185]
$11.4 \pm 1.3$	Average of various approaches (Prades, de Rafael and Vainshtein [189])
$10.47 \pm 0.54$	This work, lightest Pseudoscalar and Vector Resonance saturation

Table 4.4: Our result for  $a_\mu^{P,HLbL}$  in eq. (4.26) is compared to other determinations. The method employed in each of them is also given. We specify those works that approximate  $a_\mu^{P,HLbL}$  by the pseudoscalar pole contribution. It is understood that all others consider the complete pseudoscalar exchange contribution.

As it happened in the  $\pi^0$  case, the  $\eta^{(\prime)}$ -pole approximation underestimates clearly the  $HLbL$  contribution, by  $\sim 30(45)\%$ , and the error, by a factor of roughly two. This is confirmed by comparing our results in eq. (4.23) with those obtained in ref. [187]

$$a_\mu^{\eta,HLbL} = (1.38 \pm 0.16) \cdot 10^{-10}, \quad a_\mu^{\eta',HLbL} = (1.22 \pm 0.09) \cdot 10^{-10} \quad (4.25)$$

which agree within errors.

Taking into account our determinations of  $a_\mu^{\pi^0,HLbL}$  (4.22),  $a_\mu^{\eta,HLbL}$  and  $a_\mu^{\eta',HLbL}$  (4.24),

we obtain for the contribution of the three lightest pseudoscalars

$$a_\mu^{P,HLbL} = (10.47 \pm 0.54) \cdot 10^{-10}. \quad (4.26)$$

This number is compared to other determinations in the literature in Table 4.4. Again, the method employed in each determination is also given for reference.

## 4.7 Genuine probe of the $\pi$ TFF

Currently, there are no experimental data that can give us the behavior of the  $\pi$ TFF with both photons off-shell. Looking forward to fixing parameters from an observable with both photons off-shell we study the cross section  $\sigma(e^+e^- \rightarrow \mu^+\mu^-\pi^0)$ , which can be obtained through the process shown in figure 4.9.

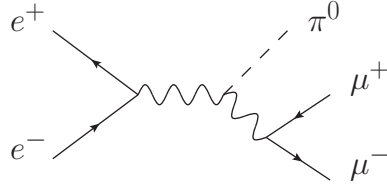


Figure 4.9: The  $e^+e^- \rightarrow \mu^+\mu^-\pi^0$  scattering as a probe for  $\pi$ TFF with both photons off-shell.

In this process the center of mass squared energy  $p^2 = s$  is the electron-positron invariant mass and the di-muon invariant mass will give the other photon squared four-momenta  $s_1 = q^2$ . Since now  $s$  and  $s_1$  are time-like, we must change the factors  $1/(M_R^2 - x) \rightarrow D_R(x)$  since now both four-momenta span the resonances region and such effect must be taken into account. By using the values of the couplings as discussed in the previous section

$$\begin{aligned} F_V &= \sqrt{3}F(1.0 \pm 0.1), \quad c_{125} = 0, \quad c_{1256} = -\frac{N_C M_V}{32\sqrt{2}\pi^2 F_V}, \\ d_3 &= -\frac{N_C M_V^2}{64\pi^2 F_V^2} + \frac{F^2}{8F_V^2} + \frac{4\sqrt{2}P_2}{F_V}, \quad P_2 = -(1.13 \pm 0.12) \cdot 10^{-3} \text{ GeV} \end{aligned} \quad (4.27)$$

we can predict the dependence of the cross section with the center of mass energy, as well as the dependence on the cross section with  $s_1$  for a fixed center of mass energy. In terms of suitable invariants [186],

$$s \equiv k^2, \quad s_1 \equiv k'^2, \quad t_0 \equiv (q_+ - p_\pi)^2, \quad t_1 \equiv (q_+ - p_+)^2, \quad u_1 \equiv (k - p_+)^2, \quad (4.28)$$

the corresponding spin-averaged and unpolarized squared matrix element reads

$$\begin{aligned} \sum \overline{|\mathcal{M}|^2} = & \frac{512\alpha^4\pi^4}{s^2s_1^2} \left| \mathcal{F}_{\pi^0\gamma\gamma}(k^2, k'^2) \right|^2 \left\{ -2m_\mu^4 s^2 \right. \\ & + m_\mu^2 s \left[ m_\mu^4 + m_\pi^2 (m_\pi^2 + s + s_1 - 2t_0 - 4t_1 + 2u_1) \right. \\ & + m_\pi^4 + m_\pi^2 (-3s + s_1 - 3t_0 - 2t_1 + u_1) + 3s^2 - 4ss_1 + 5st_0 + 6st_1 \\ & - 3su_1 + s_1^2 - 3s_1t_0 - 2s_1t_1 + s_1u_1 + 3t_0^2 + 4t_0t_1 - 2t_0u_1 + 4t_1^2 - 4t_1u_1 + u_1^2] \\ & + \frac{1}{4} [2s (s_1 - 2m_\mu^2) (s + t_1 - u_1) (-m_\mu^2 - m_\pi^2 + s + t_0 + t_1) \\ & + 4 (m_\mu^2 - t_1) (s + t_1 - u_1) (m_\mu^2 + m_\pi^2 - s - t_0 - t_1) \\ & (s - s_1 + t_0 + t_1 - u_1) + s (s_1 - 2m_\mu^2) (-m_\mu^2 - m_\pi^2 + s + t_0 + t_1)^2 \\ & - 2(s + t_1 - u_1)^2 (-m_\mu^2 - m_\pi^2 + s + t_0 + t_1)^2 - 2s^2 (s_1 - 2m_\mu^2)^2 \\ & - 2(m_\mu^2 - t_1)^2 (s - s_1 + t_0 + t_1 - u_1)^2 + s (s_1 - 2m_\mu^2) (s - s_1 + t_0 + t_1 - u_1)^2 \\ & + 2s (2m_\mu^2 - s_1) (m_\mu^2 - t_1) (s - s_1 + t_0 + t_1 - u_1) \\ & \left. \left. + s (s_1 - 2m_\mu^2) (s + t_1 - u_1)^2 + s (s_1 - 2m_\mu^2) (m_\mu^2 - t_1)^2 \right] \right\}, \quad (4.29) \end{aligned}$$

where we have neglected the electron mass. Since the flavor facilities can measure this cross-section at very small values of  $k^2$  –close to the threshold of  $(2m_\mu + m_\pi)^2$ – we kept  $m_\mu \neq 0$  and  $m_\pi \neq 0$  in eq. (4.29) as we have done in the numerics. The cross-section can be written [186]

$$\begin{aligned} \sigma = & \frac{1}{2^7\pi^4 s^2} \int_{4m_\mu^2}^{(\sqrt{s}-m_\pi)^2} \frac{ds_1}{\lambda^{1/2}(s, s_1, m_\pi^2)} \int_{t_0^-}^{t_0^+} \frac{dt_0}{\sqrt{1-\xi^2}} \\ & \int_{u_1^-}^{u_1^+} \frac{du_1}{\lambda^{1/2}(s, m_\mu^2, u_1)\sqrt{1-\eta^2}} \int_{t_1^-}^{t_1^+} \frac{dt_1}{\sqrt{1-\zeta^2}} \overline{|\mathcal{M}|^2}, \quad (4.30) \end{aligned}$$

with the definitions

$$\zeta = (\omega - \xi\eta) [(1 - \xi^2)(1 - \eta^2)]^{-1/2} \quad (4.31)$$

$$\omega = (s - m_\mu^2 - u_1 + 2t_1)\lambda^{-1/2}(s, m_\mu^2, u_1), \quad (4.32)$$

$$\eta = [2ss_1 - (s + m_\mu^2 - u_1)(s + s_1 - m_\pi^2)]\lambda^{-1/2}(s, m_\mu^2, u_1)\lambda^{-1/2}(s, s_1, m_\pi^2), \quad (4.33)$$

$$\xi = \frac{s - m_\pi^2 - s_1 + 2t_0}{\lambda^{1/2}(s, s_1, m_\pi^2)},$$

and the  $t_0$ ,  $u_1$  and  $t_1$  integration limits

$$\begin{aligned} t_0^\pm &= m_\pi^2 - \frac{s + m_\pi^2 - s_1}{2} \pm \frac{\lambda^{1/2}(s, m_\pi^2, s_1)}{2}, \\ u_1^\pm &= s + m_\mu^2 - \frac{s + s_1 - m_\pi^2}{2} \pm \frac{\sqrt{s_1(s_1 - 4m_\mu^2)\lambda(s, s_1, m_\pi^2)}}{2s_1} \\ t_1^\pm &= m_\mu^2 - \frac{s + m_\mu^2 - u_1}{2} + \frac{\lambda^{1/2}(s, m_\mu^2, u_1)}{2} \left[ \xi\eta \pm \sqrt{(1 - \xi^2)(1 - \eta^2)} \right]. \end{aligned} \quad (4.34)$$

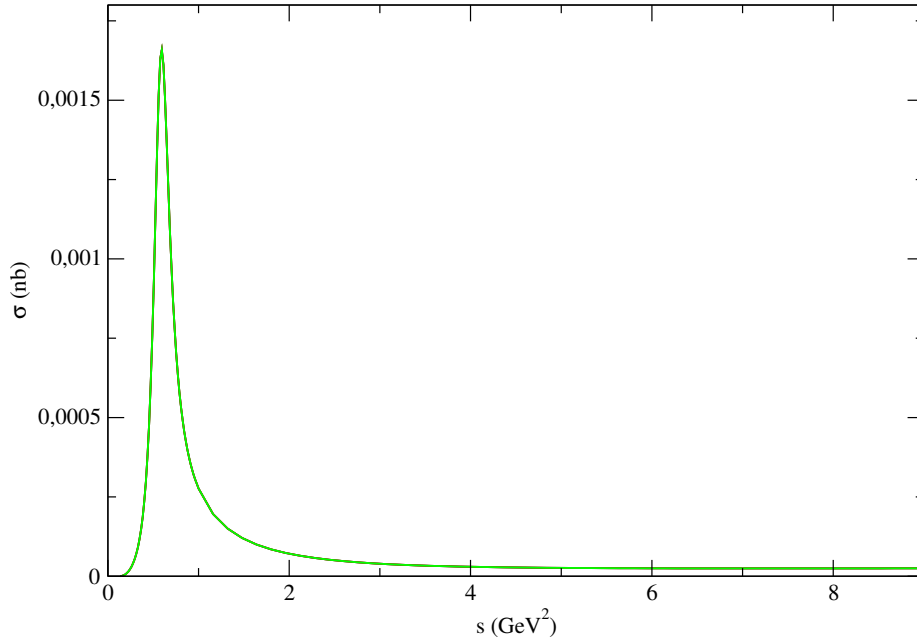


Figure 4.10: Our prediction for  $\sigma(e^+e^- \rightarrow \mu^+\mu^-\pi^0)$  at different center of mass energies using the couplings in eq. 4.27.

We therefore obtain the cross section for different center of mass energy shown in figure 4.10, and the cross section dependence on  $s_1$  with  $s = (1.02 \text{ GeV})^2$  in fig. 4.11,

since at that center of mass energy operates the KLOE experiment. By varying the parameters an upper and a lower bound is obtained for both figures, however, the central value almost overlaps with both limits cannot be discerned in both figures. The  $\rho(770)$  peak shows neatly and, at higher energies the cross section approaches a plateau. The excitations of the  $\rho(770)$  and their associated uncertainties are negligible. The profile of the  $\frac{d\sigma}{dI}$  observable makes it appealing for its measurement at KLOE, this is why we show its spectrum at  $\sqrt{s} = M_\phi$  GeV. Although the plot for  $M_{Y(4s)}$  is not shown, it would be very valuable to measure the behavior of the TFF at high virtualities of both photons to check the predicted asymptotic behaviors. This process would provide complementary information to that of BaBar and Belle, constraining the whole problematic mixed soft-hard regions needed to compute the internal vertex (the one which does not include the real photon) of the diagrams in fig 4.6.

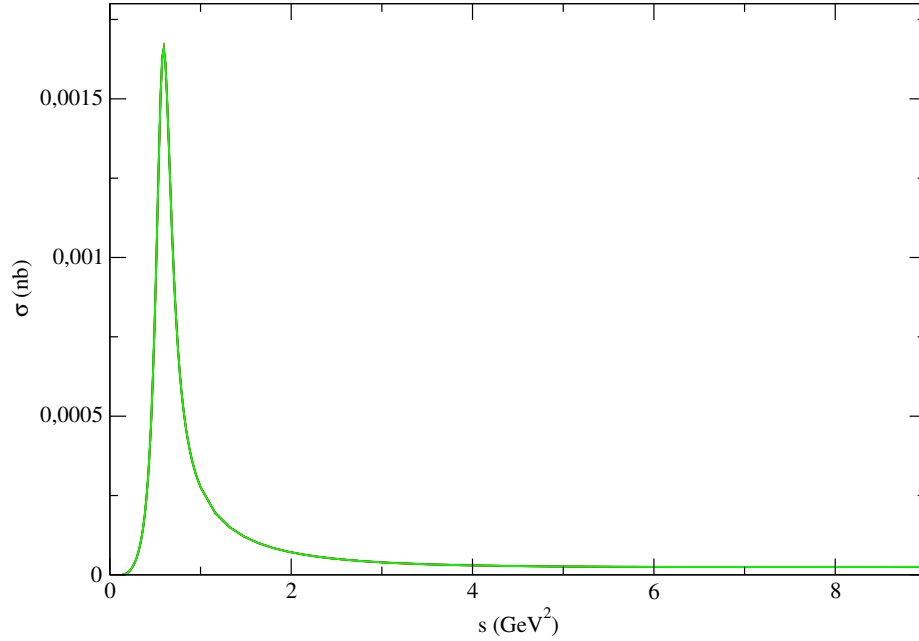


Figure 4.11: Our prediction for  $\mu^+\mu^-$  distribution at  $s = (1.02 \text{ GeV})^2$  using the couplings in eq. 4.27.

Using the relations between  $\eta^{(\prime)}$ TFF and the  $\pi$ TFF shown below in section 4.5, we computed the  $\sigma(e^+e^- \rightarrow \mu^+\mu^-\eta)$  cross section in a completely analogous way to the pion case. The total cross section and  $\frac{d\sigma}{ds_1}$  distribution are shown in fig. 4.12 at



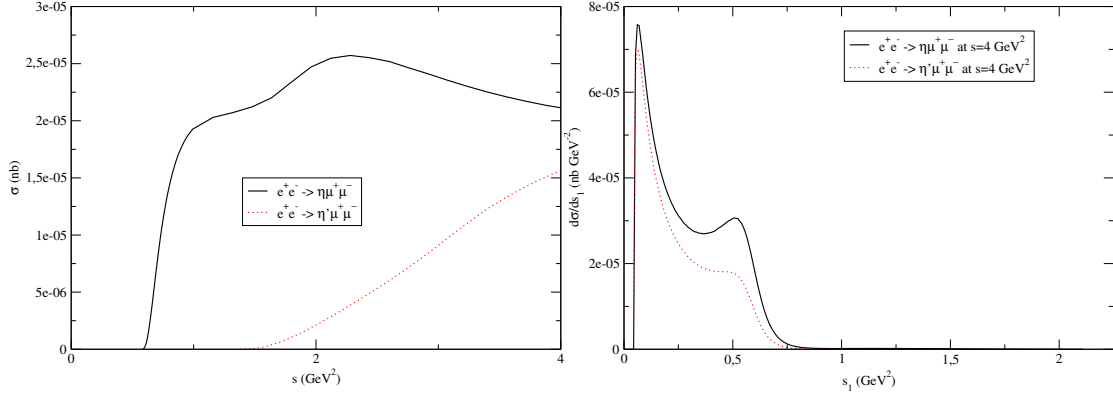


Figure 4.12: Our prediction for the  $\sigma(e^+e^- \rightarrow \mu^+\mu^-\eta)$  cross section (left) and  $\mu^+\mu^-$  distribution at 4  $\text{GeV}^2$  (right).

$s = M_\phi^2$ . The effect of the contribution of higher excited states is negligible in  $\frac{d\sigma}{ds_1}$  and is at the same level induced by the uncertainties on the  $\eta - \eta'$  mixing in the cross-section plot. They are of order 30(20)% for the  $\eta(\eta')$  cases. The  $\eta$  distribution at this energy will be less prominent and no hadronic structure will be appreciated since the available phase space is not enough, while the  $\eta'$  cannot even be produced.

## 4.8 Conclusions

A previous analysis of these TFF given by [129] confirms the expressions obtained by us of the completely off-shell TFF, however the main difference between our work [170] and the previous one comes from the more robust analysis of the error. This stems from the low energy behavior of the TFF, giving a correction to the classic WZW functional result which gives the dominant uncertainty in the  $a_\mu^{\pi^0, HLbL}$ . Also, we use a high energy constraint and Belle data, which appeared after the publication of ref [129].

We have made a proposal of a new observable, namely the  $e^+e^- \rightarrow \mu^+\mu^-\pi^0$  cross section and its dependence on the di-muon invariant mass, that would give us relevant information of the  $\pi$ TFF in the whole problematic soft-hard regions needed to fully describe the TFF for two off-shell photons, complementary to the  $e^+e^- \rightarrow e^+e^-\pi^0$  data. These observables could be measured in Belle-II and KLOE.

$a_\mu^{HLbL} \cdot 10^{10}$	Contributions
$11.6 \pm 4.0$	F. Jegerlehner y A. Nyffeler [150]
$10.5 \pm 2.6$	Prades, De Rafael y Vainshtein [189]
$13.7^{+2.7}_{-1.5}$	Erler and Toledo Sánchez [190]
$11.8 \pm 2.0$	Our contribution[170]

Table 4.5: Our contribution to the  $a_\mu^{HLbL}$  compared to previous computations.

We have obtained a total pseudoscalar exchange contribution  $a_\mu^{P,HLbL} = (10.47 \pm 0.54) \times 10^{-10}$  which is in good agreement with those reported in previous analysis, namely  $(9.9 \pm 1.6) \times 10^{-10}$  [150] and  $(11.4 \pm 1.3) \times 10^{-10}$  [189]. The contribution for the whole HLbL is obtained by adding the rest of the contributions in fig 4.5, which are obtained from ref [150], giving  $a_\mu^{HLbL} = (11.8 \pm 2.0) \times 10^{-10}$ . The previous result is compared with previous reported analyses in table 4.5.

We can see that there is a very good agreement within errors with both results shown. Adding in quadrature the errors from the LO HVP and the our HLbL contribution instead of that in ref. [191], we see that the uncertainty is  $\pm 5.1 \times 10^{-10}$ , which is a 16% smaller.

# Chapter 5

## Conclusions

We have computed several processes relevant for the search of BSM interactions due to the precision test that will be done in high intensity frontier experiments in the very near future. Since most of the processes studied in these facilities involve hadronic effects with an energy scale in which pQCD cannot give a reliable result, a better alternative to deal with this problem is the use of R $\chi$ T as an effective field theory of QCD.

By relying on the chiral symmetry of the fundamental field theory it is possible to construct an Effective Field Theory that has been used to compute processes that otherwise is not possible to calculate. These theories have a very wide range of applicability, meaning they can be used in any problem below certain energy scale so that one can consistently compute amplitudes in a perturbative way, and even renormalize the theory to get further precision in its predictions.

In chapter 1 we showed the first computation of the  $BR(\tau \rightarrow \pi \ell^+ \ell^- \nu_\tau)$  decays, which gives us an effect that will be measurable at Belle-II. This process is a very important background for processes with lepton number or lepton flavor violation. It may be an important background in the search for processes with lepton universality violation, since it gives different decay widths for different decay channels.

This induced non-universality of leptons took us to try to explain the  $R_K$  anomaly measured at LHCb, which comes to be an observable free from hadronic-pollution in certain energy ranges, where we found that the energy range probed by LHCb for this observable is free from hadronic pollution, giving a very clean window for the search of phenomena beyond the SM. The different strong and weak phases led us to calculate a CP asymmetry that is large and in agreement with experimental data.

Looking forward to improve the experimental constraints on new charged currents, we studied the decay  $\tau \rightarrow \pi\eta\gamma\nu_\tau$ , which is a very important background for the search of this kind of currents. By cutting the energy of the photon and taking values below that cut the background can be drastically reduced in one order of magnitude. Despite the fact that this would be enough for the  $\eta$  channel, it is not so for the  $\eta'$  channel since it cannot be determined due to the great uncertainty of the non radiative process.

We also found the important result that neglecting the contributions from two resonances exchange gives a very good estimation and also, a significantly reduced uncertainty. The importance of this results rely in the fact that these form factors will be inserted in the TAUOLA generator, so that this approximation will significantly simplify the codes (the computation time and the uncertainty) to make them more efficient.

Looking to provide a cleaner stage for the search of BSM effects, we computed the HLbL contributions to the  $a_\mu$ , where we managed to reduce the uncertainty and at the same time, give a more robust estimation of the uncertainty. Since a full description of the TFF will not be given by the current data fits, we proposed the measurement of (and predicted) the cross section  $e^+e^- \rightarrow \mu^+\mu^-\pi^0$  and the invariant muon mass spectrum at a fixed center of mass energy, so that the TFF can be fitted to an observable which involves both photons off-shell.

# Products derived from our research

We have published the following works:

- P. Roig, A. Guevara, G. López Castro, *Weak radiative pion vertex in  $\tau^- \rightarrow \pi^- \nu_\tau \ell^+ \ell^-$  decays*, Phys. Rev. D **88** (2013) 033007
- P. Roig, A. Guevara, G. López Castro,  *$VV'P$  form factors in resonance chiral theory and the  $\pi - \eta - \eta'$  light-by-light contribution to the muon  $g-2$* , Phys. Rev. D **89** (2014) 073016
- A. Guevara, G. López Castro, P. Roig and S. L. Tostado, *Long-distance weak annihilation contribution to the  $B^\pm \rightarrow (\pi^\pm, K^\pm) \ell^+ \ell^-$  decays*, Phys. Rev. D **92** (2015) 054035
- A. Guevara, G. López Castro, P. Roig,  *$\tau^- \rightarrow \eta^{(\prime)} \pi^- \nu_\tau \gamma$  decays as backgrounds in the search for second class currents*, Phys. Rev. D **95** (2017) 054015
- A. Guevara,  *$W^* \gamma^* \pi$  form factors in the  $\tau^- \rightarrow \pi^- \nu_\tau \ell^+ \ell^-$  decays*, J. Phys. Conf. Ser. **761** (2016) 012088,  
presented as a poster at the XIV Mexican Workshop on Particle Physics in November 2013
- A. Guevara, G. López Castro, P. Roig and S. L. Tostado, *A new long distance contribution to  $B^\pm \rightarrow (\pi^\pm, K^\pm) \ell^+ \ell^-$  decays*, Moriond QCD (2015) Conf. Proc. 107-110,  
talk given by the first author at the 50<sup>th</sup> Rencontres de Moriond on QCD and High Energy Interactions in march 2015
- A. Guevara, *Hadronic light-by-light contribution to the muon  $g-2$*  J. Phys. Conf. Ser. **761** (2016) 012009,  
talk given at the 30<sup>th</sup> Annual Meeting of the Particles and Fields division in may 2016

## Appendix A: Kinematics for cross section $\sigma(kk' \rightarrow k_1k_2k_3)$

### Introduction

As part of an almost finished work with the Ph.D. student Bryan Larios (student of Dr. Lorenzo Díaz Cruz), the author computed the phase space for a cross section of two-to-three particles as a function of two-particle invariant masses. This was done to compute the cross section of  $e^-(k)e^+(k') \rightarrow \tilde{G}(k_1)\tilde{G}(k_2)\gamma(k_3)$ , where  $\tilde{G}$  is a gravitino as a function of the mass of the gravitino, of a virtual neutralino and the energy spectrum of the photon. This is a simplification to the case where the amplitude does not depend on the angle between  $\mathbf{k}_2$  and  $\mathbf{k}$ .

### Differential cross section

The general expression for the differential cross section can be obtained from Quantum Field Theory books, in the following we will use Peskin and Schroeder definition [192]

$$d\sigma = \frac{1}{2E2E'|\mathbf{v} - \mathbf{v}'|} \left( \prod_f^3 \frac{d^3k_f}{2E_f} \right) |\mathcal{M}|^2 (2\pi)^4 \delta^{(4)}(k + k' - \Sigma k_f), \quad (5.1)$$

where  $k$  and  $k'$  are the electron and positron four-momentum and  $k_f$  are the four-momenta of the final state particles with mass  $m_f$  and energy  $E_X$ . The term in the denominator can be expressed as a function of the center of mass energy and the masses of the initial state particles using the relation  $\mathbf{v}_X = \mathbf{k}_X/E_X$ , with  $\mathbf{k}$  the three-momentum,

$$\begin{aligned} 2E \cdot 2E' |\mathbf{v} - \mathbf{v}'| &= 4EE' \left| \frac{\mathbf{k}}{E} - \frac{\mathbf{k}'}{E'} \right| = 4EE' \left| \frac{\mathbf{k}}{E} + \frac{\mathbf{k}}{E'} \right| \\ &= 4|\mathbf{k}|(E + E') = 4E_{CM}|\mathbf{k}|, \end{aligned} \quad (5.2)$$

where  $E_{CM}$  is the center of mass energy. For initial state particles with same mass, the energy of both must be equal in the center of mass reference frame (CM), since from the dispersion relation one has  $|\mathbf{k}| = \sqrt{E^2 - m^2} = \sqrt{E'^2 - m'^2} =$  and  $E + E' = E_{CM}$ . Now, if initial state particles have equal masses  $|\mathbf{k}|$  can be expressed as a function of the center of mass energy and the mass of initial state particles

$$|\mathbf{k}| = \sqrt{E^2 - m^2} = \frac{1}{2} \sqrt{E_{CM}^2 - 4m^2} = \frac{E_{CM}}{2} \sqrt{1 - \frac{4m^2}{E_{CM}^2}} = \frac{E_{CM}}{2} \sigma_m(E_{CM}^2) \quad (5.3)$$

where  $\sigma_X(p^2) = \sqrt{1 - \frac{4X^2}{p^2}}$ , being  $m_X$  the mass of particle  $X$ . And thus, the factor can be expressed as

$$\boxed{2E \cdot 2E' |\mathbf{v} - \mathbf{v}'| = 2Q^2 \sigma_m(Q^2)}, \quad (5.4)$$

where  $Q = k + k'$ , *i.e.*,  $Q^2 = E_{CM}^2$ .

To express the cross section as a function of the invariant masses of particles with four-momenta  $k_1 - k_2$  and  $k_2 - k_3$ , we introduce the variables  $k_{12}$  and  $k_{23}$ , and the invariant masses  $s = (k_1 + k_2)^2$  and  $t = (k_2 + k_3)^2$  by using integrals which are trivially equal to 1,

$$\int \delta^{(4)}(k_{12} - k_1 - k_2) d^4 k_{12}, \quad (5.5a)$$

$$\int \delta^{(4)}(k_{23} - k_2 - k_3) d^4 k_{23}, \quad (5.5b)$$

$$\int \delta [s - (Q - k_3)^2] ds, \quad (5.5c)$$

$$\int \delta [t - (Q - k_1)^2] dt, \quad (5.5d)$$

So that the differential cross section takes the form

$$d\sigma(Q^2) = \frac{|\mathcal{M}|^2}{2Q^2 \sigma_m(Q^2)} \frac{1}{(2\pi)^5} Idsdt, \quad (5.6)$$

where  $I = I_1 I_2$ , and

$$I_1 = \int d^4 k_{12} \frac{d^3 k_3}{2E_3} \delta[s - (Q - k_3)^2] \delta^{(4)}(Q - k_{12} - k_3), \quad (5.7a)$$

$$I_2 = \int d^4 k_{23} ds dt \frac{d^3 k_1 d^3 k_2}{4E_1 E_2} \delta^{(4)}(k_{12} - k_1 - k_2) \delta^{(4)}(k_{23} - k_2 - k_3) \delta[t - (Q - k_1)^2]. \quad (5.7b)$$

Since  $\frac{d^3 k_3}{2E_3} = \int d^4 k \delta(k_3^2 - m_3^2)$ , where  $m_3$  is the mass of the particle with  $k_3$  four-momentum with positive time component,  $I_1$  is a Lorentz scalar and can be computed in any reference frame. By choosing the CM, one gets

$$\begin{aligned} I_1 &= \int \frac{d^3 k_3}{2E_3} dk_{12}^0 d^3 k_{12} \delta\left(\sqrt{Q^2} - k_{12}^0 - E_3\right) \delta^{(3)}(\mathbf{k}_{12} + \mathbf{k}_3) \delta(s - k_{12}^0{}^2 - \mathbf{k}_{12}^2) \\ &= \int \frac{d^3 k_3}{2E_3} \frac{dk_{12}^0 d^3 k_{12}}{2\sqrt{\mathbf{k}_{12}^2 + s}} \delta\left(\sqrt{Q^2} - \sqrt{\mathbf{k}_{12}^2 + s} - E_3\right) \delta^{(3)}(\mathbf{k}_{12} + \mathbf{k}_3) \delta\left(k_{12}^0 - \sqrt{\mathbf{k}_{12}^2 + s}\right), \\ &= \int \frac{d^3 k_3}{2\sqrt{\mathbf{k}_3^2 + m_3^2}} \frac{\|\mathbf{k}_{12}\|^2 d\|\mathbf{k}_{12}\| d\Omega_{12}}{2\sqrt{\mathbf{k}_{12}^2 + s}} \delta\left(\sqrt{Q^2} - \sqrt{\mathbf{k}_{12}^2 + s} - \sqrt{\mathbf{k}_3^2 + m_3^2}\right) \delta^{(3)}(\mathbf{k}_{12} + \mathbf{k}_3), \\ &= \int \frac{4\pi}{2\sqrt{\mathbf{k}_{12}^2 + m_3^2}} \frac{\|\mathbf{k}_{12}\|^2 d\|\mathbf{k}_{12}\|}{2\sqrt{\mathbf{k}_{12}^2 + s}} \delta\left(\sqrt{Q^2} - \sqrt{\mathbf{k}_{12}^2 + s} - \sqrt{\mathbf{k}_{12}^2 + m_3^2}\right), \end{aligned} \quad (5.8)$$

In the second line we used the delta function property  $\delta[f(x)] = \sum_i \frac{1}{|f'(x_i)|} \delta(x - x_i)$ , where  $x_i \in \ker f$ . In the third line  $d\Omega_{12}$  is the differential solid angle subtended by  $d\|\mathbf{k}_{12}\|$ . For the delta function in the last expression we get the following expression

$$\delta\left(\sqrt{Q^2} - \sqrt{\mathbf{k}_{12}^2 + s} - \sqrt{\mathbf{k}_{12}^2 + m_3^2}\right) = \left(\frac{\|\mathbf{k}_{12}\|}{\sqrt{\mathbf{k}_{12}^2 + s}} + \frac{\|\mathbf{k}_{12}\|}{\sqrt{\mathbf{k}_{12}^2 + m_3^2}}\right)^{-1} \delta(\|\mathbf{k}_{12}\| - \|\mathbf{k}_{12}\|_0), \quad (5.9)$$

where  $\|\mathbf{k}_{12}\|_0$  is found as the root of the function of  $\|\mathbf{k}_{12}\|$  in the delta function. This



root is found analytically in the following way

$$\begin{aligned}
\sqrt{Q^2} - \sqrt{\mathbf{k}_{12}^2 + s} - \sqrt{\mathbf{k}_{12}^2 + m_3^2} &= 0 \\
\left( \sqrt{Q^2} - \sqrt{\mathbf{k}_{12}^2 + s} \right)^2 &= \mathbf{k}_{12}^2 + m_3^2 \\
Q^2 - 2\sqrt{Q^2}\sqrt{\mathbf{k}_{12}^2 + s} + \mathbf{k}_{12}^2 + s &= \mathbf{k}_{12}^2 + m_3^2 \\
Q^2 + s - m_3^2 &= 2\sqrt{Q^2}\sqrt{\mathbf{k}_{12}^2 + s} \\
\left( \frac{Q^2 + s - m_3^2}{2\sqrt{Q^2}} \right)^2 &= \|\mathbf{k}_{12}\|_0^2 + s \frac{4Q^2}{4Q^2} \\
\|\mathbf{k}_{12}\|_0^2 &= \frac{Q^4 + s^2 + m_3^4 + 2Q^2s - 2Q^2m_3^2 - 2sm_3^2 - 4Q^2s}{4Q^2} \\
&= \frac{\lambda(Q^2, s, m_3^2)}{4Q^2} \\
\|\mathbf{k}_{12}\|_0 &= \frac{\lambda^{1/2}(Q^2, s, m_3^2)}{2\sqrt{Q^2}}, \tag{5.10}
\end{aligned}$$

where the positive root has been chosen, since otherwise  $\|\cdot\|$  would not be a norm. Here  $\lambda(a, b, c) := a^2 + b^2 + c^2 - 2ab - 2ac - 2bc$  is the Källen function. Now, the factor in parenthesis in eq (5.9) can be expressed in a more simple manner

$$\left( \frac{\|\mathbf{k}_{12}\|}{\sqrt{\mathbf{k}_{12}^2 + s}} + \frac{\|\mathbf{k}_{12}\|}{\sqrt{\mathbf{k}_{12}^2 + m_3^2}} \right)^{-1} = \frac{\frac{1}{\|\mathbf{k}_{12}\|} \sqrt{\mathbf{k}_{12}^2 + s} \sqrt{\mathbf{k}_{12}^2 + m_3^2}}{\sqrt{\mathbf{k}_{12}^2 + m_3^2} + \sqrt{\mathbf{k}_{12}^2 + s}} = \frac{\sqrt{\mathbf{k}_{12}^2 + s} \sqrt{\mathbf{k}_{12}^2 + m_3^2}}{\sqrt{Q^2} \|\mathbf{k}_{12}\|}, \tag{5.11}$$

where, in the last line we made use of the fact that  $\|\mathbf{k}_{12}\|$  must be a root of the argument of the delta function in the lhs of eq (5.9). Thus, by inserting the previous expression in eq. (5.8), substituting the root  $\|\mathbf{k}_{12}\|_0$  and trivially integrating over  $d\|\mathbf{k}_{12}\|$  we get

$$\boxed{I_1 = \frac{\pi}{2} \frac{\lambda^{1/2}(Q^2, s, m_3^2)}{Q^2}} \tag{5.12}$$

By the same argument used for  $I_1$ , it is showed that  $I_2$  is Lorentz invariant,

so that we can choose a reference frame to integrate it. For the sake of simplicity we used the reference frame in which  $\mathbf{k}_{12} = 0$ , so that  $k_{12}^2 = (k_{12}^0, \mathbf{0})^2 = s$  and therefore  $k_{12} = (\sqrt{s}, \mathbf{0})$ . In order to compute the integrals of  $I_2$  we need to obtain an expression for  $\|\mathbf{Q}\|$  and  $E = \sqrt{Q^2 + \mathbf{Q}^2}$  in this reference frame. Since  $\mathbf{Q} = \gamma m \mathbf{v}$  is a three-momentum,  $E = \gamma m$  is the time component of the four-momentum vector  $Q = (E, \mathbf{Q})$ , where  $m = \sqrt{Q^2}$  and  $\gamma$  is the Lorentz factor associated with  $\mathbf{v}$ , the relative velocity between this frame and the CM one. Therefore, the relative speed is

$$v := \|\mathbf{v}\| = \frac{\|\mathbf{Q}\|}{E}. \quad (5.13)$$

By squaring  $k_3 = Q - k_{12}$  one can find that  $Q^2 + s - 2Ek_{12}^0 = m_3^2$ , and by clearing for  $E$  we find

$$E = \frac{Q^2 + s - m_3^2}{2\sqrt{2}}, \quad (5.14)$$

and since  $Q^2 = E^2 - \mathbf{Q}^2$ , we get

$$\|\mathbf{Q}\| = \frac{\lambda^{1/2}(Q^2, s, m_3^2)}{2\sqrt{s}}, \quad (5.15)$$

so that  $Q^T = \|\mathbf{Q}\|(0, 0, -1)$ , since we have chosen  $\mathbf{k}_{12}$  to be parallel to the third direction in the CM reference frame. This last expression will help us later to express contractions of four-momenta in terms of Lorentz scalars. Thus, now we can follow a development for  $I_2$  similar to that of  $I_1$ ,

$$\begin{aligned} I_2 &= \int \frac{d^4 k_{23} d^3 k_1 d^3 k_2}{4E_1 E_2} \delta^{(4)}(k_{12} - k_1 - k_2) \delta^{(4)}(k_{23} - k_{12} - Q + 2k_1) \delta(t - k_{23}^2) \\ &= \int \frac{d^4 k_{23} d^3 k_1 d^3 k_2 \delta^{(3)}(\mathbf{k}_1 + \mathbf{k}_2)}{4E_1 \sqrt{\mathbf{k}_2^2 + m_2^2}} \delta\left(\sqrt{s} - E_1 - \sqrt{\mathbf{k}_2^2 + m_2^2}\right) \delta^{(4)}(\dots) \delta(t - k_{23}^2) \\ &= \int \frac{d^4 k_{23} d^3 k_1}{4\sqrt{\mathbf{k}_1^2 + m_1^2} \sqrt{\mathbf{k}_1^2 + m_2^2}} \delta\left(\sqrt{s} - E_1 - \sqrt{\mathbf{k}_1^2 + m_2^2}\right) \delta^{(4)}(\dots) \delta(t - k_{23}^2). \end{aligned} \quad (5.16)$$

Following the procedure used in eqs. (5.9) and (5.10), we find that

$$\delta\left(\sqrt{s} - \sqrt{\mathbf{k}_1^2 + m_1^2} - \sqrt{\mathbf{k}_2^2 + m_2^2}\right) = \frac{\sqrt{\mathbf{k}_1^2 + m_1^2}\sqrt{\mathbf{k}_1^2 + m_2^2}}{\sqrt{s}\|\mathbf{k}_1\|}\delta\left(\|\mathbf{k}_1\| - \frac{\lambda^{1/2}(s, m_1^2, m_2^2)}{2\sqrt{s}}\right). \quad (5.17)$$

Substituting the delta function by the expressions found in the previous equation in the  $I_2$  integrals we get

$$\begin{aligned} I_2 &= \int d^4k_{23} \frac{\|\mathbf{k}_1\|d\|\mathbf{k}_1\|d\Omega_1}{4\sqrt{s}} \delta(\|\mathbf{k}_1\| - \|\mathbf{k}_1\|_0) \delta(t - k_{23}^2) \delta^{(4)}(k_{23} - k_{12} - Q + 2k_1) \\ &= \int d^4k_{23} d\Omega_1 \frac{\|\mathbf{k}_1\|_0}{4\sqrt{s}} \delta(t - k_{23}^2) \delta^{(4)}(k_{23} - k_{12} - Q + 2k_1) \\ &= \frac{\lambda^{1/2}(s, m_1^2, m_2^2)}{8s} \int \frac{dk_{23}^0 d^3k_{23}}{2\sqrt{\mathbf{k}_{23}^2 + t}} d\Omega_1 \delta\left(k_{23}^0 - \sqrt{\mathbf{k}_{23}^2 + t}\right) \times \\ &\quad \delta\left(k_{23}^0 - \sqrt{s} - E + 2\frac{s + m_1^2 + m_2^2}{2\sqrt{s}}\right) \delta^{(3)}(\mathbf{k}_{23} - \mathbf{Q} + 2\mathbf{k}_1) \\ &= \frac{\lambda^{1/2}(s, m_1^2, m_2^2)}{16s} \int \frac{d^3k_{23}}{\sqrt{\mathbf{k}_{23}^2 + t}} d\Omega_1 \delta\left[\sqrt{\mathbf{k}_{23}^2 + t} - \sqrt{s} - E + \frac{s + m_1^2 - m_2^2}{\sqrt{s}}\right] \times \\ &\quad \delta^{(3)}(\mathbf{k}_{23} - \mathbf{Q} + 2\mathbf{k}_1) \\ &= \frac{\lambda^{1/2}(s, m_1^2, m_2^2)}{16s} \int d\Omega_1 \frac{\delta\left[\sqrt{(\mathbf{Q} - 2\mathbf{k}_1)^2 + t} - \sqrt{s} - E + \frac{s + m_1^2 - m_2^2}{\sqrt{s}}\right]}{\sqrt{(\mathbf{Q} - 2\mathbf{k}_1)^2 + t}} \end{aligned} \quad (5.18)$$

In the third line we used the relation  $E_1 = \sqrt{\mathbf{k}_1^2 + m_1^2}$  along with the  $\|\mathbf{k}_1\| = \|\mathbf{k}_1\|_0$  from eq. (5.17). By realizing the expansion  $(\mathbf{Q} - 2\mathbf{k}_1)^2 = 4\mathbf{k}_1^2 + \mathbf{Q}^2 - 4\|\mathbf{k}_1\|\|\mathbf{Q}\|\cos(\theta_1)$  in order to obtain the  $\cos(\theta_1)$  dependance explicitly, the derivative  $\frac{d(\mathbf{Q} - 2\mathbf{k}_1)^2}{d\cos(\theta_1)} = -4\|\mathbf{k}_1\|\|\mathbf{Q}\|$  was obtained which will be needed to integrate the delta

function. So, the delta function can be expressed as

$$\begin{aligned}
& \delta \left[ \sqrt{(\mathbf{Q} - 2\mathbf{k}_1)^2 + t} - \sqrt{s} - E + \frac{s + m_1^2 - m_2^2}{\sqrt{s}} \right] \\
&= \delta \left[ \sqrt{4\mathbf{k}_1^2 + \mathbf{Q}^2 - 4\|\mathbf{k}_1\|\|\mathbf{Q}\|\cos(\theta_1) + t} - E - \frac{s + m_1^2 - m_2^2}{\sqrt{s}} \right] \\
&= \left| \frac{-\|\mathbf{k}_1\|\|\mathbf{Q}\|}{\sqrt{(\mathbf{Q} - 2\mathbf{k}_1)^2 + t}} \right|^{-1} \delta \left\{ \cos(\theta_1) - \frac{[(Q^2 + 3s - m_3^2)\lambda^{1/2}(s, m_1^2, m_2^2) - s(2s + sQ^2 - m_3^2)]}{4\|\mathbf{Q}\|\|\mathbf{k}_1\|s} \right\} \\
&= \frac{\sqrt{(\mathbf{Q} - 2\mathbf{k}_1)^2 + t}}{4\|\mathbf{Q}\|\|\mathbf{k}_1\|} \delta[(\cos(\theta_1) - \cos(\theta_1)_0)]
\end{aligned} \tag{5.19}$$

Finally, substituting the delta function in the expression for  $I_2$  and integrating trivially the azimuthal angle  $\phi_1$  we get

$$\begin{aligned}
I_2 &= \frac{\lambda^{1/2}(s, m_1^2, m_2^2)}{16s} \frac{2\pi}{\sqrt{(\mathbf{Q} - 2\mathbf{k}_1)^2 + t}} \frac{\sqrt{(\mathbf{Q} - 2\mathbf{k}_1)^2 + t}}{4\|\mathbf{k}_1\|\|\mathbf{Q}\|} \int d\cos(\theta_1) \delta[(\cos(\theta_1) - \cos(\theta_1)_0)] \\
&= 2\pi \frac{\lambda^{1/2}(s, m_1^2, m_2^2)}{16s} \frac{4s}{4\lambda^{1/2}(Q^2, s, m_3^2)\lambda^{1/2}(s, m_1^2, m_2^2)}
\end{aligned} \tag{5.20}$$

And thus we get

$$\boxed{I_2 = \frac{\pi}{8\lambda^{1/2}(Q^2, s, m_3^2)}}. \tag{5.21}$$

Since  $I = I_2 I_2$ , we get by using the boxed expressions for each integral

$$I = \frac{\pi^2}{16Q^2}, \tag{5.22}$$

and substituting the value of  $I$  and that of equation 5.4 we find the expression of the differential cross section as a function of  $s$  and  $t$ ,

$$\boxed{\frac{d\sigma}{dt ds} = \frac{|\mathcal{M}|^2}{1024\pi^3 Q^4 \sigma_m(Q^2)}} \tag{5.23}$$

In order to be able to compute the total cross section for any process, the range of  $s$

and  $t$  must be specified. If we take  $s$  as the last-to-be-integrated variable we find its minimum  $s_-$  by taking  $\mathbf{k}_1 = \mathbf{k}_2 = 0$  and its maximum  $s_+$  by taking  $\mathbf{k}_3 = 0$

$$s_- = (k_1 + k_2)^2 = (m_1 + m_2)^2, \quad (5.24a)$$

$$s_+ = (Q - k_3)^2 = (\sqrt{Q^2} - m_3)^2. \quad (5.24b)$$

We compute  $t$  in the  $\mathbf{k}_{12} = 0$  frame, so that

$$t = (Q - k_1)^2 = (E - E_1)^2 - (\mathbf{Q} - \mathbf{k}_1)^2, \quad (5.25)$$

where

$$\left( \begin{array}{c} \max \\ \min \end{array} \right) [(\mathbf{Q} - \mathbf{k}_1)^2] = Q^2 + \|\mathbf{k}_1\|^2 \pm 2\|\mathbf{Q}\|\|\mathbf{k}_1\| = (\|\mathbf{Q}\| \pm \|\mathbf{k}_1\|)^2, \quad (5.26)$$

Now, substituting the values for  $E$ ,  $E_1$ ,  $\|\mathbf{Q}\|$  and  $\|\mathbf{k}_1\|$  from eqs. (5.14), (5.15) and (5.17) in the expression for  $t$  we find

$$\begin{aligned} t_{\pm} &= (E - E_1)^2 - (\|\mathbf{Q}\| \mp \|\mathbf{k}_1\|)^2 \\ &= \left( \frac{Q^2 + s - m_3^2}{2\sqrt{s}} - \frac{s + m_1^2 + m_2^2}{2\sqrt{s}} \right)^2 - \left( \frac{\lambda^{1/2}(Q^2, s, m_3^2)}{2\sqrt{s}} - \frac{\lambda^{1/2}(s, m_1^2, m_2^2)}{2\sqrt{s}} \right)^2. \end{aligned} \quad (5.27)$$

So that the range of both variables are determined to be

$$\boxed{(m_1 + m_2)^2 \leq s \leq (\sqrt{Q^2} - m_3)^2} \quad (5.28a)$$

$$\boxed{t_{\pm} = \frac{1}{4s} \left\{ (Q^2 + m_1^2 - m_2^2 - m_3^2)^2 - [\lambda^{1/2}(Q^2, s, m_3^2) \mp \lambda^{1/2}(s, m_1^2, m_2^2)]^2 \right\}} \quad (5.28b)$$

The scalar products among final-state particles four-momenta are easily find from the definitions of  $s$ ,  $t$  and the relation  $Q^2 = (k_1 + k_2 + k_3)^2$ . Since  $s = (k_1 + k_2)^2$ ,

$$k_1 \cdot k_2 = \frac{1}{2}(s - m_1^2 - m_2^2). \quad (5.29)$$

Analogously, from  $t = (k_2 + k_3)^2$

$$k_2 \cdot k_3 = \frac{1}{2}(t - m_2^2 - m_3^2). \quad (5.30)$$

By using the previous equations in  $Q^2$  we can clear the remaining scalar product

$$k_1 \cdot k_3 = \frac{1}{2}(Q^2 - s - t + m_2^2). \quad (5.31)$$

To compute the scalar products between the initial state particles momenta and the final state particles we must make a Lorentz boost to the  $\mathbf{k}_{12} = 0$  frame. First note that  $Q^2 = k^2 + k'^2 + 2k \cdot k'$ , so that  $k \cdot Q = k' \cdot Q = Q^2/2$ . The expressions for  $v$ ,  $E$  and  $\|\mathbf{Q}\|$  are given in eqs. (5.13), (5.14) and (5.15) respectively. So that by expressing  $k$  as perpendicular to  $\mathbf{k}_{12}$  in the CM reference frame and boosting it to the  $\mathbf{k}_{12} = 0$  frame we get

$$k^{CM \rightarrow 12} \doteq \begin{pmatrix} \gamma & 0 & 0 & -\beta\gamma \\ 0 & 1 & 0 & 0 \\ 0 & 0 & 1 & 0 \\ -\beta\gamma & 0 & 0 & \gamma \end{pmatrix} \begin{pmatrix} \frac{1}{2}\sqrt{Q^2} \\ k^1 \\ k^2 \\ 0 \end{pmatrix} = \begin{pmatrix} \frac{1}{2}\sqrt{Q^2}\gamma \\ k^1 \\ k^2 \\ \frac{1}{2}\sqrt{Q^2}\beta\gamma \end{pmatrix}, \quad (5.32)$$

where  $\beta$  is  $v$  in eq. (5.13), and thus we must substitute the values of  $E$  and  $\mathbf{Q}$  in eqs. (5.14) and (5.15). Therefore,

$$\beta = \frac{\|\mathbf{Q}\|}{E} = \frac{\lambda^{1/2}(Q^2, s, m_3^2)}{Q^2 + s - m_3^2} = \left(1 - \frac{4Q^2 s}{(Q^2 + s - m_3^2)^2}\right)^{1/2}, \quad (5.33)$$

from which we can obtain the Lorentz factor  $\gamma = (1 - \beta^2)^{-1/2}$

$$\gamma = \left[1 - \left(1 - \frac{4Q^2 s}{(Q^2 + s - m_3^2)^2}\right)\right]^{-1/2} = \frac{Q^2 + s - m_3^2}{2\sqrt{Q^2 s}}. \quad (5.34)$$

And thus, the time component of the four momenta  $k$  can be expressed in the following

way

$$k^0 = \frac{1}{2} \sqrt{Q^2} \frac{Q^2 + s - m_3^2}{2\sqrt{Q^2 s}} = \frac{Q^2 + s - m_3^2}{4\sqrt{s}}. \quad (5.35)$$

With this last expression, we find that

$$k \cdot k_3 = k \cdot Q - k \cdot k_{12} = \frac{1}{2} Q^2 - 2k^0 \sqrt{s} = \frac{Q^2 - s + m_3^2}{4}. \quad (5.36)$$

On the other hand, we will also be needing the expressions for  $v$ ,  $E$  and  $\|\mathbf{Q}\|$  in the  $\mathbf{k}_{23} = 0$  reference frame. So, in a completely analogous way we find that

$$\|\mathbf{Q}\|^* = \frac{\lambda^{1/2}(Q^2 + t - m_1^2)}{2\sqrt{t}}, \quad (5.37a)$$

$$E^* = \frac{Q^2 + t - m_1^2}{2\sqrt{t}}, \quad (5.37b)$$

$$\beta^* = \left( 1 - \frac{4Q^2 t}{(Q^2 + t - m_1^2)^2} \right)^{1/2}, \quad (5.37c)$$

$$\gamma^* = \frac{Q^2 + t - m_1^2}{2\sqrt{Q^2 t}}, \quad (5.37d)$$

so that the time component of the  $k$  four-vector is

$$k^{0*} = \frac{Q^2 + t - m_1^2}{4\sqrt{t}}. \quad (5.38)$$

Therefore,

$$k \cdot k_1 = k \cdot Q - k \cdot k_{23} = Q^2 - 2k^{0*} \sqrt{t} = \frac{Q^2 - t + m_1^2}{4}. \quad (5.39)$$

Finally, the last Lorentz invariant remaining is obtained by contracting the  $k$  four-momentum with  $Q$  and using the two previous contractions

$$k \cdot k_2 = k \cdot (Q - k_1 - k_3) = \frac{1}{2} Q^2 - \frac{Q^2 - t + m_1^2}{4} - \frac{Q^2 - s + m_3^2}{4} = \frac{s + t - m_1^2 - m_2^2}{4}. \quad (5.40)$$

To obtain the cross section as a function of the energy of the final state particle with four-momentum  $k_3$  and a mass invariant pair we first obtain the dependence of  $s$  in

$E_3$ ,

$$s = (Q - k_3)^2 = Q^2 - 2Q \cdot k_3 + m_3^2 = Q^2 - 2\sqrt{Q^2}E_3 + m_3^2, \quad (5.41)$$

so that  $\frac{ds}{dE_3} = -2\sqrt{Q^2}$ , with which we obtain

$$\boxed{\frac{d\sigma}{dE dt} = \left| \frac{ds}{dE_3} \right| \frac{d\sigma}{ds dt} = \frac{\sqrt{Q^2} |\mathcal{M}|^2}{512\pi^3 Q^4 \sigma_m(Q^2)}}. \quad (5.42)$$

The kinematical limits for the energy  $E_3$  are obtained by taking the two extremal cases where  $\mathbf{k}_3 = 0$  and when  $\mathbf{k}_{12} = 0$ . In the latter, eq. (5.41) can be used by substituting  $s \rightarrow (m_1 + m_2)^2$ ; in the former we just make use of the dispersion relation  $E_3 = \sqrt{\mathbf{k}_3^2 + m_3^2}$ . Thus,

$$m_3 \leq E_3 \leq \frac{Q^2 + m_3^2 - (m_1 + m_2)^2}{2\sqrt{Q^2}}. \quad (5.43)$$



## Appendix B: Contributions to the $\tau \rightarrow \pi \ell^+ \ell^- \nu_\tau$ decay amplitude

We collect in this appendix the results of summing over polarizations and averaging over that of the tau the different contributions to the squared matrix element. We refrain from writing the lengthy outcome of the contraction of the indices which was used in our programs.

$$\begin{aligned}
\overline{|\mathcal{M}_{IB}|^2} &= 16G_F^2 |V_{ud}|^2 \frac{e^4}{k^4} F_\pi^2 M_\tau^2 \ell_{\mu\nu} \left[ \frac{-\tau^{\mu\nu} k^2}{(k^2 - 2k \cdot p_\tau)^2} + \frac{4p^\mu q^\nu k \cdot p_\tau}{(k^2 + 2k \cdot p)(k^2 - 2k \cdot p_\tau)} \right. \\
&+ \frac{4p_\tau^\mu q^\nu k \cdot p_\tau}{(k^2 - 2k \cdot p_\tau)^2} - \frac{2g^{\mu\nu} k \cdot p_\tau k \cdot q}{(k^2 - 2k \cdot p_\tau)^2} - \frac{4p^\mu p_\tau^\nu k \cdot q}{(k^2 + 2k \cdot p)(k^2 - 2k \cdot p_\tau)} \\
&- \frac{4p_\tau^\mu p_\tau^\nu k \cdot q}{(k^2 - 2k \cdot p_\tau)^2} + \frac{8p^\mu p_\tau^\nu p_\tau \cdot q}{(k^2 + 2k \cdot p)(k^2 - 2k \cdot p_\tau)} \\
&\left. + \frac{4p^\mu p^\nu p_\tau \cdot q}{(k^2 + 2k \cdot p)^2} + \frac{4p_\tau^\mu p_\tau^\nu p_\tau \cdot q}{(k^2 - 2k \cdot p_\tau)^2} \right], \tag{5.44}
\end{aligned}$$

$$2\Re e [\overline{\mathcal{M}_{IB} \mathcal{M}_V^*}] = -32G_F^2 |V_{ud}|^2 \frac{e^4}{k^4} F_\pi M_\tau^2 \Im m \left\{ F_V^*(p \cdot k, k^2) \ell_{\nu'}^\mu \epsilon^{\mu' \nu' \rho' \sigma'} k_{\rho'} p_{\sigma'} \mathcal{V}_{\mu\mu'} \right\},$$

$$2\Re e [\overline{\mathcal{M}_{IB} \mathcal{M}_A^*}] = -64G_F^2 |V_{ud}|^2 \frac{e^4}{k^4} F_\pi M_\tau^2 \ell_{\mu'}^{\nu'} \Re e \left[ \mathcal{A}_{\mu'\nu'}^* \mathcal{V}^{\mu\mu'} \right],$$

$$\overline{|\mathcal{M}_V|^2} = 16G_F^2 |V_{ud}|^2 \frac{e^4}{k^4} \left| F_V(p \cdot k, k^2) \right|^2 \epsilon_{\mu'\nu'\rho'\sigma'} \epsilon_{\mu\nu\rho\sigma} k^\rho p^\sigma k^{\rho'} p^{\sigma'} \ell^{\nu\nu'} \tau^{\mu\mu'},$$

$$\overline{|\mathcal{M}_A|^2} = 64G_F^2 |V_{ud}|^2 \frac{e^4}{k^4} \ell_{\nu\nu'} \tau_{\mu\mu'} \mathcal{A}^{\mu\nu} \mathcal{A}^{\mu'\nu'*},$$

$$2\Re e [\overline{\mathcal{M}_V \mathcal{M}_A^*}] = -64G_F^2 |V_{ud}|^2 \frac{e^4}{k^4} \Im m \left[ F_V(p \cdot k, k^2) \epsilon_{\mu\nu\rho\sigma} k^\rho p^\sigma \ell_{\nu'}^\mu \tau^{\mu\mu'} \mathcal{A}_{\mu'}^{\nu'*} \right],$$

where we have defined

$$\begin{aligned}
\ell^{\mu\nu} &= p_-^\mu p_+^\nu + p_-^\nu p_+^\mu - g^{\mu\nu}(m_\ell^2 + p_- \cdot p_+) \\
\tau^{\mu\nu} &= p_\tau^\mu q^\nu + p_\tau^\nu q^\mu - g^{\mu\nu} p_\tau \cdot q, \\
\mathcal{A}^{\mu\nu} &= F_A(p \cdot k, k^2) [(k^2 + p \cdot k)g^{\mu\nu} - k^\mu p^\nu] + B(k^2)k^2 \left[ g^{\mu\nu} - \frac{(p+k)^\mu p^\nu}{k^2 + 2p \cdot k} \right], \\
\mathcal{V}_{\mu\nu} &= \frac{2p_\mu q_\nu}{2k \cdot p + k^2} + \frac{-g_{\mu\nu}k \cdot q + 2q_\nu p_{\tau\mu} - i\epsilon_{\mu\nu\rho\sigma}k^\rho q^\sigma + k_\nu q_\mu}{k^2 - 2k \cdot p_\tau},
\end{aligned} \tag{5.45}$$

and used the conservation of the electromagnetic currents implying  $k_\mu \ell^{\mu\nu} = 0 = \ell^{\mu\nu} k_\nu$ .

## Appendix C: Form factors results according to Resonance Chiral Lagrangians in $\tau^\pm \rightarrow \pi^\pm \eta \gamma \nu_\tau$ decays

In this appendix we include the different contributions to the (axial-)vector form factors obtained using  $R\chi L$ . Only the anomalous contribution was included in section 3.4.1. Here we explicitly quote the analytic expressions for the model-dependent (resonant-mediated) contributions to these form factors following the order in the figures. We start with fig. 3.5, giving rise to  $a_{i=1,2,3,4}^{1R}$  in  $R\chi L$ :

$$\begin{aligned}
a_1^{1R} = & -\frac{4C_q}{F^2 M_V m_\rho^2 D_\rho [(p_0 + k)^2]} (k \cdot p_0 ((F_V - 2G_V) (- (8c_3 + 2c_5 + 3c_7) m_\eta^2 + 8c_3 m_\pi^2 + 2(c_5 + c_7) p \cdot p_0) \\
& + m_\rho^2 ((c_7 + c_{1256}) F_V - 2c_7 G_V)) - \frac{1}{2} (F_V - 2G_V) k \cdot p (4c_5 k \cdot p_0 + 2(c_5 - 4c_3) m_\eta^2 - (2c_5 + c_{1256}) m_\rho^2 + 8c_3 m_\pi^2) \\
& - 2c_7 (F_V - 2G_V) (k \cdot p_0)^2 + \frac{1}{2} m_\rho^2 (m_\eta^2 ((2(8c_3 + c_5 + c_7) + c_{1256}) F_V - 4(4c_3 + c_5 + c_7) G_V) \\
& + 16c_3 m_\pi^2 (G_V - F_V) - (2(c_5 + c_7) - c_{1256}) p \cdot p_0 (F_V - 2G_V)) \\
& + ((4c_3 + c_5 + c_7) m_\eta^2 - 4c_3 m_\pi^2) (F_V - 2G_V) (p \cdot p_0 - m_\eta^2)) \\
& + \frac{4F_A}{F^2 D_{a_1} [(p + p_0 + k)^2]} (-C_q (-(\kappa_5^A + \kappa_6^A - \kappa_7^A + \kappa_{16}^A) (k \cdot p + m_\pi^2) - (\kappa_3^A + 2\kappa_8^A + \kappa_{15}^A) k \cdot p_0 \\
& + 2m_\pi^2 (2\kappa_9^A - \kappa_{10}^A + 2\kappa_{11}^A + \kappa_{14}^A) + (-3\kappa_3^A + 4\kappa_4^A + \kappa_5^A + \kappa_6^A + \kappa_7^A - 2\kappa_8^A - \kappa_{15}^A) p \cdot p_0) \\
& - C_q (-(\kappa_5^A + \kappa_6^A + \kappa_7^A) k \cdot p_0 + 2m_\pi^2 (\kappa_{14}^A + 2(\kappa_9^A + \kappa_{11}^A)) + m_\eta^2 (\kappa_3^A - \kappa_5^A - \kappa_6^A - \kappa_7^A + 2\kappa_8^A + \kappa_{15}^A) \\
& + (-2\kappa_3^A + 4\kappa_4^A + \kappa_5^A + \kappa_6^A - \kappa_7^A + \kappa_{16}^A) p \cdot p_0) - 2\sqrt{2}\kappa_9^A C_s (m_\pi^2 - 2m_K^2) + \sqrt{2} (2\kappa_9^A - \kappa_{10}^A) C_s (2m_K^2 - m_\pi^2)) \\
& - \frac{4F_A}{F^2 m_{a_1}^2 D_{a_1} [(p + k)^2]} ((m_{a_1}^2 - k \cdot p) (C_q (\kappa_{16}^A (2k \cdot p + m_\pi^2) + \kappa_{16}^A (2(k \cdot p_0 + p \cdot p_0) + m_\eta^2) \\
& - (\kappa_3^A + 2\kappa_8^A + \kappa_{15}^A) (k \cdot p_0 + m_\eta^2 + p \cdot p_0) - 2m_\pi^2 (2\kappa_9^A + \kappa_{10}^A + 2\kappa_{11}^A + \kappa_{12}^A)) + \sqrt{2} (2\kappa_9^A + \kappa_{10}^A) C_s (2m_K^2 - m_\pi^2)) \\
& + \sqrt{2} C_s (2m_K^2 - m_\pi^2) (-2\kappa_9^A (-m_{a_1}^2 + 2k \cdot p + m_\pi^2 + p \cdot p_0) - \kappa_{10}^A p \cdot p_0) \\
& + C_q (p \cdot p_0 (-m_{a_1}^2 (\kappa_3^A + \kappa_{15}^A) + (\kappa_3^A + \kappa_{15}^A - \kappa_{16}^A) (2k \cdot p + m_\pi^2) + 2m_\pi^2 (2\kappa_9^A + \kappa_{10}^A + 2\kappa_{11}^A + \kappa_{12}^A) \\
& + m_\eta^2 (\kappa_3^A + 2\kappa_8^A + \kappa_{15}^A - \kappa_{16}^A)) - (4m_\pi^2 (\kappa_9^A + \kappa_{11}^A) + m_\eta^2 (\kappa_3^A + \kappa_{15}^A)) (m_{a_1}^2 - 2k \cdot p - m_\pi^2) \\
& + k \cdot p_0 ((\kappa_3^A + \kappa_{15}^A) (-m_{a_1}^2 + 2k \cdot p + m_\pi^2) + (\kappa_3^A + 2\kappa_8^A + \kappa_{15}^A - 2\kappa_{16}^A) p \cdot p_0) + (\kappa_3^A + 2\kappa_8^A + \kappa_{15}^A - 2\kappa_{16}^A) (p \cdot p_0)^2)) \\
& - \frac{4F_V C_q}{F^2 m_\rho^2} \left( \frac{2\sqrt{2} C_s (2m_K^2 - m_\pi^2) \kappa_{13}^V}{C_q} + \frac{2\sqrt{2} C_s (2m_K^2 - m_\pi^2) (\kappa_{13}^V + \kappa_{18}^V)}{C_q} \right. \\
& - (\kappa_1^V + \kappa_2^V + \kappa_3^V + \kappa_6^V + \kappa_7^V + \kappa_8^V) k \cdot p_0 - (\kappa_6^V + \kappa_8^V + 2\kappa_{12}^V + \kappa_{16}^V - 2\kappa_{17}^V) k \cdot p_0 \\
& + (-\kappa_1^V + \kappa_2^V - \kappa_3^V + \kappa_7^V + \kappa_{17}^V) k \cdot p - m_\eta^2 \kappa_1^V - m_\pi^2 (\kappa_1^V + 2(-\kappa_4^V + \kappa_{10}^V + 2(\kappa_{13}^V + \kappa_{14}^V + \kappa_{15}^V))) \\
& - 2m_\pi^2 (-\kappa_4^V + 2\kappa_9^V + \kappa_{10}^V + 2(\kappa_{13}^V + \kappa_{14}^V + \kappa_{15}^V + \kappa_{18}^V)) + m_\pi^2 (\kappa_2^V - \kappa_3^V + \kappa_7^V) - m_\eta^2 (\kappa_2^V + \kappa_3^V + \kappa_6^V + \kappa_7^V + \kappa_8^V) \\
& - m_\eta^2 (\kappa_6^V + \kappa_8^V + 2\kappa_{12}^V + \kappa_{16}^V - \kappa_{17}^V) + p \cdot p_0 \kappa_1^V + p \cdot p_0 (\kappa_1^V + \kappa_2^V + \kappa_3^V - 4\kappa_5^V - \kappa_6^V - \kappa_7^V - \kappa_8^V) \\
& \left. - p \cdot p_0 (-3\kappa_2^V + 3\kappa_3^V + 4\kappa_5^V + \kappa_6^V - \kappa_7^V + \kappa_8^V + 2\kappa_{12}^V + \kappa_{16}^V - \kappa_{17}^V) \right), \tag{5.46}
\end{aligned}$$

where  $c_{1256} \equiv c_1 - c_2 - c_5 + 2c_6$  was used. Its value is fixed by eqs. (A3.50).

$$\begin{aligned}
a_2^{1R} = & \frac{4C_q(F_V - 2G_V)}{F^2 M_V m_\rho^2 D_\rho [(p_0 + k)^2]} (c_7 k \cdot p_0 + (4c_3 + c_5 + c_7) m_\eta^2 - 4c_3 m_\pi^2) (-2k \cdot p_0 - m_\eta^2 + m_\rho^2) \\
& + \frac{4F_A}{F^2 D_{a_1} [(p + p_0 + k)^2]} (C_q (- (\kappa_5^A + \kappa_6^A + \kappa_7^A) k \cdot p_0 + 2m_\pi^2 (\kappa_{14}^A + 2 (\kappa_9^A + \kappa_{11}^A))) \\
& + m_\eta^2 (\kappa_3^A - \kappa_5^A - \kappa_6^A - \kappa_7^A + 2\kappa_8^A + \kappa_{15}^A) + (-2\kappa_3^A + 4\kappa_4^A + \kappa_5^A + \kappa_6^A - \kappa_7^A + \kappa_{16}^A) p \cdot p_0) + 2\sqrt{2}\kappa_9^A C_s (m_\pi^2 - 2m_K^2) \\
& + \frac{4F_A}{F^2 m_{a_1}^2 D_{a_1} [(p + k)^2]} \left( \sqrt{2} C_s (2m_K^2 - m_\pi^2) (2\kappa_9^A (m_{a_1}^2 - 2k \cdot p - m_\pi^2) - (2\kappa_9^A + \kappa_{10}^A) p \cdot p_0) \right. \\
& + C_q (p \cdot p_0 (-m_{a_1}^2 (\kappa_3^A + \kappa_{15}^A) + (\kappa_3^A + \kappa_{15}^A - \kappa_{16}^A) (2k \cdot p + m_\pi^2) + 2m_\pi^2 (2\kappa_9^A + \kappa_{10}^A + 2\kappa_{11}^A + \kappa_{12}^A) \\
& \quad \left. + m_\eta^2 (\kappa_3^A + 2\kappa_8^A + \kappa_{15}^A - \kappa_{16}^A)) - (4m_\pi^2 (\kappa_9^A + \kappa_{11}^A) + m_\eta^2 (\kappa_3^A + \kappa_{15}^A)) (m_{a_1}^2 - 2k \cdot p - m_\pi^2) \right. \\
& + k \cdot p_0 ((\kappa_3^A + 2\kappa_8^A + \kappa_{15}^A - 2\kappa_{16}^A) p \cdot p_0 - (\kappa_3^A + \kappa_{15}^A) (m_{a_1}^2 - 2k \cdot p - m_\pi^2)) + (\kappa_3^A + 2\kappa_8^A + \kappa_{15}^A - 2\kappa_{16}^A) (p \cdot p_0)^2) \\
& + \frac{4F_V C_q}{F^2 m_\rho^2} \left( \frac{2\sqrt{2} C_s (2m_K^2 - m_\pi^2) (\kappa_{13}^V + \kappa_{18}^V)}{C_q} - (\kappa_1^V + \kappa_2^V + \kappa_3^V + \kappa_6^V + \kappa_7^V + \kappa_8^V) k \cdot p_0 - m_\eta^2 \kappa_1^V \right. \\
& \quad \left. - 2m_\pi^2 (-\kappa_4^V + 2\kappa_9^V + \kappa_{10}^V + 2 (\kappa_{13}^V + \kappa_{14}^V + \kappa_{15}^V + \kappa_{18}^V)) - m_\eta^2 (\kappa_2^V + \kappa_3^V + \kappa_6^V + \kappa_7^V + \kappa_8^V) \right. \\
& \quad \left. + p \cdot p_0 (\kappa_1^V + \kappa_2^V + \kappa_3^V - 4\kappa_5^V - \kappa_6^V - \kappa_7^V - \kappa_8^V) \right), \tag{5.47}
\end{aligned}$$

$$\begin{aligned}
a_3^{1R} = & \frac{16G_V C_q}{F^2 M_V [m_\eta^2 + 2(k \cdot p + k \cdot p_0 + p \cdot p_0)] D_\rho [(p_0 + k)^2]} \left[ -(c_{1256} + 8c_3) \frac{m_\eta^2}{2} + c_{1256} k \cdot p_0 + 4c_3 m_\pi^2 \right] \\
& + \frac{4F_A}{F^2 m_{a_1}^2 D_{a_1} [(p + p_0 + k)^2]} \left( \kappa_{10}^A (\sqrt{2} C_s (2m_K^2 - m_\pi^2) - 2m_\pi^2 C_q) - m_{a_1}^2 (\kappa_5^A + \kappa_6^A - \kappa_7^A + \kappa_{16}^A) C_q \right) \\
& + \frac{4F_A}{F^2 m_{a_1}^2 D_{a_1} [(p + k)^2]} \left( C_q (\kappa_{16}^A (m_{a_1}^2 + 2k \cdot p_0 + m_\eta^2 + 2p \cdot p_0) - (\kappa_3^A + 2\kappa_8^A + \kappa_{15}^A) (k \cdot p_0 + m_\eta^2 + p \cdot p_0) \right. \\
& \quad \left. - 2m_\pi^2 (2\kappa_9^A + \kappa_{10}^A + 2\kappa_{11}^A + \kappa_{12}^A)) + \sqrt{2} (2\kappa_9^A + \kappa_{10}^A) C_s (2m_K^2 - m_\pi^2) \right) \\
& + \frac{4F_V C_q}{F^2 m_\rho^2} (3\kappa_1^V - 3\kappa_2^V + 3\kappa_3^V - \kappa_6^V + \kappa_7^V - \kappa_8^V), \tag{5.48}
\end{aligned}$$

$$\begin{aligned}
a_4^{1R} = & \frac{4C_q(F_V - 2G_V)}{F^2 M_V m_\rho^2 D_\rho [(p_0 + k)^2]} \left( (c_5 + c_7) (2k \cdot p_0 + m_\eta^2) + 4c_3 (m_\eta^2 - m_\pi^2) + \left( -c_5 - c_7 + \frac{c_{1256}}{2} \right) m_\rho^2 \right) \\
& - \frac{4F_A C_q}{F^2 D_{a_1} [(p + p_0 + k)^2]} (\kappa_3^A - 2\kappa_5^A - 2\kappa_6^A + 2\kappa_8^A + \kappa_{15}^A - \kappa_{16}^A) \\
& - \frac{4F_A}{F^2 m_{a_1}^2 D_{a_1} [(p + k)^2]} \left( C_q (\kappa_{16}^A (m_{a_1}^2 + 2k \cdot p_0 + m_\eta^2 + 2p \cdot p_0) - (\kappa_3^A + 2\kappa_8^A + \kappa_{15}^A) (k \cdot p_0 + m_\eta^2 + p \cdot p_0) \right. \\
& \left. - 2m_\pi^2 (2\kappa_9^A + \kappa_{10}^A + 2\kappa_{11}^A + \kappa_{12}^A)) + \sqrt{2} (2\kappa_9^A + \kappa_{10}^A) C_s (2m_K^2 - m_\pi^2) - C_q (\kappa_{16}^A - 2\kappa_8^A) (m_{a_1}^2 - 2k \cdot p - m_\pi^2) \right) \\
& - \frac{4F_V C_q}{F^2 m_\rho^2} (2\kappa_1^V - 4\kappa_2^V + 6\kappa_3^V - 2\kappa_6^V - 2\kappa_8^V + 2\kappa_{12}^V - \kappa_{16}^V - \kappa_{17}^V) .
\end{aligned} \tag{5.49}$$

The two-resonance mediated contributions to the axial-vector form factors, corresponding to figs. 3.6, are given in the following:

$$\begin{aligned}
a_1^{2R} = & -\frac{8F_A C_q}{F^2 M_V m_\rho^2 D_{a_1} [(p + p_0 + k)^2] D_\rho [(p_0 + k)^2]} \\
& \left( -2\sqrt{2}(k \cdot p)^2 \left( \frac{1}{2} (2c_5 + c_{1256}) m_\rho^2 - c_5 (m_\eta^2 + 2k \cdot p_0) + 4c_3 (m_\eta^2 - m_\pi^2) \right) \lambda'' \right. \\
& - ((c_5 + c_7) m_\eta^2 + k \cdot p_0 c_7 - 4c_3 (m_\pi^2 + m_\eta^2)) (m_\eta^2 - m_\rho^2 + 2k \cdot p_0) \left( -2\sqrt{2}(k \cdot p + p \cdot p_0) \lambda'' - 2m_\pi^2 (2\lambda_1 + \lambda_2) \right. \\
& \quad \left. + (m_\eta^2 + 2k \cdot p_0) \lambda_4 \right) - \frac{1}{2} k \cdot p \left( -4\sqrt{2} p \cdot p_0 (8c_3 m_\pi^2 - c_7 m_\eta^2 + (c_7 - c_{1256}) m_\rho^2) \lambda'' \right. \\
& \quad \left. + 2c_5 (4\lambda_4 (k \cdot p_0)^2 + (m_\eta^2 - m_\rho^2) (m_\eta^2 \lambda_4 - 2m_\pi^2 (2\lambda_1 + \lambda_2))) \right. \\
& - 8c_3 (m_\pi^2 - m_\eta^2) (2(2\lambda_1 + \lambda_2) m_\pi^2 - m_\eta^2 \lambda_4 + m_\rho^2 (\lambda_3 - 2\lambda_5)) + c_{1256} m_\rho^2 (2(2\lambda_1 + \lambda_2) m_\pi^2 + m_\eta^2 (\lambda_3 - \lambda_4 - 2\lambda_5)) \\
& + 2k \cdot p_0 \left( 4\sqrt{2} p \cdot p_0 c_7 \lambda'' + 2c_5 ((2m_\eta^2 - m_\rho^2) \lambda_4 - 2m_\pi^2 (2\lambda_1 + \lambda_2)) + 8c_3 ((4\lambda_1 + \lambda_4) m_\pi^2 + m_\rho^2 \lambda_3 - 2m_\eta^2 \lambda_4) \right. \\
& + c_{1256} m_\rho^2 (\lambda_3 - \lambda_4 - 2\lambda_5)) + p \cdot p_0 (4c_3 (m_\pi^2 + m_\eta^2) (2(2\lambda_1 + \lambda_2) m_\pi^2 - m_\eta^2 \lambda_4 + p \cdot p_0 (2\lambda_2 - \lambda_4 - 2\lambda_5)) \\
& \quad \left. - (c_5 + c_7) (-4\lambda_4 (k \cdot p_0)^2 - m_\eta^2 (-2(2\lambda_1 + \lambda_2) m_\pi^2 + m_\eta^2 \lambda_4 + p \cdot p_0 (-2\lambda_2 + \lambda_4 + 2\lambda_5))) \right) \\
& \quad \left. + k \cdot p_0 ((-c_{1256} \lambda_3 m_\rho^2 - 4p \cdot p_0 (c_5 + c_7) \lambda_2) m_\pi^2 \right. \\
& + p \cdot p_0 (-4\sqrt{2} p \cdot p_0 (c_5 + c_7) \lambda'' + 4(-4c_3 + c_5 + c_7) m_\eta^2 \lambda_4 + 8m_\pi^2 (-(-4c_3 + c_5 + c_7) \lambda_1 - c_3 \lambda_4)) \\
& \quad \left. - m_\rho^2 (c_{1256} (4\lambda_1 m_\pi^2 + p \cdot p_0 (\lambda_3 - \lambda_4 - 2\lambda_5)) + 2p \cdot p_0 ((c_5 + c_7) \lambda_4 + 4c_3 (\lambda_3 - 2(\lambda_4 + \lambda_5)))) \right) \\
& \quad - m_\rho^2 \left( -\sqrt{2} (p \cdot p_0)^2 (2(c_5 + c_7) - c_{1256}) \lambda'' + 4m_\pi^2 \left( \frac{1}{2} (8c_3 + c_{1256}) m_\eta^2 - 4c_3 m_\pi^2 \right) \lambda_1 \right. \\
& \quad \left. + \frac{1}{2} m_\pi^2 (2p \cdot p_0 (c_{1256} - 2(c_5 + c_7)) \lambda_2 + ((8c_3 + c_{1256}) m_\eta^2 - 8c_3 m_\pi^2) \lambda_3) \right. \\
& \quad \left. + p \cdot p_0 \left( \frac{1}{2} m_\eta^2 (2(c_5 + c_7) \lambda_4 + c_{1256} (\lambda_3 - \lambda_4 - 2\lambda_5) + 8c_3 (\lambda_3 - 2(\lambda_4 + \lambda_5))) \right. \right. \\
& \quad \left. \left. \left( \left( c_5 + c_7 - \frac{c_{1256}}{2} \right) \lambda_1 + c_3 (\lambda_3 - 2\lambda_5) \right) \right) \right) \\
& \quad + \frac{8F_A C_q \kappa_1^{SA} (c_d p \cdot p_0 + m_\pi^2 c_m)}{F^2 D_{a_1} [(p + p_0 + k)^2] D_{a_0} [(p + p_0)^2]} ,
\end{aligned} \tag{5.50}$$

$$\begin{aligned}
a_2^{2R} = & -\frac{8F_A C_q}{F^2 M_V m_\rho^2 D_{a_1} [(p + p_0 + k)^2] D_\rho [(p_0 + k)^2]} \\
& (c_7 k \cdot p_0 + (c_5 + c_7) m_\eta^2 - 4c_3 (m_\eta^2 + m_\pi^2)) (2k \cdot p_0 + m_\eta^2 - m_\rho^2) \\
& \left( \lambda_4 (2k \cdot p_0 + m_\eta^2) - 2\sqrt{2} \lambda'' k \cdot p - 2(2\lambda_1 + \lambda_2) m_\pi^2 - 2\sqrt{2} p \cdot p_0 \lambda'' \right) \\
& - \frac{4F_A C_q \kappa_1^{SA} (c_d p \cdot p_0 + m_\pi^2 c_m)}{F^2 D_{a_1} [(p + p_0 + k)^2] D_{a_0} [(p + p_0)^2]} ,
\end{aligned} \tag{5.51}$$

$$a_3^{2R} = -\frac{4\sqrt{2}F_A C_q (\lambda' + \lambda'')}{F^2 M_V D_{a_1} [(p + p_0 + k)^2] D_\rho [(p_0 + k)^2]} \left( 2(8c_3 + c_{1256}) k \cdot p_0 + (8c_3 + c_{1256}) m_\eta^2 - 8c_3 m_\pi^2 \right), \quad (5.52)$$

$$\begin{aligned} a_4^{2R} = & -\frac{8F_A C_q}{F^2 M_V m_\rho^2 D_{a_1} [(p + p_0 + k)^2] D_\rho [(p_0 + k)^2]} \left( \frac{1}{2} (2\lambda_2 - \lambda_3) m_\rho^2 (c_{1256} (2k \cdot p_0 + m_\eta^2) + 8c_3 (m_\eta^2 - m_\pi^2)) \right. \\ & \left. - 2\sqrt{2}\lambda'' k \cdot p \left( - (c_5 + c_7) (2k \cdot p_0 + m_\eta^2) + 4c_3 (m_\eta^2 + m_\pi^2) + \frac{1}{2} (2(c_5 + c_7) - c_{1256}) m_\rho^2 \right) \right. \\ & + 2k \cdot p_0 \left( (c_5 + c_7) (\lambda_4 (m_\rho^2 - 2m_\eta^2) + 2(2\lambda_1 + \lambda_2) m_\pi^2) + 4c_3 (2\lambda_4 m_\eta^2 + (\lambda_4 - 4\lambda_1) m_\pi^2) + 2\sqrt{2} (c_5 + c_7) p \cdot p_0 \lambda'' \right) \\ & - 4(c_5 + c_7) \lambda_4 (k \cdot p_0)^2 - (4c_3 (m_\eta^2 + m_\pi^2) - (c_5 + c_7) m_\eta^2) (-\lambda_4 m_\eta^2 + 2(2\lambda_1 + \lambda_2) m_\pi^2 + (2\lambda_2 - \lambda_4 - 2\lambda_5) p \cdot p_0) \\ & \left. - m_\rho^2 \left( \lambda_4 (4c_3 (m_\eta^2 + m_\pi^2) - (c_5 + c_7) m_\eta^2) + (2(c_5 + c_7) - c_{1256}) (2\lambda_1 + \lambda_2) m_\pi^2 + \sqrt{2} (2(c_5 + c_7) - c_{1256}) p \cdot p_0 \lambda'' \right) \right). \end{aligned} \quad (5.53)$$

We will display separately the contributions from the last diagram in the first line of figure 3.6, due to the length of the corresponding expressions.



$$\begin{aligned}
a_1^{W^- \rightarrow (a_1^-) \eta \rightarrow \pi^- (\rho^0) \eta \rightarrow \pi^- \gamma \eta} = & + \frac{8F_V}{F^2 m_{a_1}^2 m_\rho^2 D_{a_1} [(p+k)^2]} \left( 8m_\pi^2 C_q m_\pi^2 m_\eta^2 \lambda_1 \kappa_3^A + 16k \cdot p C_q m_\pi^2 m_\eta^2 \lambda_1 \kappa_3^A \right. \\
& - 8C_q m_\pi^2 m_{a_1}^2 m_\eta^2 \lambda_1 \kappa_3^A - 2m_\pi^2 C_q m_{a_1}^2 m_\eta^2 \lambda_2 \kappa_3^A + 2k \cdot p C_q m_{a_1}^2 m_\eta^2 \lambda_2 \kappa_3^A + 2p^4 C_q m_\eta^2 \lambda_2 \kappa_3^A - 4(k \cdot p)^2 C_q m_\eta^2 \lambda_2 \kappa_3^A \\
& + 2m_\pi^2 k \cdot p C_q m_\eta^2 \lambda_2 \kappa_3^A + 2k \cdot p C_q m_{a_1}^2 m_\eta^2 \lambda_4 \kappa_3^A - 4(k \cdot p)^2 C_q m_\eta^2 \lambda_4 \kappa_3^A - 2m_\pi^2 k \cdot p C_q m_\eta^2 \lambda_4 \kappa_3^A + 4k \cdot p C_q m_{a_1}^2 m_\eta^2 \lambda_5 \kappa_3^A \\
& - 8(k \cdot p)^2 C_q m_\eta^2 \lambda_5 \kappa_3^A - 4m_\pi^2 k \cdot p C_q m_\eta^2 \lambda_5 \kappa_3^A + 8C_q m_\pi^2 p_0^4 \kappa_8^A \lambda_1 + 8k \cdot p C_q m_\pi^2 m_\eta^2 \kappa_8^A \lambda_1 - 8C_q m_\pi^2 m_{a_1}^2 m_\eta^2 \kappa_8^A \lambda_1 \\
& + 32m_\pi^2 C_q m_\pi^4 \kappa_9^A \lambda_1 + 64k \cdot p C_q m_\pi^4 \kappa_9^A \lambda_1 + 16\sqrt{2} m_\pi^2 C_s m_\pi^4 \kappa_9^A \lambda_1 + 32\sqrt{2} k \cdot p C_s m_\pi^4 \kappa_9^A \lambda_1 - 32\sqrt{2} m_\pi^2 C_s m_K^2 m_\pi^2 \kappa_9^A \lambda_1 \\
& - 64\sqrt{2} k \cdot p C_s m_K^2 m_\pi^2 \kappa_9^A \lambda_1 - 32C_q m_\pi^4 m_{a_1}^2 \kappa_9^A \lambda_1 - 16\sqrt{2} C_s m_\pi^4 m_{a_1}^2 \kappa_9^A \lambda_1 + 32\sqrt{2} C_s m_K^2 m_\pi^2 m_{a_1}^2 \kappa_9^A \lambda_1 + 8k \cdot p C_q m_\pi^4 \kappa_{10}^A \lambda_1 \\
& + 4\sqrt{2} k \cdot p C_s m_\pi^4 \kappa_{10}^A \lambda_1 - 8\sqrt{2} k \cdot p C_s m_K^2 m_\pi^2 \kappa_{10}^A \lambda_1 - 8C_q m_\pi^4 m_{a_1}^2 \kappa_{10}^A \lambda_1 - 4\sqrt{2} C_s m_\pi^4 m_{a_1}^2 \kappa_{10}^A \lambda_1 + 8\sqrt{2} C_s m_K^2 m_\pi^2 m_{a_1}^2 \kappa_{10}^A \lambda_1 \\
& + 8C_q m_\pi^4 m_\eta^2 \kappa_{10}^A \lambda_1 + 4\sqrt{2} C_s m_\pi^4 m_\eta^2 \kappa_{10}^A \lambda_1 - 8\sqrt{2} C_s m_K^2 m_\pi^2 m_\eta^2 \kappa_{10}^A \lambda_1 + 32m_\pi^2 C_q m_\pi^4 \kappa_{11}^A \lambda_1 + 64k \cdot p C_q m_\pi^4 \kappa_{11}^A \lambda_1 \\
& - 32C_q m_\pi^4 m_{a_1}^2 \kappa_{11}^A \lambda_1 + 8k \cdot p C_q m_\pi^4 \kappa_{12}^A \lambda_1 - 8C_q m_\pi^4 m_{a_1}^2 \kappa_{12}^A \lambda_1 + 8C_q m_\pi^4 m_\eta^2 \kappa_{12}^A \lambda_1 + 8m_\pi^2 C_q m_\pi^2 m_\eta^2 \kappa_{15}^A \lambda_1 \\
& + 16k \cdot p C_q m_\pi^2 m_\eta^2 \kappa_{15}^A \lambda_1 - 8C_q m_\pi^2 m_{a_1}^2 m_\eta^2 \kappa_{15}^A \lambda_1 - 4C_q m_\pi^2 p_0^4 \kappa_{16}^A \lambda_1 - 8(k \cdot p)^2 C_q m_\pi^2 \kappa_{16}^A \lambda_1 - 4m_\pi^2 k \cdot p C_q m_\pi^2 \kappa_{16}^A \lambda_1 \\
& + 4m_\pi^2 C_q m_\pi^2 m_{a_1}^2 \kappa_{16}^A \lambda_1 + 8k \cdot p C_q m_\pi^2 m_{a_1}^2 \kappa_{16}^A \lambda_1 - 4m_\pi^2 C_q m_\pi^2 m_\eta^2 \kappa_{16}^A \lambda_1 - 12k \cdot p C_q m_\pi^2 m_\eta^2 \kappa_{16}^A \lambda_1 + 4C_q m_\pi^2 m_{a_1}^2 m_\eta^2 \kappa_{16}^A \lambda_1 \\
& - 4k \cdot p C_q p_0^4 \kappa_8^A \lambda_2 - 4m_\pi^2 C_q m_{a_1}^2 m_\eta^2 \kappa_8^A \lambda_2 - 4(k \cdot p)^2 C_q m_\eta^2 \kappa_8^A \lambda_2 - 8\sqrt{2} p^4 C_s m_K^2 \kappa_9^A \lambda_2 + 16\sqrt{2} (k \cdot p)^2 C_s m_K^2 \kappa_9^A \lambda_2 \\
& - 8\sqrt{2} m_\pi^2 k \cdot p C_s m_K^2 \kappa_9^A \lambda_2 + 8p^4 C_q m_\pi^2 \kappa_9^A \lambda_2 - 16(k \cdot p)^2 C_q m_\pi^2 \kappa_9^A \lambda_2 + 8m_\pi^2 k \cdot p C_q m_\pi^2 \kappa_9^A \lambda_2 + 4\sqrt{2} p^4 C_s m_\pi^2 \kappa_9^A \lambda_2 \\
& - 8\sqrt{2} (k \cdot p)^2 C_s m_\pi^2 \kappa_9^A \lambda_2 + 4\sqrt{2} m_\pi^2 k \cdot p C_s m_\pi^2 \kappa_9^A \lambda_2 + 8\sqrt{2} m_\pi^2 C_s m_K^2 m_{a_1}^2 \kappa_9^A \lambda_2 - 8\sqrt{2} k \cdot p C_s m_K^2 m_{a_1}^2 \kappa_9^A \lambda_2 \\
& - 8m_\pi^2 C_q m_\pi^2 m_{a_1}^2 \kappa_9^A \lambda_2 + 8k \cdot p C_q m_\pi^2 m_{a_1}^2 \kappa_9^A \lambda_2 - 4\sqrt{2} m_\pi^2 C_s m_\pi^2 m_{a_1}^2 \kappa_9^A \lambda_2 + 4\sqrt{2} k \cdot p C_s m_\pi^2 m_{a_1}^2 \kappa_9^A \lambda_2 \\
& + 4\sqrt{2} (k \cdot p)^2 C_s m_K^2 \kappa_{10}^A \lambda_2 - 4(k \cdot p)^2 C_q m_\pi^2 \kappa_{10}^A \lambda_2 - 2\sqrt{2} (k \cdot p)^2 C_s m_\pi^2 \kappa_{10}^A \lambda_2 + 4\sqrt{2} m_\pi^2 C_s m_K^2 m_{a_1}^2 \kappa_{10}^A \lambda_2 \\
& - 4m_\pi^2 C_q m_\pi^2 m_{a_1}^2 \kappa_{10}^A \lambda_2 - 2\sqrt{2} m_\pi^2 C_s m_\pi^2 m_{a_1}^2 \kappa_{10}^A \lambda_2 + 4\sqrt{2} k \cdot p C_s m_K^2 m_\eta^2 \kappa_{10}^A \lambda_2 - 4k \cdot p C_q m_\pi^2 m_\eta^2 \kappa_{10}^A \lambda_2 + 8p^4 C_q m_\pi^2 \kappa_{11}^A \lambda_2 \\
& - 2\sqrt{2} k \cdot p C_s m_\pi^2 m_\eta^2 \kappa_{10}^A \lambda_2 - 16(k \cdot p)^2 C_q m_\pi^2 \kappa_{11}^A \lambda_2 + 8m_\pi^2 k \cdot p C_q m_\pi^2 \kappa_{11}^A \lambda_2 - 8m_\pi^2 C_q m_\pi^2 m_{a_1}^2 \kappa_{11}^A \lambda_2 + 8k \cdot p C_q m_\pi^2 m_{a_1}^2 \kappa_{11}^A \lambda_2 \\
& - 4(k \cdot p)^2 C_q m_\pi^2 \kappa_{12}^A \lambda_2 - 4m_\pi^2 C_q m_\pi^2 m_{a_1}^2 \kappa_{12}^A \lambda_2 - 4k \cdot p C_q m_\pi^2 m_\eta^2 \kappa_{12}^A \lambda_2 - 2m_\pi^2 C_q m_{a_1}^2 m_\eta^2 \kappa_{15}^A \lambda_2 + 2k \cdot p C_q m_{a_1}^2 m_\eta^2 \kappa_{15}^A \lambda_2 \\
& + 2p^4 C_q m_\eta^2 \kappa_{15}^A \lambda_2 - 4(k \cdot p)^2 C_q m_\eta^2 \kappa_{15}^A \lambda_2 + 2m_\pi^2 k \cdot p C_q m_\eta^2 \kappa_{15}^A \lambda_2 + 2k \cdot p C_q p_0^4 \kappa_{16}^A \lambda_2 + 2p^4 C_q m_{a_1}^2 \kappa_{16}^A \lambda_2 + 4m_\pi^2 k \cdot p C_q m_{a_1}^2 \kappa_{16}^A \lambda_2 \\
& + 2m_\pi^2 C_q m_{a_1}^2 m_\eta^2 \kappa_{16}^A \lambda_2 + 6(k \cdot p)^2 C_q m_\eta^2 \kappa_{16}^A \lambda_2 + 2m_\pi^2 k \cdot p C_q m_\eta^2 \kappa_{16}^A \lambda_2 + 4(k \cdot p)^3 C_q \kappa_{16}^A \lambda_2 + 2m_\pi^2 (k \cdot p)^2 C_q \kappa_{16}^A \lambda_2 \\
& - 2(p \cdot p_0)^2 \left( \sqrt{2} C_s (2m_K^2 - m_\pi^2) \kappa_{10}^A + C_q ((m_\pi^2 - m_{a_1}^2 + 2k \cdot p) \kappa_3^A + 2(m_\pi^2 - m_{a_1}^2 - m_\eta^2 + k \cdot p) \kappa_8^A - 2m_\pi^2 \kappa_{10}^A \right. \\
& - 2m_\pi^2 \kappa_{12}^A + m_\pi^2 \kappa_{15}^A - m_{a_1}^2 \kappa_{15}^A + 2k \cdot p \kappa_{15}^A - m_\pi^2 \kappa_{16}^A + 2m_{a_1}^2 \kappa_{16}^A + m_\eta^2 \kappa_{16}^A) \lambda_2 - 2k \cdot p C_q p_0^4 \kappa_8^A \lambda_4 + 2k \cdot p C_q m_{a_1}^2 m_\eta^2 \kappa_8^A \lambda_4 \\
& - 2(k \cdot p)^2 C_q m_\eta^2 \kappa_8^A \lambda_4 + 16\sqrt{2} (k \cdot p)^2 C_s m_K^2 \kappa_9^A \lambda_4 + 8\sqrt{2} m_\pi^2 k \cdot p C_s m_K^2 \kappa_9^A \lambda_4 - 16(k \cdot p)^2 C_q m_\pi^2 \kappa_9^A \lambda_4 \\
& - 8m_\pi^2 k \cdot p C_q m_\pi^2 \kappa_9^A \lambda_4 - 8\sqrt{2} (k \cdot p)^2 C_s m_\pi^2 \kappa_9^A \lambda_4 - 4\sqrt{2} m_\pi^2 k \cdot p C_s m_\pi^2 \kappa_9^A \lambda_4 - 8\sqrt{2} k \cdot p C_s m_K^2 m_{a_1}^2 \kappa_9^A \lambda_4 \\
& + 8k \cdot p C_q m_\pi^2 m_{a_1}^2 \kappa_9^A \lambda_4 + 4\sqrt{2} k \cdot p C_s m_\pi^2 m_{a_1}^2 \kappa_9^A \lambda_4 + 2\sqrt{2} (k \cdot p)^2 C_s m_K^2 \kappa_{10}^A \lambda_4 - 2(k \cdot p)^2 C_q m_\pi^2 \kappa_{10}^A \lambda_4 \\
& - \sqrt{2} (k \cdot p)^2 C_s m_\pi^2 \kappa_{10}^A \lambda_4 - 2\sqrt{2} k \cdot p C_s m_K^2 m_{a_1}^2 \kappa_{10}^A \lambda_4 + 2k \cdot p C_q m_\pi^2 m_{a_1}^2 \kappa_{10}^A \lambda_4 + \sqrt{2} k \cdot p C_s m_\pi^2 m_{a_1}^2 \kappa_{10}^A \lambda_4 \\
& + 2\sqrt{2} k \cdot p C_s m_K^2 m_\eta^2 \kappa_{10}^A \lambda_4 - 2k \cdot p C_q m_\pi^2 m_\eta^2 \kappa_{10}^A \lambda_4 - \sqrt{2} k \cdot p C_s m_\pi^2 m_\eta^2 \kappa_{10}^A \lambda_4 - 16(k \cdot p)^2 C_q m_\pi^2 \kappa_{11}^A \lambda_4 - 8m_\pi^2 k \cdot p C_q m_\pi^2 \kappa_{11}^A \lambda_4 \\
& + 8k \cdot p C_q m_\pi^2 m_{a_1}^2 \kappa_{11}^A \lambda_4 - 2(k \cdot p)^2 C_q m_\pi^2 \kappa_{12}^A \lambda_4 + 2k \cdot p C_q m_\pi^2 m_{a_1}^2 \kappa_{12}^A \lambda_4 - 2k \cdot p C_q m_\pi^2 m_\eta^2 \kappa_{12}^A \lambda_4 + 4(p \cdot p_0)^3 C_q (\kappa_8^A - \kappa_{16}^A) \lambda_2 \\
& + 2k \cdot p C_q m_{a_1}^2 m_\eta^2 \kappa_{15}^A \lambda_4 - 4(k \cdot p)^2 C_q m_\eta^2 \kappa_{15}^A \lambda_4 - 2m_\pi^2 k \cdot p C_q m_\eta^2 \kappa_{15}^A \lambda_4 + k \cdot p C_q p_0^4 \kappa_{16}^A \lambda_4 - 2(k \cdot p)^2 C_q m_{a_1}^2 \kappa_{16}^A \lambda_4
\end{aligned}$$



$$\begin{aligned}
a_2^{W^- \rightarrow (a_1^-) \eta \rightarrow \pi^- (\rho^0) \eta \rightarrow \pi^- \gamma \eta} = & + \frac{8F_V}{F^2 m_{a_1}^2 m_\rho^2 D_{a_1} [(p+k)^2]} \left( 2 \left( C_q m_\eta^2 \kappa_3^A - 4\sqrt{2} C_s m_K^2 \kappa_9^A + 4C_q m_\pi^2 \kappa_9^A + 2\sqrt{2} C_s m_\pi^2 \kappa_9^A \right. \right. \\
& + 4C_q m_\pi^2 \kappa_{11}^A + C_q m_\eta^2 \kappa_{15}^A - C_q m_\eta^2 \kappa_{16}^A + k \cdot p_0 C_q (\kappa_3^A + \kappa_{15}^A) + p \cdot p_0 C_q (\kappa_3^A + \kappa_{15}^A - \kappa_{16}^A) \left. \right) (2\lambda_2 + \lambda_4 + 2\lambda_5) (k \cdot p)^2 \\
& + (-8p \cdot p_0 C_q m_\pi^2 \lambda_1 \kappa_3^A - 8C_q m_\pi^2 m_\eta^2 \lambda_1 \kappa_3^A - 2p \cdot p_0 C_q m_{a_1}^2 \lambda_2 \kappa_3^A - 2C_q m_{a_1}^2 m_\eta^2 \lambda_2 \kappa_3^A + 4p \cdot p_0 C_q m_\eta^2 \lambda_2 \kappa_3^A \\
& + 4(p \cdot p_0)^2 C_q \lambda_2 \kappa_3^A - p \cdot p_0 C_q m_{a_1}^2 \lambda_4 \kappa_3^A - C_q m_{a_1}^2 m_\eta^2 \lambda_4 \kappa_3^A - 2p \cdot p_0 C_q m_{a_1}^2 \lambda_5 \kappa_3^A - 2C_q m_{a_1}^2 m_\eta^2 \lambda_5 \kappa_3^A \\
& - 32C_q m_\pi^4 \kappa_9^A \lambda_1 - 16\sqrt{2} C_s m_\pi^4 \kappa_9^A \lambda_1 + 32\sqrt{2} C_s m_K^2 m_\pi^2 \kappa_9^A \lambda_1 - 32C_q m_\pi^4 \kappa_{11}^A \lambda_1 - 8p \cdot p_0 C_q m_\pi^2 \kappa_{15}^A \lambda_1 \\
& - 8C_q m_\pi^2 m_\eta^2 \kappa_{15}^A \lambda_1 + 8p \cdot p_0 C_q m_\pi^2 \kappa_{16}^A \lambda_1 + 8C_q m_\pi^2 m_\eta^2 \kappa_{16}^A \lambda_1 + 4C_q p_0^4 \kappa_8^A \lambda_2 + 8p \cdot p_0 C_q m_\eta^2 \kappa_8^A \lambda_2 + 4(p \cdot p_0)^2 C_q \kappa_8^A \lambda_2 \\
& - 16\sqrt{2} p \cdot p_0 C_s m_K^2 \kappa_9^A \lambda_2 + 16p \cdot p_0 C_q m_\pi^2 \kappa_9^A \lambda_2 + 8\sqrt{2} p \cdot p_0 C_s m_\pi^2 \kappa_9^A \lambda_2 + 8\sqrt{2} C_s m_K^2 m_{a_1}^2 \kappa_9^A \lambda_2 - 8C_q m_\pi^2 m_{a_1}^2 \kappa_9^A \lambda_2 \\
& - 4\sqrt{2} C_s m_\pi^2 m_{a_1}^2 \kappa_9^A \lambda_2 - 4\sqrt{2} p \cdot p_0 C_s m_K^2 \kappa_{10}^A \lambda_2 + 4p \cdot p_0 C_q m_\pi^2 \kappa_{10}^A \lambda_2 + 2\sqrt{2} p \cdot p_0 C_s m_\pi^2 \kappa_{10}^A \lambda_2 - 4\sqrt{2} C_s m_K^2 m_\eta^2 \kappa_{10}^A \lambda_2 \\
& + 4C_q m_\pi^2 m_\eta^2 \kappa_{10}^A \lambda_2 + 2\sqrt{2} C_s m_\pi^2 m_\eta^2 \kappa_{10}^A \lambda_2 + 16p \cdot p_0 C_q m_\pi^2 \kappa_{11}^A \lambda_2 - 8C_q m_\pi^2 m_{a_1}^2 \kappa_{11}^A \lambda_2 + 4p \cdot p_0 C_q m_\pi^2 \kappa_{12}^A \lambda_2 + 4C_q m_\pi^2 m_\eta^2 \kappa_{12}^A \lambda_2 \\
& - 2p \cdot p_0 C_q m_{a_1}^2 \kappa_{15}^A \lambda_2 - 2C_q m_{a_1}^2 m_\eta^2 \kappa_{15}^A \lambda_2 + 4p \cdot p_0 C_q m_\eta^2 \kappa_{15}^A \lambda_2 + 4(p \cdot p_0)^2 C_q \kappa_{15}^A \lambda_2 - 2C_q p_0^4 \kappa_{16}^A \lambda_2 \\
& + 4p \cdot p_0 C_q m_{a_1}^2 \kappa_{16}^A \lambda_2 - 6p \cdot p_0 C_q m_\eta^2 \kappa_{16}^A \lambda_2 + 2C_q p_0^4 \kappa_8^A \lambda_4 + 4p \cdot p_0 C_q m_\eta^2 \kappa_8^A \lambda_4 + 2(p \cdot p_0)^2 C_q \kappa_8^A \lambda_4 \\
& + 4\sqrt{2} C_s m_K^2 m_{a_1}^2 \kappa_9^A \lambda_4 - 4C_q m_\pi^2 m_{a_1}^2 \kappa_9^A \lambda_4 - 2\sqrt{2} C_s m_\pi^2 m_{a_1}^2 \kappa_9^A \lambda_4 - 2\sqrt{2} p \cdot p_0 C_s m_K^2 \kappa_{10}^A \lambda_4 + 2p \cdot p_0 C_q m_\pi^2 \kappa_{10}^A \lambda_4 \\
& + \sqrt{2} p \cdot p_0 C_s m_\pi^2 \kappa_{10}^A \lambda_4 - 2\sqrt{2} C_s m_K^2 m_\eta^2 \kappa_{10}^A \lambda_4 + 2C_q m_\pi^2 m_\eta^2 \kappa_{10}^A \lambda_4 + \sqrt{2} C_s m_\pi^2 m_\eta^2 \kappa_{10}^A \lambda_4 - 4C_q m_\pi^2 m_{a_1}^2 \kappa_{11}^A \lambda_4 \\
& + 2p \cdot p_0 C_q m_\pi^2 \kappa_{12}^A \lambda_4 + 2C_q m_\pi^2 m_\eta^2 \kappa_{12}^A \lambda_4 - p \cdot p_0 C_q m_{a_1}^2 \kappa_{15}^A \lambda_4 - C_q m_{a_1}^2 m_\eta^2 \kappa_{15}^A \lambda_4 - C_q p_0^4 \kappa_{16}^A \lambda_4 - 3p \cdot p_0 C_q m_\eta^2 \kappa_{16}^A \lambda_4 \\
& - 2(p \cdot p_0)^2 C_q \kappa_{16}^A \lambda_4 + 4C_q p_0^4 \kappa_8^A \lambda_5 + 8p \cdot p_0 C_q m_\eta^2 \kappa_8^A \lambda_5 + 4(p \cdot p_0)^2 C_q \kappa_8^A \lambda_5 + 8\sqrt{2} C_s m_K^2 m_{a_1}^2 \kappa_9^A \lambda_5 \\
& - 8C_q m_\pi^2 m_{a_1}^2 \kappa_9^A \lambda_5 - 4\sqrt{2} C_s m_\pi^2 m_{a_1}^2 \kappa_9^A \lambda_5 - 4\sqrt{2} p \cdot p_0 C_s m_K^2 \kappa_{10}^A \lambda_5 + 4p \cdot p_0 C_q m_\pi^2 \kappa_{10}^A \lambda_5 + 2\sqrt{2} p \cdot p_0 C_s m_\pi^2 \kappa_{10}^A \lambda_5 \\
& - 4\sqrt{2} C_s m_K^2 m_\eta^2 \kappa_{10}^A \lambda_5 + 4C_q m_\pi^2 m_\eta^2 \kappa_{10}^A \lambda_5 + 2\sqrt{2} C_s m_\pi^2 m_\eta^2 \kappa_{10}^A \lambda_5 - 8C_q m_\pi^2 m_{a_1}^2 \kappa_{11}^A \lambda_5 + 4p \cdot p_0 C_q m_\pi^2 \kappa_{12}^A \lambda_5 \\
& + 4C_q m_\pi^2 m_\eta^2 \kappa_{12}^A \lambda_5 - 2p \cdot p_0 C_q m_{a_1}^2 \kappa_{15}^A \lambda_5 - 2C_q m_{a_1}^2 m_\eta^2 \kappa_{15}^A \lambda_5 - 2C_q p_0^4 \kappa_{16}^A \lambda_5 - 6p \cdot p_0 C_q m_\eta^2 \kappa_{16}^A \lambda_5 - 4(p \cdot p_0)^2 C_q \kappa_{16}^A \lambda_5 \\
& + m_\pi^2 \left( -4\sqrt{2} C_s m_K^2 \kappa_9^A + 2(\sqrt{2} C_s + 2C_q) m_\pi^2 \kappa_9^A + 4C_q m_\pi^2 \kappa_{11}^A + C_q m_\eta^2 (\kappa_3^A + \kappa_{15}^A - \kappa_{16}^A) + p \cdot p_0 C_q (\kappa_3^A + \kappa_{15}^A - \kappa_{16}^A) \right) \\
& (2\lambda_2 + \lambda_4 + 2\lambda_5) + k \cdot p_0 C_q \left( -8m_\pi^2 \lambda_1 (\kappa_3^A + \kappa_{15}^A) - (2\lambda_2 + \lambda_4 + 2\lambda_5) [(m_{a_1}^2 - m_\pi^2)(\kappa_3^A + \kappa_{15}^A) + 2m_\eta^2 (\kappa_{16}^A - \kappa_8^A)] \right. \\
& \left. + 2p \cdot p_0 [2\lambda_2 (\kappa_3^A + \kappa_8^A + \kappa_{15}^A) + (\lambda_4 + 2\lambda_5)(\kappa_8 - \kappa_{16})] \right) k \cdot p \\
& + 2 \left( C_q m_{a_1}^2 (p \cdot p_0 + m_\eta^2) (m_\pi^2 \lambda_1 + p \cdot p_0 \lambda_2) \kappa_3^A + 2m_\pi^2 \lambda_1 \left\{ -2C_q \kappa_8^A [m_\eta^2 + p \cdot p_0]^2 - [\sqrt{2} C_s (2m_K^2 - m_\pi^2) - m_\pi^2 C_q] \right. \right. \\
& \left. \left[ 2m_{a_1}^2 \kappa_9^A - (p \cdot p_0 + m_\eta^2) \kappa_{10}^A \right] + C_q [(p \cdot p_0 + m_\eta^2) (m_{a_1}^2 \kappa_{15}^A + (m_\eta^2 + 2p \cdot p_0) \kappa_{16}^A - m_\pi^2 \kappa_{12}^A)] \right\} \\
& + p \cdot p_0 \lambda_2 \left\{ -C_q (m_{a_1}^2 + p \cdot p_0) [2\kappa_8^A (m_\eta^2 + p \cdot p_0) + 2m_\pi^2 \kappa_{12}^A - \kappa_{16}^A (2p \cdot p_0 + m_\eta^2)] - C_q m_{a_1}^2 [4m_\pi^2 \kappa_{11}^A + \kappa_{15}^A (p \cdot p_0)] \right. \\
& \left. + [\sqrt{2} C_s (2m_K^2 - m_\pi^2) - m_\pi^2 C_q] [m_{a_1}^2 \kappa_9^A + (p \cdot p_0 + m_{a_1}^2) \kappa_{10}^A] \right\} + 2(k \cdot p_0)^2 p \cdot p_0 C_q (\kappa_{16}^A - \kappa_8^A) \lambda_2 \\
& + m_\pi^2 \left( C_q (\kappa_3^A + \kappa_{15}^A + \kappa_{16}^A) \lambda_2 (p \cdot p_0)^2 + \left( 2\sqrt{2} C_s (m_\pi^2 - 2m_K^2) \lambda_2 \kappa_9^A + C_q m_\eta^2 (\kappa_3^A + \kappa_{15}^A) \lambda_2 \right. \right. \\
& \left. \left. + C_q (m_{a_1}^2 \lambda_2 \kappa_{16}^A + m_\pi^2 (-2\lambda_1 \kappa_3^A - 2\kappa_{15}^A \lambda_1 + 2\kappa_{16}^A \lambda_1 + 4\kappa_9^A \lambda_2 + 4\kappa_{11}^A \lambda_2)) \right) p \cdot p_0 \right. \\
& \left. - 2m_\pi^2 \left( 2\sqrt{2} C_s (m_\pi^2 - 2m_K^2) \kappa_9^A + 4C_q m_\pi^2 (\kappa_9^A + \kappa_{11}^A) + C_q m_\eta^2 (\kappa_3^A + \kappa_{15}^A - \kappa_{16}^A) \right) \lambda_1 \right)
\end{aligned}$$

$$\begin{aligned}
& +k \cdot p_0 \left( C_q \left( p \cdot p_0 \left( \kappa_3^A + \kappa_{15}^A + \kappa_{16}^A \right) \lambda_2 - 2m_\pi^2 \left( \kappa_3^A + \kappa_{15}^A \right) \lambda_1 \right) m_\pi^2 + 2C_q m_\pi^2 \left( \left( \kappa_3^A + \kappa_{15}^A \right) m_{a_1}^2 + 2m_\eta^2 \left( \kappa_{16}^A - \kappa_8^A \right) \right) \lambda_1 \right. \\
& \quad \left. + 4 \left( p \cdot p_0 \right)^2 C_q \left( \kappa_{16}^A - \kappa_8^A \right) \lambda_2 + p \cdot p_0 \left( \sqrt{2} C_s \left( 2m_K^2 - m_\pi^2 \right) \lambda_2 \kappa_{10}^A + C_q m_\eta^2 \left( \kappa_{16}^A - 2\kappa_8^A \right) \lambda_2 \right. \right. \\
& \quad \left. \left. + C_q \left( -2 \left( 2\lambda_1 \kappa_8^A - 2\kappa_{16}^A \lambda_1 + \left( \kappa_{10}^A + \kappa_{12}^A \right) \lambda_2 \right) m_\pi^2 - m_{a_1}^2 \left( \kappa_3^A + 2\kappa_8^A + \kappa_{15}^A - 2\kappa_{16}^A \right) \lambda_2 \right) \right) \right) , \quad (5.54)
\end{aligned}$$

$$\begin{aligned}
a_3^{W^- \rightarrow (a_1^-) \eta \rightarrow \pi^- (\rho^0) \eta \rightarrow \pi^- \gamma \eta} = & + \frac{8F_V}{F^2 m_{a_1}^2 m_\rho^2 D_{a_1} [(p+k)^2]} \left( 2C_q m_{a_1}^2 m_\eta^2 \lambda_2 \kappa_3^A - 2m_\pi^2 C_q m_\eta^2 \lambda_2 \kappa_3^A - 4k \cdot p C_q m_\eta^2 \lambda_2 \kappa_3^A \right. \\
& + 8C_q m_\pi^4 \kappa_{10}^A \lambda_1 + 4\sqrt{2} C_s m_\pi^4 \kappa_{10}^A \lambda_1 - 8\sqrt{2} C_s m_K^2 m_\pi^2 \kappa_{10}^A \lambda_1 + 8C_q m_\pi^4 \kappa_{12}^A \lambda_1 - 4C_q m_\pi^2 m_{a_1}^2 \kappa_{16}^A \lambda_1 - 4C_q m_\pi^2 m_\eta^2 \kappa_{16}^A \lambda_1 \\
& + 4C_q m_{a_1}^2 m_\eta^2 \kappa_8^A \lambda_2 - 4k \cdot p C_q m_\eta^2 \kappa_8^A \lambda_2 + 8\sqrt{2} m_\pi^2 C_s m_K^2 \kappa_9^A \lambda_2 + 16\sqrt{2} k \cdot p C_s m_K^2 \kappa_9^A \lambda_2 - 8m_\pi^2 C_q m_\pi^2 \kappa_9^A \lambda_2 \\
& - 16k \cdot p C_q m_\pi^2 \kappa_9^A \lambda_2 - 4\sqrt{2} m_\pi^2 C_s m_\pi^2 \kappa_9^A \lambda_2 - 8\sqrt{2} k \cdot p C_s m_\pi^2 \kappa_9^A \lambda_2 - 8\sqrt{2} C_s m_K^2 m_{a_1}^2 \kappa_9^A \lambda_2 + 8C_q m_\pi^2 m_{a_1}^2 \kappa_9^A \lambda_2 \\
& + 4\sqrt{2} C_s m_\pi^2 m_{a_1}^2 \kappa_9^A \lambda_2 + 4\sqrt{2} k \cdot p C_s m_K^2 \kappa_{10}^A \lambda_2 - 4k \cdot p C_q m_\pi^2 \kappa_{10}^A \lambda_2 - 2\sqrt{2} k \cdot p C_s m_\pi^2 \kappa_{10}^A \lambda_2 - 4\sqrt{2} C_s m_K^2 m_{a_1}^2 \kappa_{10}^A \lambda_2 \\
& + 4C_q m_\pi^2 m_{a_1}^2 \kappa_{10}^A \lambda_2 + 2\sqrt{2} C_s m_\pi^2 m_{a_1}^2 \kappa_{10}^A \lambda_2 - 8m_\pi^2 C_q m_\pi^2 \kappa_{11}^A \lambda_2 - 16k \cdot p C_q m_\pi^2 \kappa_{11}^A \lambda_2 + 8C_q m_\pi^2 m_{a_1}^2 \kappa_{11}^A \lambda_2 \\
& - 4k \cdot p C_q m_\pi^2 \kappa_{12}^A \lambda_2 + 4C_q m_\pi^2 m_{a_1}^2 \kappa_{12}^A \lambda_2 + 2C_q m_{a_1}^2 m_\eta^2 \kappa_{15}^A \lambda_2 - 2m_\pi^2 C_q m_\eta^2 \kappa_{15}^A \lambda_2 - 4k \cdot p C_q m_\eta^2 \kappa_{15}^A \lambda_2 - 2m_\pi^2 C_q m_{a_1}^2 \kappa_{16}^A \lambda_2 \\
& \quad - 2k \cdot p C_q m_{a_1}^2 \kappa_{16}^A \lambda_2 - 2C_q m_{a_1}^2 m_\eta^2 \kappa_{16}^A \lambda_2 + 2k \cdot p C_q m_\eta^2 \kappa_{16}^A \lambda_2 + 4 \left( k \cdot p_0 \right)^2 C_q \left( \kappa_8^A - \kappa_{16}^A \right) \lambda_2 \\
& + 4 \left( p \cdot p_0 \right)^2 C_q \left( \kappa_8^A - \kappa_{16}^A \right) \lambda_2 - 2k \cdot p C_q m_\eta^2 \kappa_8^A \lambda_4 + 2\sqrt{2} k \cdot p C_s m_K^2 \kappa_{10}^A \lambda_4 - 2k \cdot p C_q m_\pi^2 \kappa_{10}^A \lambda_4 - \sqrt{2} k \cdot p C_s m_\pi^2 \kappa_{10}^A \lambda_4 \\
& - 2k \cdot p C_q m_\pi^2 \kappa_{12}^A \lambda_4 + k \cdot p C_q m_{a_1}^2 \kappa_{16}^A \lambda_4 + k \cdot p C_q m_\eta^2 \kappa_{16}^A \lambda_4 - 4k \cdot p C_q m_\eta^2 \kappa_8^A \lambda_5 + 4\sqrt{2} k \cdot p C_s m_K^2 \kappa_{10}^A \lambda_5 \\
& - 4k \cdot p C_q m_\pi^2 \kappa_{10}^A \lambda_5 - 2\sqrt{2} k \cdot p C_s m_\pi^2 \kappa_{10}^A \lambda_5 - 4k \cdot p C_q m_\pi^2 \kappa_{12}^A \lambda_5 + 2k \cdot p C_q m_{a_1}^2 \kappa_{16}^A \lambda_5 + 2k \cdot p C_q m_\eta^2 \kappa_{16}^A \lambda_5 \\
& \quad + 8C_q m_\pi^2 m_\eta^2 \kappa_8^A \lambda_1 + 2p \cdot p_0 \left( C_q \left( - \left( m_\pi^2 - m_{a_1}^2 + 2k \cdot p \right) \lambda_2 \kappa_3^A + 2m_{a_1}^2 \kappa_8^A \lambda_2 + 2m_\eta^2 \kappa_8^A \lambda_2 \right. \right. \\
& \quad \left. \left. - 2k \cdot p \kappa_8^A \lambda_2 - m_\pi^2 \kappa_{15}^A \lambda_2 + m_{a_1}^2 \kappa_{15}^A \lambda_2 - 2k \cdot p \kappa_{15}^A \lambda_2 - m_\pi^2 \kappa_{16}^A \lambda_2 - 2m_{a_1}^2 \kappa_{16}^A \lambda_2 - m_\eta^2 \kappa_{16}^A \lambda_2 \right. \right. \\
& \quad \left. \left. + 2m_\pi^2 \left( 2\lambda_1 \kappa_8^A - 2\kappa_{16}^A \lambda_1 + \left( \kappa_{10}^A + \kappa_{12}^A \right) \lambda_2 \right) - k \cdot p \kappa_8^A \lambda_4 + k \cdot p \kappa_{16}^A \lambda_4 - 2k \cdot p \kappa_8^A \lambda_5 + 2k \cdot p \kappa_{16}^A \lambda_5 \right) \right. \\
& \quad \left. - \sqrt{2} C_s \left( 2m_K^2 - m_\pi^2 \right) \kappa_{10}^A \lambda_2 \right) + 2k \cdot p_0 \left( C_q \left( - \left( m_\pi^2 - m_{a_1}^2 + 2k \cdot p \right) \lambda_2 \kappa_3^A + 2m_{a_1}^2 \kappa_8^A \lambda_2 + 2m_\eta^2 \kappa_8^A \lambda_2 - 2k \cdot p \kappa_8^A \lambda_2 \right. \right. \\
& \quad \left. \left. + 4p \cdot p_0 \kappa_8^A \lambda_2 - m_\pi^2 \kappa_{15}^A \lambda_2 + m_{a_1}^2 \kappa_{15}^A \lambda_2 - 2k \cdot p \kappa_{15}^A \lambda_2 - m_\pi^2 \kappa_{16}^A \lambda_2 - 2m_{a_1}^2 \kappa_{16}^A \lambda_2 - m_\eta^2 \kappa_{16}^A \lambda_2 - 4p \cdot p_0 \kappa_{16}^A \lambda_2 \right. \right. \\
& \quad \left. \left. + 2m_\pi^2 \left( 2\lambda_1 \kappa_8^A - 2\kappa_{16}^A \lambda_1 + \left( \kappa_{10}^A + \kappa_{12}^A \right) \lambda_2 \right) - k \cdot p \kappa_8^A \lambda_4 + k \cdot p \kappa_{16}^A \lambda_4 - 2k \cdot p \kappa_8^A \lambda_5 + 2k \cdot p \kappa_{16}^A \lambda_5 \right) \right. \\
& \quad \left. - \sqrt{2} C_s \left( 2m_K^2 - m_\pi^2 \right) \kappa_{10}^A \lambda_2 \right) \right) , \quad (5.55)
\end{aligned}$$

$$\begin{aligned}
a_4^{W^- \rightarrow (a_1^-) \eta \rightarrow \pi^- (\rho^0) \eta \rightarrow \pi^- \gamma \eta} = & + \frac{16F_V}{F^2 m_{a_1}^2 m_\rho^2 D_{a_1} [(p+k)^2]} \left( C_q \left( -(p \cdot p_0) m_{a_1}^2 \lambda_2 \kappa_3^A + m_\pi^2 m_\eta^2 \lambda_2 \kappa_3^A - m_{a_1}^2 m_\eta^2 \lambda_2 \kappa_3^A \right. \right. \\
& + 2k \cdot p m_\eta^2 \lambda_2 \kappa_3^A + m_\pi^2 p \cdot p_0 \lambda_2 \kappa_3^A + 2k \cdot p p \cdot p_0 \lambda_2 \kappa_3^A + 4(k \cdot p)^2 \kappa_8^A \lambda_2 - 2(p \cdot p_0)^2 \kappa_8^A \lambda_2 - 2k \cdot p m_{a_1}^2 \kappa_8^A \lambda_2 \\
& - 2p \cdot p_0 m_{a_1}^2 \kappa_8^A \lambda_2 - 2m_{a_1}^2 m_\eta^2 \kappa_8^A \lambda_2 - 2p \cdot p_0 m_\eta^2 \kappa_8^A \lambda_2 + 2m_\pi^2 k \cdot p \kappa_8^A \lambda_2 - p \cdot p_0 m_{a_1}^2 \kappa_{15}^A \lambda_2 + m_\pi^2 m_\eta^2 \kappa_{15}^A \lambda_2 \\
& - m_{a_1}^2 m_\eta^2 \kappa_{15}^A \lambda_2 + 2k \cdot p m_\eta^2 \kappa_{15}^A \lambda_2 + m_\pi^2 p \cdot p_0 \kappa_{15}^A \lambda_2 + 2k \cdot p p \cdot p_0 \kappa_{15}^A \lambda_2 + 2(p \cdot p_0)^2 \kappa_{16}^A \lambda_2 + m_\pi^2 m_{a_1}^2 \kappa_{16}^A \lambda_2 + 2k \cdot p m_{a_1}^2 \kappa_{16}^A \lambda_2 \\
& + 2p \cdot p_0 m_{a_1}^2 \kappa_{16}^A \lambda_2 + m_{a_1}^2 m_\eta^2 \kappa_{16}^A \lambda_2 + p \cdot p_0 m_\eta^2 \kappa_{16}^A \lambda_2 + m_\pi^2 p \cdot p_0 \kappa_{16}^A \lambda_2 + 2k \cdot p p \cdot p_0 \kappa_{16}^A \lambda_2 - 2(k \cdot p_0)^2 (\kappa_8^A - \kappa_{16}^A) \lambda_2 \\
& + k \cdot p_0 \left( (m_\pi^2 - m_{a_1}^2 + 2k \cdot p) \kappa_3^A - 2m_{a_1}^2 \kappa_8^A - 2m_\eta^2 \kappa_8^A + m_\pi^2 \kappa_{15}^A - m_{a_1}^2 \kappa_{15}^A + 2k \cdot p \kappa_{15}^A + m_\pi^2 \kappa_{16}^A + 2m_{a_1}^2 \kappa_{16}^A + m_\eta^2 \kappa_{16}^A \right. \\
& + 2k \cdot p \kappa_{16}^A - 4p \cdot p_0 (\kappa_8^A - \kappa_{16}^A) \left. \right) \lambda_2 - 2m_\pi^2 (2(m_\pi^2 - m_{a_1}^2 + 2k \cdot p) \kappa_8^A \lambda_1 - (2(m_\pi^2 - m_{a_1}^2 + 2k \cdot p) \kappa_9^A - m_{a_1}^2 \kappa_{10}^A \\
& - p \cdot p_0 \kappa_{10}^A + 2m_\pi^2 \kappa_{11}^A - 2m_{a_1}^2 \kappa_{11}^A + 4k \cdot p \kappa_{11}^A - m_{a_1}^2 \kappa_{12}^A - p \cdot p_0 \kappa_{12}^A - k \cdot p_0 (\kappa_{10}^A + \kappa_{12}^A)) \lambda_2) + 2(k \cdot p)^2 \kappa_8^A \lambda_4 \\
& - k \cdot p m_{a_1}^2 \kappa_8^A \lambda_4 + m_\pi^2 k \cdot p \kappa_8^A \lambda_4 + 4(k \cdot p)^2 \kappa_8^A \lambda_5 - 2k \cdot p m_{a_1}^2 \kappa_8^A \lambda_5 + 2m_\pi^2 k \cdot p \kappa_8^A \lambda_5) \\
& \left. - \sqrt{2} C_s (2m_K^2 - m_\pi^2) (2(m_\pi^2 - m_{a_1}^2 + 2k \cdot p) \kappa_9^A - (m_{a_1}^2 + k \cdot p_0 + p \cdot p_0) \kappa_{10}^A) \lambda_2 \right). \quad (5.56)
\end{aligned}$$

We turn now to the vector factors, with the one-resonance exchange contributions (fig. 3.7) listed next:

$$\begin{aligned}
v_1^{1R} = & \frac{4\sqrt{2}C_q}{3F^2 M_V^2 m_\rho^2 D_\rho [(p+k)^2]} \left( 2k \cdot p (4(c_5 + c_7) (m_\rho^2 - 2m_\pi^2) ((c_5 + c_7) (k \cdot p_0 + m_\eta^2) + 4c_3 (m_\pi^2 - m_\eta^2)) \right. \\
& + p \cdot p_0 (8(c_5 + c_7) (2c_3 m_\eta^2 - (2c_3 + c_5 + c_7) m_\pi^2) + (4(c_5 + c_7)^2 + c_{1256}^2) m_\rho^2)) \\
& + 4(c_5 + c_7) m_\pi^2 (m_\rho^2 - m_\pi^2) ((c_5 + c_7) (k \cdot p_0 + m_\eta^2) + 4c_3 (m_\pi^2 - m_\eta^2)) \\
& \left. - 16(c_5 + c_7) (k \cdot p)^2 ((c_5 + c_7) (k \cdot p_0 + m_\eta^2 + p \cdot p_0) + 4c_3 (m_\pi^2 - m_\eta^2)) \right) \\
& + p \cdot p_0 (-8c_3 (m_\pi^2 - m_\eta^2) ((c_{1256} - 2(c_5 + c_7)) m_\rho^2 + 2(c_5 + c_7) m_\pi^2) + (4(c_5 + c_7)^2 (m_\rho^2 - m_\pi^2) + c_{1256}^2 m_\rho^2) m_\pi^2) \\
& + \frac{4\sqrt{2}C_q}{3F^2 M_V^2 m_\omega^2 D_\omega [(p_0+k)^2]} \left( 16c_3 m_\pi^2 k \cdot p_0 ((c_5 + c_7) (2k \cdot p_0 + m_\eta^2) + 4c_3 (m_\eta^2 - m_\pi^2)) \right. \\
& - m_\omega^2 ((c_{1256} (8c_3 + 3c_{1256}) m_\eta^2 + 16c_3 (c_5 + c_7) m_\pi^2) k \cdot p_0 + 2c_{1256}^2 (k \cdot p_0)^2 + 64c_3^2 m_\pi^2 m_\eta^2 \\
& \left. + c_{1256} (8c_3 + c_{1256}) m_\eta^4 - 64c_3^2 m_\pi^4) \right) \\
& - \frac{8\sqrt{2}C_q \lambda_{15}^S}{3F^2 D_{a_0} [(p+p_0)^2]} (c_m m_\pi^2 + c_d p \cdot p_0) \\
& - \frac{2C_q F_V}{3F^2 m_\omega^2} \left( -(\lambda_{13}^V - \lambda_{14}^V - \lambda_{15}^V) (k \cdot p_0 + m_\eta^2 + p \cdot p_0) + 4m_\pi^2 \lambda_6^V + 2p \cdot p_0 (\lambda_{11}^V + \lambda_{12}^V) \right), \quad (5.57)
\end{aligned}$$

$$\begin{aligned}
v_2^{1R} = & \frac{4\sqrt{2}C_q}{3F^2 M_V^2 m_\rho^2 D_\rho [(p+k)^2]} \left( m_\rho^2 \left( - \left( (3c_{1256}^2 m_\pi^2 - 8c_3 (2(c_5 + c_7) + c_{1256}) (m_\pi^2 - m_\eta^2)) \right) k \cdot p + 2c_{1256}^2 (k \cdot p)^2 \right. \right. \\
& + c_{1256} m_\pi^2 (8c_3 m_\eta^2 + (c_{1256} - 8c_3) m_\pi^2) \left. \right) - 16c_3 (c_5 + c_7) (m_\pi^2 - m_\eta^2) k \cdot p (2k \cdot p + m_\pi^2) \\
& - \frac{16\sqrt{2}C_q}{3F^2 M_V^2 m_\omega^2 D_\omega [(p_0+k)^2]} \left( -\frac{1}{2} k \cdot p_0 (p \cdot p_0 (8(c_5 + c_7) (4c_3 m_\pi^2 - (2c_3 + c_5 + c_7) m_\eta^2) \right. \\
& + (4(c_5 + c_7)^2 + c_{1256}^2) m_\omega^2) - 4(4c_3 - c_5 - c_7) m_\pi^2 (-2(2c_3 + c_5 + c_7) m_\eta^2 + (c_5 + c_7) m_\omega^2 + 4c_3 m_\pi^2) \\
& + (c_5 + c_7) k \cdot p ((c_5 + c_7) (2k \cdot p_0 + m_\eta^2) + 4c_3 (m_\eta^2 - m_\pi^2)) (2k \cdot p_0 + m_\eta^2 - m_\omega^2) \\
& + 4(c_5 + c_7) (k \cdot p_0)^2 ((c_5 + c_7) (m_\pi^2 + p \cdot p_0) - 4c_3 m_\pi^2) + \frac{1}{4} m_\omega^2 (16c_3 m_\pi^2 ((c_5 + c_7) (m_\pi^2 + 2p \cdot p_0) - 4c_3 m_\pi^2) \\
& - m_\eta^2 (4((c_5 + c_7)^2 - 16c_3^2) m_\pi^2 + (c_{1256}^2 + 8c_3 c_{1256} + 4(c_5 + c_7) (4c_3 + c_5 + c_7)) p \cdot p_0) \\
& + (4c_3 m_\pi^2 - (4c_3 + c_5 + c_7) m_\eta^2) (4c_3 m_\pi^2 p \cdot p_0 - m_\eta^2 ((c_5 + c_7) (m_\pi^2 + p \cdot p_0) - 4c_3 m_\pi^2)) \\
& + \frac{8\sqrt{2}C_q \lambda_{15}^S}{3F^2 D_{a_0} [(p+p_0)^2]} (c_m m_\pi^2 + c_d p \cdot p_0) \\
& - \frac{2C_q F_V}{3F^2 m_\omega^2} \left( -(\lambda_{13}^V - \lambda_{14}^V - \lambda_{15}^V) (k \cdot p_0 + m_\eta^2 + p \cdot p_0) + 4m_\pi^2 \lambda_6^V + 2p \cdot p_0 (\lambda_{11}^V + \lambda_{12}^V) \right), \\
\end{aligned} \tag{5.58}$$

$$\begin{aligned}
v_3^{1R} = & -\frac{4\sqrt{2}C_q}{3F^2 M_V^2 m_\rho^2 D_\rho [(p+k)^2]} \left( 16c_3 (c_5 + c_7) (m_\pi^2 - m_\eta^2) (2k \cdot p + m_\pi^2) - m_\rho^2 (2c_{1256}^2 k \cdot p \right. \\
& - 8c_3 (2(c_2 + 4c_3 + c_7) - c_{1256}) m_\eta^2 + (c_{1256}^2 + 8c_3 (2(c_5 + c_7) - c_{1256})) m_\pi^2 \\
& + 2(4c_3 - c_5) (2c_5 - 2c_6 + c_{1256}) p \cdot p_0) \\
& + \frac{16\sqrt{2}C_q}{3F^2 M_V^2 m_\omega^2 D_\omega [(p_0+k)^2]} (c_5 + c_7) ((c_5 + c_7) (2k \cdot p_0 + m_\eta^2) + 4c_3 (m_\eta^2 - m_\pi^2)) (2k \cdot p_0 + m_\eta^2 - m_\omega^2) \\
& - \frac{2C_q F_V}{3F^2 m_\omega^2} (\lambda_{13}^V - \lambda_{14}^V - \lambda_{15}^V), \\
\end{aligned} \tag{5.59}$$

$$\begin{aligned}
v_4^{1R} = & -\frac{4\sqrt{2}C_q}{3F^2M_V^2m_\rho^2D_\rho[(p+k)^2]}4(c_5+c_7)^2(2k\cdot p+m_\pi^2)(2k\cdot p-m_\rho^2+m_\pi^2) \\
& -\frac{4\sqrt{2}C_q}{3F^2M_V^2m_\omega^2D_\omega[(p_0+k)^2]}(m_\omega^2(c_{1256}(c_{1256}(2k\cdot p_0+m_\eta^2)+8c_3m_\eta^2)-16c_3(c_5+c_7)m_\pi^2) \\
& +16c_3m_\pi^2((c_5+c_7)(2k\cdot p_0+m_\eta^2)+4c_3(m_\eta^2-m_\pi^2))) \\
& +\frac{2C_qF_V}{3F^2m_\omega^2}(\lambda_{13}^V-\lambda_{14}^V-\lambda_{15}^V) .
\end{aligned}
\tag{5.60}$$

Finally, we will give the two-resonance mediated contributions to the vector form factors (figure 3.8):

$$\begin{aligned}
v_1^{2R} = & \frac{8F_V C_q}{3F^2 M_V m_\omega^2 D_\rho [(p+p_0+k)^2] D_\omega [(p_0+k)^2]} \left( m_\omega^2 (k \cdot p_0 (2(8c_3 + 3c_{1256}) d_3 m_\eta^2 \right. \\
& + m_\pi^2 (-(16c_3 d_3 + (2(c_5 + c_7) + c_{1256}) d_{12})) + 2(2(c_5 + c_7) + c_{1256}) d_3 p \cdot p_0) + 4c_{1256} d_3 (k \cdot p_0)^2 \\
& + (8c_3 m_\pi^2 - (8c_3 + c_{1256}) m_\eta^2) (d_{12} m_\pi^2 - 2d_3 (m_\eta^2 + p \cdot p_0))) \\
& + 2d_3 k \cdot p (m_\omega^2 ((2(c_5 + c_7) + c_{1256}) k \cdot p_0 + (8c_3 + c_{1256}) m_\eta^2 - 8c_3 m_\pi^2) \\
& + 2k \cdot p_0 (4c_3 (m_\pi^2 - m_\eta^2) - (c_5 + c_7) (2k \cdot p_0 + m_\eta^2))) \\
& - 2k \cdot p_0 (2d_3 p \cdot p_0 - d_{12} m_\pi^2) ((c_5 + c_7) (2k \cdot p_0 + m_\eta^2) + 4c_3 (m_\eta^2 - m_\pi^2))) \\
& - \frac{8F_V C_q}{3F^2 M_V m_\rho^2 D_\rho [(p+p_0+k)^2] D_\rho [(p+k)^2]} \left( -16c_5 d_2 m_\pi^6 \right. \\
& + 16c_5 d_2 m_\rho^2 m_\pi^4 + 16c_7 d_2 m_\rho^2 m_\pi^4 - 16p \cdot p_0 c_5 d_2 m_\pi^4 - 16p \cdot p_0 c_7 d_2 m_\pi^4 - 2p \cdot p_0 c_5 d_3 m_\pi^4 - 2p \cdot p_0 c_7 d_3 m_\pi^4 - 2p \cdot p_0 c_5 d_4 m_\pi^4 \\
& - 2p \cdot p_0 c_7 d_4 m_\pi^4 + 16p \cdot p_0 c_5 d_2 m_\rho^2 m_\pi^2 + 16p \cdot p_0 c_7 d_2 m_\rho^2 m_\pi^2 - 8p \cdot p_0 c_{1256} d_2 m_\rho^2 m_\pi^2 + 2p \cdot p_0 c_5 d_3 m_\rho^2 m_\pi^2 \\
& + 2p \cdot p_0 c_7 d_3 m_\rho^2 m_\pi^2 - 2p \cdot p_0 c_{1256} d_3 m_\rho^2 m_\pi^2 + 2p \cdot p_0 c_5 d_4 m_\rho^2 m_\pi^2 + 2p \cdot p_0 c_7 d_4 m_\rho^2 m_\pi^2 - 4(p \cdot p_0)^2 c_5 d_3 m_\pi^2 - 16c_7 d_2 m_\pi^6 \\
& - 4(p \cdot p_0)^2 c_7 d_3 m_\pi^2 + 4(p \cdot p_0)^2 c_5 d_3 m_\rho^2 + 4(p \cdot p_0)^2 c_7 d_3 m_\rho^2 - 2(p \cdot p_0)^2 c_{1256} d_3 m_\rho^2 \\
& - 8(k \cdot p)^2 (c_5 + c_7) ((-d_3 + d_4 + d_{12}) m_\eta^2 + (k \cdot p_0 + p \cdot p_0) (d_3 + d_4) + 8d_2 (m_\pi^2 - m_\eta^2)) \\
& + 2k \cdot p_0 ((c_5 + c_7) (d_3 + d_4) (m_\rho^2 - m_\pi^2) m_\pi^2 + p \cdot p_0 d_3 ((2(c_5 + c_7) - c_{1256}) m_\rho^2 - 2(c_5 + c_7) m_\pi^2)) \\
& - m_\eta^2 (2(c_5 + c_7) (8d_2 + d_3 - d_4 - d_{12}) m_\pi^2 (m_\rho^2 - m_\pi^2) - p \cdot p_0 (8d_2 - d_{12}) (2(c_5 + c_7) m_\pi^2 + (c_{1256} - 2(c_5 + c_7)) m_\rho^2)) \\
& + 4k \cdot p (-2(c_5 + c_7) d_3 (p \cdot p_0)^2 + ((c_5 + c_7 - c_{1256}) d_3 \\
& + (c_5 + c_7) d_4) m_\rho^2 + (c_5 + c_7) ((8d_2 - d_{12}) m_\eta^2 - 2(4d_2 + d_3 + d_4) m_\pi^2)) p \cdot p_0 \\
& - (c_5 + c_7) (8d_2 m_\pi^2 + (-8d_2 - d_3 + d_4 + d_{12}) m_\eta^2) (2m_\pi^2 - m_\rho^2) - k \cdot p_0 (c_5 + c_7) (2p \cdot p_0 d_3 + (d_3 + d_4) (2m_\pi^2 - m_\rho^2)) \\
& + \frac{8F_V C_q \lambda_3^{SV}}{3F^2 D_\rho [(p+p_0+k)^2] D_{a0} [(p+p_0)^2]} (c_d p \cdot p_0 + c_m m_\pi^2) \\
& - \frac{16F_V C_q}{3F^2 M_V m_\rho^2 m_\omega^2 D_\rho [(p+k)^2]} \left( k \cdot p (2((c_5 + c_7) k \cdot p_0 + (c_5 + c_7) m_\eta^2 + 4c_3 (m_\pi^2 - m_\eta^2)) \right. \\
& (m_\pi^2 (d_1 + 8d_2 + d_3 + 2d_4) - d_4 m_\rho^2) + p \cdot p_0 (2c_5 (m_\pi^2 (d_1 + 8d_2 + d_3 + 2d_4) - d_4 m_\rho^2) + 2c_7 d_1 m_\pi^2 + 16c_7 d_2 m_\pi^2 \\
& + c_{1256} d_3 m_\rho^2 + 2c_7 d_3 m_\pi^2 + 8c_3 d_4 (m_\pi^2 - m_\eta^2) - 2c_7 d_4 m_\rho^2 + 4c_7 d_4 m_\pi^2)) \\
& + m_\pi^2 (m_\pi^2 - m_\rho^2) (d_1 + 8d_2 + d_3 + d_4) ((c_5 + c_7) k \cdot p_0 + (c_5 + c_7) m_\eta^2 + 4c_3 (m_\pi^2 - m_\eta^2)) \\
& + \frac{1}{2} p \cdot p_0 (8c_3 (m_\pi^2 - m_\eta^2) (m_\pi^2 (d_1 + 8d_2 + d_3 + d_4) - (d_3 + d_4) m_\rho^2) + m_\pi^2 (2c_5 (m_\pi^2 - m_\rho^2) (d_1 + 8d_2 + d_3 + d_4) \\
& + 2c_7 (m_\pi^2 - m_\rho^2) (d_1 + 8d_2 + d_3 + d_4) + c_{1256} (-(d_1 + 8d_2)) m_\rho^2)) \\
& + 4d_4 (k \cdot p)^2 ((c_5 + c_7) k \cdot p_0 - 4c_3 m_\eta^2 + c_5 m_\eta^2 + c_7 m_\eta^2 + 4c_3 m_\pi^2 + (c_5 + c_7) p \cdot p_0)) \\
& + \frac{\sqrt{2} F_V^2 C_q}{3F^2 m_\rho^2 m_\omega^2 D_\rho [(p+p_0+k)^2]} (2k \cdot p_0 + m_\eta^2 + m_\rho^2 + 2p \cdot p_0) \\
& ((\lambda_3^{VV} + \lambda_4^{VV} + 2\lambda_5^{VV}) (k \cdot p_0 + m_\eta^2 + p \cdot p_0) + 4m_\pi^2 \lambda_6^{VV} + 4p \cdot p_0 (\lambda_1^{VV} + \lambda_2^{VV})) ,
\end{aligned}
\tag{5.61}$$



where  $d_{12} \equiv d_1 + 8d_2$  is fixed by the short-distance constraints (3.50).

$$\begin{aligned}
v_2^{2R} = & \frac{8F_V C_q}{3F^2 M_V m_\omega^2 D_\rho [(p + p_0 + k)^2] D_\omega [(p_0 + k)^2]} (8c_3 d_3 m_\omega^2 m_\pi^4 - 8c_3 d_4 m_\omega^2 m_\pi^4 + 8c_3 d_{12} m_\omega^2 m_\pi^4 - 8p \cdot p_0 c_3 d_{12} m_\pi^4 \\
& + 64p \cdot p_0 c_3 d_2 m_\omega^2 m_\pi^2 - 16p \cdot p_0 c_5 d_2 m_\omega^2 m_\pi^2 + 8p \cdot p_0 c_3 d_3 m_\omega^2 m_\pi^2 - 8p \cdot p_0 c_3 d_4 m_\omega^2 m_\pi^2 - 8p \cdot p_0 c_3 d_{12} m_\omega^2 m_\pi^2 \\
& - 2p \cdot p_0 c_7 d_{12} m_\omega^2 m_\pi^2 + p \cdot p_0 c_{1256} d_{12} m_\omega^2 m_\pi^2 + 8p \cdot p_0 c_3 (d_{12} - 8d_2) m_\omega^2 m_\pi^2 - 2p \cdot p_0 c_5 (d_{12} - 8d_2) m_\omega^2 m_\pi^2 \\
& + 16(p \cdot p_0)^2 c_3 d_3 m_\pi^2 - 2(4c_3 + c_5 + c_7) (p \cdot p_0 (d_3 + d_4) - (d_3 - d_4 + d_{12}) m_\pi^2) m_\eta^4 + 4(p \cdot p_0)^2 c_5 d_3 m_\omega^2 \\
& + 4(p \cdot p_0)^2 c_7 d_3 m_\omega^2 - 2(p \cdot p_0)^2 c_{1256} d_3 m_\omega^2 + 8(k \cdot p_0)^2 (c_5 + c_7) ((d_3 - d_4 + d_{12}) m_\pi^2 - p \cdot p_0 (d_3 + d_4)) \\
& + 2m_\eta^2 (-2(4c_3 + c_5 + c_7) d_3 (p \cdot p_0)^2 + ((c_5 + c_7) d_{12} + 4c_3 (d_3 + d_4 + d_{12})) m_\pi^2 + ((-4c_3 + c_5 + c_7 - c_{1256}) d_3 \\
& + (4c_3 + c_5 + c_7) d_4) m_\omega^2) p \cdot p_0 - (d_3 - d_4 + d_{12}) m_\pi^2 (4c_3 m_\pi^2 + (4c_3 + c_5 + c_7) m_\omega^2)) \\
& + 4k \cdot p_0 (-2(c_5 + c_7) d_3 (p \cdot p_0)^2 + (((c_5 + c_7 - c_{1256}) d_3 + (c_5 + c_7) d_4) m_\omega^2 + 4c_3 (d_3 + d_4) (m_\pi^2 - m_\eta^2) \\
& + (c_5 + c_7) (d_{12} m_\pi^2 - 2(d_3 + d_4) m_\eta^2)) p \cdot p_0 + (d_3 - d_4 + d_{12}) m_\pi^2 (4c_3 (m_\eta^2 - m_\pi^2) + (c_5 + c_7) (2m_\eta^2 - m_\omega^2))) \\
& + 2k \cdot p (-4(c_5 + c_7) (d_3 + d_4) (k \cdot p_0)^2 + 2((d_3 + d_4) (4c_3 m_\pi^2 - 2(2c_3 + c_5 + c_7) m_\eta^2 + (c_5 + c_7) m_\omega^2) \\
& - 2p \cdot p_0 (c_5 + c_7) d_3) k \cdot p_0 + (d_3 + d_4) (4c_3 m_\pi^2 - (4c_3 + c_5 + c_7) m_\eta^2) (m_\eta^2 - m_\omega^2) \\
& + p \cdot p_0 d_3 (8c_3 m_\pi^2 - 2(4c_3 + c_5 + c_7) m_\eta^2 + (2(c_5 + c_7) - c_{1256}) m_\omega^2))) \\
& - \frac{8F_V C_q}{3F^2 M_V m_\rho^2 D_\rho [(p + p_0 + k)^2] D_\rho [(p + k)^2]} \\
& (4(k \cdot p)^2 (c_{1256} d_3 m_\rho^2 - (c_5 + c_7) (2d_3 (k \cdot p_0 + p \cdot p_0) + (d_{12} - 8d_2) m_\eta^2 + 8d_2 m_\pi^2)) \\
& + k \cdot p (m_\rho^2 (2(2(c_5 + c_7) + c_{1256}) d_3 (k \cdot p_0 + p \cdot p_0) - (2(c_5 + c_7) + c_{1256}) (8d_2 - d_{12}) m_\eta^2 \\
& + 2m_\pi^2 (4(2(c_5 + c_7) + c_{1256}) d_2 + 3c_{1256} d_3)) - 2(c_5 + c_7) m_\pi^2 (2d_3 (k \cdot p_0 + p \cdot p_0) + (d_{12} - 8d_2) m_\eta^2 + 8d_2 m_\pi^2)) \\
& + c_{1256} m_\pi^2 m_\rho^2 (2d_3 (k \cdot p_0 + m_\pi^2 + p \cdot p_0) + (d_{12} - 8d_2) m_\eta^2 + 8d_2 m_\pi^2)) \\
& + \frac{8F_V C_q \lambda_3^{SV}}{3F^2 D_\rho [(p + p_0 + k)^2] D_{a_0} [(p + p_0)^2]} (c_d p \cdot p_0 + c_m m_\pi^2) \\
& - \frac{8F_V C_q}{3F^2 M_V m_\rho^2 m_\omega^2 D_\rho [(p + k)^2]} (k \cdot p (8c_3 (m_\pi^2 - m_\eta^2) (m_\pi^2 (d_1 + 8d_2 + d_3 + d_4) + (d_3 - d_4) m_\rho^2) \\
& + c_{1256} m_\pi^2 m_\rho^2 (d_1 + 8d_2 - 2d_3)) + m_\pi^2 (d_1 + 8d_2) m_\rho^2 (c_{1256} m_\pi^2 - 8c_3 (m_\pi^2 - m_\eta^2)) \\
& + 2(k \cdot p)^2 (8c_3 d_4 (m_\pi^2 - m_\eta^2) - c_{1256} d_3 m_\rho^2)) \\
& + \frac{\sqrt{2} F_V^2 C_q}{3F^2 m_\rho^2 m_\omega^2 D_\rho [(p + p_0 + k)^2]} (2k \cdot p_0 + m_\eta^2 + m_\rho^2 + 2p \cdot p_0) \\
& ((\lambda_3^{VV} + \lambda_4^{VV} + 2\lambda_5^{VV}) (k \cdot p + m_\pi^2 + p \cdot p_0) + 4m_\pi^2 \lambda_6^{VV} + 4p \cdot p_0 (\lambda_1^{VV} + \lambda_2^{VV})) ,
\end{aligned} \tag{5.62}$$

$$\begin{aligned}
v_3^{2R} = & -\frac{16F_V C_q (d_3 - d_4)}{3F^2 M_V m_\omega^2 D_\rho [(p + p_0 + k)^2] D_\omega [(p_0 + k)^2]} (4c_3(m_\pi^2 - m_\eta^2) - (c_5 + c_7)(2k \cdot p_0 + m_\eta^2)) (m_\omega^2 - m_\eta^2 - 2k \cdot p_0) \\
& + \frac{16F_V C_q}{3F^2 M_V m_\rho^2 D_\rho [(p + p_0 + k)^2] D_\rho [(p + k)^2]} \left( \frac{m_\rho^2}{2} (2d_3 (c_{1256} (2k \cdot p + k \cdot p_0 + p \cdot p_0) \right. \\
& - 2(c_5 + c_7) (k \cdot p_0 + p \cdot p_0)) + (2(c_5 + c_7) - c_{1256}) (8d_2 - d_{12}) m_\eta^2 + 2m_\pi^2 (4(c_{1256} - 2(c_5 + c_7)) d_2 + c_{1256} d_3)) \\
& \left. + (c_5 + c_7) (2k \cdot p + m_\pi^2) (2d_3 (k \cdot p_0 + p \cdot p_0) + (d_{12} - 8d_2) m_\eta^2 + 8d_2 m_\pi^2) \right) \\
& - \frac{8F_V C_q}{3F^2 M_V m_\rho^2 m_\omega^2 D_\rho [(p + k)^2]} (8c_3 (m_\pi^2 - m_\eta^2) (m_\pi^2 (d_1 + 8d_2 + d_3 + d_4) - (d_3 + d_4) m_\rho^2) \\
& + c_{1256} m_\pi^2 (-(d_1 + 8d_2)) m_\rho^2 + 2k \cdot p (c_{1256} d_3 m_\rho^2 + 8c_3 d_4 (m_\pi^2 - m_\eta^2))) \\
& - \frac{\sqrt{2} F_V^2 C_q}{3F^2 m_\rho^2 m_\omega^2 D_\rho [(p + p_0 + k)^2]} (\lambda_3^{\text{VV}} + \lambda_4^{\text{VV}} + 2\lambda_5^{\text{VV}}) (2k \cdot p_0 + m_\eta^2 + m_\rho^2 + 2p \cdot p_0) ,
\end{aligned} \tag{5.63}$$

$$\begin{aligned}
v_4^{2R} = & \frac{16F_V C_q (d_3 - d_4)}{3F^2 M_V m_\omega^2 D_\rho [(p + p_0 + k)^2] D_\omega [(p_0 + k)^2]} \left( \frac{1}{2} m_\omega^2 (4c_{1256} d_3 k \cdot p_0 + 2(c_{1256} - 2(c_5 + c_7)) d_3 k \cdot p \right. \\
& + 2(8c_3 + c_{1256}) d_3 m_\eta^2 - 16c_3 d_3 m_\pi^2 + 2c_5 d_{12} m_\pi^2 + 2c_7 d_{12} m_\pi^2 - c_{1256} d_{12} m_\pi^2 + 2(c_{1256} - 2(c_5 + c_7)) d_3 p \cdot p_0) \\
& \left. + (2d_3 (k \cdot p + p \cdot p_0) - d_{12} m_\pi^2) ((c_5 + c_7) (2k \cdot p_0 + m_\eta^2) + 4c_3 (m_\eta^2 - m_\pi^2)) \right) \\
& - \frac{16F_V C_q (c_5 + c_7) (d_3 - d_4)}{3F^2 M_V m_\rho^2 D_\rho [(p + p_0 + k)^2] D_\rho [(p + k)^2]} (2k \cdot p + m_\pi^2) (2k \cdot p - m_\rho^2 + m_\pi^2) \\
& + \frac{16F_V C_q (c_5 + c_7)}{3F^2 M_V m_\rho^2 m_\omega^2 D_\rho [(p + k)^2]} (-2k \cdot p + m_\rho^2 - m_\pi^2) (m_\pi^2 (d_1 + 8d_2 + d_3 + d_4) + 2d_4 k \cdot p) \\
& + \frac{\sqrt{2} F_V^2 C_q}{3F^2 m_\rho^2 m_\omega^2 D_\rho [(p + p_0 + k)^2]} (\lambda_3^{\text{VV}} + \lambda_4^{\text{VV}} + 2\lambda_5^{\text{VV}}) (2k \cdot p_0 + m_\eta^2 + m_\rho^2 + 2p \cdot p_0) .
\end{aligned} \tag{5.64}$$

## Appendix D: Off-shell width of meson resonances

For completeness we explain in this appendix the expressions that we have used for the off-shell width of meson resonances relevant to our study. The  $\rho(770)$  width is basically driven by Chiral Perturbation Theory results

$$\Gamma_\rho(s) = \frac{sM_\rho}{96\pi F^2} \left[ \sigma_\pi^{3/2}(s)\theta(s - 4m_\pi^2) + \frac{1}{2}\sigma_K^{3/2}(s)\theta(s - 4m_K^2) \right], \quad (5.65)$$

where  $\sigma_P(s) = \sqrt{1 - 4\frac{m_P^2}{s}}$ . We note that the definition of the vector meson width is independent of the realization of the spin-one fields [76]. Given the narrow character of the  $\omega(782)$  resonance the off-shellness of its width can be neglected. A similar comment would apply to the  $\phi(1020)$  meson, although it does not contribute to the considered processes in the ideal-mixing scheme for the  $\omega - \phi$  mesons that we are following.

The  $a_1(1260)$  meson energy-dependent width was derived in Ref. [90] applying the Cutkosky rules to the analytical results for the form factors into  $3\pi$  [90] and  $KK\pi$  channels [135] that are the main contributions to this width. Since its computation requires the time-consuming numerical calculation of the corresponding correlator over phase-space, we computed  $\Gamma_{a_1}(s)$  at 800 values of  $s$  and use linear interpolation to obtain the width function at intermediate values.

Finally, the  $a_0(980)$  meson is also needed as an input in the analyses. We have used the functional dependence advocated in eqs. (19) and (20) of Ref. [124] which take into account the main absorptive parts given by the  $\pi\eta$ ,  $K\bar{K}$  and  $\pi\eta'$  cuts. The very low-energy (G-parity violating)  $\pi\pi$  cut has been neglected.

We point out that we are considering only the imaginary parts of the meson-meson loop functions giving rise to the resonance widths. On the contrary, we are disregarding the corresponding real parts. Although this procedure violates analyticity at NNLO in the chiral expansion, the numerical impact of this violation is negligible (see e.g. Ref. [82]) and, for simplicity, we take this simplified approach in our study.

## Appendix E: Integration formulas needed to compute the $a_\mu^{P,HLbL}$

This appendix collects some formulae used for the evaluation of the pion pole/exchange contribution to the hadronic light-by-light muon anomalous magnetic moment in Chapter. 4. We will follow the notation of ref. [169], where angular integrations of the relevant two-loop integrals were first performed analytically using the method of Gegenbauer polynomials. The remaining two-dimensional integrations can be readily performed numerically provided the  $\pi$ TFF can be written

$$\mathcal{F}_{\pi^0\gamma\gamma}(q_1^2, q_2^2) = \frac{F}{3} \left[ f(q_1^2) - \sum_{M_{V_i}} \frac{1}{q_2^2 - M_{V_i}^2} g_{M_{V_i}}(q_1^2) \right]. \quad (5.66)$$

Then, the hadronic light-by-light contribution to  $a_\mu$  reads

$$a_\mu^{\pi^0, HLbL} = \left( \frac{\alpha}{\pi} \right)^3 \left[ a_\mu^{\pi^0(1), HLbL} + a_\mu^{\pi^0(2), HLbL} \right], \quad (5.67)$$

with

$$a_\mu^{\pi^0(1), HLbL} = \int_0^\infty dQ_1 \int_0^\infty dQ_2 \left[ w_{f_1}(Q_1, Q_2) f^{(1)}(Q_1^2, Q_2^2) + \sum_{M_{V_i}} w_{g_1}(M_{V_i}, Q_1, Q_2) g_{M_{V_i}}^{(1)}(Q_1^2, Q_2^2) \right], \quad (5.68)$$

and

$$a_\mu^{LbL, \pi^0(2), HLbL} = \int_0^\infty dQ_1 \int_0^\infty dQ_2 \sum_{M=m_\pi, M_{V_i}} w_{g_2}(M, Q_1, Q_2) g_M^{(2)}(Q_1^2, Q_2^2). \quad (5.69)$$

In the previous equation,  $w_{\{f/g\}_i}(q_1^2, q_2^2)$  are weight factors, whose expressions can be found in ref. [169].  $\{f/g\}^{(i)}$  are generalized form factors given by

$$\begin{aligned} f^{(1)}(Q_1^2, Q_2^2) &= \frac{F}{3} f(-Q_1^2) \mathcal{F}_{\pi^0\gamma\gamma}(-Q_2^2, 0), \quad g_{M_{V_i}}^{(1)}(Q_1^2, Q_2^2) = \frac{F}{3} \frac{g_{M_{V_i}}(-Q_1^2)}{M_{V_i}^2} \mathcal{F}_{\pi^0\gamma\gamma}(-Q_2^2, 0), \\ g_{m_\pi}^{(2)}(Q_1^2, Q_2^2) &= \frac{F}{3} \mathcal{F}_{\pi^0\gamma\gamma}(-Q_1^2, -Q_2^2) \left[ f(0) + \sum_{M_{V_i}} \frac{g_{M_{V_i}}(0)}{M_{V_i}^2 - m_\pi^2} \right], \\ g_{M_{V_i}}^{(2)}(Q_1^2, Q_2^2) &= \frac{F}{3} \mathcal{F}_{\pi^0\gamma\gamma}(-Q_1^2, -Q_2^2) \frac{g_{M_{V_i}}(0)}{m_\pi^2 - M_{V_i}^2}. \end{aligned} \quad (5.70)$$

Our expressions for the  $\pi$ TFF in the case of virtual (4.7) and real pion (4.8) can indeed be written according to eq. (5.66):

$$\begin{aligned} f(q^2) &= \frac{2}{F^2} \left[ \frac{-2\sqrt{2}c_{1256}F_V(M_V^2 - 2q^2)}{M_V(M_V^2 - q^2)} - \frac{N_C}{8\pi^2} - \frac{4d_3F_V^2}{M_V^2 - q^2} \right], \\ g_{M_V}(q^2) &= \frac{2}{F^2} \left[ 2\sqrt{2}c_{1256}F_V M_V + 4d_3F_V^2 \frac{M_V^2 + q^2}{M_V^2 - q^2} \right], \end{aligned} \quad (5.71)$$

for on-shell pion, and the additional contributions

$$\begin{aligned} \Delta f(q^2, r^2) &= \frac{2r^2}{F^2} \frac{-16\sqrt{2}P_2F_V}{(M_V^2 - q^2)(M_P^2 - r^2)}, \\ \Delta g_{M_V}(q^2, r^2) &= \frac{2r^2}{F^2} \left\{ \frac{4d_{123}F_V^2}{M_V^2 - q^2} - \frac{16\sqrt{2}P_2F_V}{M_P^2 - r^2} + \frac{16F_V^2P_3}{(M_V^2 - q^2)(M_P^2 - r^2)} \right\} \end{aligned} \quad (5.72)$$

for the general situation in which the pion is off its mass-shell. The predicted vanishing of the  $c_{1235}$ ,  $c_{125}$  and  $P_1$  couplings according to asymptotic constraints has already been taken into account to simplify eqs. (5.71) and (5.72).

In the latter case, eqs. (5.67)-(5.69) should be replaced by [150]

$$\begin{aligned} a_\mu^{\pi^0, H L b L} &= -\frac{2\alpha^3}{3\pi^2} \int_0^\infty dQ_1 \int_0^\infty dQ_2 \int_{-1}^{+1} dt \sqrt{1-t^2} Q_1^3 Q_2^3 \left[ \frac{F_1(Q_1^2, Q_2^2, t)}{Q_2^2 + m_\pi^2} I_1(Q_1, Q_2, t) \right. \\ &\quad \left. + \frac{F_2(Q_1^2, Q_2^2, t)}{Q_3^2 + m_\pi^2} I_2(Q_1, Q_2, t) \right], \end{aligned} \quad (5.73)$$

where  $Q_3 = (Q_1 + Q_2)$ ,  $t = \cos(\widehat{Q_1, Q_2})$ ,

$$\begin{aligned} F_1(Q_1^2, Q_2^2, t) &= \mathcal{F}_{\pi\gamma\gamma}(-Q_1^2, -Q_3^2, -Q_2^2) \mathcal{F}_{\pi\gamma\gamma}(-Q_2^2, 0, -Q_2^2) \\ F_2(Q_1^2, Q_2^2, t) &= \mathcal{F}_{\pi\gamma\gamma}(-Q_1^2, -Q_2^2, -Q_3^2) \mathcal{F}_{\pi\gamma\gamma}(-Q_3^2, 0, -Q_3^2), \end{aligned} \quad (5.74)$$

and the integration kernels  $I_1(Q_1, Q_2, t)$  and  $I_2(Q_1, Q_2, t)$  can be found in ref. [150].

# References

- [1] E. Rutherford, Philosophical magazine. Series 6 **21** (1911) 669
- [2] J. Chadwick, Nature. **129** (1932) 312
- [3] D. Ivanenko, Nature **129** (1932) 798
- [4] W. Heisenberg Z. Phys. **77** (1932) 11
- [5] E. Fermi, Nuovo Cim. **11** (1934) 1
- [6] G. Gamow and E. Teller, Phys.Rev. **49** (1936) 895
- [7] T.D. Lee and C.N. Yang, Phys. Rev. **104** (1956) 254
- [8] C.S. Wu, E. Ambler, R. H. Hayward, D. D. Hoppes and R. P. Hudson, Phys. Rev. **105** (1957) 1413
- [9] R. Garwin, L. Lederman and M. Weinrich, Phys. Rev. **105** (1957) 1415
- [10] A. Salam, Nuovo Cim. **5** (1957) 299
- [11] L. Michel, Proc. Phys. Soc. **A 63** (1950) 514
- [12] R. P. Feynman and M. Gell-Mann, Phys. Rev. **109** (1958) 193
- [13] E. C. Sudarshan and R. E. Marshak, Phys. Rev. **109** (1958) 1860
- [14] J. Schwinger, Annals Phys. **2** (1957) 407
- [15] S. L. Glashow, Nucl. Phys. **22** (1961) 579
- [16] T. Nakano and K. Nishijima, Prog. Theor. Phys. **10** (1953) 581
- [17] K. Nishijima, Prog. Theor. Phys. **13** (1955) 285
- [18] M. Gell-Mann, Nuovo Cim. **4** (1956) 848
- [19] A. Salam and J. C. Ward, Phys. Rev. Lett. **5** (1960) 390
- [20] J. Goldstone, Nuovo Cim. **19** (1960) 154
- [21] J. Goldstone, A. Salam and S. Weinberg, Phys. Rev. **127** (1962) 965
- [22] F. Englert and R. Brout, Phys. Rev. Lett. **13** (1964) 321
- [23] P. Higgs, Phys. Rev. **145** (1965) 1156
- [24] S. Weinberg, Phys. Rev. Lett. **19** (1967) 1264
- [25] G. Danby, J-M. Gaillard, K. Goulianos, L. M. Lederman, N. Mistry, M. Schwartz, and J. Steinberger, Phys. Rev. Lett. **9** (1962) 36
- [26] A. Salam and J. C. Ward, Phys. Lett. **13** (1964) 168

- [27] A. Salam, Conf. Proc. **C68-05-19** (1968) 367
- [28] S. Sakata, Progr. Theor. Phys. **16** (1956) 686
- [29] Y. Ne'eman, Nucl. Phys. **26** (1961) 222
- [30] M. Gell-Mann, Phys. Rev. **125** (1961) 1067
- [31] N. Cabibbo, Phys. Rev. Lett. **10** (1963) 531
- [32] M. Gell-Mann and M. Lèvy, Nuovo Cim. **16** (1960) 705
- [33] G. Zweig, *An  $SU(3)$  model for strong interaction symmetry and its breaking* CERN-TH-412 and CERN-TH-401 (1964),
- [34] M. Gell-Mann, Phys. Lett. **8** (1964) 214
- [35] M. Y. Han and Y. Nambu, Phys. Rev. **139** (1965) B1006
- [36] O. Greenberg, Phys. Rev. Lett. **13** (1964) 598
- [37] V. E. Barnes *et al*, Phys. Rev. Lett. **12** (1964) 204
- [38] K. Brueckner, Phys. Rev. **86** (1952) 106
- [39] J. D. Bjorken, Phys. Rev. **179** (1968) 1547
- [40] S. L. Glashow, J. Iliopoulos and L. Maiani, Phys. Rev. **D2** (1970) 1285
- [41] J. Iliopoulos, Quantum Field Theory lectures during the 2015 CERN Latin American of High Energy Physics at Ibarra, Ecuador. (2015)
- [42] W. Bardeen, H. Fritzsch and M. Gell-Mann, Scale and conformal symmetry in hadron physics proceedings. CERN-TH-1538 (1972)
- [43] J. H. Christenson, J. W. Cronin, V. L. Fitch and R. Turlay, Phys. Rev. Lett. **13** (1964) 138
- [44] M. Kobayashi and T. Maskawa, Prog. Theor. Phys. **49** (1973) 652
- [45] S. W. Herb, D. C. Hom, L. M. Lederman, J. C. Sens, H. D. Snyder, J. K. Yoh, J. A. Appel, B. C. Brown, C. N. Brown, W. R. Innes, K. Ueno, T. Yamanouchi, A. S. Ito, H. Jöstlein, D. M. Kaplan, and R. D. Kephart, Phys. Rev. Lett. **39** (1977) 252
- [46] S. Abachi *et al.* (D0 Collab.) Phys. Rev. Lett. **74** (1995) 2422; F. Abe *et al.* (CDF Collab.) Phys. Rev. Lett. **74** (1995) 2626
- [47] M. L. Perl *et al.*, Phys. Rev. Lett. **35** (1975) 1489
- [48] K. Kodama *et al.*, Phys. Lett. **B504** (2001) 218



- [49] S. Chatrchyan *et al.* (CMS Collab.) Phys. Lett. **B716** (2012) 30; G. Aad *et al.* (ATLAS collab.) Phys. Lett. **B716** (2012) 1.
- [50] G. Ecker, Prog. Part. Nucl. Phys. **35** (1995) 1
- [51] A. Pich, Rept. Prog. Phys. **58** (1995) 563; AIP Conf. Proc. **317** (1994) 95
- [52] S. Scherer, Adv. Nucl. Phys. **27** (2003) 277
- [53] S. Weinberg, Phys. Rev. **166** (1968) 1568
- [54] S. Coleman, J. Wess and B. Zumino, Phys. Rev. **177** (1969) 2247; C. Callan, S. Coleman, J. Wess and B. Zumino, Phys. Rev. **177** (1969) 2247
- [55] S. Weinberg, Physica **96A** (1979) 327
- [56] J. Wess and B. Zumino, Phys. Lett. B **37** (1971) 95. E. Witten, Nucl. Phys. B **223** (1983) 422.
- [57] J. Gasser and H. Leutwyler, Annals Phys. **158** (1984) 142;
- [58] J. Gasser and H. Leutwyler, Nucl. Phys. B **250** (1985) 465.
- [59] J. Bijnens, G. Colangelo and G. Ecker, JHEP **9902** (1999) 020.
- [60] J. Bijnens, L. Girlanda and P. Talavera, Eur. Phys. J. C **23** (2002) 539.
- [61] G. 't Hooft, Nucl. Phys. B **72** (1974) 461, Nucl. Phys. B **75** (1974) 461. E. Witten, Nucl. Phys. B **160** (1979) 57.
- [62] A. Manohar, *Large N QCD*, talk given at Les Houches Summer School in Theoretical Physics, Session 68: Probing the Standard Model of Particle Interactions. (1997) 1091
- [63] G. Ecker, J. Gasser, A. Pich and E. de Rafael, Nucl. Phys. **B321** (1989) 311
- [64] G. Ecker, J. Gasser, H. Leutwyler, A. Pich and E. de Rafael, Phys. Lett. **B223** (1989) 425
- [65] G. Ciezarek, M. Franco Sevilla, B. Hamilton, R. Kowalewski, T. Kuhr, V. Lüth and Y. Sato, arXiv:1703.01766
- [66] E. Arganda, M. Herrero and J. Portolés, JHEP **0806** (2008) 079
- [67] A. Celis, V. Cirigliano, E. Passemar, Phys. Rev. **D89** (2014) 013008
- [68] A. Celis, V. Cirigliano, E. Passemar, Phys. Rev. **D89** (2014) 095014
- [69] A. Lami, J. Portolés, P. Roig, Phys. Rev. **D93** (2016) 076008
- [70] Z. -H. Guo and P. Roig, Phys. Rev. D **82** (2010) 113016.
- [71] G. López Castro, N. Quintero, Phys. Rev. **D85** (2012) 076006, **86** (2012) 079904 (erratum); Michel Hernández Villanueva, Ms. Sc. Thesis *Estudio de sensibilidad del proceso  $B^0 \rightarrow D^- \pi^- \mu^+ \mu^+$  en el experimento Belle II* (2014) Cinvestav, México

- [72] C. Patrignani *et al.* (Particle Data Group), Chin. Phys. C, **40**, 100001 (2016).
- [73] J. Bijnens, G. Ecker and J. Gasser, Nucl. Phys. B **396** (1993) 81.
- [74] P. Roig, A. Guevara, G. López Castro, Phys. Rev. D **88** (2013) 033007
- [75] A. Flores-Tlalpa, PhD Thesis, *Modelo de dominancia de mesones para decaimientos semilep-  
tónicos de sabores pesados.* (2008) Cinvestav, Mexico, DF
- [76] D. Gómez Dumm, A. Pich and J. Portolés, Phys. Rev. D **62** (2000) 054014.
- [77] A. Pich, J. Portolés, Phys. Rev. D **63** (2001) 093005.
- [78] J. F. De Trocóniz and F. J. Ynduráin, Phys. Rev. D **65** (2002) 093001.
- [79] B. Ananthanarayan, I. Caprini and I. S. Imsong, Phys. Rev. D **83** (2011) 096002.
- [80] C. Hanhart, Phys. Lett. B **715** (2012) 170.
- [81] D. G. Dumm and P. Roig, Eur. Phys. J. C **73** (2013).2528
- [82] D. R. Boito, R. Escribano and M. Jamin, Eur. Phys. J. C **59** (2009) 821.
- [83] B. Aubert *et al.* [BABAR Collaboration], Phys. Rev. Lett. **103** (2009) 231801.
- [84] E. G. Floratos, S. Narison and E. de Rafael, Nucl. Phys. B **155** (1979) 115.
- [85] S. Peris, M. Perrottet and E. de Rafael, JHEP **9805** (1998) 011; M. Knecht, S. Peris, M. Per-  
rottet and E. de Rafael, Phys. Rev. Lett. **83** (1999) 5230; S. Peris, B. Phily and E. de Rafael,  
Phys. Rev. Lett. **86** (2001) 14.
- [86] F. Guerrero and A. Pich, Phys. Lett. B **412** (1997) 382.
- [87] M. Jamin, A. Pich and J. Portolés, Phys. Lett. B **640** (2006) 176.
- [88] S. Weinberg, Phys. Rev. Lett. **18** (1967) 507.
- [89] P. Roig and J. J. Sanz Cillero, Phys. Lett. B **733** (2014) 158.
- [90] D. G. Dumm, P. Roig, A. Pich and J. Portolés, Phys. Lett. B **685** (2010) 158.
- [91] I. M. Nugent, T. Przedzinski, P. Roig, O. Shekhovtsova and Z. Was, Phys. Rev. D **88** (2013)  
093012. We used the improved results updating O. Shekhovtsova, I. M. Nugent, T. Przedzinski,  
P. Roig and Z. Was, arXiv:1301.1964 [hep-ph]. Talk given at the 12th International Workshop  
on Tau Lepton Physics (TAU 2012). Nucl. Phys. Proc. Suppl. 253-255 (2014) 73.
- [92] O. Shekhovtsova, T. Przedzinski, P. Roig and Z. Was, Phys. Rev. D **86** (2012) 113008.
- [93] L. Wolfenstein, Phys. Rev. Lett. **51** (1983) 1945
- [94] R. Aaij *et al.* (LHCb Collab.), Phys. Rev. Lett. **113** (2014) 151301

- [95] C. Bobeth, G. Hiller and G. Piranishvili, JHEP **0712** (2007) 040
- [96] A. Guevara, G. López Castro and P. Roig, Phys. Rev. D **92** (2015) 054035
- [97] G. J. Gounaris and J. J. Sakurai, Phys. Rev. Lett. **21** (1968) 244
- [98] M. Beneke, T. Feldmann and D. Seidel, Eur. Phys. J. C **41** (2005) 173; M. Beneke, G. Buchalla, M. Neubert and C. T. Sachrajda, Nucl. Phys. **591** (2000) 313;
- [99] M. Beneke, T. Feldmann and D. Seidel, Nucl. Phys. B **612** (2001) 25
- [100] A. Khodjamirian, T. Mannel, Y. M. Wang, JHEP **1302** (2013) 010
- [101] G. Amorós, S. Noguera and J. Portolés, Eur. Phys. J. C **27** (2003) 243
- [102] P. Ball and R. Zwicky, Phys. Rev. D **71** (2005) 014029
- [103] S. J. Brodsky and G. R. Farrar, Phys. Rev. Lett. **31** (1973) 1153. G. P. Lepage and S. J. Brodsky, Phys. Rev. D **22** (1980) 2157.
- [104] V. Cirigliano, G. Ecker and H. Neufeld JHEP **0208** (2002) 002
- [105] A. Pich and J. Portolés, Nucl. Phys. Proc. Suppl. **121** (2003) 179
- [106] P. Roig and Z. Was, Phys. Rev. D **86** (2012) 11300; D. Gómez Dumm and P. Roig, Eur.Phys. J. C **73** (2013) 8, 2528
- [107] J.P. Lees *et al.* (BaBar Collab.) Phys.Rev. D **88** (2013) 032013
- [108] J. P. Lees *et al.* (BaBar Collab.) Phys.Rev. D **86** (2012) 032013
- [109] A. Ali, A. Ya. Parkhomenko, and A. V. Rusov, Phys. Rev. D **89** (2014) 094021
- [110] PDG K.A. Olive *et al.* (Particle Data Group) Chin. Phys. C **38** (2014) 090001
- [111] J. Charles, *et al.* (CKM fitter Group) Phys.Rev. D **91** (2015) 073007
- [112] R. Aaij *et al.* (LHCb Collab.), JHEP **1212** (2012) 125
- [113] W.S. Hou, M. Khonda and F. Xu, Phys.Rev. D **90** (2014) 013002
- [114] C. Hambrock, A. Khodjamirian and A. Rusov, Phys.Rev. D **92** (2015) 074020
- [115] S. Weinberg, Phys. Rev. **112**, 1375 (1958).
- [116] C. Leroy and J. Pestieau, Phys. Lett. B **72**, 398 (1978).
- [117] V. Cirigliano, G. Ecker and H. Neufeld, JHEP **0208**, 002 (2002).
- [118] J. Bijnens, G. Ecker and J. Gasser, Nucl. Phys. B **396**, 81 (1993).

- [119] C. A. Domínguez, Phys. Rev. D **20**, 802 (1979); S. Tisserant and T. N. Truong, Phys. Lett. B **115** (1982) 264; A. Pich, Phys. Lett. B **196**, 561 (1987); A. Bramon, S. Narison and A. Pich, Phys. Lett. B **196**, 543 (1987); E. Berger and H. Lipkin, Phys. Lett. B **189**, 226 (1987); Y. Meurice, Mod. Phys. Lett. A **2**, 699 (1987); Phys. Rev. D **36**, 2780 (1987); C. K. Zachos and Y. Meurice, Mod. Phys. Lett. A **2**, 247 (1987); S. Fajfer and R. J. Oakes, Phys. Lett. B **213**, 376 (1988); H. Pietschmann and H. Rupertsberger, Phys. Rev. D **40**, 3115 (1989); J. O. Eeg and O. Lie-Svendsen, Phys. Lett. B **200**, 182 (1988); M. Suzuki, Phys. Rev. D **36**, 950 (1987); E. Braaten, R. J. Oakes and S. M. Tse, Int. J. Mod. Phys. A **5**, 2737 (1990); J. L. Díaz-Cruz and G. López Castro, Mod. Phys. Lett. A **6**, 1605 (1991); H. Neufeld and H. Rupertsberger, Z. Phys. C **68** (1995) 91.
- [120] P. del amo Sánchez et al [BaBar collaboration], Phys. Rev. D **83**, 032002 (2011).
- [121] B. Aubert *et al.* [BaBar Collaboration], Phys. Rev. D **77** (2008) 112002.
- [122] K. Hayasaka [Belle Collaboration], PoS EPS **-HEP2009**, 374 (2009).
- [123] F. E. Low, Phys. Rev. **110** (1958) 974.
- [124] R. Escribano, S. González-Solís and P. Roig, Phys. Rev. D **94** (2016) 034008.
- [125] D. M. Asner *et al.* [CLEO Collaboration], Phys. Rev. D **61** (2000) 012002.
- [126] S. Uehara *et al.* [Belle Collaboration], Phys. Rev. D **80** (2009) 032001.
- [127] Z. H. Guo, J. A. Oller and J. Ruiz de Elvira, Phys. Rev. D **86** (2012) 054006.
- [128] J. F. Donoghue, C. Ramírez and G. Valencia, Phys. Rev. D **39** (1989) 1947;
- [129] K. Kampf and J. Novotny, Phys. Rev. D **84** (2011) 014036.
- [130] V. Cirigliano, G. Ecker, M. Eidemüller, R. Kaiser, A. Pich and J. Portolés, Nucl. Phys. B **753** (2006) 139.
- [131] D. Gómez Dumm, A. Pich and J. Portolés, Phys. Rev. D **69** (2004) 073002.
- [132] P. D. Ruiz-Femenía, A. Pich and J. Portolés, JHEP **0307** (2003) 003.
- [133] K. G. Wilson, Phys. Rev. **179** (1969) 1499.
- [134] Z. -H. Guo, Phys. Rev. D **78** (2008) 033004.
- [135] D. G. Dumm, P. Roig, A. Pich and J. Portolés, Phys. Rev. D **81** (2010) 034031.
- [136] V. Cirigliano, G. Ecker, M. Eidemüller, R. Kaiser, A. Pich and J. Portolés, JHEP **0504** (2005) 006.
- [137] B. Ananthanarayan and B. Moussallam, JHEP **0406** (2004) 047.

- [138] V. Cirigliano, G. Ecker, M. Eidemuller, A. Pich and J. Portolés, Phys. Lett. B **596** (2004) 96.
- [139] M. Jamin, J. A. Oller and A. Pich, Nucl. Phys. B **587** (2000) 331; **622** (2002) 279.
- [140] J. Bijnens and I. Jemos, Nucl. Phys. B **854** (2012) 631.
- [141] S. Z. Jiang, Y. Zhang, C. Li and Q. Wang, Phys. Rev. D **81** (2010) 014001.
- [142] D. G. Dumm and P. Roig, Phys. Rev. D **86** (2012) 076009.
- [143] Y. H. Chen, Z. H. Guo and H. Q. Zheng, Phys. Rev. D **85** (2012) 054018.
- [144] Y. H. Chen, Z. H. Guo and H. Q. Zheng, Phys. Rev. D **90** (2014) no.3, 034013.
- [145] Y. H. Chen, Z. H. Guo and B. S. Zou, Phys. Rev. D **91** (2015) 014010.
- [146] A. Guevara, G. López Castro and P. Roig, Phys. Rev. D **95** (2017) 054015
- [147] W. Gerlach and O. Stern, Z. Phys. **9** (1922) 349-352 and 353-355
- [148] J. E. Nafe, E. B. Nelson and I. I. Rabi, Phys. Rev. **71** (1947) 914
- [149] J. S. Schwinger, Phys. Rev. **73** (1948) 416
- [150] F. Jegerlehner and A. Nyffeler, Phys. Rept. **477** (2009) 1.
- [151] K. Ackerstaff *et al.* [OPAL Collab.] Phys. Lett. B **431** (1998) 188; M. Acciarri *et al.* [L3 Collab.] Phys. Lett. B **434** (1998) 169; W. Lohmann, Nucl. Phys. Proc. Suppl. **144** (2005)
- [152] T. Aoyama, M. Hayakawa, T. Kinoshita and M. Nio, Phys. Rev. Lett. **109** (2012) 111808
- [153] G. Venanzoni, [E989 Collab.] arXiv1411.2555 [hep-ph] (2014)
- [154] B. Shwartz, PHIPSI15 conference talk (2015)
- [155] H. H. Elend, Phys. Lett. **20** (1966) 682; H. H. Elend, Phys. Lett. **21** (1966) 720 (erratum)
- [156] S. Laporta and E. Remiddi, Phys. Lett. B **379** (1996) 283
- [157] M. Hoferichter, G. Colangelo, M. Procura, P. Stoffer, Int. J. Mod. Phys. Conf. Ser. **35** (2014) 1460400
- [158] G. Colangelo, M. Hoferichter, B. Kubis, M. Procura and P. Stoffer, Phys. Lett. B **735** (2014) 90
- [159] G. Colangelo, M. Hoferichter, M. Procura and P. Stoffer, JHEP **1409** (2014) 091
- [160] G. Colangelo, M. Hoferichter, M. Procura and P. Stoffer, Phys. Lett. B **738** (2014) 6
- [161] V. Pauk and M. Vanderhaeghen, Phys. Rev. D **90** (2014) 113012
- [162] G. Colangelo, M. Hoferichter, M. Procura and P. Stoffer, JHEP **1509** (2015) 074

- [163] G. Colangelo, M. Hoferichter, M. Procura and P. Stoffer, *Dispersion relation for hadronic light-by-light scattering: two-pion contributions*, CERN-TH-2017-014 (2017)
- [164] T. Blum, S. Chowdhury, M. Hayakawa and T. Izubuchi, Phys. Rev. Lett. **114** (2015) 012001
- [165] T. Blum, N. Christ, M. Hayakawa, T. Izubuchi, L. Jin and C. Lehner, Phys. Rev. D **93** (2016) 014503
- [166] E. de Rafael, Phys. Lett. B **322** (1994) 239.
- [167] M. Hayakawa, T. Kinoshita and A. I. Sanda Phys. Rev. Lett. **75** (1995) 790; Phys. Rev. D **54** (1996) 3137.
- [168] J. Bijnens, E. Pallante, J. Prades, Phys. Rev. Lett. **75** (1995) 1447; Nuclear Phys. B 474 (1996) 379; J. Bijnens, E. Pallante, J. Prades, Phys. Rev. Lett. **75** (1995) 3781 (erratum); J. Bijnens, E. Pallante, J. Prades, Nuclear Phys. B 626 (2002) 410 (erratum)
- [169] M. Knecht, A. Nyffeler, Phys. Rev. D **65** (2002) 073034.
- [170] P. Roig, A. Guevara and G. López Castro, Phys. Rev. D **89** (2014) 073016
- [171] B. Aubert *et al.* [BaBar Collaboration], Phys. Rev. D **80** (2009) 052002.
- [172] S. Uehara *et al.* [Belle Collaboration], Phys. Rev. D **86** (2012) 092007.
- [173] H. J. Behrend *et al.* [CELLO Collaboration], Z. Phys. C **49** (1991) 401.
- [174] J. Gronberg *et al.* [CLEO Collaboration], Phys. Rev. D **57** (1998) 33.
- [175] R. Kaiser and H. Leutwyler, In \*Adelaide 1998, Nonperturbative methods in quantum field theory\* 15-29, Eur. Phys. J. C **17** (2000) 623.
- [176] J. Schechter, A. Subbaraman and H. Weigel, Phys. Rev. D **48** (1993) 339. T. Feldmann, P. Kroll and B. Stech, Phys. Rev. D **58** (1998) 114006; Phys. Lett. B **449** (1999) 339. T. Feldmann, Int. J. Mod. Phys. A **15** (2000) 159.
- [177] M. Ramsey-Musolf and M. Wise, Phys. Rev. Lett. **89** (2002) 041601
- [178] K. Engel, H. Patel and M. Ramsey-Musolf, Phys. Rev. D **86** (2012) 037502
- [179] Y. Nambu and G. Jona-Lasinio, Phys. Rev. **122** (1961) 345; **124** (1961) 246.
- [180] M. Hayakawa and T. Kinoshita, Phys. Rev. D **57** (1998) 465; 66 (2002) 019902 (erratum) ;
- [181] K. Melnikov and A. Vainshtein, Phys. Rev. D **70** (2004) 113006.
- [182] D. K. Hong and D. Kim, Phys. Lett. B **680** (2009) 480.
- [183] L. Cappiello, O. Catà and G. D'Ambrosio, Phys. Rev. D **83** (2011) 093006.
- [184] P. Masjuan and M. Vanderhaeghen, J. Phys. G **42** (2015), 125004

- [185] A. E. Dorokhov, A. E. Radzhabov and A. S. Zhevlakov, Eur. Phys. J. C **72** (2012) 2227, C **71** (2011) 1702.
- [186] R. Kumar, Phys. Rev. **185** (1969) 1865.
- [187] R. Escribano, P. Masjuan and P. Sánchez-Puertas, Phys. Rev. D **89** (2014) 034014.
- [188] P. Masjuan, E. Ruiz Arriola and W. Broniowski, Phys. Rev. D **87** (2013) 014005.
- [189] J. Prades, E. de Rafael and A. Vainshtein, Advanced series on directions in high energy physics. **20** (2009) 303
- [190] J. Erler and G. Toledo Sánchez, Phys. Rev. Lett. **97** (2006) 161801
- [191] A. Nyffeler, Phys. Rev. D **79** (2009) 073012.
- [192] M. Peskin and D. Schroeder, *An introduction to quantum field theory* first ed. Addison-Wesley. (1995) USA